A STUDY OF THE BIOPHYSICAL MECHANISMS OF DAMAGE BY IONIZING RADIATION TO MAMMALIAN CELLS 'IN VITRO'

Chun-Zhang Chen

A Thesis Submitted for the Degree of PhD
at the
University of St Andrews

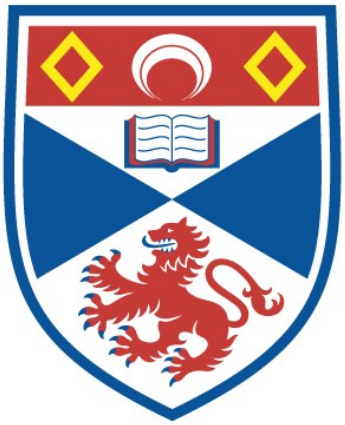

1988

A Study of Biophysical Mechanisms of Damage by Ionizing Radiation to Mammalian Cells *in vitro*

A STUDY OF BIOPHYSICAL MECHANISMS OF DAMAGE BY IONIZING RADIATION TO MAMMALIAN CELLS *in vitro*

by Chun-Zhang Chen
(Research Assistant, M.Sc.)

A thesis presented
for the degree of
Doctor of Philosophy

University of St. Andrews
St. Andrews, Fife KY16 9SS
Scotland, United Kingdom
June, 1987

University of St. Andrews
Thesis Copyright Declaration Form

"In submitting this thesis to the University of St. Andrews I understand that I am giving permission for it to be made available for public use in accordance with the regulations of the University Library for the time being in force, subject to any copyright vested in the work not being affected thereby. I also understand that the title and abstract will be published, and that a copy of the work may be made and supplied to any *bona fide* library or research worker."

Declaration

I wish to exercise the above option.

Signature

Date

23 Sept. 1987

Declaration

I hereby declare that this thesis has been composed by myself, that it is a record of my own work, and that it has not previously been presented for a higher degree.

This research was carried out in the Department of Physics, in the University of St. Andrews under the supervision of Dr. D. E. Watt.

Chun-Zhang Chen

Certificate

I hereby certify that the candidate, Chun-Zhang Chen, has fulfilled the conditions of the Resolution and Regulations of the University of St. Andrews appropriate to the Degree of Ph.D.

David E. Watt
Research Supervisor

Acknowledgements

I wish to thank Dr. D.E. Watt, for his sincere support and many conductive discussions throughout the course of the research. I should like to acknowledge Dr. A.C. Riches, for his interest and supervision on biological aspects, and his encouragement on monolayer cell culture studies.

I am grateful for the assistance of the department workshop for constructing mechanical apparatus. The advisory staff of the computing laboratory are appreciated for their computational service. The academic staff who offered help in both the Department of Physics and the Department of Anatomy and Experimental Pathology, particularly, Professor W. Sibbett, Professor D.B. Thomas, are acknowledged for their concern and providing the necessary facilities for the experiments, and Dr. P.E. Bryant and Mrs. C. Briscoe are acknowledged for their helpful discussion and assistance.

Financial support from the Chinese Academy of Sciences, the Development Office of St. Andrews University, the Sino-British Fellowship Trust and the Universities' China Committee is gratefully acknowledged. I am obliged to Mrs. M. Aikman for her moral support.

Finally, I should like to record my appreciation to Professors G.E. Adams, J.H. Martin, S.Z. Bei, L.S. Cheng and Dr. X. Shen for initially introducing me into the present research field and for their continous encouragement.

I am thankful to my colleagues, of the Institute of Biophysics, the Chinese Academy of Sciences, and friends, abroad and home, for their support and encouragement.

List of Publications

from the thesis:

Watt, D.E., Al-Affan, I.A.M., Chen, C.-Z. and Thomas, G.E. (1985), Identification of biophysical mechanisms of damage by ionizing radiation. Radiat. Prot. Dosi. (Microdosimetry, Procs. Ninth Symp. Microdos., May 20-24, Toulouse, France), **13**(1-4), 285-294.

Chen, C.-Z. and Watt, D.E. (1986), Biophysical mechanism of radiation damage to mammalian cells by x and γ-rays. Int. J. Radiat. Biol., **49**(1), 131-142.

Watt, D.E., Chen, C.-Z., Kadiri, L. and Younis, A. (1987), Towards a unified system for expression of biological damage by ionizing radiation. BNES Conf. on Health Effects of Low Dose Ionizing Radiations- Recent Advances and their Implications. 11-14 May, 1987. London.

Chen, C.-Z., McGuire, A. and Watt, D.E. (1987), Test of a DNA-rupture model of radiation action. Eighth Int. Congr. Radiat. Res., Session **B32-1V.** 19-24 July, 1987, Edinburgh.

other publications:

Shen Xun, Tang De-jiang, Chen Chun-zhang, Nie Yu-sheng, Li Xin-yuan, Zhang Yin, Guo Sheng-wu, Pang Su-zhen, Dai Jun and Ma Hai-guan (1981), A Conventional Flash Photolysis Apparatus Using Spectrophotometry and Observations on Some Transient Photolysis Species. *Acta Biochimica et Biophysica Sinica*, **13**(2), 165-174.

Zhang Yin, Tang De-jiang and Chen Chun-zhang (1981), Potassium Ferrioxalate Actinometer and Its Application in Flash Photolysis. Biochemistry and Biophysics (China), No.2(April), 62-65.

Chen Chun-zhang, Shen Xun, Li Xin-yuan (1983), A Simple Home-made Radio-chromatogram Scanner and Its Performance. Chinese J. Radiol. Med. Prot., **6**, 53-56.

Ma Hei-guan and Chen Chun-zhang (1983), A Microsecond Flash Photolysis Apparatus. 2nd Natl. Symp. on Biophysics, Shijiazhuang, China, 14-19 Nov., 1983.

Tang De-jiang, Li Xin-yuan, Chen Chun-zhang and Shen Xun (1983), The measurement of a small transient signal superposed on a large electric current. J. Electronics (in Chinese), **5**(2), 84-90; (1984), ibid (in English), **1**(1), 28-35.

Pang Su-zhen, Chen Chun-zhang and Shen Xun (1984), A flash photolysis study of an aqueous solution of bovine serum albumin. *Acta Biochemica et Biophysica Sinica*, **16**(6), 533-539.

This thesis is dedicated to my parents.

Abstract

An extensive survey made of published survival data of damage by ionizing radiation to mammalian cells *in vitro* has led to the new conclusion that the damage is determined by the specific ionization or the mean free path between ionizing events along the charged particle tracks. The optimum damage is observed when the mean free path is equivalent to the DNA double strand spacing of 1.8 nm. Therefore, the biological mechanism of ionizing radiation to mammalian cells *in vitro* is intra track dominant.

A 100 keV electron accelerator has been constructed and commissioned to produce a broad beam irradiation field of greater than 1 cm diameter. The fluence rate may be adjusted from 10^8 cm^{-2}-sec^{-1} downwards to enable further development as a chronic irradiation facility. Another new feature of the accelerator is that it incorporates a differential vacuum system which permits irradiation of the monolayer cell cultures to be carried out in normal pressure.

Experiments of irradiation to Chinese hamster cells, by ^{241}Am alpha particles at low fluence rate, have supplied satisfactory data for testing a new DNA-rupture model which is under development. For V79 cells irradiated at a low fluence rate of 10^5 cm^{-2}-min^{-1}, when survival data were fitted into the model, new biophysical parameters were extracted and a proposal was made that the repair phenomenon of cellular survival at very low doses is determined by three time factors: the irradiation time, the damage fixation time and the repair time. The values obtained were 3-4 hours for the mean repair time, and more than 10 hours for the damage to be considered permanent.

Details of the monolayer cell culture technique developed and used in the present experiments are described.

Consideration has been given to the significance of the results obtained from the study in radiation protection and in radiotherapy. In future studies it is recommended that more attention should be paid to measure the ionization events of the radiation studied.

Towards the objective of producing a unified dosimeter, more studies are needed to correlate the results for electrons and neutrons for which less data are available.

In this thesis the background and the basic theories are introduced in Chapters I and II. Experimental details are described in Chapter III on physical aspects and Chapter IV on biological aspects. Finally the results and discussion are presented in Chapter V.

CONTENTS

CHAPTER I INTRODUCTION

1.1 Purpose of the Project

Radiation is an important factor in our daily life. It is important not only because the oldest application of x-rays for the therapeutic treatment of skin cancer has been extended to the application of gamma-rays, high energy electrons and fast neutrons to the treatment of almost every type of cancer. It is also because in the last two decades, radiation facilities have proved to be invaluable in many industrial applications:

i) tracer application, *e.g.*, the extensively used technique in the detection of leaks from underground pipework;

ii) physical quality measurements, *e.g.*, as thickness and density gauges and for analysis of elements in a sample;

iii) processing such as sterilizing of medical products, improving the properties of various plastic products, tubes, and car tyres *etc.*, killing insects, organisms and bacteria for food preservation.

Furthermore, nuclear power stations supply about 15% of the total electricity in the world, and there has been an increasing use of nuclear power to supply electricity because of the potential shortage of fossil fuels in the natural world before alternative energy supplies can be brought into production.

The biological effects of ionizing radiation at high doses has been long ago a matter of public knowledge. Because of the problem of safe disposal of radiation waste from nuclear reactors, and the remote possibility of reactor accident, the general public feel threatened by possible effects at low dose levels. However, this anxiety is justified as we are unable to correlate the biological effects at low level in vitro to those in vivo of human beings, for example, the manifestation of potential cancer incidence.

Therefore, radiation research, especially at low dose levels, is necessary for purposes of radiation protection and radiotherapy, and all other peaceful uses of nuclear energy. It is necessary to pursue study of the mechanisms of interaction between radiation and biological media, to assess the effects of radiation from the cosmic rays, ultraviolet exposure, and radioactivity in the natural environment and in the surroundings of nuclear installations. From such studies information can be obtained to enable more accurate assessment of risk to both classified workers and the general population.

The existing theories of assessing the mechanisms of the effects of ionizing radiation damage to biological systems are based on the concept of energy transfer or energy deposition reflected in the quantities of the absorbed dose D, in units of J/kg, and the quality factor Q adopted in radiation protection legislation (ICRP, 1977). Although Q is unitless, it is related to the linear energy transfer LET, in units of keV/μm, see Table 1.1. Comparison of damage effects due to different types of radiation is quantified, *e.g.*,

for mathematical modelling, by the relative biological effectiveness (RBE).

Table 1.1 LET-Q Relation

Particles	LET(keV/um)	Q
x,γ,e	< 3.5	1
	7	2
n,ions	23	5
	53	10
alpha	>175	20

The RBE of some test readiation (r) with respect to x-rays (formally 250-kV x-rays) reference radiation (x) is defined by the ratio D_x/D_r, where D_x and D_r are, respectively, the doses of x-rays and the test radiation required to produce the same biological end-point.

Difficulties have been met in either interrelating the radiation damage models commonly used in the literature to give rise to a universal explanation of the biological end-point induced by different ionizing radiation particles (dose effect), or developing further these models to involve a time factor (dose-rate effect) so as to be able to predict the forthcoming radiation damage.

The proposed project aims to study published biological damage data, to analyse the results in terms of parameters expressed in units excluding energy, and to propose biophysical mechanisms of damage based on the new parameters. From these studies, the strategic challenge is to develop and carry out tests of

the proposed model, and to suggest what physical parameters be measured, and how to relate these to the biological effects of ionizing radiation.

The detailed research programme includes a brief review of the present status of the existing theories; an analysis of the extensive published data; a design of the experimental installation for the relevant research to be carried out, and to establish necessary facilities for future research. Theoretical calculations for the analyses are undertaken to some extent.

1.2 Ionizing Radiation

Biological systems are notably sensitive to radiations, due to the subsequent events or products produced in the interaction of incident particles with the systems. Such radiation particles may include, in the electromagnetic spectrum, ultraviolet radiation, infra-red to microwave radiation and 'ionizing radiation'. The latter applies, to radiation which can ionize matter directly. The term 'indirectly ionizing' is used if the action is due to secondary charged particle radiation. In the present research, only ionizing radiation will be dealt with although other so called 'non-ionizing' radiation (*e.g.*, UV radiation) has been receiving more and more attention. In the following text, the short term 'radiation' will stand for 'ionizing radiation' unless otherwize stated.

Radiation charged particles and photons interact mainly with the electrons of an atom or of a molecule of the medium under risk, for example, with those of water, which is of great biological

interest. These interactions can be excitation events, in which case one or more electrons in an atom or molecule are raised to higher energy levels, or ionization events, *i.e.*, the radiation particle has sufficient energy to eject one or more orbital electrons from the atom or molecule. Usually, the primary radiations dealt with have much higher energy compared to that required in interact ions to ionize or excite atoms or molecules of any material. In traversing matter, however, the energy of the primary particle is degraded in producing secondary charged particles. Fast neutrons, being electrically neutral, interact with matter mainly through elastic scattering to produce charged particles which can be treated as primaries in a simplified analysis. The primary particles and secondaries may be finally stopped, transmitted, or recoiled depending on their energy. A detailed account of the complete process is difficult and each aspect should be treated individually.

In radiation research, studies on low-level ionizing radiations related to radiation protection or radiotherapy are always useful since questions on low radiation dose, of the order of, or below 1 gray, can be controversial. For example, do such low doses have a linear or a non-linear response for production of somatic damage? It is not clear, because there are not sufficient good direct experimental results to be demonstrative (cf. Brown, 1977; Cohen, 1980; Coggle, 1985). It is expected that through studies on the effects of low-dose or low dose-rate radiation to biological systems at different levels (*e.g.*, at cellular level), information obtained can improve our understanding of the relationship between damage

effect and radiation quantity and/or quality. This, in turn, can give us clearer guidance in the peaceful applications of atomic energy (cf. Upton, 1977; Pochin, 1983; Elkind, 1984).

1.3 Physical Background of Radiation Biophysics

1.3.1 Interactions of radiation with matter

The process of the interaction of ionizing particles with matter is complex. It varies with and depends on the type and energy of the primary particle. However, these types of interactions in general, according to the type of the incident particles can be listed in the following three categories:

i) electromagnetic interaction: x-rays and γ-rays;

ii) neutral interaction: ions, electrons.

iii) charged particle interaction: ions, electrons.

i) X-ray and γ-ray photons are 'indirectly ionizing' radiations. Since the secondary electrons of the photons rather than the photons themself produce chemical or biological damages in the matter the photons traverse. The process of interaction of x-rays or γ-rays with matter can be the processes of attenuation, scattering and absorption. A photon can lose its entire energy through the photoelectric effect (absorption) resulting in attenuation of the total beam of photons, or lose part of its energy through Compton effect, in which case the incident photon is scattered. The Compton effect is dominant in low Z materials. The

linear attenuation coefficient, μ, is equal to the product of the collision cross-section per atom, σ, and the number of atoms per unit volume, N, *i.e.*, $\mu = \sigma N$. Then the fraction of photons which can pass through a thickness x of density ρ is $I/I_0 = e^{-\mu x} = e^{-(\mu/\rho)(\rho x)}$.

Where $\mu/\rho = \rho N_A/A$ is the mass attenuation coefficient, a more convenient parameter in use. The total mass attenuation coefficient is (ICRU, 1980)

$$\frac{\mu}{\rho} = \frac{\tau}{\rho} + \frac{\sigma_c}{\rho} + \frac{\sigma_{coh}}{\rho} + \frac{\kappa}{\rho} \qquad (1.1)$$

where the components refer to the photoelectric effect, Compton effect, coherent scattering, and pair production, respectively. Photon energy of x-rays or γ-rays below 2 MeV is important to the present discussion. Therefore, the last two terms on the right of Eq.(1.1) can be ignored.

For the theoretical calculation of absorbed dose, the mass energy transfer coefficient μ_{tr}/ρ and the mass absorption coefficient μ_{en}/ρ are important,

$$\frac{\mu_{tr}}{\rho} = \frac{\tau}{\rho} f_\tau + \frac{\sigma_c}{\rho} f_c \qquad (1.2)$$

where $f_\tau = 1 - \bar{E}_{fr}/h\upsilon_0$, E_{fr} is the average energy emitted as

fluorescent radiation per photon absorbed ($\bar{E}_{fr}=\phi E_b$, the product of the fluorescence yield and the binding energy of the target molecule); $f_c=\bar{E}_C/h\upsilon_0$, $\bar{E}_C$ the average energy of the Compton electron per scattered photon of energy $h\upsilon_0$. In low Z elements, μ_{en}/ρ and μ_{tr}/ρ are approximately equal. Through these effects, the secondary energetic charged particles (usually electrons) are generated and these in turn produce most of the excitation and ionization. The subsequent quantitative treatment is similar to that for charged particle interactions.

ii) Many dose effect experiments have been performed with fast neutrons (0.5-14 MeV) which can be obtained from spontaneous fission sources (*e.g.* ^{252}Cf); in a nuclear reactor, or from a Cyclotron through (d,n) reactions. Interaction between a neutron and an atom of the matter, according to the energy conservation law and the momentum conservation law, is considered as an elastic collision between the neutron and the nucleus. A recoil nucleus having mass A can obtain energy E_A, from the neutron of mass M_n and energy E_n,

$$E_A = \frac{4\ M_n A}{(M_n + A)^2}\ E_n \cos^2\theta \qquad (1.3)$$

where θ is the angle between the incident neutron and the recoil nucleus. Let $M_n=1$, then A will have a minimum value from zero to

a maximum $E_{A,max}=E_n 4A/(1+A)^2$ at $\theta=0$. As the theoretical energy distributions for both the scattered recoil nucleus and the scattered neutrons are rectangular, therefore, the mean energies imparted to the target nucleus and the scattered neutrons are $\bar{E}_A=E_n 2A/(1+A)^2$, and $E_{n,s}=E_n(1+A^2)/(1+A)^2$. In the liquid water system of interest, the hydrogen nucleus has a mass $A=M_n=1$. From the above equation, the simplified energy spectrum in a hydrogenous medium can be taken as

$$\bar{E}_A = \bar{E}_{n,s} = E_n/2 \qquad (1.4)$$

The neutron can also interact through absorption but this is less important in biological effects and therefore is excluded in the discussion.

iii) Fast energetic charged particles produce ionization and excitation through direct Coulomb-force interactions with the electrons of the matter being traversed. This interaction is the most common. The relevant mathematical expression for the rate of energy loss is given in the next section.

1.3.2 Energy transfer and energy deposition

Incident charged particles are subject to an energy transfer process. For dosimetric purpose, one needs to know the W value, the mean energy expended in a gas per ion pair formed, which is defined as (ICRU, 1980)

$$W = E/\bar{N} \qquad (1.5)$$

where $\bar{N}$ is the mean number of ion pairs formed when the initial kinetic energy E of a charged particle is completely dissipated in the gas. For electrons in dry air, the recommended value is 33.85-33.97 eV (ICRU, 1979; Boutillon & Perroche-Roux, 1987). The mean excitation energy, I, is an important parameter used to calculate the stopping power, defined in Eq.(1.6), where the summation is made over all excitation levels E_i and weighted by a transition frequency, f_i, termed the oscillator strengths representing the fraction of electron orbitals available to be excited to the level with value E_i

$$Z \ln I = \Sigma f_i \ln E_i \qquad (1.6)$$

in which I and E_i are in units of eV. The Bethe-Bloch formula (1933) described a differential energy loss (the stopping power or LET, the acronym of linear energy transfer first used by Zirkle *et al.* in 1952, in radiobiology research), of charged particle per unit path length travelled. The definition of LET is given by ICRU (ICRU, 1970).

In the last decade, many theoretical works have been pursued to make the Bethe-Bloch formula fit the experimental data better, and results of the calculation of the stopping power of electrons and positrons have been tabulated (ICRU, 1984). Let all the relevant constants and numerals in the theoretical expression for stopping power be collected together as

$$k_L = 2\pi N_A r_e^2 mc^2 = 0.1535 \text{ MeV-cm}^2/\text{mol}, \qquad (1.7)$$

then the corrected formula for calculating the stopping power of heavy ions, of charge number z, is given by

$$-\frac{1}{\rho} S_{col} = 2 k_L \frac{Z z^2}{A \beta^2} L(\beta) \qquad (1.8)$$

where L(β) is the stopping number per atomic electron. Other symbols have their usual meanings. The detailed formulae are given in Appendix A. An analogous formula is given for electrons, but then the total stopping power is separated into the collision stopping power and the radiative one. The latter can be neglected at low energy

$$-\frac{1}{\rho} S_{col} = k_L \frac{Z z^2}{A \beta^2} L_e(\beta) \qquad (1.9)$$

The stopping power formula S_{col}/ρ refers to the mass stopping power having units of MeV-cm^2/g. This is extensively used in application. S_{col} or $-(dE/dX)_{col}$ can be called the linear collision stopping power. In radiation protection, S_{col} is equivalent in quantity (although not in concept) to LET or L_∞ (the infinite symbol ∞ will be omitted in the following text), which is usually expressed as keV/μm. Calculated results for alpha particles, ^{244}Am(5.80 MeV), and for electrons (10-100 keV) based on the above equations are given in Appendix A. These radiations will be used in the experimental work to be described.

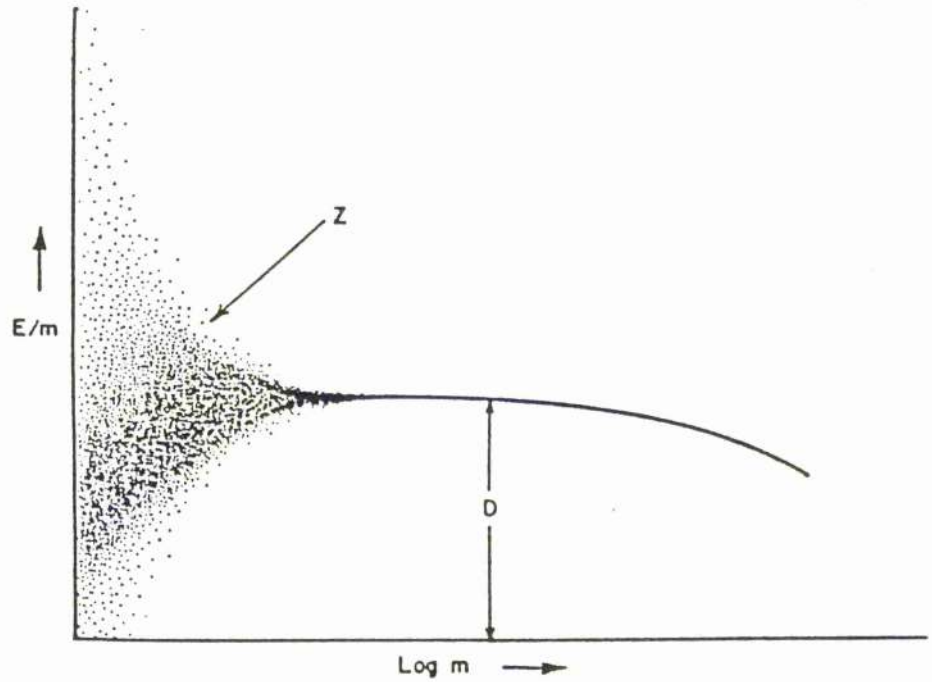

Fig. 1.1 Energy density as a function of the mass for which energy density is determined. The horizontal line covers the region in which the absorbed dose can be established in a single measurement. The shaded portion represents the range where statistical fluctuations are important (After Rossi, 1968).

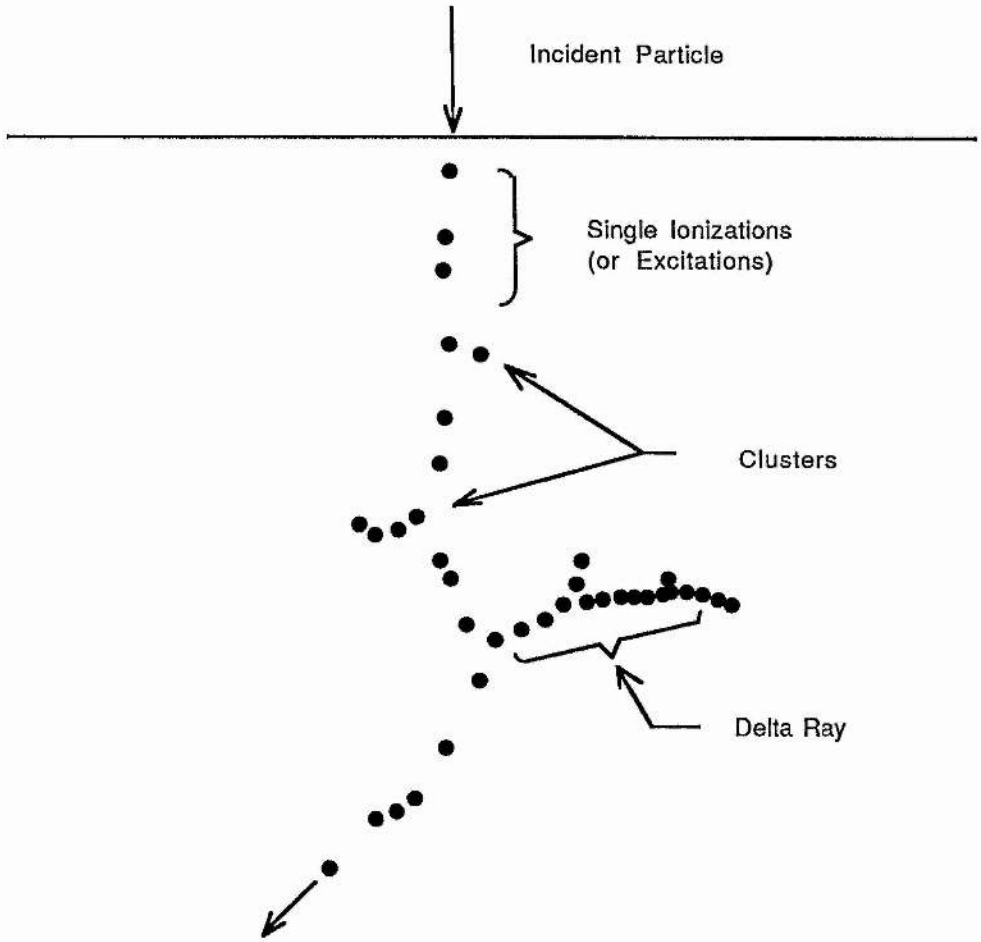

Fig.1.2 Diagrammatic representation of the track of an ionizing particle in matter. Two main types of interaction are (a) a localized excitation or ionization in the track of the ionizing particle, (b) a larger energy transfer producing further ionizing events which may be an ion cluster of a few ion pairs or a separated track known as delta ray. Primary tracks (or the track "core") of heavy ions particle are essentially straight and may be clearly separated from their delta ray tracks. But the situation is complicated for electrons as the delta ray track is comparable at high energies or devious at low energies.

1.3.3 Restricted LET and track average LET

In microdosimetry (ICRU, 1983) and in radiobiological modelling of track-structure theory, attention is focused on the concept of energy deposition, *i.e.*, energy 'imparted locally'. The fraction of the energy lost by an electron in the medium in the vicinity of the electron track, is given approximately by $L_\Delta/S_{col}(T)$, where L_Δ is the restricted collision stopping power or restricted LET in comparison with the unrestricted LET or linear stopping power. L_Δ, is the quotient of dE by dl, where dl is the distance traversed by the particle and dE the mean energy loss due to collisions with energy transfers less than some specified value, Δ, or the cut-off energy. For example, if an interesting site is chosen to be 1 μm, then $\Delta \leq 6$ keV must be set in to the calculation as electron energies of greater than 6 keV can be considered to act as separate tracks since their range is >1 μm. A schematic demonstration of the meaning of L_Δ is given by ICRU (1970, p7). The corresponding formula to calculate L_Δ is found in Appendix A. It is noted that the cut-off energy Δ may be selected by an author for his interest, usually from 100 eV to 10 keV depending on the sensitive site chosen. Eq.(A1.11) is valid for Δ larger than the binding energies of the atomic electrons in the target material, and should be at least comparable with the K-shell binding energy (ICRU, 1984).

Both L and L_Δ discussed above are applicable to monoenergetic particle beams. Often one encounters a continuous

spectrum of particle beams such as induced by x-ray spectra in which case the averaged track LET, $\bar{L}_T$, can be used and is given by

$$\bar{L}_T = \int_{L_{min}}^{L_{max}} t(L)\, L\, dL \qquad (1.10)$$

where t(L) is the fraction of the tracks which have LET from L to L+dL, in the LET spectrum. Similarly, the dose averaged LET, L_D, is also defined with d(L), the fraction of dose, and substitute t(L) in Eq.(1.12) to get L_D. A cut-off value can be chosen, to get $L_{T,\Delta}$, or $L_{D,\Delta}$, to analyse the experimental results (*e.g.* Virsik *et al.*, 1982).

1.3.4 Microdosimetry

One of the basic physical parameters used to describe the biological effects of radiation, is the absorbed dose, D. The absorbed dose is defined as the quotient of $d\bar{\varepsilon}$ by dm, where $d\bar{\varepsilon}$ is the energy imparted by ionizing radiation to matter in a volume of mass dm (ICRU, 1980).

As D and LET are both non-stochastic quantities in dosimetry, for study at the cellular or molecular levels, the physicists were aware of the need to deal with the stochastics of the local energy density, which may diverge dramatically from the average observed D values. Fig 1.1 is a schematic representation of various values of the ratio E/m that will be observed within a limited volume of the irradiated material as m is changed.

Rossi *et al.* first established the concepts of microdosimetry.

In their frame work (Rossi *et al.*, 1955-1972), the stochastic quantity, z, the specific energy (imparted), is defined as the quotient of ε by m, where ε is the energy imparted by ionizing radiation to matter of mass m, *i.e.*

$$z = \varepsilon/m \qquad (1.11)$$

Similarly, the lineal energy, y, is the quotient of ε by $\bar{l}$, where ε is the energy imparted to the matter in a volume by a single energy deposition event and $\bar{l}$ is the mean chord length in that volume:

$$y = \varepsilon/\bar{l} \qquad (1.12)$$

Both z and y have the same units as the absorbed dose D and the linear energy transfer LET, respectively (ICRU, 1983). In the following text, microdosimetric quantities may be mentioned without further discussion.

1.3.5 Linear primary ionization

Both theoretical and experimental studies on parameters such as the linear energy transfer LET, and/or microdosimetric lineal energy y have improved greatly our knowledge of the basic phenomena and principal mechanisms of radiation damage effects. Briefly, as found in the literature, these effects are analysed in the physical terms of energy transfer or energy deposition.

One of the main interests in this research is to use an alternative physical parameter, *i.e.* the linear primary ionization (or IMFP, inverse of mean free path) which does not include the concept of energy deposition, to analyse the experimental results.

Theoretical calculations of linear primary ionization at low electron energies have been developed recently (see Hamm *et al.*, 1975; Ritchie *et al.*, 1978; Tung and Chen, 1982). In this section, the useful formulae for calculating the linear primary ionization (for heavy ions, alternative term radiation yield may be used) are compiled but the detailed theoretical considerations will not be described.

For heavy charged particles having charge number z and total energy E (or sometimess expressed as the relativistic speed β, $\beta=(E^2-E_0^2)^{1/2}/E$, and $E=E_0+E_k$, where E_0 and E_k are the rest energy and the kinetic energy respectively, the LET is calculated according to Eq.(1.8). However, studies on LET have led to the development of the track theory. Many secondary electrons, or δ-rays which stand for those electrons having sufficient energy to produce further ionizations, are produced along the track 'core', cf. Fig.1.2.

The δ-rays may be visualized as the bristles around a test-tube brush (Katz *et al.*, 1971). Modification was made, from studies in photographic emulsions, first to the effective charge number, z, substituted by z^* (Barkas, 1963)

$$z^* = z\,[1-\exp(-125\,\beta / z^{2/3})] \qquad (1.13)$$

and later by the parameter z^{*2}/β^2 which was used to develop a track theory of heavy ions (Mozumder & Magee, 1966; Butts & Katz, 1967; Katz *et al.*, 1972), and the two component model was

established.

The calculation on z^{*2}/β^2 gives a quantity approximately proportional to the ionization numbers per unit length. The primary ionizations of δ-rays of energies T per unit track length, n_δ, can be deduced from the number of collisions between T_{min} and T_{max},

$$\frac{1}{\rho} n_\delta = C \frac{z^{*2}}{\beta^2} \int_{T_{min}}^{T_{max}} \frac{dT}{T^2} \qquad (cm^2/g) \qquad (1.14)$$

where $C=k_L Z/A=2\pi Ne^4/(mc^2)$, k_L is given is Eq.(1.7), the minimum T is the first ionization potential I_1 and the maximum possible is

$$T_{max} = \frac{2\, mc^2 \beta^2}{1 - \beta^2} \qquad (1.15)$$

Then, n_δ or I_s, the total number of δ-rays per unit ion path length (in μm) is given by Mott formula (Watt *et al.*, 1985) as

$$I_s = k \frac{z^{*2}}{\beta^2} \left(\frac{1}{I_1} - \frac{1}{T_{max}} \right) \qquad (1.16)$$

where $k=0.01535\rho Z/A$ keV/μm, when T in keV, ρ in g/cm^3.

For electrons, the formula for the number of ionizations produced per unit track length is fundamentally related to the stopping power equation, but contains two parameters M_i^2 and c_i which are constants for a given material, *viz.*

$$\frac{1}{\rho} I_s = \frac{8\pi a_0^2 R N_A}{mc^2} \frac{M_i^2 z^2}{A\beta^2} \ln\left(\frac{mc^2 \beta^2 c_i}{2}\right) \qquad (1.17)$$

$$= 1.117 \times 10^3 \frac{z^2}{\beta^2} M \ln(2.555 \times 10^5 \beta^2 c_i) \quad (m^2/kg)$$

where $M=M_i^2/A$, and M^2 is called the dipole matrix element squared, it gives the summation of energy transfers to the set of possible ionized states. R=13.7 eV is the Rydberg energy and a_0= 5.291×10^{-11} m is the Bohr radius. For hydrocarbon absorbers experiments suggest M~0.3 and c_i~0.091 eV^{-1}. As z=1, therefore we have for unit density (Chen & Watt, 1986)

$$I_s = \frac{0.3387}{2\beta^2} \ln(2.325 \times 10^4 \beta^2) \quad (ions./\mu m) \qquad (1.18)$$

Eq.(1.17) is valid for E_e>300 eV, it is modified by a factor of 2 in the denominator as this is found to give better normalization to ensure a smooth join to the calculated results for electrons energies below 10 keV in liquid water (Tung & Chen, 1982).

The Monte-Carlo calculation on electron interaction probabilities (IMFP, inverse mean free path) showed that the IMFP for the elastic interaction process increases from E_e<10 keV and becomes dominant at <10 eV. This does not necessarily imply that elastic scattering is more important than inelastic scattering since pronounced forward elastic scattering may be relatively ineffective in causing electron attenuation in matter (Ritchie *et al.*, 1978). It

should be mentioned here that the analyses to be made later, on the specific ionization values are therefore based on the inelastic quantity.

1.3.6 Discussion

Some aspects of radiation research related to the interests of radiation protection and radiotherapy is introduced and a general outline of the background of the theory of charged particle interactions deduced from classical physics to more relevant microdosimetry is given. Current studies require usually the calculation of the physical quality parameters of the ionizing particles, essentially the LET and the absorbed dose, therefore, the relevant formulae and conditions of application are discussed.

Secondary electrons (or δ-rays) produced by the charged particles have sufficient energy to continue interactions and in turn produce more low energy electrons. The spatial structure of the secondary electrons can be calculated and the mean linear primary ionization determined. In the last section, the concept and the calculation of the specific primary ionization for both heavy ions and electrons are introduced. As will be seen in the next chapter, the present study has shown that the primary ionization can be a good parameter for describing dose-effect results satisfactorily, and it may be a parameter which offers a challenge to LET and dose for the expression of biological effectiveness.

CHAPTER II

STUDY ON MECHANISMS OF RADIATION DAMAGE

Since the manifestation of the effects of radiation action to a biological system at various levels is different, the proposed mechanisms of radiation damage are therefore complex and some are controversial. As far as cellular damage is concerned, the existing mathematical models are numerous and are continually under development.

In this chapter, the basic theories of radiation action are described. Among the many models three conventional types of radiation damage models are briefly discussed, and the repair mechanisms, which are recognized to be important biologically are reviewed in Sec.2.1. The attention of the present study is paid mainly to the biological end-point of cell death or cell inactivation, although damage at molecular and subcellular levels are also introduced in Sec.2.2.

Studies on mechanisms of ionizing radiation by x-ray and γ-ray photons, and by heavy ions are then presented in Sec.2.3. Interesting results and important conclusions are researched, based on the analysis of the published data in correlation with the

linear primary ionizations.

2.1 Review of the Theories of Radiation Damage Effects

2.1.1 Time scale of radiation action

The time scale of the complicated chain of events arising from radiation action were divided into some characteristic stages by Platzman (1958, 1962) who also estimated the order of magnitude of the reaction time, in particular in a liquid water system as follows (Dertinger & Jung, 1970):

Physical stage	10^{-13} sec;
Physico-chemical stage	10^{-10} sec;
Chemical stage	10^{-6} sec;
Biological stage	secs to years.

At the physical stage, the energy of an incident particle is transferred to the medium, producing primary excitation and ionization products which are unstable and undergo instantaneous secondary reactions followed in the physico-chemical stage. When the thermo equilibrium state is reached, the chemical stage starts in which case the active products, often free radicals, play some important role in the damage process. The damage effect in the biological stage is considered to be the combined actions of the previous processes. The damage effect can be called 'direct action' or 'indirect action' which will be discussed in the next section.

2.1.2 Direct and indirect radiation action

It is only meaningful to distinguish the direct action and the indirect action at the molecular level. If the radiation absorption occurs directly in the molecule damaged, the action is called direct, while, the indirect action occurs when the absorption of the radiation energy and the reaction of such absorption occurs at different molecules.

Quantitative analysis of the two types of action on a molecule at risk, *e.g.*, a DNA macromolecule, in relation to causing cellular death is at present not very clear. From experiments on oxygen effect, *i.e.*, irradiate a sample under oxygen saturation, an agreed reaction with a free radical $R\cdot$ is $R\cdot+O_2 \rightarrow RO\cdot_2$, which is believed produce nonrestorable damage, and so the (indirect) action efficiency is enhanced. The ratio of hypoxic to aerated doses to achieve the same biological effect in the same system is called the oxygen enhancement ratio (OER). The OER is observed higher at lower LET (cf. Sec.2.3.2). Therefore, it is considered by some authors (*e.g.*, Hall, 1978) that sparse ionization from x-rays of low-LET causes mainly indirect action in comparison with dense ionization from neutrons or alpha particles of high-LET which acts directly. But this consideration is controversial (*e.g.* Goodhead, 1987). The two radiation actions can directly or, through free radicals, indirectly produce damage within a cell, in synthetic enzymes, or in bases and hydrogen bonds between the two strands of the DNA double helix. When DNA damage occurs, single strand breaks (SSBs) or double strand breaks (DSBs) are produced. For

this in turn the cell is rendered unable to differentiate so an inactivation will finally occur. More details will be given later.

An ideal study on radiobiology would enable prediction of all subsequent reactions between an initial physical interaction of an incident particle with the medium, to the final manifestation of biological effect. In the present stage of knowledge, the study on radiation effects is based on physical calculations such as LET, and primary ionization and then related to short term biological effects such as cell inactivation or chromosome aberrations. However, the consequence of the relation between two conjunctive stages is not clear, the study of intermediate processes is still undergoing development.

2.1.3 From hit theory to damage models

The theories of radiation biophysics have had only a short history. Due to the development of physics, chemistry and biology, from about 1920s, mathematical and statistical methods were introduced into the field, to describe quantitatively the phenomenon of radiation action on the medium transferred. The hit-target theory was first introduced by Dessauer (1922) and Crowther (1926) and developed mainly by Lea (1946). Lea in 1946, and Timofeeff-Ressovsky and Zimmer in 1947, published their books in which detailed studies of radiation action on living organisms were systematically surveyed. Through the analysis by statistical methods, of the dose-response curves obtained from experiments, the 'hit-target' theory was first formed.

The 'hit-target' theory is based on the following assumptions (Dertinger & Jung, 1970):

i) ionizing radiation deposits energy in discrete packages;

ii) events of radiation interaction are independent of each other and have a Poisson distribution; and

iii) a reaction in a specified 'target' with a volume V occurs after it has been 'hit' n times.

As the product h=VxD represents the average 'hit' numbers in the 'target volume' which has received a dose D, the probability of exactly n 'hits' is given by the Poisson distribution

$$P(n) = h^n e^{-h}/n! \qquad (2.1)$$

In the dose-response curve, the end-point is expressed as the survival fraction N/N_0, where N is the surviving number and N_0 the number before irradiation. Hence, any entity receiving n-1 or less 'hits' will survive. The final survival fraction is the sum of 0, 1, 2, ..., n-1 'hits' *viz.*

$$N/N_0 = e^{-h} \sum_{k=0}^{n-1} \frac{h^k}{k!} \qquad (2.2)$$

In larger entities, *e.g.*, in cellular systems, which is supposed to contain m targets ($m \geq 1$), the surviving fraction according to the probability theory for single-hit multi-target effect is

$$N/N_0 = 1 - (1 - e^{-VD})^m \qquad (2.3)$$

V is also called radiosensitivity in unit of kg/J, or often appeared as

$$S = 1 - (1 - e^{-D / D_0})^m \qquad (2.4)$$

where S stands for the survival fraction N/N_0, D_0 is the dose required to reduce the number of clonogenic cells to 37% survival of their former value. If m=1, by which D_{37} is used

$$S = e^{-D / D_{37}} \qquad (2.5)$$

D_0 or D_{37} (m=1) is the reciprocal of the slope on S versus D plotting, and is determined from the straight portion of the dose response curve or from the non-linear fitting.

It is noted that, in track segment experiments where the thickness of target material irradiated is small compared with the range of the charged particle tracks, the effect cross-section σ_e can be used such that the 'hit' number h is expressed as $h= \sigma_e \phi$, where σ_e (cm^2) is also the probability of the effect being induced by an incident particle. $\phi(cm^{-2})$ is the total fluence of incident particles. This is found suitable to apply to the situation of single-hit single-target to compare the effect cross-sections explicitly by the same particles.

In the literature, various other modelling methods as well as the 'hit-target' model have been applied in an attempt to interpret the cellular radiation results of dose-response curves. Many established mammalian cell-lines characterizing a shoulder at low doses in the survival curves by low LET irradiation but mostly a pure exponential response by high LET irradiation. This has led to

a controversial outcome in the past twenty years.

As the hit-target model does not give a finite initial slope and does not account for the physical quantities of the particle, one of the two-component models based on the track theory developed by Katz *et al.* (1971, 1972) can give the initial slope as well as the final one at high dose, *viz.* the total survival fraction is the product of two components, *i.e.* F_i, the fraction of cells surviving ion kill, and F_γ, the fraction of cells surviving gamma kill which is similar to the situation of single-hit multi-target, then the model is given by

$$S = F_i \, F_\gamma$$

$$= e^{-\sigma D / L} \{1 - [1 - e^{-(1 - P_i) D / D_\gamma}]^m\} \qquad (2.6a)$$

where P_i is the probability of ion kill. It is noticed that when the contribution of ion kill is dominant or $P_i=1$, the model reduces into the form of single-hit single-target model. However, in the literature, this model is often quoted a simple form as

$$S = e^{-D / D_1} [1 - (1 - e^{-D / D_2})^m] \qquad (2.6b)$$

Once again a shortcoming of the two-component model is that, it does not explain the continuous curvature of the survival curve sometimes observed at high doses.

The theory of microdosimetry was developed in 1955 after Rossi and co-workers developed experimental methods to analyse the microdosimetric distribution of energy deposition in small volumes of irradiated matter. This has influenced the study of

radiation dosimetry to a great extent since then. Extensive work has been done in measuring the microdosimetric stochastic quantities: *e.g.*, z and y, and the associated spectral distributions. Thereafter, the dual-action theory was introduced, and the 'site model' or, later after more strict treatment, the 'distance model' was established (Kellerer and Rossi, 1972, 1978). Basically the format of the model is:

$$S = e^{-y(D)} = e^{-\alpha D - \beta D^2} \tag{2.7}$$

where α and β are the respective constants simply related to single-event damage or intra-track action proportional to D and to two-event damage or inter-track action proportional to D^2. In the 'distance model', however, y(D), the number of expected lesions, is said that it can be expressed by an integral over two functions s(x) and t(x). The proximity function s(x) characterizes the geometry of the sensitive 'matrix' in the cell nucleus; t(x) the spatial distribution of energy transfers. Then, they deduced that

$$y(D) = \frac{c^2 \rho V}{2} D \left[\int_0^\infty \frac{g(x)\ t(x)\ s(x)}{4 \pi x^2} dx + \rho\ D \int_0^\infty g(x)\ s(x)\ dx \right]$$

$$= k\ (\xi D + D^2) \tag{2.8}$$

where c is a constant and the coefficient k is given by

$$k = \frac{c^2 \rho^2 V}{2} \int_0^\infty s(x)\ g(x)\ dx \tag{2.9}$$

and

$$\xi = \int_0^\infty \frac{s(x)\ g(x)\ t(x)}{4\pi\rho x^2}\,dx \Big/ \int_0^\infty s(x)\ g(x)\ dx \qquad (2.10)$$

In the early site model, the combination probability g(x) is taken to be constant, ξ is the average of specific energy z, $\bar{z}_D$, as s(x)dx is equal to the domain of volume of interest, $\int s(x)dx=V$,

$$\bar{z}_D = \int_0^\infty z^2 f_1(z)\,dz \Big/ \int_0^\infty z\, f_1(z)\,dz = \frac{1}{m}\int_0^\infty \frac{s(x)\ t(x)}{4\pi x^2}\,dx \qquad (2.11)$$

where $f_1(z)$ is the single event distribution of z. This relation was applicable to both x-rays and high RBE neutron irradiations; and they also predicted that at lower doses the intra-track component is dominant. At higher doses, the inter-track component becomes increasingly important (Kellerer & Rossi, 1978). In Eq.(2.9), k is radiation quality independent since s(x) and g(x) are so. However, Watt *et al.* (1984) found that from studying data of monoenergetic ions (Blakely *et al.*, 1979), k is dependent on LET, and therefore an alternative version of the dual-action model was suggested.

Explicit comparison among the main three most popular models has led us to conclude that: firstly, existing models can fit the experimental data well with little differences of the statistical error (*e.g.*, Millar *et al.*, 1978); secondly, one model differs from and conflicts with the other according to the authors' premises, each model has its advantages or disadvantages concerning the physical parameters adopted; and finally, on the whole, none of the

existing models can adequately explain the radiation effect in the area of interest as for example, in radiological protection (Watt, 1975; Thomas & Watt, 1984; Watt *et al.*, 1984).

Basically, difficulties with modelling models which remain unsolved are: how to cope with the physical factors (despite the many complicated biological and chemical factors). These are the time factor (dose-rate), and the quality factor (LET). It is therefore questioned whether the cell will be able to recover or repair the damage introduced by the incident ionizing radiation particles before an event of death occurs or whether the physical parameters, (*e.g.*, the quantity absorbed dose, D) are inappropriate (Watt *et al.*, 1985).

Very recently, Goodhead (Goodhead, 1987) reviewed a few major features and differences of models proposed for mammalian cells. He divided models into two main groups, they are 'phenomenological' and 'mechanistic'. And some may overlap. An explicit comparison of the models reviewed by Goodhead has been summarized in Table 2.1. He raised and answered some critical questions (Table 2.2) to assist future development of the models as well as of the radiation damage theories. However, he treated only these models which are based on energy deposition.

As can be seen from the above discussions, the models are numerous; the theories are comprehensive; the mechanisms are various. Nevertheless, the latest favoured conclusions seem to be that repair phenomena are important. Lesions produced by sublesions, *e.g.*, DNA strand breaks as claimed by many models (cf.

Table 2.1 Explicit comparison of models (after Goodhead, 1987)

Authors	Sublesion				Lesion				Quality parameters	Comments model's type
	Nature specified		Due to	Repair	Nature specified		Due to	Repair		
Kellerer & Rossi, 1972	no		sgl. ion.	yes	no	sublesion		yes	dose-mean specific energy z	replaced
Kellerer & Rossi, 1978	DNA ssb?		sgl. ion.	yes	no	2-sublesions		yes	proximity function t(x)	sgl. ion. strictly
Chadwick & Leenhouts, 1981	DNA ssb		·OH	yes	DNA dsb	2-ssb		yes	LET, ß	predicts non-linear dose response for DNA dsb's
Curtis, 1986	(DNA dsb?)		cluster		no	clusters?		no	z^2/β^2, LET	
Katz et al., 1971	no		ion, -kill	?	no	m-sublsn		no	z^2/β^2	phenomenological
Gunther & Schulz, 1983	DNA(dsb?)		cluster	yes	DNA-sublesion				LET, z	phenom/mechan
Bond & Varma, 1983	not considered				no	energy		?	z, y	phenom, low doses
Goodhead, 1982	not required				DNA	clusters		yes	f(E)	mechanic
Pohlit & Heyder, 1981	not required				dose			constant		

* sgl. ion. : single ionizaion

Table 2.2 Questions and answers to the reviewed models by Goodhead (after Goodhead, 1987)

Questions	Answers
Critical initial damage (sublesion or lesion) by?	Clusters other than by single ionization
Importance of water radical ('indirect effect')?	Direct effects in DNA predominate for all ion. rad.
How is DNA dsb in cells depend on dose?	Usually linearly (fairly low doses?)
Initial slope of acute low-LET radiation zero?	Evidence against this
Initial slopes vary with dose-rate?	Yes (contrary to many models)
Primary critical damage same for, qualitatively, high- and low-LET?	Most models assume it is
Quantitative differences of high- and low-LET?	All models assume spatial (track structure) differences
Same basic mechanisms dominant at low(1-track) & high(m-track) doses?	Most unlikely
Any substantial interaction of sublesions?	Little direct evidence
Any repair processes non-linear with dose?	Depend on particular biological system
In what systems do 'reverse' dose-rate effects occur?	None of the models is adequate on this (on transformation and carcinogenesis)
How far can developed and tested models be applied to practical (carcinogenesis and genetics)?	This link will remain tenuous

Sec.2.2), seem to be the predominant in causing cell death according to most of the theories. Therefore, in the next section, the proposed repair mechanisms are discussed in combination with another repair model in an effort to extract the parameters determining the repair processes.

2.1.4 Damage repair in cellular systems

As already mentioned above, the survival curve or dose-effect of a high LET particle is usually pure exponential whereas for low LET it is always a shouldered curve as far as the mammalian cellular system is concerned. When studies on dose-rate are involved, it is difficult to interpret a relationship of the difference between them due to the fact that there is no universal model able to describe the mechanisms of radiation damage satisfactorily. In other words, one can say that a specified model can be used only within some limited conditions. Therefore, further study to interpret the results via a different approach is necessary even if establishing a universal model should prove to be impossible.

The phenomenon of the shouldered survival curves on low LET has received a great deal of study in both physical modelling and biological experiments. The popular conclusion from these studies is that there are some different repair processes involved in the damage. The two defined processes (ICRU, 1979; Elkind, 1984) are potentially lethal damage (PLD) and sublethal damage (SLD). They can be described as follows (Hall, 1978). PLD is that component of radiation damage which can be influenced by

post-irradiation environmental conditions. SLD is the damage which under normal circumstances can be repaired within a matter of hours unless additional sublethal damage is added (*e.g.*, from a second dose of radiation) with which it can interact to form lethal damage, which is irreversible and irrepairable leading to cell death by definition.

Both PLD and SLD are found repaired in certain conditions. The expression of PLD can be modified by some post irradiation experiments to study further the influence of biological factors. The sublethal damage recovery was found first by Jacobson, in 1957, in algae and then Elkind *et al.* in 1959, in mammalian cells as well as being demonstrated in mouse tumour in situ irradiation which showed a radiotherapeutic significance (Little *et al.*, 1973). The SLD repair can be explained by the split-dose experiments. A total dose was delivered in two fractions at time intervals from zero to several hours. During the intervals the cells were either maintained at room temperature (24 ^{0}C incubation, or starving condition, see Metting *et al.*, 1985) to reduce the rate at which cells moving through the cell cycle, or maintained at normal condition (37 ^{0}C incubation, asynchronous cells in growth medium). The difference between the two incubation conditions showed that, in the former case, the survival fractions increased and then remained constant after two-hour intervals, while in the latter case, the survivals increased after two-hour intervals but further fluctuated depending on the cell cycle (Fig.2.1). But as seen in Fig.2.1, the PLD repair was not observed in the split-dose in

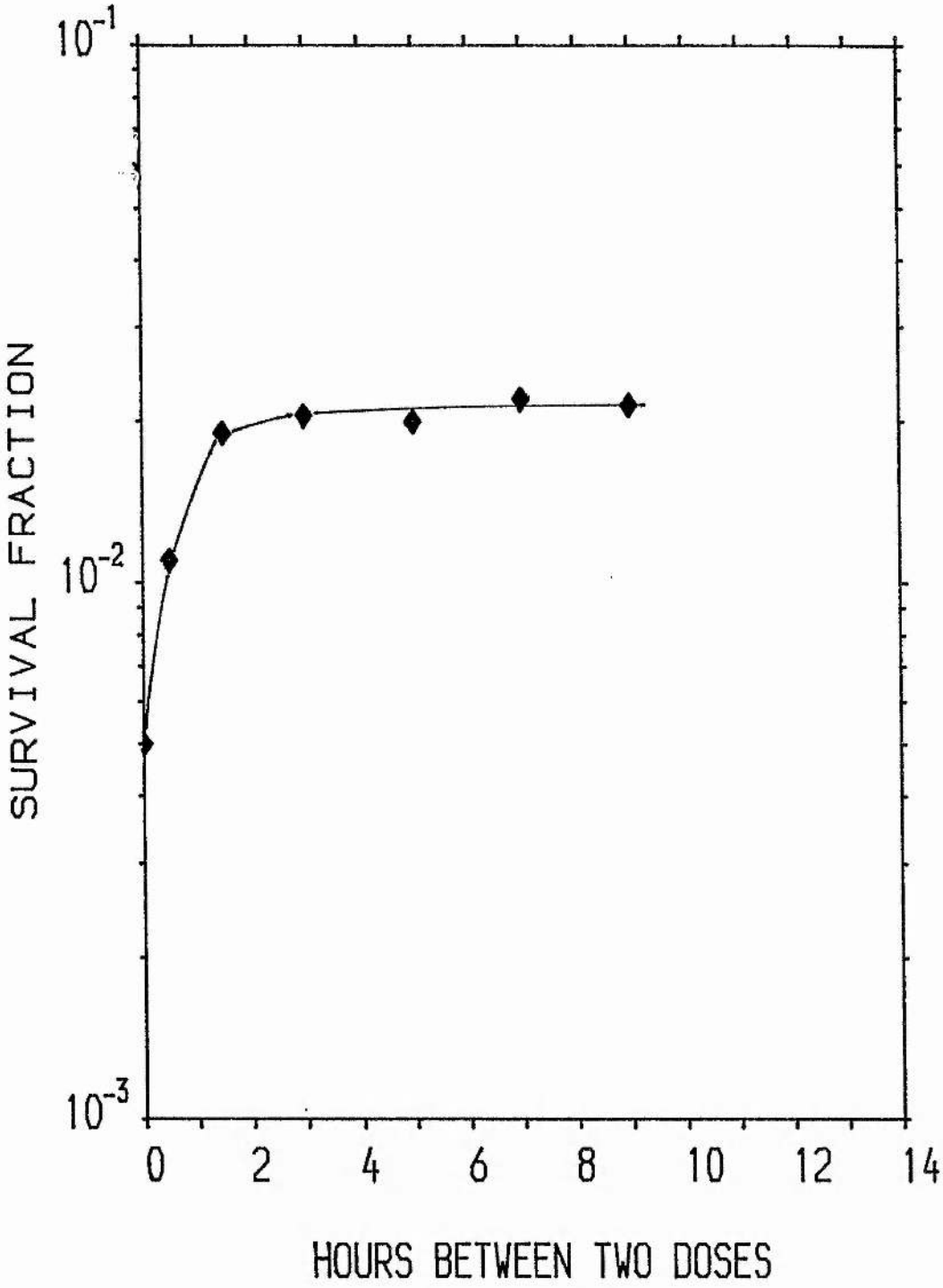

Fig. 2.1(a) Split-dose experiment of Chinese hamster cells, V79-379A, exposed to 2.5 MV X-rays of 7.63+7.95 Gy, incubated in 24 °C between the two doses (Elkind et al, 1965).

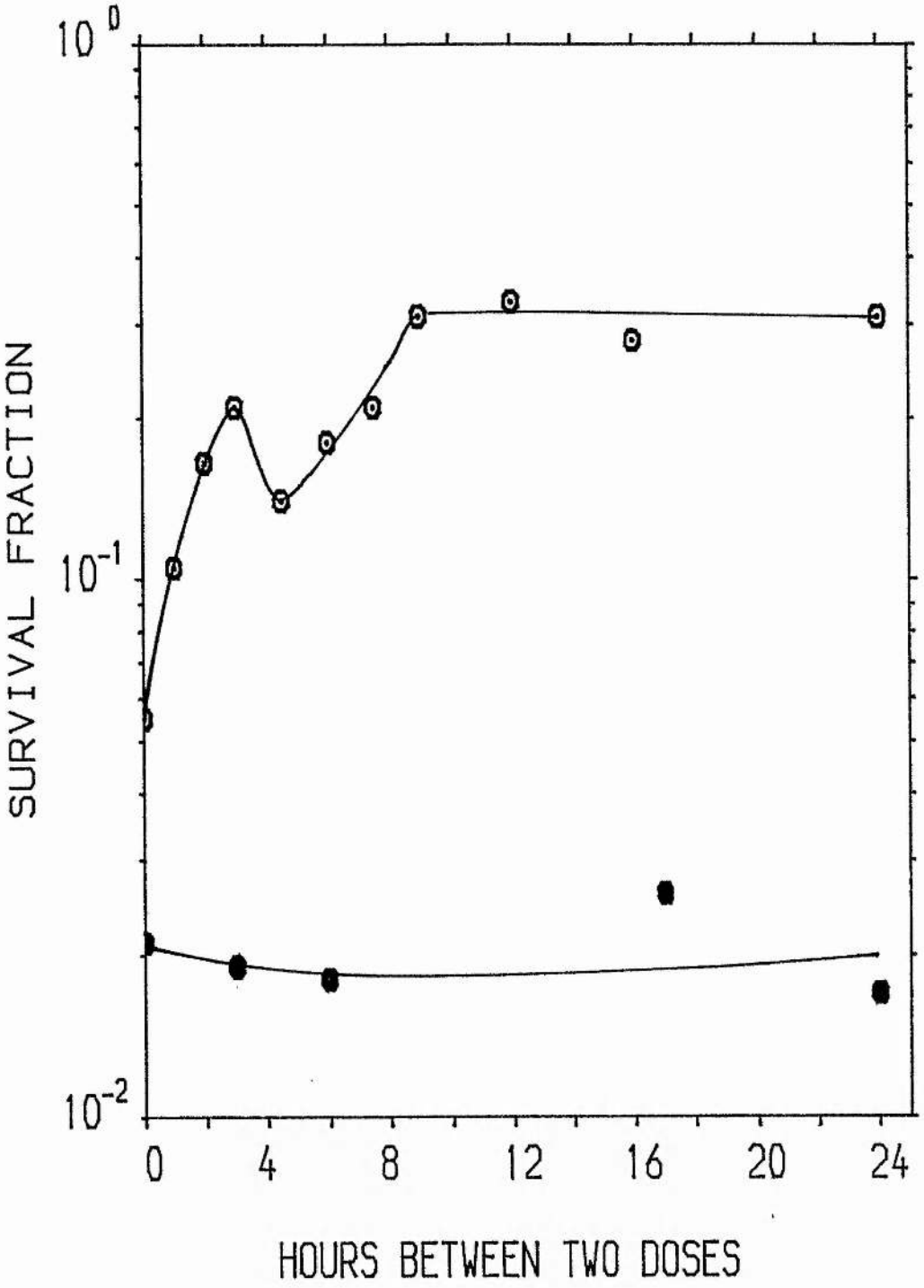

Fig. 2.1 (b) Split-dose experiment of C3H-10T1/2 mouse embryo cells, up: exposed to 50 kV X-rays of 3.50 +3.50 Gy; below: JANUS neutrons of 1.89 + 1.89 Gy. Incubation in 37°C between the two doses (Elkind et al, 1984).

neutron irradiation (Elkind *et al.*, 1984).

The implications from these experiments are that, there is a repair process taking approximately two hours, for Chinese hamster cells, for example; the incubation condition or the kinetic distribution of the cells in the cycle, during long-term irradiation, can cover this repair process; in the case of neutron irradiation, high LET particles, this repair phenomenon is not observed, see Fig.2.1(b).

The proposal of sublethal damage repair also led to many dose-rate effect studies. For x- or γ-rays, the principal effect of dose-rate is observed between 1 to 10^{-3} Gy/min. At higher dose-rates the effect is less certain for mammalian cells, and at lower dose-rates cell proliferation continues during the irradiation, and the ultimate outcome is a complex function of radiosensitivity, dose and other factors (Hall, 1972).

An example of a study on repair in dose-rate effect experiments was reported by Braby and Roesch (1978). They reviewed many models in the literature from the point of view of repair in relation to dose-rate $\dot{D}$, and one can extract the following three common parameters, whatever the expression of the models:

k_1- rate of cell damage;

k_2- rate of damaged cell killing; and

t_r- mean recovery or repair time of damaged cells.

However, when they fitted their dose-rate test data, on *C. reinhardi*, an ideal cell which does not change in radiosensitivity

during irradiation, they showed that all the models produced a family of curves except the so-called accumulation model which gave a single curve without dose-rate dependence. The accumulation model is based on the hit theory for low-LET radiation (Roesch, 1972), in analogy to the dual-action model.

In the more recent study on dose-rate of CHO cells at plateau phase (Metting *et al.* , 1985), the accumulation model developed was expressed as follows,

$$- \ln S/D^2 - C/D = A/t^2 (e^{-t} - 1 + t) \qquad (2.12)$$

where C is a parameter related to the probability of producing lethal damage by a single event and A is related to the probability of pairs of sublethal events interacting to become lethal, $t=t_1/t_r$, t_1 is the irradiation time.

Plotting, at different dose-rate, - lnS/D vs. D, for $D \ll \dot{D}t_r$, or $t_1 \ll t_r$, $-\ln S/D = C + AD/2$, C and A were determined for CHO (Chinese hamster ovary) cells by x-rays as C=0.225, A=0.092. The single-event damage was separated from the two-event damage, by plotting $-\ln S/D^2$ vs. t_1, and finally they obtained the mean recovery or repair time t_r, 70±30 mins, see Table 2.3.

They concluded that through such a study on the dose-rate effects, many models proved unsuitable and tested may be rejected in future. However, this model is very susceptible to the systematic error in the data which is always large in biological experiments. Nevertheless, their extensive test with x-rays has shown that, i) at very low dose-rate, CHO cell populations exhibited a high

Table 2.3 Mean repair time, t_r, obtained by the dose-rate effect study, for different cell lines (after Metting *et al.*, 1985)

Cell-line	Dose-rate, Gy/min	t_r, min	Reference
CHO	0.0031-1.0	70 ± 30	Metting *et al.*, 1985
V-79	0.002-2.0	240 ± 60	Szechter & Schwarz, 1977
HeLa	0.0092-1.43	45 ± 50	Mitchell *et al.*, 1979

incidence of repair; implying that below a certain value the damage is dose or single-event dependent; ii) or at very low dose-rate, sublesions can be repaired and; iii) the order of repair time can be predicted if a proper model is used. Further discussion on this will be presented in Sec.2.4.

2.2 Introduction to Damage in Biological Entities

2.2.1 Entities smaller than cells

In the early studies, radiation effect on enzymes was considered (Okada *et al.* , 1970). An enzyme can play an important role in a biochemical reaction, *e.g.*, in DNA synthesis. However, more than twenty to several thousands grays are needed to cause an appreciable inactivation of an enzyme. Depending on many factors, the radiosensitivity of a specific enzyme, in aqueous solution, is proportional to its concentration C (in g/ml) and the reciprocal of its molecular weight. The following is an example of data for ^{60}Co irradiations abstracted from more extensive tables (Chen, 1984).

Enzymes	C,mg/ml	D,Gy/min	D_{37}	Reference
RNase	0.06	15.0	130	Adams *et al.*, 1971
Trypsin	0.12	5.7	76	Lynn, 1971
DNase	0.50	50.0	400	Gehrmann, 1957
RNase	20.00	900.0	4408	Hunt *et al.*, 1962

Unfortunately, in the absence of knowledge of the

concentration of a specific enzyme in the cell of interest, it is not possible to discuss the relationship between the enzyme inactivation and cell death. But it is known that only about 1-2 Gy will kill 63% of a population of mammalian cells which is more than ten times sensitive to radiation than is the enzyme. For this reason, discussion on the analysis of cell inactivation in the following text will not involve the role of damage by enzymes nor of RNA.

2.2.2 DNA strand breaks

A normal macromolecule deoxyribonucleic acid, DNA, will carry the genetic information correctly in the integrity of its complementary double helix. Since DNA replication is essential for cell division, damage to its single strand or double strands have long been believed to be the main candidates causing cell inactivation (Okada, 1970). Studies in the primary effects in matter, and analysing the dose response relationship of DNA strand breaks with that of cell survival fraction, had led to the linear-quadratic form of the dual-action model by Sinclair in 1966 and by Chadwick and Leenhouts in 1973. In order to understand the cell damage mechanisms, it is necessary to know as a prelude, the cause of radiation damage in DNA molecules (refer to Fig.2.2).

i) **DNA base damage**: Apart from the cross linkages, which is a radiation-induced binding of nucleotides with proteins in the cell (mainly the binding of bases, ribose with amino acids, *e.g.*, Shen & Fu, 1983), there are three types of recognized damage to DNA,

they are base damage, single strand break SSB, and double strand break DSB. According to Monte-Carlo calculation, about 80% of $OH^{\cdot}$, the main damaging radical, attack bases 20% of them attack ribose (Chatterijee & Magee, 1985). Free radicals can alter a base sequence and give rise to an altered phenotype or mutation of the cell. As reviewed by Chadwick and Leenhouts (1981), although radiation-induced base damage, for example, the thymine base damage in Chinese hamster ovary cells, predominates over SSB induction, no direct evidence is available, showing that the thymine base damage forms a biologically important lesion. Experiments also indicated that the unrepaired base damage in prokaryotes was an important determinant of survival, the higher cells seemed to be able to tolerate or repair a large amount of this damage, although there is an increasing evidence that similar damage may be important (Coggle, 1983).

ii) **DNA single strand breaks:** DNA single strand breaks can be detected by the alkaline sucrose gradient velocity sedimentation technique, which is a time consuming method, or the improved alternative DNA unwinding hydroxylapatite (HAP) chromatography method described by Ahnstron and associates in 1973. The alkaline elution method developed by Kohn in 1973 permits the detection of extremely low level of DNA damage, but both require large amounts of cellular DNA compared with the latest alkaline agarose gel electrophoresis method, which requires about one tenth of the cellular DNA (non-radioactive) of the foregoing two methods (Freeman *et al.*, 1986). The separation of SSB DNA by the

agarose gel electrophoresis method has been improved by using unidirectional pulse field instead of static fields (Sutherland *et al.*, 1987a). More recently a method for direct and rapid quantitation of fluorescence from electrophoresis gels by using a CCD (charge coupled device) television camera has been reported (Sutherland *et al.*, 1987b).

It is estimated that SSBs can be repaired very rapidly in about 10-40 mins in mammalian cells, depending on the cell type (or enzyme controlling) and the temperature since it was found that at 0 ^{0}C no SSB repair could happen (Koch & Painter, 1975). The repaired SSBs are considered unimportant to cell death. Unrepaired SSBs may form DSBs as it has been demonstrated that there were exactly two unrepaired SSBs per DSB, which, are believed to lead to important biological effect (Chadwick & Leenhouts, 1981).

iii) **DNA double strand breaks**: The dose relationship of DNA double strand breaks has been found to be either linear in the dry state or linear-quadratic in solution. The situation of DSBs of DNA within mammalian cells is not clear. Some authors found linear and some linear-quadratic (Dugle *et al.*, 1976; Chadwick & Leenhouts, 1981; Goodhead, 1987) response curves. This may be because at low dose the detection of DSBs is more difficult at low dose by the neutral sucrose gradient velocity sedimentation method because of its poor sensitivity. Held *et al.* (1986) recently have used both hydroxylapatite chromatography and the elution technique to obtain linear dose response for V79 cells.

Many measurements carried out in different types of cells have indicated that the DSB can be rejoined or 'repaired'. However, this 'repair' may be mechanically rejoined in a wrong genetic sequence, so-called 'error-prone' which would lead to mutation. The quantitative relationship between DSBs and cell death is thus difficult to evaluate.

2.2.3 Discussion

Before discussing radiation damage to mammalian cells it is necessary to establish knowledge of the damage to the radiosensitive sites which are considered by the majority to be the DNA double strand helix within the cell nucleus. Although there has been a lot of study on enzyme inactivation. its contribution is thought to be less important.

In radiation chemistry, the G value is defined as the yield of a product, *e.g.*, the number of reactive free radicals, per 100 eV energy absorbed. The hydroxyl radical OH· (G=6.0), whose existence was demonstrated by the OH radical scavenger experiments, is believed to be the main agent causing the hydrogen bonds, the connections between the two DNA strands, to break. A SSB involves about 15 hydrogen bonds break estimated from the G values. In such cases about 3-4 pairs of nucleotides are no more combined by H-bonds. Therefore, if the distance between two SSBs is less than three nucleotides, a DSB would happen (see Dertinger & Jung, 1970). It is estimated that, 1-2 Gy dose would cause about 1000 SSBs or 50 DSBs, for example, Koch and Painter

(1975) reported about 10% SSBs were unrepaired.

Study on chromosome aberrations has significant meaning in relation to DNA strand breaks and cell mutation or inactivation. Experiments provide very strong support that an eukaryotic chromosome consists of one DNA double helix backbone extending from one end of the chromosome through the centromere to the other as a continuous molecule (Kavenoff & Zimm, 1973). For cellular studies, assuming the probability (or effect cross-section) of cell inactivation to be unity, at about 100 keV/μm, it is estimated that for cell transformation the probability is about 10^{-2}, for cell mutation is about 10^{-4}-10^{-5} (cf. Goodhead, 1984). However, there has been little attempt to relate all the information together for modelling purposes (cf. Sec. 2.1.3). Therefore, the rest of the discussion of radiation damage to cells will be on cell inactivation, in a broad sense, in relation to DNA double strand breaks.

The present section is not intended to involve many details of the damage at different subcellular levels. Nevertheless, since DSBs in the DNA have proved to be the most significant events, the possible damage mechanisms of DSBs leading to a final cell death are introduced. This discussion will be beneficial in the following analysis of the radiation damage to the whole cell which is based on this.

2.3 Radiation Damage to Mammalian Cells

2.3.1 Damage by x-ray and γ-ray photons

Irradiation by x-ray and γ-ray photons offers a conventional

tool for both radiotherapy and radiology purposes. A large number of publications of dose-response studies on biological systems can be found in the literature. Due to the difficulty of calculating the quality parameter of the continuous x-ray spectrum precisely, it is noticed that little has been done to analyse systematically the enormous amount of experimental data published.

In order to understand the mechanism of the interaction of different radiation particles with the medium, published survival data for the induction of reproductive death in mammalian cells irradiated by photons from x- and γ-ray sources have been compiled and compared with the data of heavy ions.

It was found that the majority of the published data of photon irradiations were fitted by the hit-target model Eq.(2.4), some by the two component model Eq.(2.6) and the dual action model Eq.(2.7) equally well regardless of the inherent premises involved in each model.

Data of the most commonly studied three types of mammalian cells irradiated *in vitro* are presented: human carcinoma cells (HeLa); Chinese hamster ovary cells (CHO) and Chinese hamster lung cells (V79). To justify the equivalent dose effect, among different cells, or to reduce influence of many factors, the data were chosen from air or oxygen irradiation, and no chemical sensitizers were present, and the radiation dose-rate has been limited to within two orders of magnitude in the collected data, *i.e.*, 0.14-1.6 Gy/min for HeLa cells, 0.14-9 Gy/min for CHO cells, and 1.5-50 Gy/min for V79 cells.

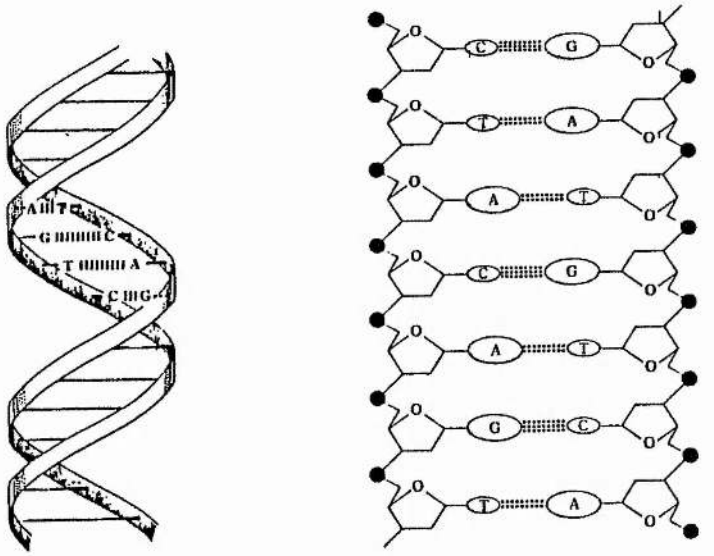

Fig. 2.2 (a) Schematic of Watson-Crick model of the DNA double helix molecule

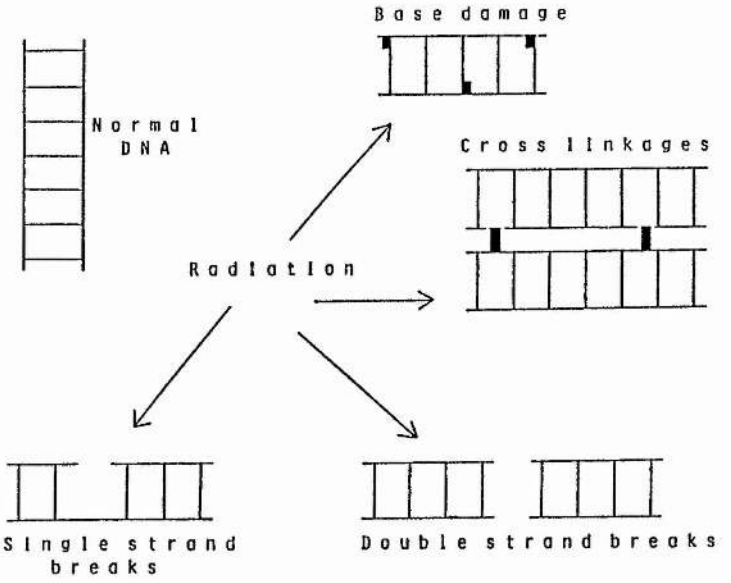

Fig. 2.2 (b) Possible types of radiation damage in DNA (after Coggle, 1983)

Two physical parameters, $\bar{L}_T$ and $\bar{I}_S$ were computed according to Eqs.(1.10) and (1.18). The reciprocal of $\bar{I}_S$ is the mean free path between ionizations. The calculation of $\bar{L}_T$ requires a series of sub-calculations; it is based on the assumption that all irradiation conditions satisfying the secondary charged particle transient equilibrium. Details are given in the publication (Chen & Watt, 1986).

The survival data were processed to give intrinsic efficiencies, σ_R, *i.e.* the ratio of the effect cross-section, σ_e, to the geometrical cross-section, σ_g, of the cell nucleus. For x-rays and γ-rays, σ_e in cm^2 was calculated from

$$\sigma_e = 1.6 \times 10^{-9} \bar{L}_T / D_0 \qquad (2.13)$$

where D_0 in gray was obtained from either the original authors or by determining the average slope over the approximately linear portion of the published survival curves. By plotting the intrinsic efficiency σ_R versus $\bar{L}_T$ and versus $\bar{I}_S$ on log-log scale respectively, we have, determined by the least squares method in Fig.2.3

$$\sigma_R = (1.91^{+0.53}_{-0.41}) \times 10^{-3} \bar{L}_T^{\,1.12 \pm 0.08}, \qquad (2.14)$$

and

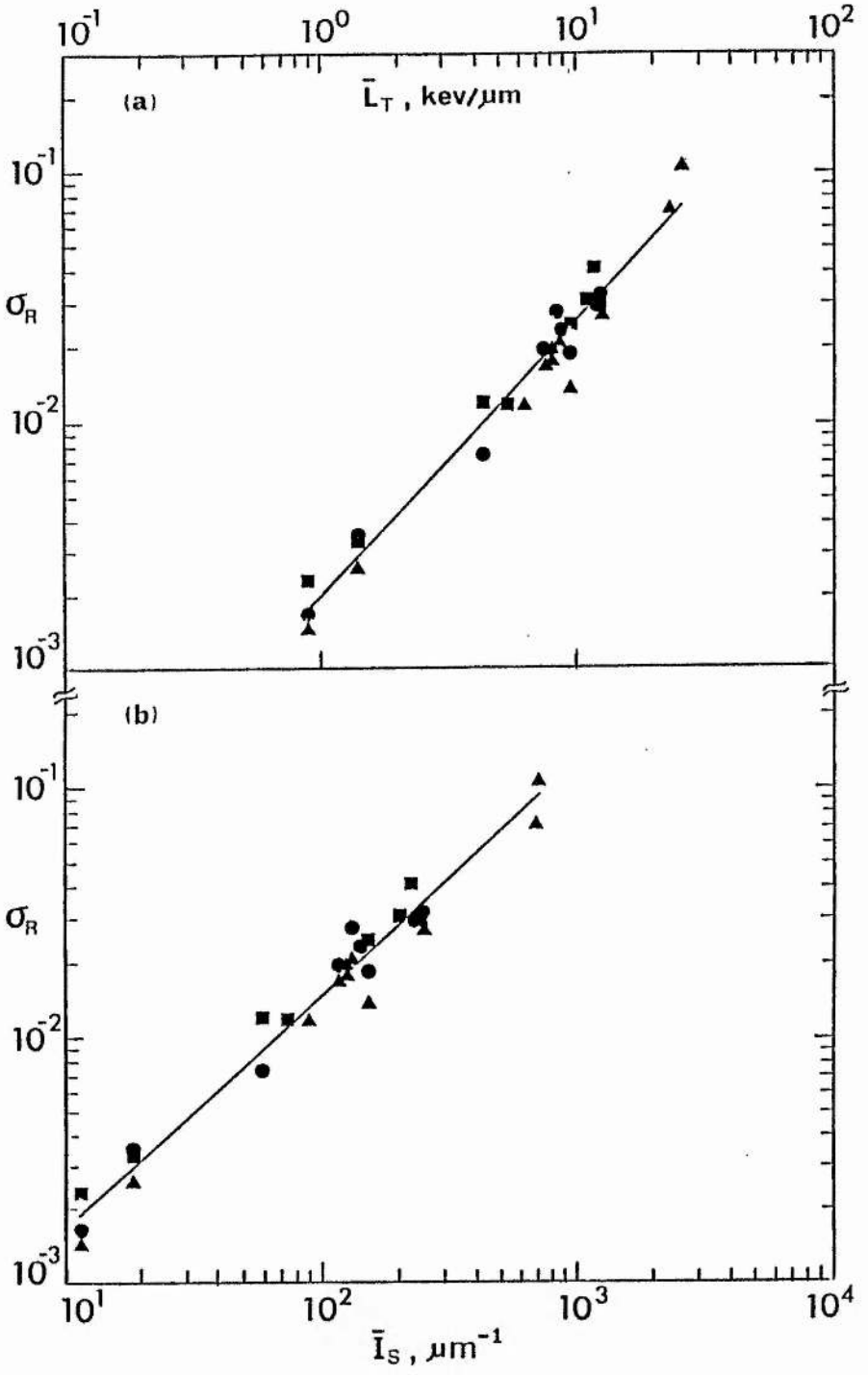

Fig. 2.3 Intrinsic efficiency, for damage by secondary electrons produced in x- and γ- irradiation of CHO (●), HeLa (■) and V-79 cells (▲), plotted as a function (a) of the track average LET, L_T, and (b) the mean specific primary ionization, I_S (After Chen, C.-Z. and Watt, D.E. (1986), Biophysical Mechanism of Radiation Damage to Mammalian Cells by x- and γ-rays. Int. J. Radiat. Biol., **49**(1), 131-142).

$$\sigma_R = (1.82^{+0.55}_{-0.42}) \times 10^{-4}\ \bar{I}_S^{\,0.95\pm 0.03} \quad . \qquad (2.15)$$

It is seen that, in Fig. 2.3 and from Eqs.(2.14) and (2.15), the intrinsic efficiency for damage by x- and γ-rays is linearly related to both $\bar{L}_T$ and to $\bar{I}_S$ on log-log plotting. Data of the soft x-rays from 1.5 keV aluminium characteristic K x-rays and from 0.3 keV carbon K x-rays are seen to be consistent with the linearity. And carbon K x-rays is at the maximum efficiency since the secondary electron of carbon K x-rays have primary ionization around the region of optimum effectiveness.

The value of the optimum effectiveness is of 5.5×10^6 ions.-cm^2/g. The reciprocal of this value is 1.8 nm, in water equivalent, being the DNA strand spacing.

Although similar linear relation is seen for σ_R versus $\bar{L}_T$, there is no relation between $\bar{L}_T$ and DNA spacing.

The ratio of $\sigma_R/\bar{I}_S$ reflects the intrinsic efficiency for damage per primary ionization (or per δ-ray). $\sigma_R/\bar{I}_S$ is found nearly a constant (slightly decreases with increasing of $\bar{I}_S$) independently of $\bar{I}_S$. This implies that, the δ-ray action is of minor importance in damaging cells.

In other words, the initial kinetic energies of electrons are relatively unimportant. It is important when they come to rest in

the cell nucleus as the probability of damage by electrons increases rapidly towards the end of the electron track. This conclusion is also seen in heavy ions result in Fig.2.4, where a comparison between the photon data and a typical set of heavy ion data is given. Of heavy ions result, more discussion will be presented in the next section.

From Fig.2.4, it is seen that, for both x- and γ-ray photons and heavy ions, firstly, there is a linear relationship below 5.5×10^6 ions.-cm^2/g or above 1.8 nm. Secondly, the magnitude of the intrinsic efficiency for photons is always very much less (~10%) than that for heavy ions with the same primary ionization. The implication may be that although the equilibrium slowing down electron spectrum from photons contains an abundance of low energy electrons (Hamm *et al.*, 1978), which are the most damaging, nevertheless, because of straggling or multiple scatter at the end of the range, the electrons are insufficient to penetrate both strands of the DNA double helix. Which in turn, leads to the third proposal that, most of the observed damage is due to intra-track effects rather than to inter-track effects. This proposal is also based on the fact that, σ_R is more closely proportional to $\bar{I}_S$ than to $(\bar{I}_S)^{1/2}$ for the photons. (Chen & Watt, 1986).

The data by Virsik *et al.* (1982), who reported a good correlation of electron, photon, and neutron data with dose-restricted LET (or $\bar{L}_{D,\Delta}$), were also processed (Watt & Chen, 1985). The original study was on the chromosome aberrations

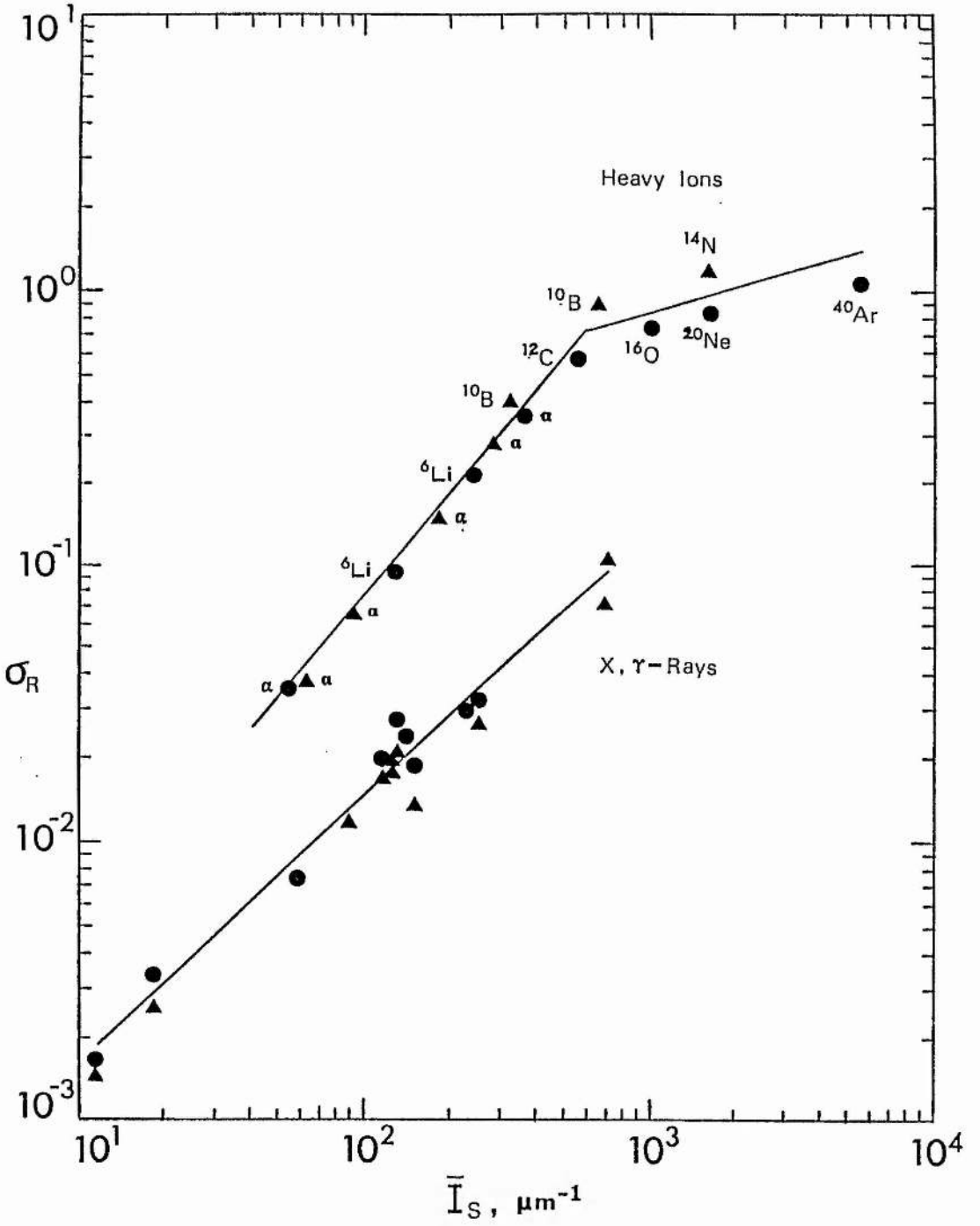

Fig. 2.4 Results for x- and γ-rays from Fig. 2.3(b) are compared with the intrinsic efficiencies for fast accelerated ions (CH cells (●), Skarsgard *et al.* (1967); V-79 cells (▲), Thacker *et al.* (1979). At the same value of I_S the photon data are about an order of magnitude smaller than the ion data. Also as σ_R is more nearly proportional to I_S than to $(I_S)^{1/2}$ for the photons, electron intratrack action appears to dominate the damage mechanism (After Chen and Watt (1986)).

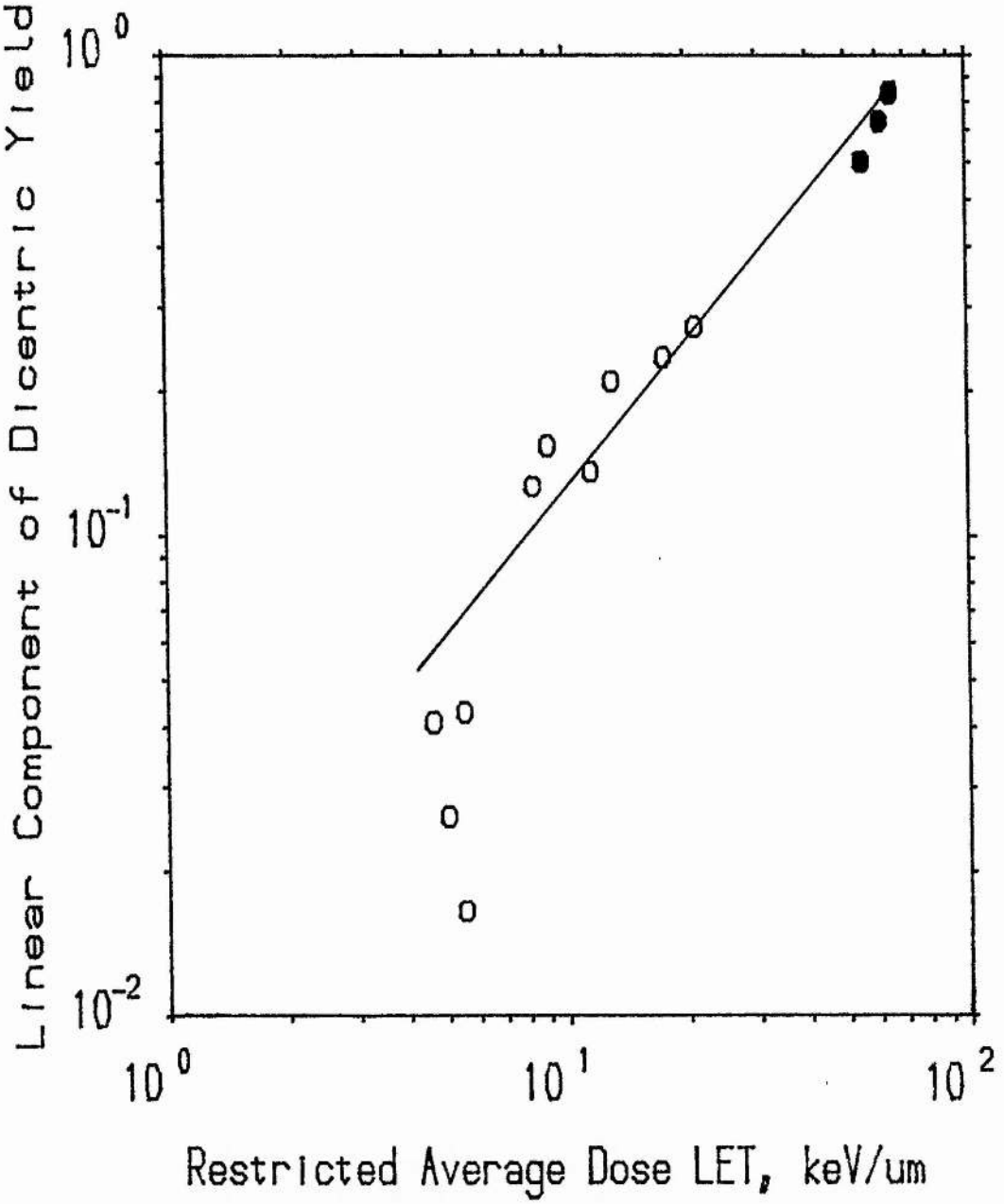

Fig. 2.5(a) Chromosome aberrations yield (dicentric) of human lymphocytes during the first mitosis, $y = \alpha D + \beta D$. Plotting of 'α-LET law' (After Virsik et al, 1982).

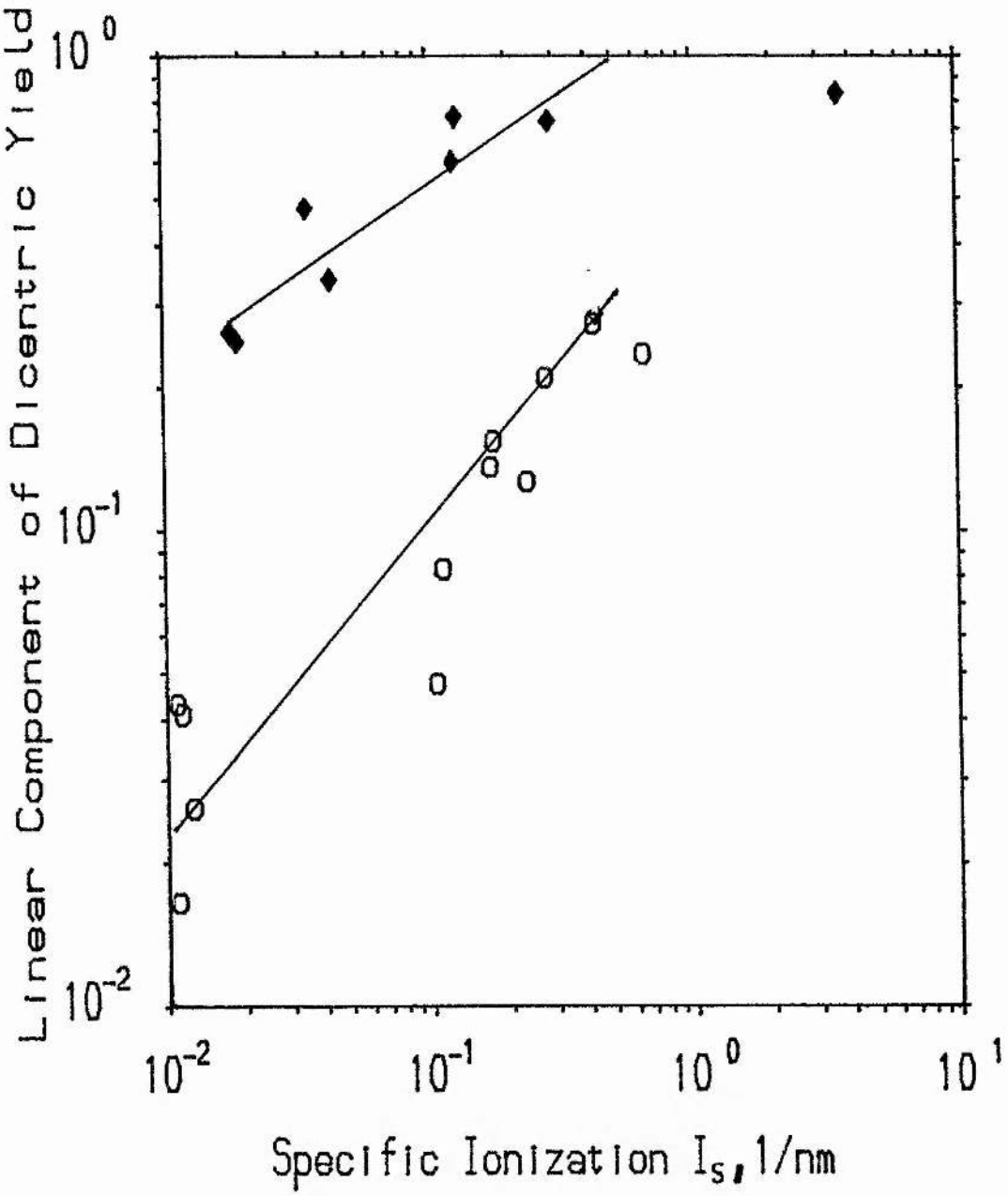

Fig. 2.5 (b) Chromosome aberrations yield (dicentric) of human lymphocytes. Plot: 'α-I_s (of secondary electrons)'. Open symbols: photons or electrons data; solid symbols: neutrons (Watt and Chen, 1985).

(dicentric data) of human lymphocytes. Plotting the linear term α of the aberration yield ($y=\alpha D+\beta D^2$) against $\bar{L}_{D,\Delta}$ (Δ could be different values in the original publication), there is a so-called 'α-LET law'. However, when the data were plotted against $\bar{I}_S$, see Fig.2.5, it is shown again that, first, α is linear to $\bar{I}_S$; second, the difference of efficiency is about one order less for photons, which is separated from the neutron data group; and third that the optimum values for both groups are seen to be 1.8 nm. From the above discussions, we are able to suggest that, the linear primary ionization is a conceptually correct parameter to be used rather than LET. The critical 1.8 nm spacing will be further demonstrated by the heavy ions results in the following.

2.3.2 Cell inactivation by heavy ions

In therapeutic treatment, in order to reduce the OER effect, high LET particles have been used. Such application in turn requires further study of the dose-effect of, *e.g.*, accelerated heavy ions at various biological levels. It is also known that for many cell lines (*e.g.*, T1-kidney cells) the relative biological effectiveness, RBE, of heavy ions increases with their LET to a maximum (at about 110 keV/μm, for T-1 kidney cells), and then decreases (Fig.2.6). When plotting RBE versus LET for different cell lines, the maximum RBEs are not unique values (cf. ICRU, 1970). For the reduction of RBE at higher LET, it was roughly interpreted as

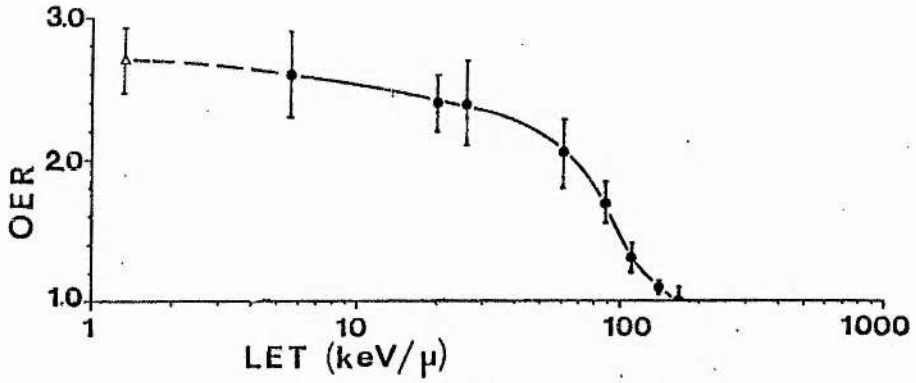

FIG. 2.6(a) OER as a function of LET. Measurements of OER were made with cultured cells of human origin. *Closed circles* refer to monoenergetic charged particles, the *open triangle* to 250-kVp x-rays with an assumed track average LET of 1.3 keV/μ. (From Barendsen GW, Koot CJ, van Kersen GR, Bewley DK, Field SB, Parnell CJ: Int J Radiat Biol 10:317–327, 1966)

FIG. 2.6(b) Variation of the OER and the RBE as a function of the LET of the radiation involved. The data were obtained by using T_1 kidney cells of human origin, irradiated with various naturally occurring α-particles or with deuterons accelerated in the Hammersmith cyclotron. Note that the rapid increase of RBE and the rapid fall of OER both occur at about the same LET, namely about 100 keV/μ. (Redrawn from Barendsen GW: in Proceedings of the Conference on Particle Accelerators in Radiation Therapy. US Atomic Energy Commission, Technical Information Center, LA-5180-C, October 1972, pp 120–125)

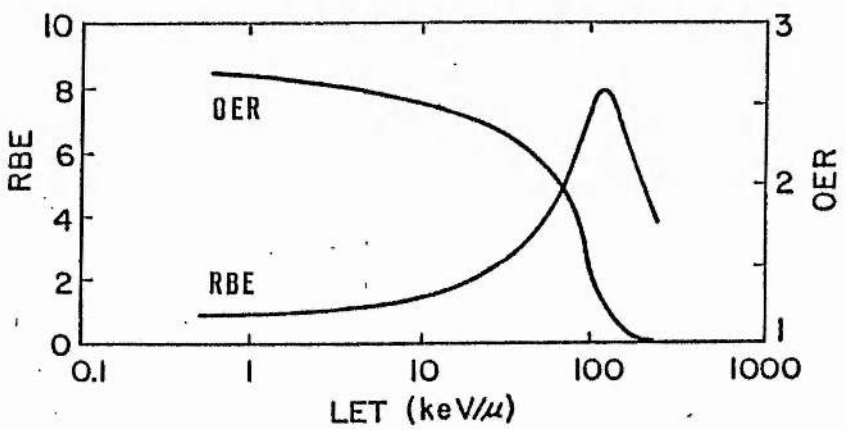

'overkill' or the waste of energy (*e.g.*, Hall, 1978). Examples of these phenomena (based on LET or energy transfer) have not been satisfactory.

Thomas and Watt (1984) proposed a statistical model for heavy ions based on the target concept incorporated with the δ-ray spectrum. By comparing the theoretical calculations with the experimental results in the literature, the general trends in cross-section ratios were adequately predicted for small targets such as enzymes, viruses.

This idea was developed to test different targets from enzymes to phages, yeast cells and mammalian cells, all irradiated by accelerated ions (Cannell & Watt, 1985).

In the literature dose response curves have been reported for ions of ^{2}H up to ^{40}Ar accelerated up to LET equal to $20x10^{3}$ MeV-cm^2/gm (Todd *et al.*, 1968) to determine the dose-response curves, for example, of Chinese hamster cell lines, or of yeast cells (Kiefer *et al.* , 1982; Kiefer, 1985). From these published data, Cannell and Watt (1985) plotted the intrinsic efficiencies as a function of primary ionization, Y, yield of the δ-ray spectrum generated by heavy charged particles, on log-log scale. For the mammalian cells and T1 phages, they found a distinctive feature of the pronounced discontinuity at Y values of about 5 ions.-cm^2/μg or about 2 nm mean free path equivalent in aqueous medium. While the data of lysozymes and ϕX-174 phages plotted did not show this inflection, instead it continued to increase monotonically. The

difference between the two groups is that, the former contain double strand DNA in their cellular nucleus, the latter do not (ϕX-174 phage contains single strand DNA).

Another important feature is that, when Y is further increased, the intrinsic efficiency increases a very little.

Since the inflection value of Y is equivalent to 1.8 nm (Table 2.4), the spacing between the two strands of DNA, it is concluded that the mechanism of fast ion inactivation in mammalian cells is dependent on the 'matching' of the mean free path of ionization events with the DNA strand separation distance, and the energy transfer (largely to the kinetic energy of the δ-rays) per event is less important, as seen in Table 2.4, the spread of δ-ray energy can be several orders, yet the σ_R at $\lambda \leq 1.8$ nm seems to be unity (Fig.2.4).

2.3.3 Discussion

Analysis of the published survival data by x-rays and γ-rays and heavy ions have shown that, the parameter $\overline{I}_S$, the specific primary ionization can be a very good quality parameter for interpreting biological effects. It supplies us the information that the optimum effect is reached at the mean free path equivalent to the DNA strand spacing; further increasing δ-ray energy (or LET) does not increase the intrinsic efficiency in cells, the quantitative

Table 2.4 Specific ionizations at discontinuity and mean free paths between ionizations for various targets. Mean value of specific ionization at discontinuity = 5.5±0.5 ions-cm^2/μg. Average mean free path λ between ionizations = 1.8±0.2 nm (after Cannell and Watt, 1985).

Target type and reference	Specific ionization at discontinuity (cm^2/μg)	Mean free path between ionizations, λ (nm)	Spread of δ-ray energies (keV)
V-79 cells Thacker *et al.*, 1979	5.95	1.7	3-24
CH2B2 cells Skarsgard *et al.*, 1967	5.4	1.9	11-22
T-1 cells Barendsen *et al.*, 1967	5.6	1.8	0.75-14
T-1 cells Blakely *et al.*, 1979	5.9	1.7	37-1635
T1-phage Fluke *et al.*, 1960; Schambra & Huchinson, 1964	5.3	1.9	7-25

comparison in Table 2.4, means that the δ-ray effect is of minor importance at cellular levels containing double strands, which in turn support the suggestion that the radiation damage to DNA is crucial.

Furthermore, these results suggest that microdosimetry should reflect the spatial distribution of events over distances of 2 nm rather than on energy deposition distributions as at present. The obvious implication for radiotherapy is that, on the basis of the damage mechanism described, optimum damage radiation should be chosen to be an accelerated ion having mean free paths for ionization of 2 nm regardless or its LET or ion type.

From comparison among electrons from photons and ions, conclusion is also made that the efficiency of the former is about ten times lower and always below the optimum specific ionization, the observed effects are therefore mainly intra-track not inter-track actions. This study was also extended to the analysis of neutron data to chromosome aberration (Watt & Chen, 1985), Fig.2.5. The result that electrons are less damaging led to the following proposal of damage effect of primary and secondary particles: the total probability of damage is given as (Watt *et al.*, 1985)

$$P_{tot} = P_i (1 + n_i P_j) \qquad (2.16)$$

where P_i is the intrinsic efficiency of damage for the radiation on the primary target alone, in which n_i ($=I_i \bar{l}$) ionizations occur on average, and P_j is the mean extrinsic efficiency of damage for the

delta ray spectrum. Extraction of P_j is now possible by looking at Fig.2.4. At the saturation condition I_i>0.55 nm^{-1}, P_i=1, in which case $P_j=(P_{tot}-1)/n_i$ represents the mean extrinsic efficiency for a single delta ray particle. The microdosimetry parameter, the defined mean cord length $\bar{l}$, can be taken as 4000 nm for Chinese hamster cell nuclei. Then the calculated P_j from primary heavy ions is $P_j=4\text{-}5X10^{-5}$ as indicated in Fig.2.4. This can be compared (from Eq.(2.15)) of the value about $2.11\text{-}5.22X10^{-5}$ for electrons from photons (assume P_i=0).

Furthermore, for comparative purposes, RBEs were compared with the simple ratio of effect cross-section defined by Eq.(2.13). The RBE of radiation type $\bar{l}$ with respect to the reference radiation type 2 is given by (Watt *et al.*, 1985)

$$RBE_{1,2} = \frac{\sigma_1 \ \bar{L}_{T,2}}{\sigma_2 \ \bar{L}_{T,1}} \qquad (2.17)$$

Note that here the LET ratio reintroduced the dependence on energy deposition but this is necessary in order to see RBE dependence on LET and on primary ionization $\bar{I}_S$. Usually the maximum RBE occurs at different LET according to ion type (see also ICRU, 1970). If the same data are shown as a function of $\bar{I}_S$ a more self consistent representation is achieved at the same position of mean free path of λ~1.8 nm, independently of both target type and radiation type as shown in Fig.2.7.

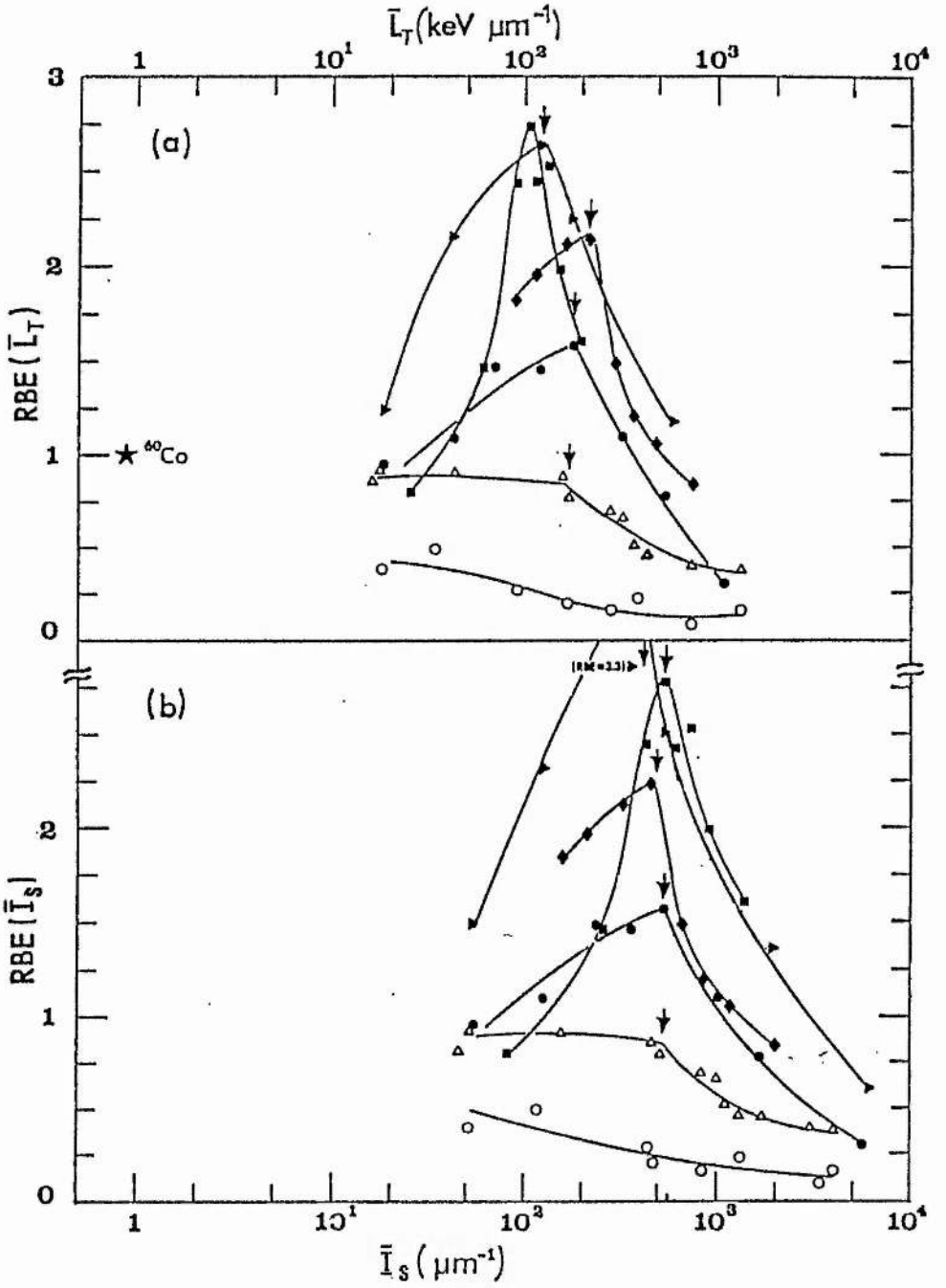

Fig. 2.7 RBEs are shown as a function of $\bar{L}_T$ and of $\bar{I}_s$. In the latter case the better grouping of the maxima (their common value of I_s ~550 μm^{-1}) and the apparent independence of both radiation type and target type is consistent with the interpretation of the damage mechanism. Symbol notations-○: ϕX-174; △: T1-phage; others: T1-cells and Chinese hamster cells by different authors (details see the text).

The above study on the mechanism of biological effect to cells, encouraged us to propose that the end-point at cellular level could be related to the damage of DNA secondary structure. It was based on the assumption that, as the dominant action observed is intra-track action, the dose-rate of the ionizing radiation particle is not important in the dose-effect. This led to the proposal of a new model- the DNA-rupture model discussed in the next section.

2.4 Damage Fixation and DNA-Rupture Model

2.4.1 Damage fixation

Despite the widely accepted sublethal damage repair proposal, the studies discussed above on heavy ions and photons showed that by analysing the intrinsic efficiency of damage the radiation effect is closely related to the DNA spacing and to the primary ionization events. A DNA-rupture model describing the cell survival based on the mechanism has been proposed (Watt, 1987) and it has been tested here with numerical data obtained in preliminary experiments.

Assuming that cell inactivation is caused by one or more DSBs in DNA by a single charged particle track, the DSBs are assumed to be capable of repair but the repair must occur within a mean time period t_f otherwise the damage becomes 'fixed' and the cell inactivation or cell transformation will occur subsequently.

2.4.2 The DNA-rupture model

Let n_0 be the mean number of segments of DNA at risk in a cell at t=0. Let p_1 stand for the probability of producing one DSB per track traversal of the target then the product of p_1 and n_0, *i.e.* $p_1 n_0$, is the efficiency for production of double strand breaks in a cell initially.

The time factor, t_f, is required for the double strand breaks to become irrepairable. Let t_r be the mean repair time. For a total irradiation time, t_i, the effect cross-section, σ_e, for the production of the biological effect in the cell, having a projected cross-section σ_g in the DNA molecules, is given by

$$\sigma_e = \sigma_g \int_0^{t_i} [1 - \exp(-p_1 n_0 e^{-(t_f - t)/t_r})] \, dt / t_i \qquad (2.18)$$

Since the yield of radiation action, y, is related to the particle fluence Φ as $y = \sigma_e \Phi$, for N_0 cells at t=0, the cell survival fraction N/N_0 is given by $S=e^{-y}$, *i.e.*

$$S = e^{-\sigma_e \Phi} \qquad (2.19)$$

The final expression of the DNA-rupture model is

$$\ln S = -\sigma_g \phi \int_0^{t_i} \{ 1 - \exp [-p_1 n_0 e^{-(t_f - t)/t_r}] \} \, dt \qquad (2.20)$$

It is seen that the survival fraction may be determined by the irradiation time at a given fluence rate or *vice versa* . For the given irradiation time t_i, the other parameters may be extracted by a non-linear fitting method applied to the experimental data.

Since logically we may expect $t_f > t_r$, for acute irradiation, *i.e.* $t_i << t_f$, Eq.(2.20) can be approximated as

$$\ln S = - \sigma_g \phi \int_0^{t_i} (1 - e^{-C}) \, dt$$

where C is the reduced constant term on the exponential or simply

$$S_a = e^{- \sigma_g \phi f(t_i)} \qquad (2.21)$$

For high-LET irradiation, if it is found $e^{-C} << 1$ (or $p_1 n_0 >> 1$, since t_f may be comparable with t_r) then the model will be reduced to a pure exponential expression. While for x- or γ-rays irradiation, e^{-C} may not be negligible (or $p_1 n_0 \sim 1$, the ratio of t_f/t_r should not be affected greatly), then the survival curve will be non-linear in response as shown by Eq.(2.21).

2.4.3 Discussion

It is noted that this model is irradiation time dependent, which eliminates the dose-rate dependence. When the irradiation time t_i is sufficiently large, the shouldered survival curve should tend, at very low dose-rate, to a near-linear response because most of the DSBs are repaired as, for example, quoted in Metting *et al.*'s

work (1985). On the other hand, for high LET, it seems that the published survival curves are most exponential. For very low dose-rate at high LET, *e.g.*, for heavy ions, the situation is not found in the reference.

The model challenges also the conventional physical qualities used in interpreting the survival results. Consequently, it is expected that the present experimental data on low LET by electrons and on high LET by alpha particles will be used in comparison with the published results to test the foregoing predictions and to appraise the validity of the theory.

To carry out the necessary experiments to provide our own data for test of the proposed theory a low energy electron accelerator was designed and commissioned for the low LET irradiation and an alpha particle irradiation facility built for the high LET experiment. Details of these and of the biological method used is introduced in the following two chapters.

CHAPTER III

EXPERIMENTAL: PHYSICAL ASPECTS

As the study in Chapter II showed, from the comparison of photons and ions, the intrinsic efficiency of radiation damage of the secondary electrons is about an order of magnitude lower than the ions. Two main conclusions are that most of the observed dose effect is intra-track action and the optimum value of damage is obtained when the mean free path of the ionization particles equals the spacing of the two strands in the DNA double helix. A prolonged experimental study is necessary to optimise the test. However in the present experimental research some preliminary tests for mammalian cell irradiation *in vitro* has been performed. This includes first a design of a low energy electron accelerator, and a facility involving two alpha irradiation sources- one for acute irradiation and the other for chronic irradiation. Relevant dosimetry techniques were also developed.

3.1 Low Energy Electron Accelerator

To build a complete low energy electron accelerator and its ancillary equipment requires a great deal of physical as well as mechanical work. In the literature, one laboratory reported a low energy (<100 keV) electron accelerator used for mammalian cell

studies (Cole *et al.*, 1963; Zermeno & Cole, 1969; Cole *et al.*, 1974; Tobleman & Cole, 1974). The reported machine, however, was conventional. It produced a spot beam therefore a precise mechanical device was needed to rotate the sample dish (1 cm diameter) during irradiation in order to imitate a large uniform radiation field impinging on a large area sample of cells. Due to the mechanical requirement, the samples were tested in a fixed short time (25 secs). To arrive at different total dose in the fixed time, the dose-rate was varied appropriately. By pipetting cells onto a membrane filter the cell dimension was less certain because the cells might overlap onto each other causing the survival curves to exhibit a tailing effect. Rigorous sterilizing conditions were required during the whole experiment. A similar facility for cellular study is not found reported elsewhere.

The present work involved design of a low energy (<100 keV) electron accelerator to produce a broad beam field. By using a differential vacuum system, the irradiation can be carried out in normal pressure while the cells are still maintained in medium surroundings. Thus, a complicated mechanical driver is avoided and longer irradiation time is allowed. Furthermore, the cell dimension is more certain permitting better quantitative analysis. The detailed description of this accelerator is given below.

3.1.1 Electron gun

Before considering the construction of the electron gun, one needs to know the beam current required to deliver an

appropriate dose rate. The beam current density can be determined from the following

$$j = e \rho \dot{D}/S \quad (A/m^2) \qquad (3.1)$$

where S is the stopping power given by Eq.(1.9). At maximum 100 keV, e.g., $S=6.592 \times 10^{11}$ J/m (=4.12 MeV-cm^2/g) in water, j is of the order of 10^{-7}A/m^2 in order to produce a dose rate of 10 Gy/min. For convenience, let S be in MeV-cm^2/g, ρ in g/cm^3, $\dot{D}$ in Gy/sec, then the required $j=\dot{D}/S$ nA/cm^2.

As the required current is low, a 0.2 mm in diameter, 2 cm in length tungsten wire is used as the filament material, for tungsten is known to have a high melting point, low vapour pressure, and relatively high electrical and thermal conductivity, and it has high mechanical strength. An ideal calculation can be made to get the optical analogue design of the electron gun electrodes. However, a modification was done on a ready-made multistage gun used for low energy electron research in this laboratory (Iskef, 1981), the gun was based on the design for producing a current of 8 μA at 30 eV with 1 mm spot size beam at 4 cm, and with maximum convergence angle of 0.035 rad (Simpson & Kuyatt, 1963). The gun was tested for the present purpose at a distance of 70 cm. The spot size was found to be about 2 mm which was thought unsuitable for the present purpose. Careful adjustments have been tried in order to obtain a broad beam which depend in a complicated way on the geometry and the electric potential applied to the electrodes of the gun. The final

arrangement of the gun is shown in Fig.3.1.

To ease the high voltage insulation at maximum 100 kV, a floating voltage supply method is adopted, the electron gun and its electrodes are insulated from the mains via an isolating transformer, the schematic diagram is given in Fig.3.2. The voltages supplied to the electrodes are selected through individual adjustment to defocus the beam and get an optimum broad field, the measured data will be given later.

3.1.2 Auto-heating circuit of electron gun

The filament current of the gun is quite low (*ca.* 5 A) compared with the maximum output of the power supply used (30 A, Kingshill), therefore, the power source is worked at the voltage stabilizing condition. Nevertheless, with either voltage stabilization (as present) or current stabilization (in rigorous condition), normally more than one hour is needed to slowly warm up the filament. An auto-preheating circuit was designed, which when the high vacuum is reached, can increase the output of the filament power supply slowly as a function of time in pre-set steps of up to more than an hour. The process is operated by the timing control circuit given in Fig.3.3 and Fig.3.4.

In Fig.3.3, Relay 1 and Relay 2 protect the two timers (T1 and T2), which delay the time intervals (0-24 hrs) through t1 and t2 respectively, so that after the rotary pump (RP) is switched on, the diffusion pump and the isolating transformer can then be switched on at two pre-set intervals determined by T1 and T2.

Consequently, after t2 is connected the third timer (T3) starts to count, and to warm up the filament. The principle circuit of timer 3 is given in Fig.3.4 (Courtesy of R.-D. Zhang for the design), and its printed circuit board is shown in Fig.3.5.

After timer 3 in Fig.3.4 is on (DC supply shown in Fig.3.3), it starts to produce clock signals as follows. Due to the function of C1, the input of NAG1 is at '0' level, and outputs '1' level which clears all the subsequent FDs, the outputs, *e.g.*, of FD6, *i.e.*, labelled 8,9,10 are all at '0' levels, and so that NAG3 outputs '1'. While C1 is charged, FD1 starts to accept the clock signal from C2R5 circuit, via NAG2 which has been functioned and consequent clock signal is produced. The following status of AG1-AG6 will decide the correspondent connection of the relay at interval determined by C2R5 which can be varied to increase or decrease the total warm up time of the filament.

AG1-6	1	2	3	4	5	6
Status	000,001	010	011	100	101	110
Relay ON	1	2	3	4	5	6

The output of the power source for the filament is adjusted by R_w as shown in Fig.3.4, R_w has been substituted by several resistors in series and controlled by the timer. The timer can be reset to zero either switch off its DC supply or more conveniently by manually pressing the reset button.

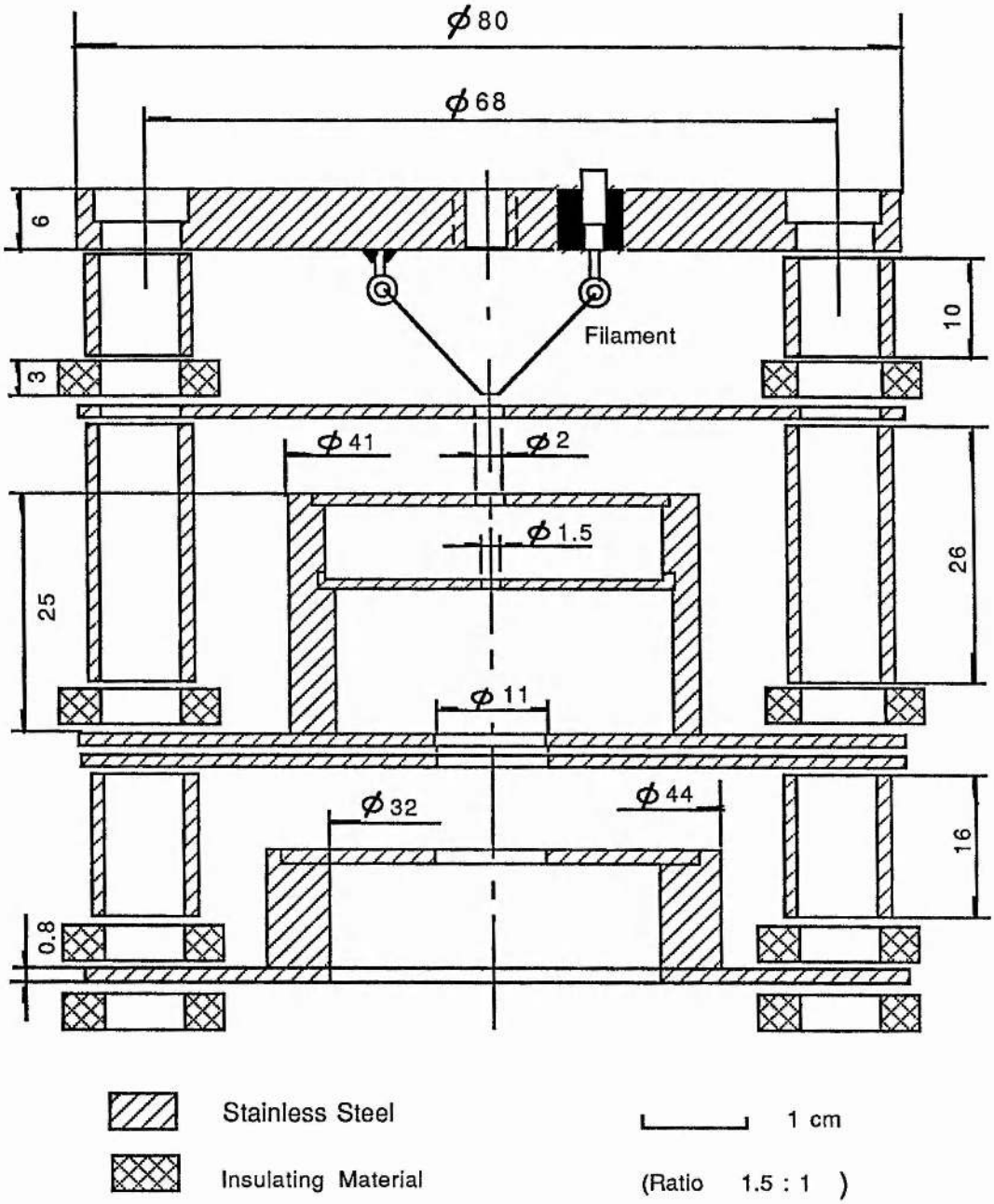

Fig. 3.1 Schematic of Electron Gun

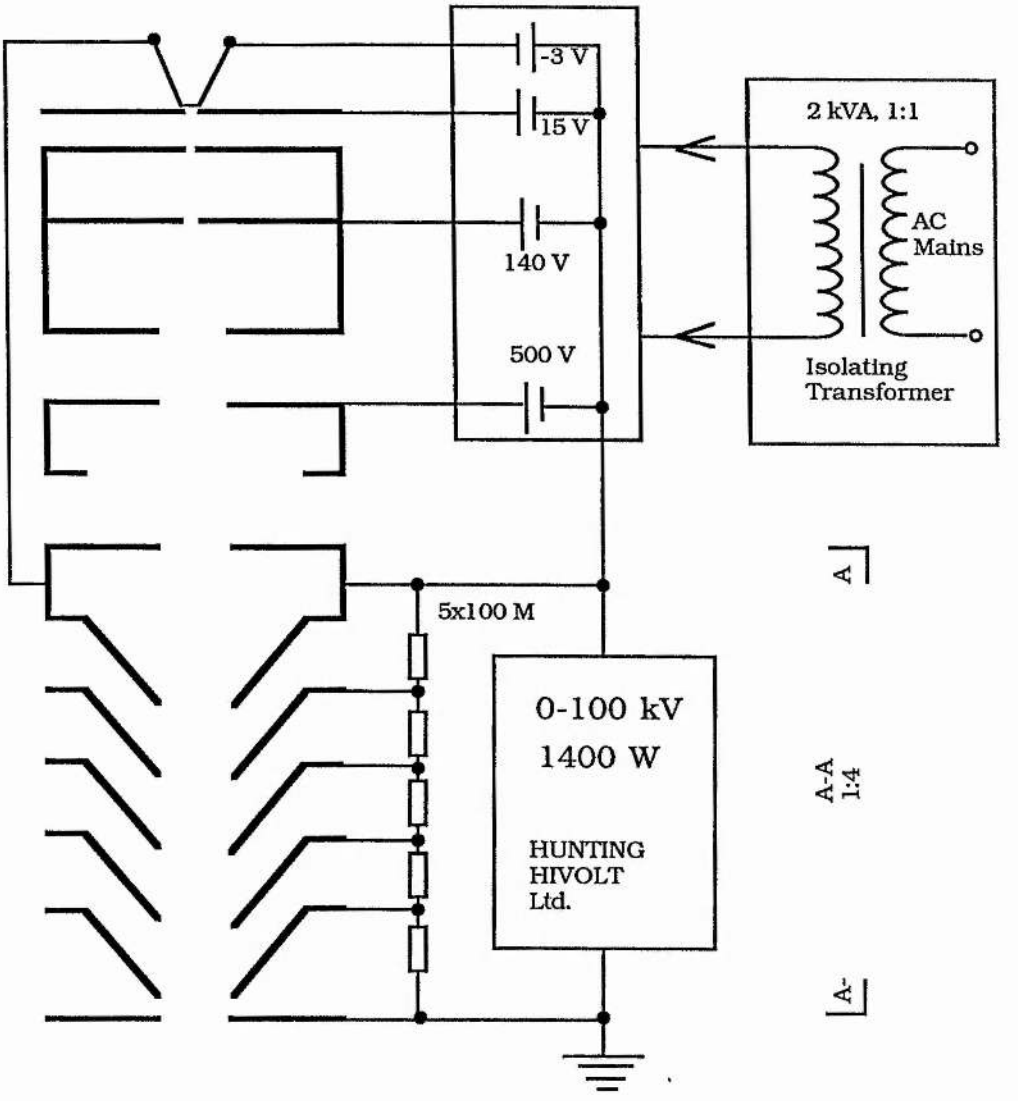

Fig. 3.2 Electron gun power supplies and the schematic of the floating high voltage supply

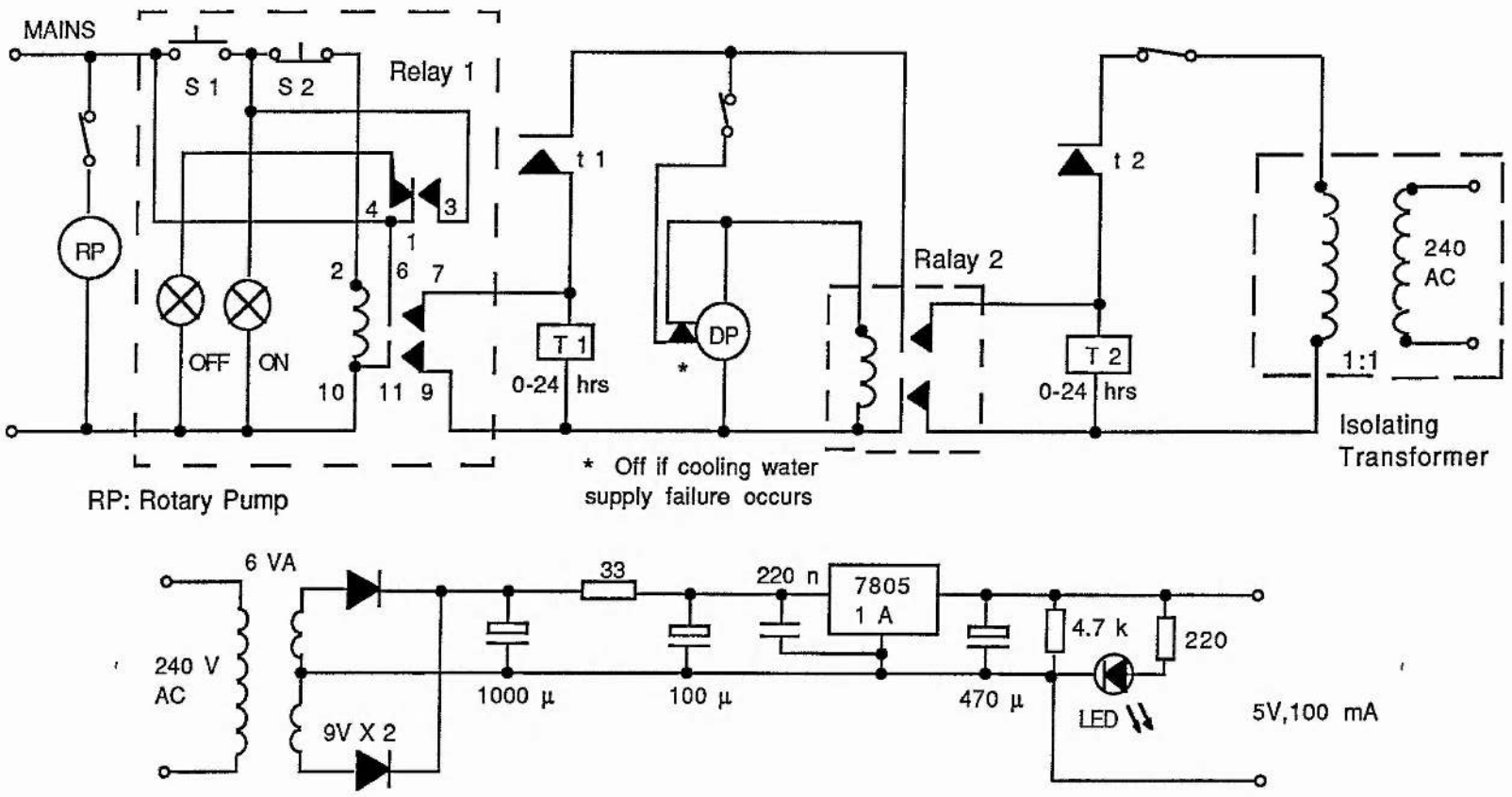

Fig. 3.3 Auto-preheating timing control circuit. Above: timer 1 (T1) controls the starting time of diffusion pump (DP) via t1, timer 2 (T2) connects the isolating transformer on via t2. Below: DC power supply of timer 3 which starts to warm up the filament of the electron gun.

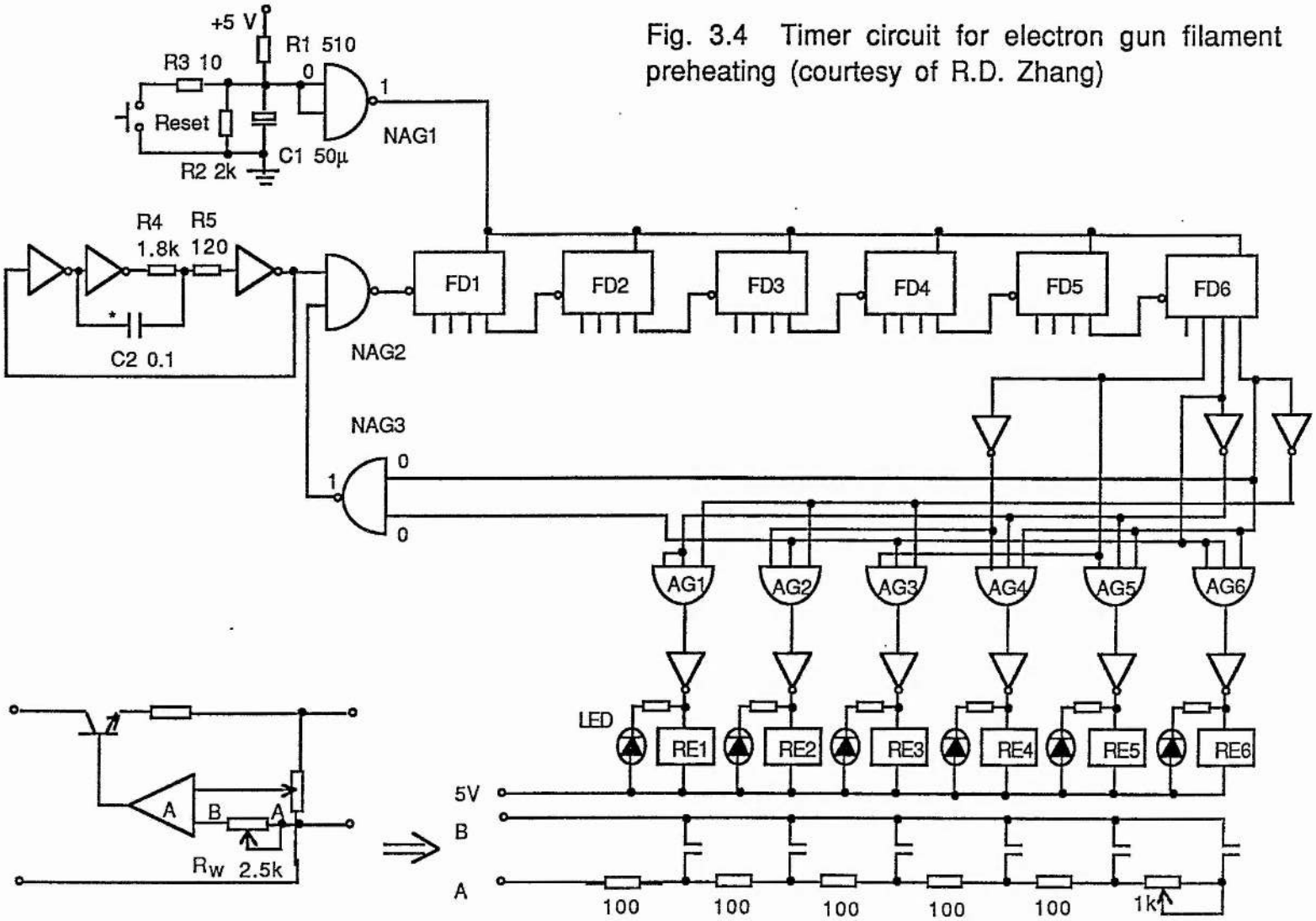

Fig. 3.4 Timer circuit for electron gun filament preheating (courtesy of R.D. Zhang)

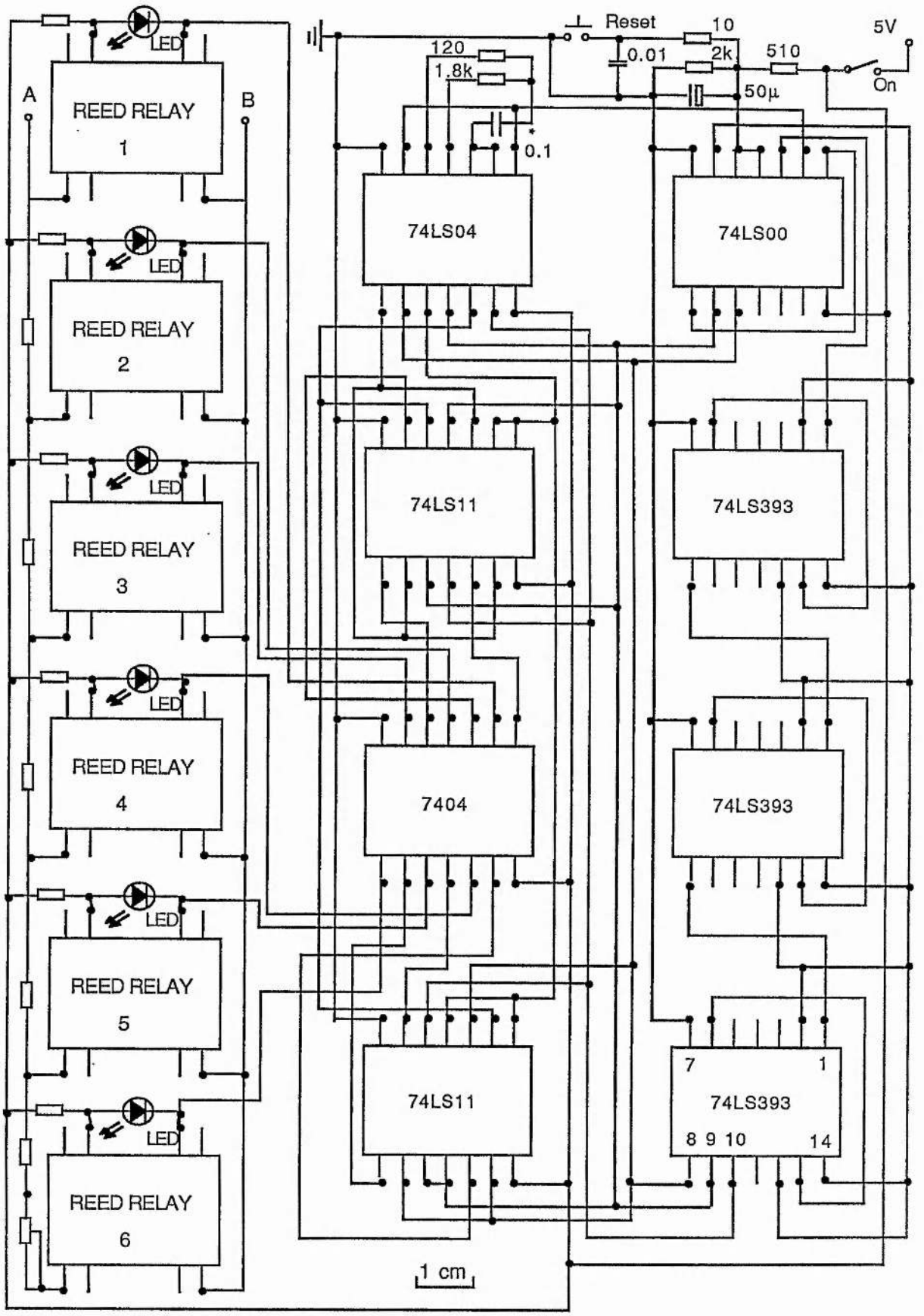

Fig. 3.5 P.C.B. of the timing circuit for electron gun filament

3.1.3 Vacuum system and irradiation chamber

As seen in Fig.3.3, the pumping system is protected by relay 1 in case an electrical failure occurs. If the cooling water is reduced, in turn, this will automatically switch off the filament power source to ensure that the electron gun is working only in the required vacuum condition.

The mechanical construction of the vacuum system as well as the body of the electron accelerator is shown in Fig.3.6 and in Fig.3.7 schematically. Two rotary pumps and one diffusion pump (Edwards Difstak, speed 280 l/sec) are used in order to obtain the designed differential vacuum. The acceleration of the electrons is maintained in the high vacuum (2.5×10^{-5} torr); while the sample irradiation has to be performed in a low vacuum. As an 100 keV electron can penetrate through less than 0.2 mm in water or 15 cm in air, therefore, the irradiation chamber has to be maintained in a certain low vacuum, which is chosen to be about or below 10 torr. The acceleration chamber and the irradiation chamber is separated by a thickness of 5 μm polyester foil (Melinex, metallized with aluminium, 1.41 g/cm^3, Goodfellow). The film thickness is checked by cutting arbitrarily several pieces of known area and weighing these on a Sartorius balance (the measured value for a 6 μm thickness, 1.39 g/cm^3, is 0.816 ± 0.029 mg/cm^2, or $t = 5.87 \pm 0.21$ μm. The error is believed to be introduced by the estimation of the film).

Ideally an irradiation should be performed at normal pressure. However, because of the said difficulty of the short range

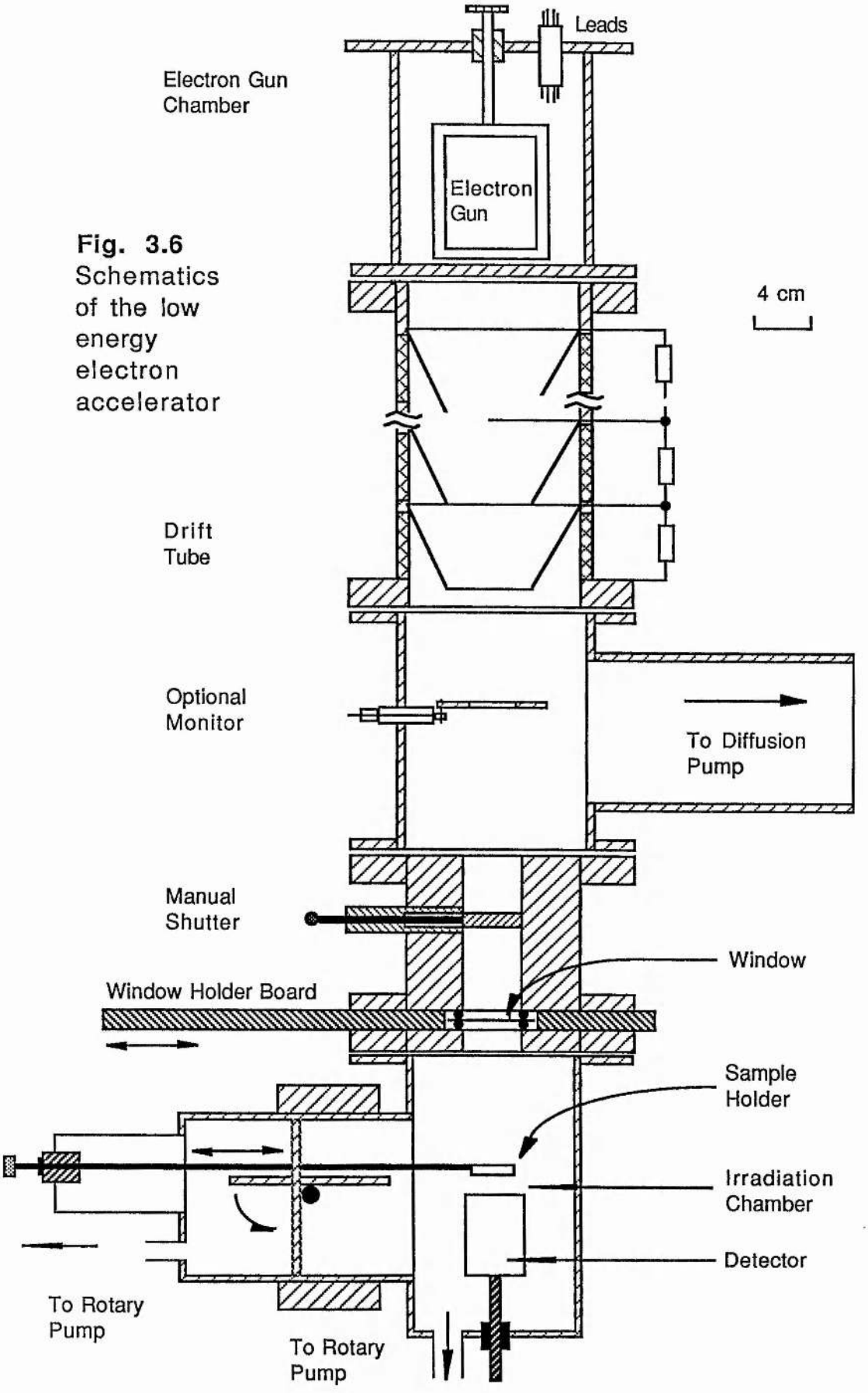

Fig. 3.6 Schematics of the low energy electron accelerator

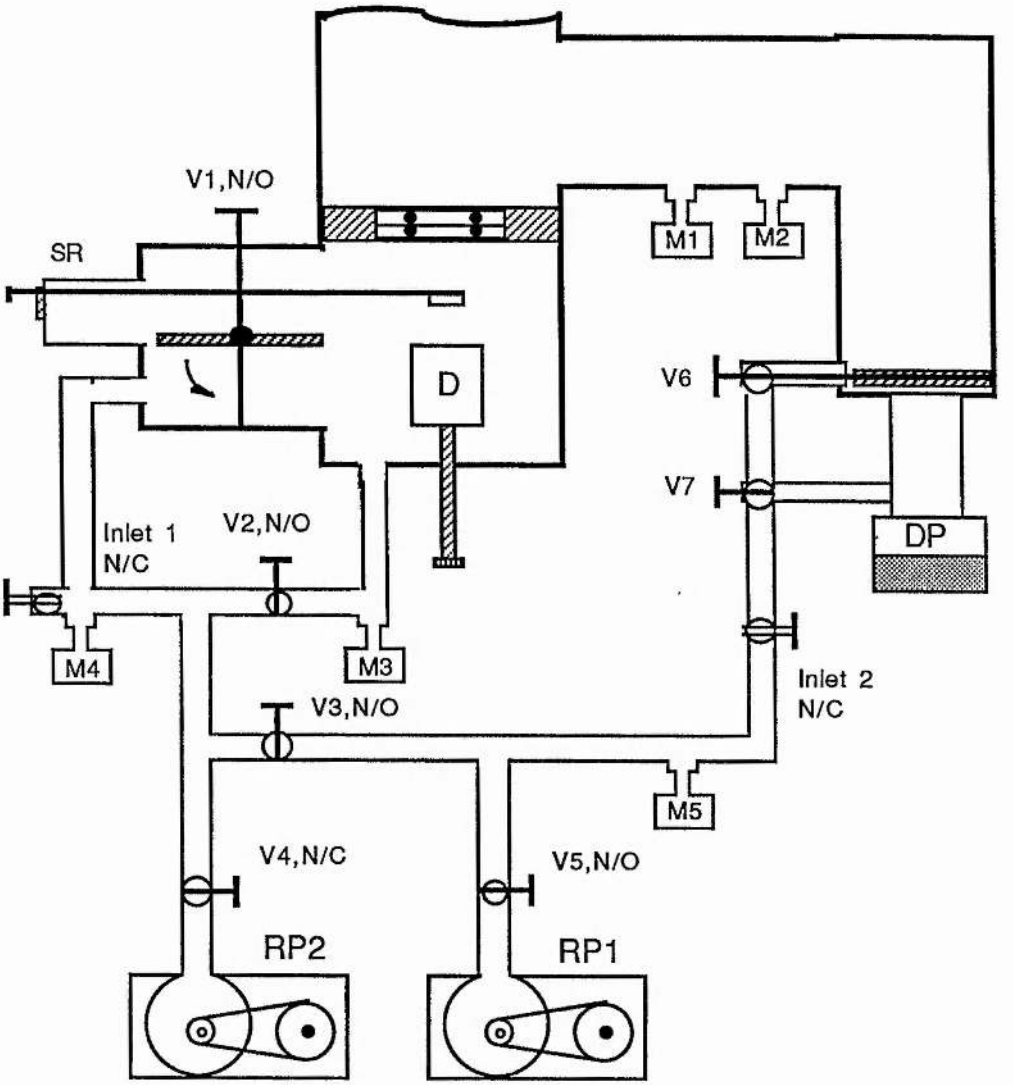

M1: Penning 8
M2: PIRAM 14
M3: PIRAM 11
M4: PIRAM 14
M5: PIRAM 12

RP: Rotary Pump
DP: Diffusion Pump
D: Detector
SR: Sampling Rod
N/O: Normally Open
N/C: Normally Close

Fig. 3.7 Principle of the differential vacuum system

of the low energy electrons, we further process the cells to be irradiated in a sealed petri dish under normal pressure as detailed in Chapter IV. An intermediate chamber was therefore designed so that the sample can be pushed to position and be brought out after exposure to the electron beam. Fig.3.7 shows the arrangement of the three chambers as well as the valves used to control the irradiation procedure.

The following steps have been organized in order to carry out the experiment in a differential vacuum condition:

1. pulling out the sampling rod so that
2. V1 can be and must be closed;
3. close V2 and V3, check that if V4 is also closed;
4. open inlet 1, noticing M1, M2, M3 and M5 readings are unaffected;
5. close inlet 1 when M4 is indicating at 1 atm.;
6. open the cover of sampling chamber, put the petri dish containing cells on the holder, then close;
7. switch on RP2 power, and gently open V4;
8. open V3, when M4 is about 10 torr;
9. open V2, and notice M3 until it is < 3 torr;
10. open V1, and the sample is ready to be tested.

3.1.4 Safety and interlocking

To avoid the potential hazards from the high voltage, some precautions must be taken. For example, one must ensure that the anode of the accelerator is well grounded and the safety interlocking system is operating. To switch off the high voltage, one can press the OFF button or turn the master key counter-clockwise. Both are arranged in the front board of the control

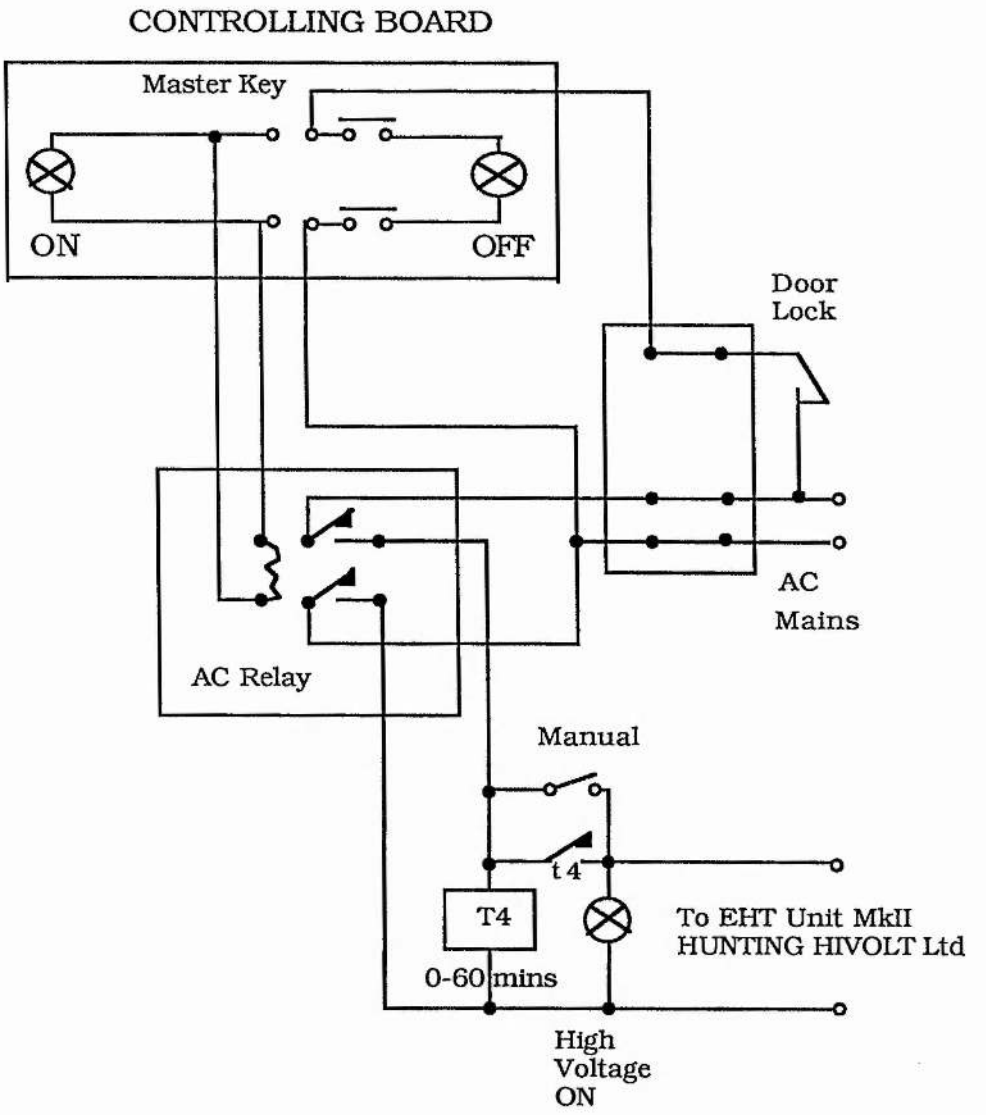

Fig. 3.8 High voltage interlocking system

deck. These are usually considered by the manufacturer of the instruments. However, for the present purpose, to ensure no personnel get access into the high voltage enclosure, the region of which is isolated by a fence with one door, a switch is mounted such that the power supply can be connected only when the door has been shut. A red bulb is lit when the high voltage is on. An irradiation timing control is also included. The arrangement is shown in Fig.3.8.

3.2 Alpha Irradiation Arrangement

Several different types of arrangement for alpha particle irradiation in cell studies have been reported. For an ideal device of alpha irradiation, two criteria are of special importance (Roos & Kellerer, 1986). First, the fluence has to be reasonablly uniform over an extended sample. Secondly, the energy needs to be sufficient for penetration of a monolayer of mammalian cells, and the dose must not vary strongly through the region of interest.

To fulfil the first condition, one could use a uniform and sufficiently large source. Its diameter would have to be three times as large as that of the sample. This ensures a uniform fluence but is necessary to also ensure uniform energy deposition and so a collimator is introduced to permit only normal incidence to the cells. For example, Simmons *et al.* used an active area of diameter of 10 cm source for the studies of human lung cell lines (Simmons *et al.*, 1983; Min *et al.*, 1985). A collimator was used to further ensure the beam to be parallel when it struck the layer of cells (a

typical collimator, reported by Roos and Kellerer, has a height of 15 mm and 3 mm diameter of its channels).

Another method is to separate source and sample by a large distance in vacuum, such that an approximately parallel beam can be obtained and yet the alpha particles will not lose much of their energy in transit to the target (*e.g.*, Barendsen & Beusker, 1960).

A most effective method, according to Roos and Kellerer, is to design a moving collimator, the fluence inhomogenicity may be reduced to 3% while the transparency of the collimator can be over 80%. To reduce energy loss in the channels of the collimator, source and collimator can be mounted in a container which is flushed with helium under normal pressure (no vacuum is needed).

In the present work, to enable a quick preliminary test of the damage model, it was considered reasonable to dispense with collimator and to perform the irradiation under fixed geometrical conditions. This means that care must be taken to calculate the interaction parameters (LET, I_1 etc.) for the spectrum of alpha particles that traverse the cellular targets.

Two alpha sources are utilized for the experiment. These are so used to obtain data that can be used to test the proposed DNA-rupture model. Also a comparison can be made to the low LET result. Of the two sources, one (^{244}Cm) is used to deliver an acute and the other (^{241}Am) is used to deliver a chronic irradiation. The arrangement of the two sources is given in Fig.3.9. The basic data of the two disc sources are as follows:

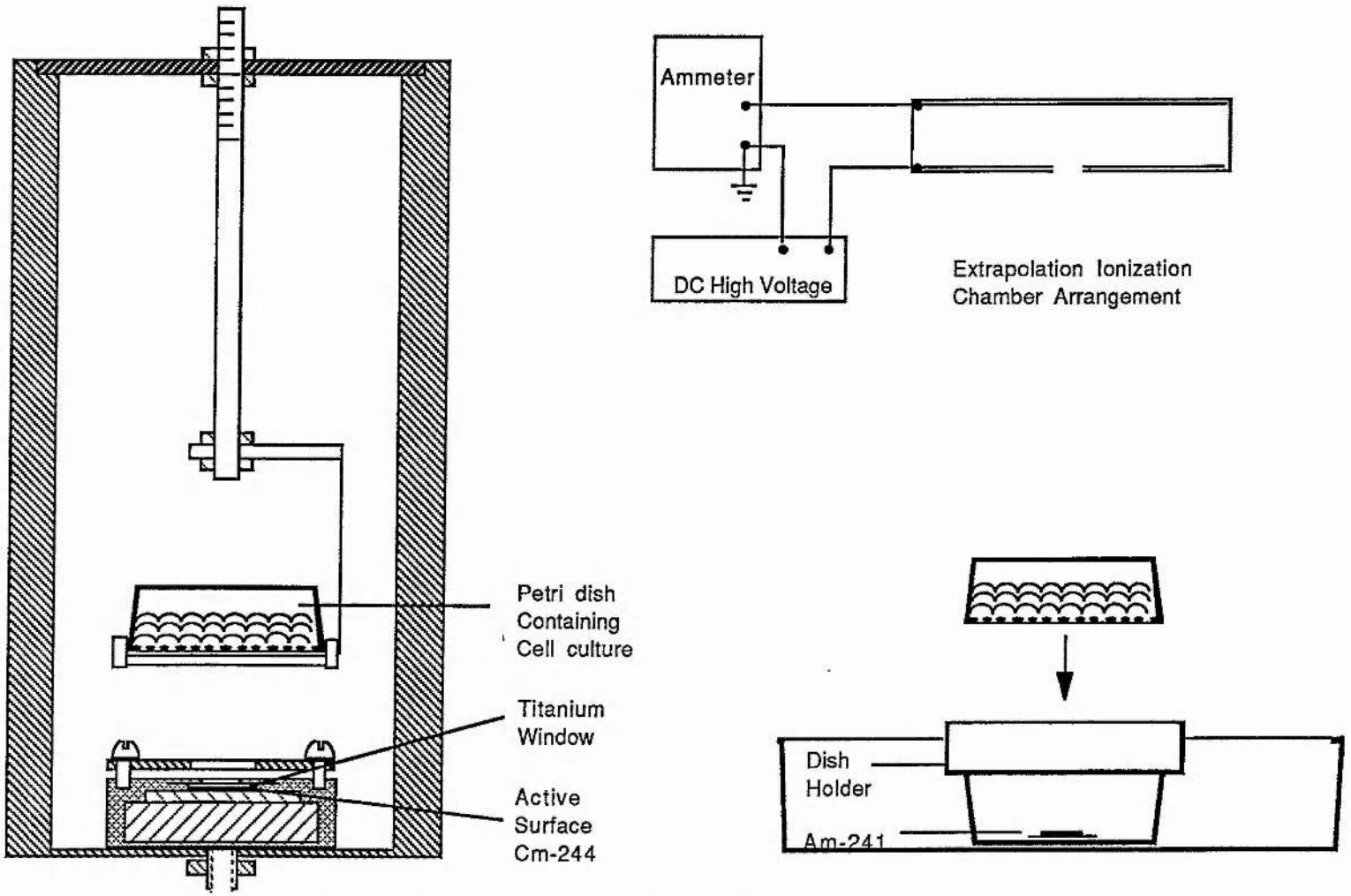

Fig. 3.9 Alpha irradiation arrangement. Left: an acute source of curium-244, 505μCi; right: a chronic source of americium-241, 1.35 μCi. Top right: an arrangement for measuring alpha-particle fluence rate on ionization chamber principle.

Isotopes	$^{244}Cm_{96}$	$^{241}Am_{95}$
Energy spectra	5.801 MeV, 76.7%;	5.477 MeV, 85.1%;
	5.759 MeV, 23.3%;	5.435 MeV, 12.6%;
		5.378 MeV, 1.7%;
Activity	505 μCi	1.35 μCi

Both isotopes have long half-life (18 and 433 years respectively) and are disc sources of 6 mm diameter. The curium is vacuum sealed with a 4 μm titanium safety window; the americium is a conventional source and its gamma-ray contribution is known to deliver a negligible dose.

3.3 Methods of Dosimetry

In most circumstances, dosimetry is the measurement of absorbed dose (or abbreviated simply as dose) by means of dosimeters. The measurement can involve basically determining the energy spectra and/or the fluence rate of the incident particles to be measured. There are a number of different dosimetric methods and they have been extensively discussed (see Attix *et al.*, 1966-1969).

Dosimeters which depend on the collection of electric charge include ionization chambers, proportional and Geiger-Müller counters. The solid state or semiconductor dosimeters are relatively new. They have better energy resolution and permit accurate measurements of energy spectra. Indirectly methods by cloud chambers and photographic emulsions may allow dosimetry of ionizing radiation over a wide range of dose, a wide range of time and a wide range of area.

In this discussion, only the dosimetric methods used for the electron and alpha particle detection in the present work will be discussed. As in the present situation, experiments on biology may be considered preliminary.

For the electron irradiation, both the calorimetric method and the Faraday cup have been used previously in this laboratory for electron energies below 10 keV (Iskef, 1981; Al-Ahmad, 1984). These two methods are reviewed and extended to the present purpose. They are discussed in Secs.3.3.1 and 3.3.2, respectively. For the alpha particles' irradiation, a simple extrapolation ionization chamber was used. This will be described in Sec.3.3.3.

3.3.1 Calorimetric method

3.3.1.1 Introduction

The calorimetric method has been developed as a convenient technique applied particularly to measurement of energy fluence of x-ray and electron beams so as to be able to measure the total absorbed dose (ICRU, 1964). For a calorimeter, it is unnecessary to consider the factors in the foregoing discussion as it measures the energy deposited in the material of interest directly. Therefore, it is often used as a calibrator of other dosimeters utilizing the secondary process, *i.e.*, the indirect measurement. It is known that the sensitivity of a calorimeter is insufficient for radiation protection purposes and also due to scattering of the incident particles and/or rejected particles, some of the energy may be

mismeasured. However such disadvantages can be overcome by appropriate precautions and corrections (Laughlin & Genna, 1966).

There are two methods of calorimetry, i.e., the isothermal one and non-isothermal one. As it is difficult to establish a thermodynamic equilibrium state to satisfy the condition of constructing an isothermal calorimeter, it is easier in practice to utilize the non-isothermal method. Among the non-isothermal methods, the 'constant temperature environmental method' is simple and explicit as long as correction for leakage is made.

3.3.1.2 Temperature change in calorimeter

Incident particles of ionising radiation traverse an energy absorber and lose part or total of its energy in the absorber. The net absorbed energy is released in the form of heat energy which results in the rise of the temperature in the absorber. The temperature variance can be measured by a thermistor and calibrated in terms of absorbed dose, *i.e.*, the energy absorbed in a unit volume, being measured.

There are two ways of measuring temperature change. One is using a thermocouple (or thermopile composed of a number of thermocouples), which is made of a pair of conductors of two different metals, to measure the electromotive force (emf) generated at their junctions. The emf is about 50 mV per ^{0}C and is detected with a potentiometer. However, the second method, resistance thermometer reveals a higher sensitivity compared with

the thermoelectric thermometer.

The resistance thermometer can be a platinum resistor or a semiconductor thermometer, known as a thermistor. The resistance-temperature relationship of a thermistor of platinum is simply linear but for a semiconductor it is approximately exponential, *i.e.*

$$R_T = R_0 \, e^{\beta(1/T - 1/T_0)} \qquad (3.2)$$

where β is the characteristic temperature constant (^{0}K) and can be determined by plotting logR versus 1/T. As the temperature coefficient is defined by $\alpha_T=(1/R)(dR/dt)$, we have, by substituting Eq.(3.2) and $dR/dT=(-\beta R_0/T^2)e^{\beta(1/T-1/T0)}$ by differentiating R with respect to T

$$\alpha_T = -\beta / T^2 \qquad (3.3)$$

for platinum, α_T (at 298 ^{0}K) is about 0.4, and for semiconductor it is about one order higher (negative). Obviously, in order to obtain higher sensitivity in measuring a small temperature change, a semiconductor thermistor is preferred.

3.3.1.3 Heat transfer loss in calorimetry

It is necessary to first discuss the mechanism of the heat transfer in a calorimeter, *i.e.*, the relation between changes in thermal energy which is transferred from the radiation energy and temperature rise caused by the incident particle and therefore the

design of the calorimeter is contributed to methods of temperature change detection and, the energy leakage correction.

According to Newton's law of cooling, the total heat transfer loss can be expressed as

$$(1/A)(dE/dt) = - \Sigma h_i (T-T_0) \qquad W/m^2 \qquad (3.4)$$

where A is the concerned area in a calorimeter, i=1,2,3 in h_i which represent for the heat transfer coefficients for convection, conduction and radiation, T and T_0 denote the temperatures of the calorimeter absorber and its surroundings respectively (Laughlin & Genna, 1966). They are briefly described in the following.

i) **Heat convection** is not observed when the Raleigh number $R=m_c d^3 \Delta T<1620$. Where d (in cm) is the separation between the two parallel plates in a specified experiment, ΔT (in degrees centigrade) is their temperature difference, and m_c (in $cm^{-3}\ ^0C^{-1}$) is the convection modulus of air. Since the convection modulus is proportional to the square of the density which in turn is proportional to the pressure, P, then no heat convection will occur when the following condition is satisfied

$$P/760 < [16.2/(d^3 \Delta T)]^{1/2} \qquad (3.5)$$

P is in torr. In the present study, let d be the separation between the calorimeter and its jacket (less than 3 cm). As ΔT is measured always less than 10 ^0C and P less than 10 torr, therefore, convection can be ignored.

ii) **Heat conduction** can transport energy through intermolecular collisions in a calorimeter from the thermistor to its surrounding air or enclosure. This can be described by the heat flow equation. In Eq.(3.4), h_2 or h_c is known in the cylindrical surfaces:

$$h_c = k/[r \ln(1+d/r)] \qquad (3.6)$$

where r is the cylinder radius, d is the separation, and the thermal conductivity, k, is proportional to $\rho v \lambda C_v$, where ρ is the density of the air, v is the mean molecular velocity, C_v is the thermal capacity at constant volume and, λ, the mean free path, which is the average distance travelled by a gas molecule before colliding with another gas molecule. In air, λ is roughly equal to 5/P(in mtorr) cm at room temperature. In practice, to obtain a lower rate of heat conduction transfer in a calorimeter, one should reduce the pressure in the system. The heat conduction loss is also transferred through electrical connection wires. The heat leakage rate is $L=kA/l$ ($W/^0K$), where A and l are the cross section area and the length of the wire respectively.

iii) **Heat radiation** loss can occur in a calorimetric dosimeter. The radiative heat transfer coefficient h_3 or h_r is

$$h_r = \sigma F(T^4-T_0^4)/(T-T_0) \qquad (3.7)$$

and factor F is a function of emissivities ε, ε_0 and areas A, A_0 of the radiative object (*e.g.*, a calorimeter) and the enclosure and F^{-1} =

$(1/\varepsilon) + (A/A_0)\,[(1/\varepsilon_0) - 1]$ (McAdams, 1942). When A/A_0 approaches zero (or ε_0 equals 1), $F=\varepsilon$, then the area of the thermistor and the temperature difference between it and its enclosure will determine the radiative energy loss. Also, it is noted that Eq.(3.4) will be in accordance with the Stefan-Boltzmann law. σ is the Stefan-Boltzmann constant. $\varepsilon=1$ if the surrounding object is considered as a 'black-body': $(1/A)(dE/dt)= \varepsilon\sigma(T^4 - T_0^4)$. It follows that, if a material with low emissivity or a polished surface (small ε) is used, the radiative loss from the calorimeter would be reduced.

3.3.1.4 Experimental detection of absorbed dose

A conventional Wheatstone Bridge is suitable for measuring the temperature change in a calorimetric dosimeter. In Fig.3.10, the practical circuit is given, where R_1-R_4 compose the bridge circuit, and R_L is the load resistance. We chose $R_T(=R_1)=R_2=R_3=R_4$, as the output signal V_L can be read on the detector so to calculate R_T from

$$R_T = \frac{V_L (R_2R_3 + R_2R_L + R_3R_L) + R_2R_LV_S}{R_LV_S - V_L(2R_2 + R_2R_L/R_3 + R_3 + R_L)} \qquad (3.8)$$

In practice, R_2 is a potentiometer so it can be adjusted to be equal to R_T at the current temperature, and R_L (optional) is

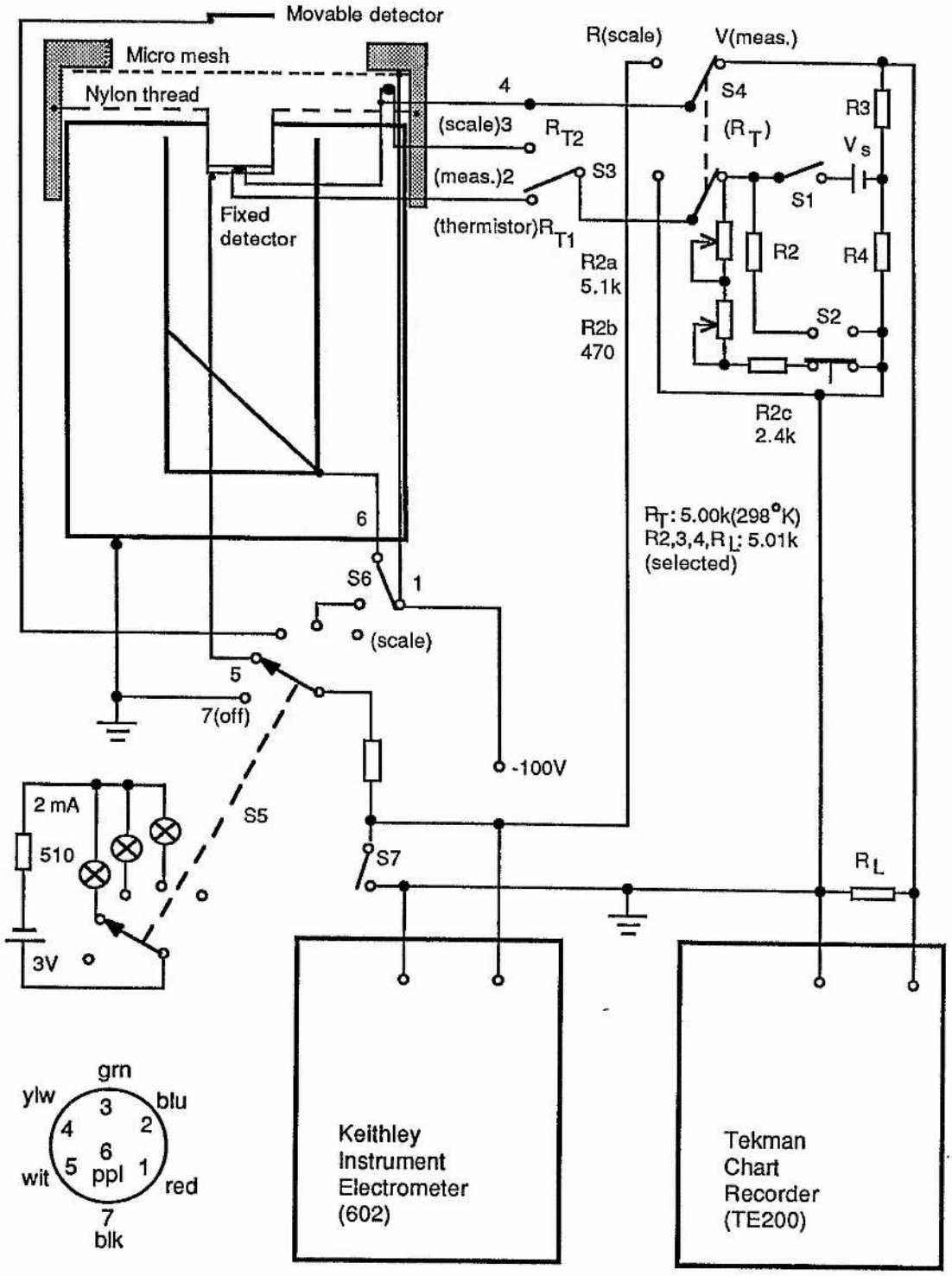

Fig.3.10 Principle circuit of dosimetric detector

shunted at the input of the chart recorder which has a very high input impedence of 10^6 ohms. If required the signal to noise ratio can be increased by adjustment of R_L.

From Eq.(3.9), the total temperature increase ΔT is detected during the time interval Δt of irradiation assuming constant dose rate,

$$T - T_0 = (TT_0/\beta) \ln(R_T/R_0) \qquad (3.9)$$

The present value of β is 3795.29 which is fitted, from the data given by the manufacturer, by the least squares method.

In Fig.3.10, two thermistors R_{T1}, R_{T2} were used. The output of R_{T1} is normally connected via S_2, S_3 to the Wheatstone Bridge circuit. R_{T2} can reflect a reference temperature to the calorimeter for calibration purposes. The resistance of the thermistors before irradiation is started is scaled via S_3 to a Keithley Instruments electrometer (KIM, input impedence $>10^{14}$ ohms as a voltmeter). A Tekman chart recorder (TCR, $>10^6$ ohms) is used to display the voltage signal from the bridge. KIM and TCR are scaled to each other before use.

The thermistor R_{T1} is embedded with a heat conductive insulating glue between two layers of 1 cm diameter copper foil (16.7 mg/cm^2). This forms the detection surface of the calorimeter and also serves as a Faraday cup whose function will be discussed later. The cup is cylinder 1 cm in height open at the top. The total

weight is 774.6 mg (including the thermistor of 58.2 mg), and its heat capacity is mc_p=774.6x10^{-6}kg x386J/kg-^{0}K=0.299 J/^{0}K.

3.3.1.5 Correction for heat leakage

The absorbed dose, D, defined (ICRU, 1969) as

$$D = E_D/\ m = E/m + E_d/m \qquad (3.10)$$

where E_d is the 'heat defect' which stands for the fraction converted from the incident particle energy into chemical energy. Let us consider the first term in the above equation here. From Eq.(3.4), since $dE=mc_p dT$, then letting $K=(A/mc_p)\Sigma h_i$ we have the heat leakage rate

$$(dT_l/dt) = - K (T_c - T_j) \qquad (3.11)$$

where the subscripts c and j denote the calorimeter absorber and jacket. The net constant rate (measured) of temperature rise of the thermistor corresponding to the constant rate of input dT_c/dt is the difference between the real rate $\dot{T}_r = (dE/dt)/(mc_p)$ which we wish to measure and the leakage term, *viz.*

$$(dT_c/dt) = \dot{T}_r - (dT_l/dt) \qquad (3.12)$$

Since T_j is considered constant, the solution of the above linear differential equation over limits T_i (initial) to T_f (final) is found to be

$$T_{cf}-T_{ci} = (\dot{T}_r/K)(1- e^{-K\Delta t}) + (T_{ci}-T_j)\ e^{-K\Delta t} \qquad (3.13)$$

where $t=t_f-t_i$, and the real rate is

$$\dot{T}_r= [K(T_{cf}-T_{ci})-K(T_{ci}-T_j)\, e^{-K\Delta t}] \,/\, (1- e^{-K\Delta t}) \qquad (3.14)$$

assuming $T_{ci}=T_j$ in Eqs.(3.13) and (3.14), and let $T_m= T_{cf}-T_{ci}$, we have

$$T_m= \dot{T}_r\, (1 - e^{-K\Delta t})/K \qquad (3.15)$$

or

$$(dT_r/dt)= T_m K/(1 - e^{-K\Delta t}) \qquad (3.16)$$

In order to determine K, a similar leakage rate is assumed as Eq.(3.11) after the end of the irradiation (Al-Ahmad, 1984), *i.e.*

$$(dT_{cf}/dt) = - K\, (T_{cf}- T_{ci}) \qquad (3.17)$$

integrating over $T_{cf}- T_{ci}$ to $T_t- T_{ci}$, K is then determined in the experiment from the following

$$(T_t- T_{ci})/\, (T_{cf}- T_{ci}) = e^{-Kt} \qquad (3.18)$$

notice that the subscript 't' in the above denotes the time after the input energy is terminated. Now the dose rate is expressed as

$$\dot{D} = (1/m)(dE/dt)= c_p\, (dT_r/dt)$$

$$= c_p\, K(T_{cf}- T_{ci})/(1- e^{-K\Delta t}) \qquad (3.19)$$

Fig.3.11 shows the principle of the calorimetric determination method. For high fluence rate ($>10^{10}cm^{-2}s^{-1}$), a measurement is shown in Fig.3.12, K is determined. Also for a small range of temperature change, R_T values are calculated then one can obtain the output voltage signals of the bridge circuit from which in turn the values of T are calculated. These results are

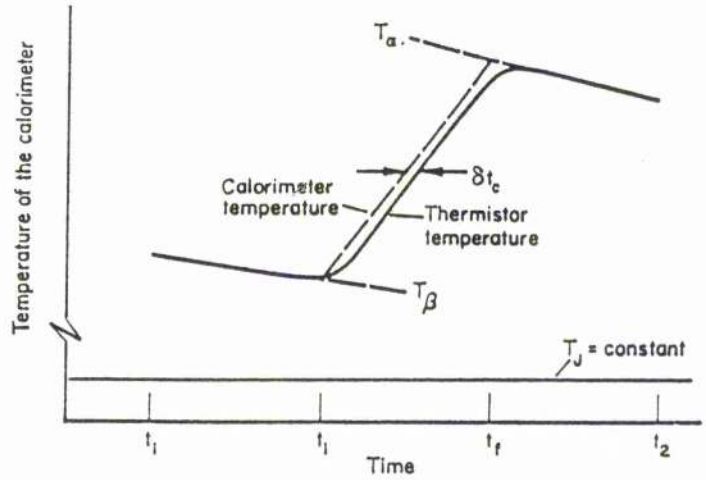

Fig. 3.11(a) Schematic calorimeter heating curve. Energy is introduced into the calorimeter at a constant rate during the X period (t_i to t_f). During the rating periods (t_i to t_i and t_f to t_2), the calorimeter temperature exponentially approaches the equilibrium temperature (jacket temperature, T_J). δt_c measures the thermal time lag between the thermistor and the calorimeter, and T_α and T_β measure the net temperature change resulting from energy input (After Laughlin & Genna, 1966).

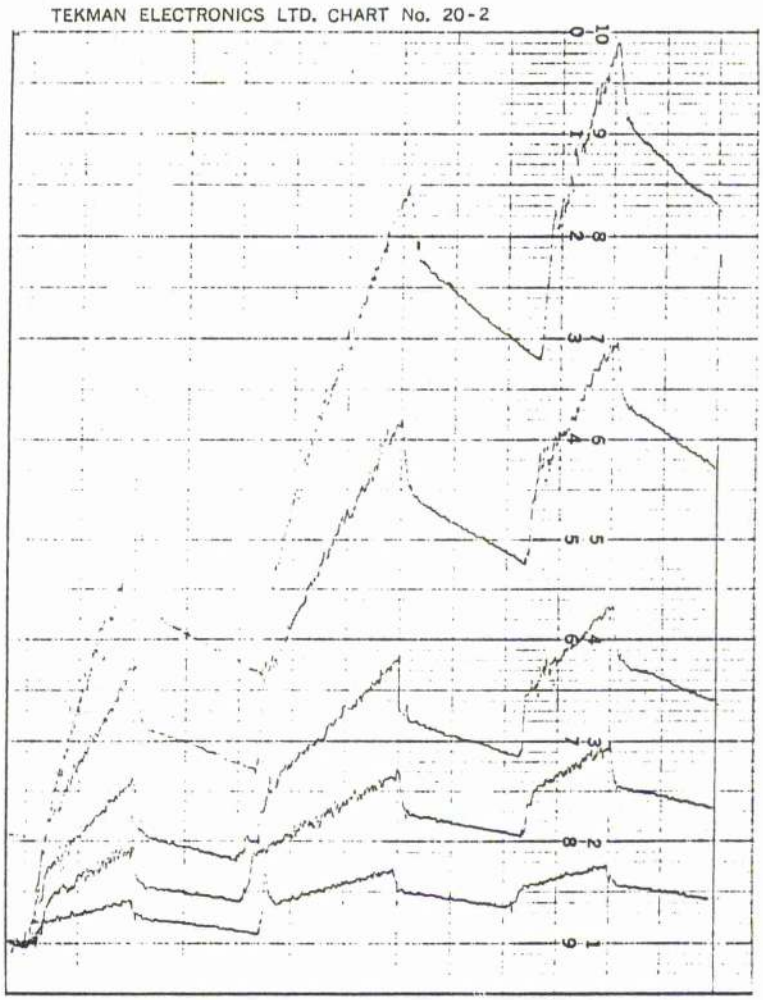

Fig. 3.11(b) Representation of measured heating curves by different electron energies (from top: 50, 40, 30, 25 and 20 keV) of focused beams. X: 60 mm/min; Y: 5 mV/cm (2 mm/div); load resistor: 1 megaohms.

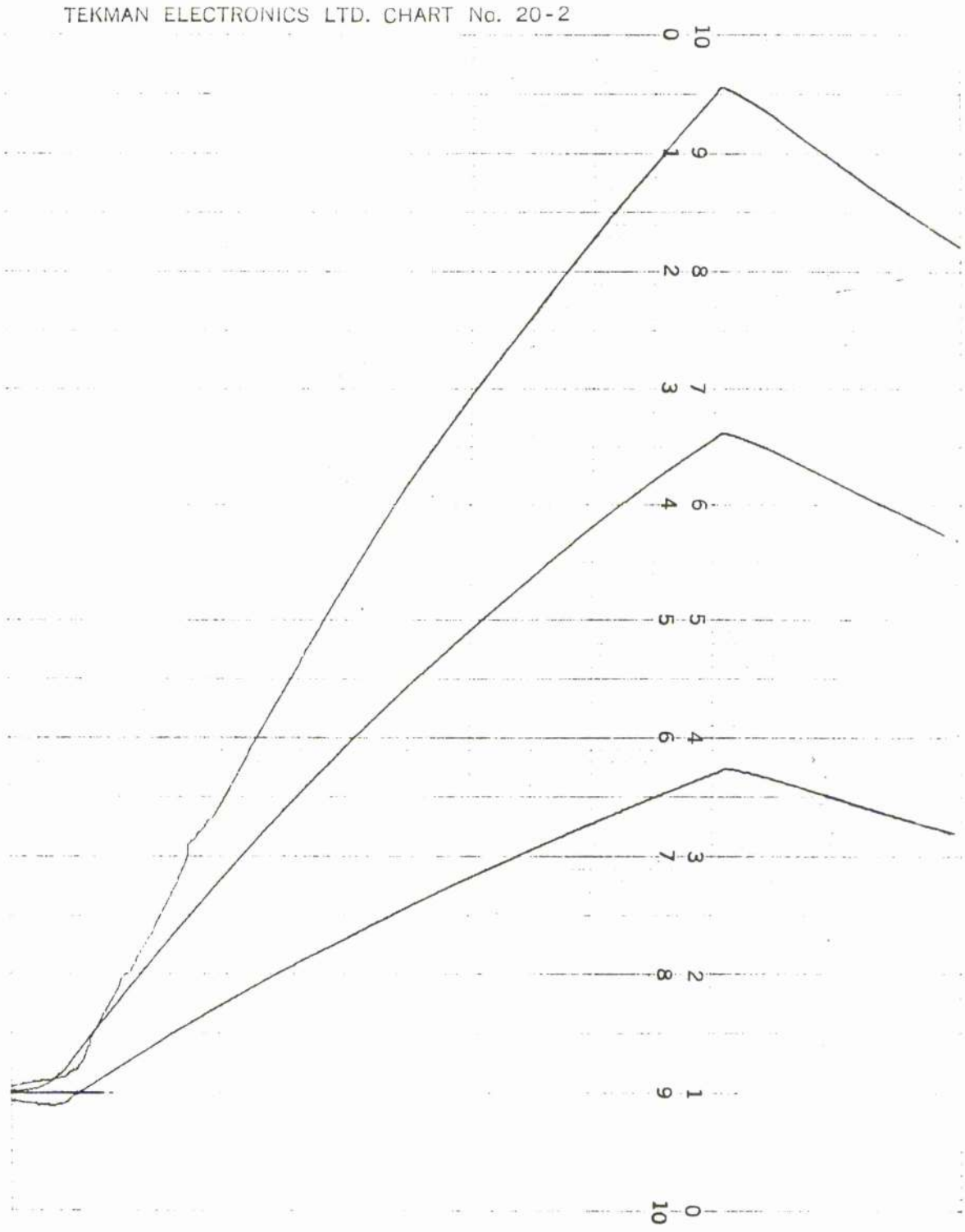

Fig. 3.12 Scaled heating curves by different electron energies (from top: 42.8, 38.5, 31.3 keV). X: 100 mm/min; Y: 0.5 mV/cm.

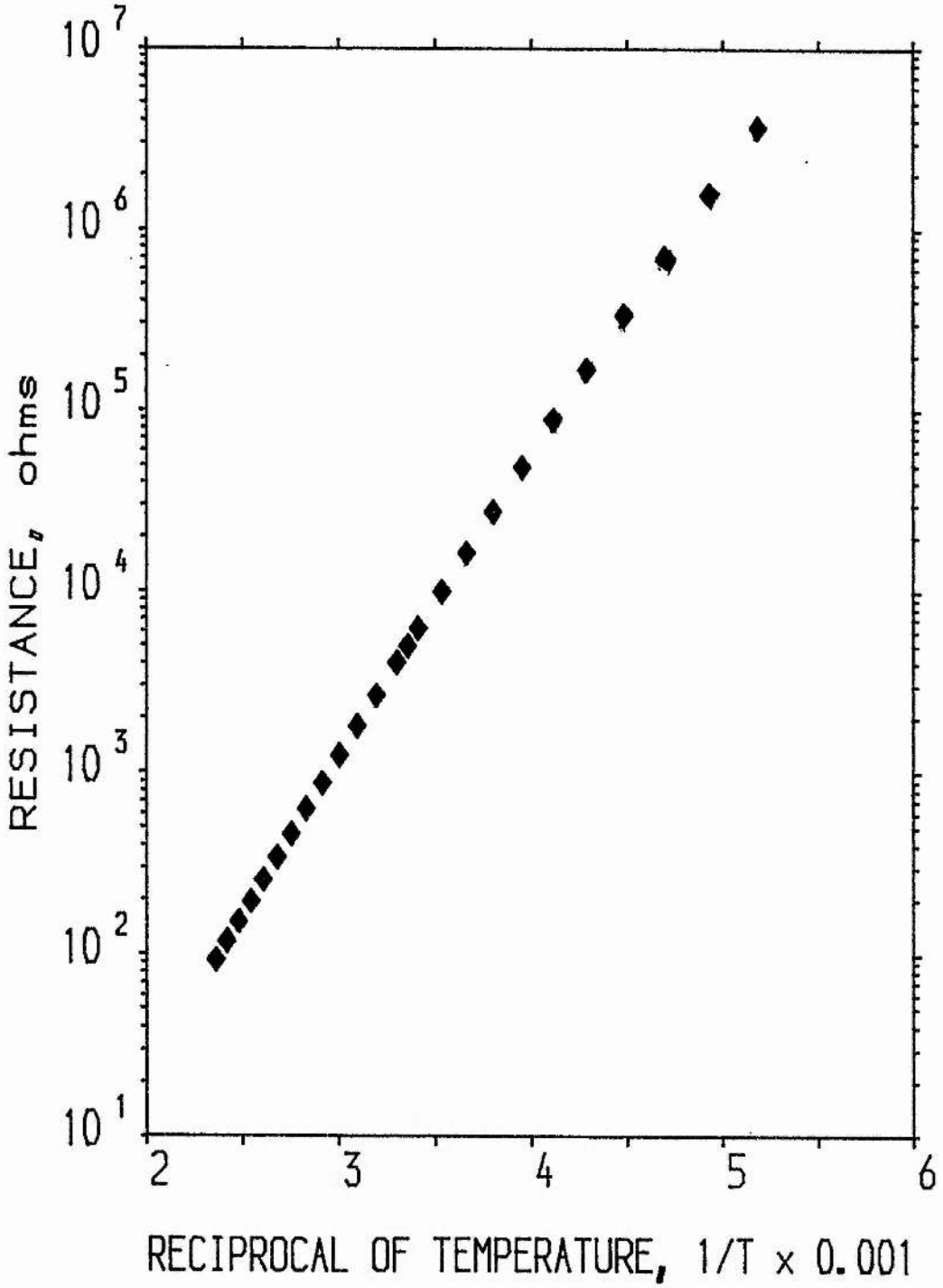

Fig. 3.13 Plotting of Log R versus reciprocal of temperature for the thermistor of 5 kiloohms at 25 degrees centigrade.

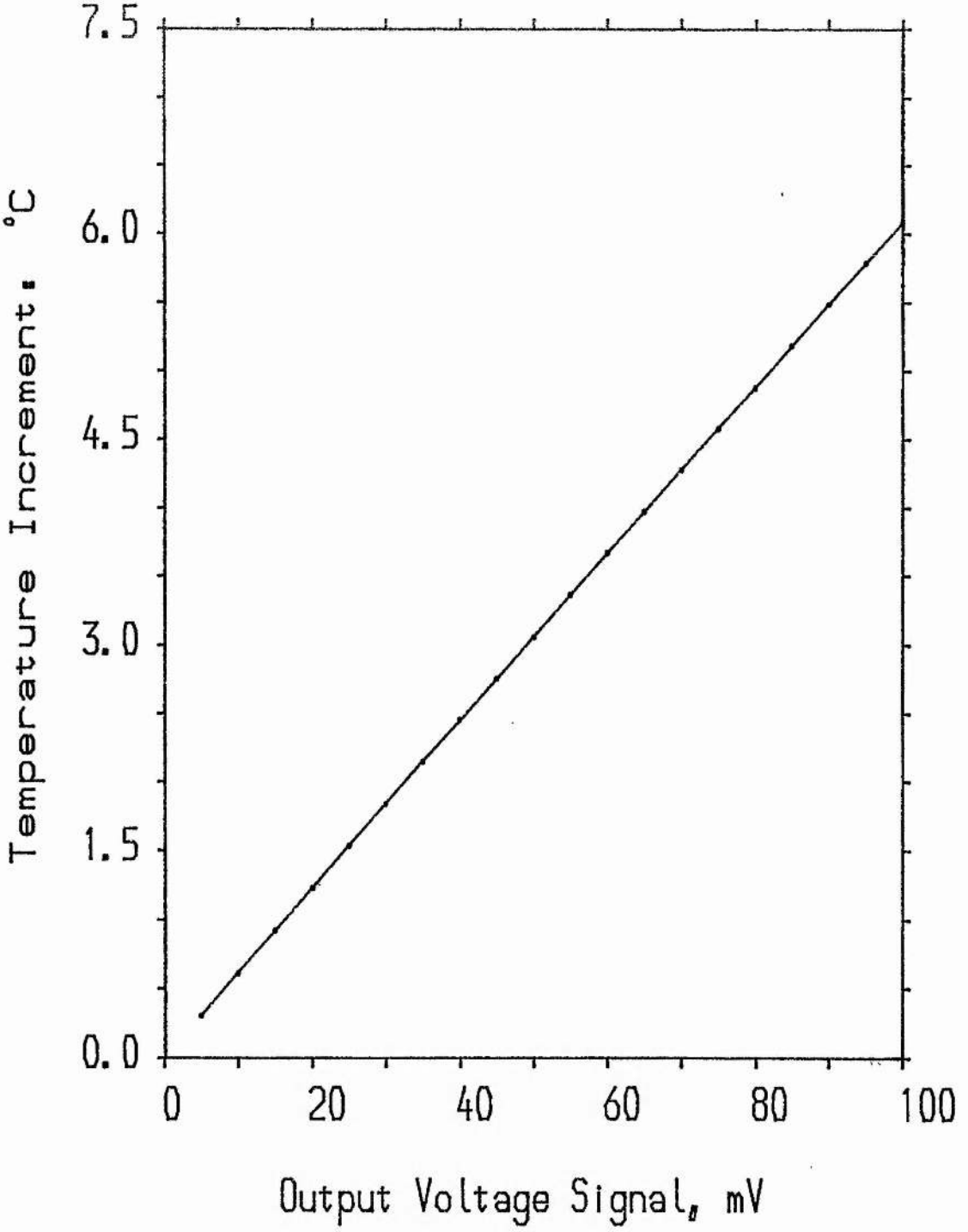

Fig. 3.14 Output voltage signals from the Wheatstone bridge circuit from temperature rise expressed as the resistance change of the thermistor.

Table 3.1 Measured voltage signals from which the leakage rate K (1/sec) is determined by the least squares method, and the temperature rise T_m and the corrected temperature or the real temperature T_r are calculated.

kV	50	45	40
t, sec	66	66	56
V_{cf}-V_{ci}, mV	8.25	5.25	2.42
K, x10 $^{-3}$	8.665	8.337	12.2
T_m, °C	0.483	0.308	0.142
T_r, °C	0.635	0.401	0.207

given in Fig.3.13, Fig.3.14 and Table 3.1.

3.3.2 Electron fluence detection method

The electrons, in the present experiment, traverse a 5 μm polyester window first and then enter into the irradiation chamber of low vacuum, within which the energy loss for >40 keV can be shown negligible. For air at 20 ^{0}C, the density $\rho=1.58\times10^{-6}P$ (g/cm^3), where P is in torr. For 40 keV electrons (which will be used in the experiment) travelling in air over a distance d=10 cm at 10 torr pressure, the stopping power at the residual energy (38.8 keV) is about 7.4 MeV-cm^2/g. Then the energy loss fraction $dE/E=dx\rho xS/E$ is about 3%. Therefore, the total energy loss in the window and in the petri dish cover (3.5 μm polyester, detail given in Chapter IV) can be found. The calculated energy loss spectra of electrons are discussed in Chapter V.

The absorbed dose for a given energy electron can be calculated now from the electron fluence. However, the total escaped electrons should be taken into consideration first. Electrons can suffer multiple scattering due to many small deflections in traversing matter. At low energies, *e.g.*, <100 keV, the plural scattering or its modification should be considered (Bichsel, 1968). However, backscattering, an extension of multiple scattering to angles larger than 90^0, is of direct interest at present because the magnitude of the fluence is affected by the fraction of the backscattered electrons. At energies below about 10 keV there is discrepancy among different authors for the value of the

backscattering coefficient, η (*e.g.*, Waibel & Grosswendt, 1978). This coefficient is treated as a parameter independent of the electron energy. However, in low Z material this may introduce an error of up to 60% according to Hunger and Küchler (1979). They have measured the backscattering coefficients in different specimens for electrons of energies of 4-40 keV, and they fitted an empirical formula to their experimental data as follows

$$\eta\,(Z,E) = E^{\,m(Z)}\, e^{C(Z)} \qquad (3.20)$$

where Z is the atomic number, E is the energy in keV.

$$m(Z) = 0.1382\text{-}0.9211\; Z^{-0.5}$$

and

$$e^{C(Z)}=0.1904\text{-}0.2236\ln Z+0.1292\ln^2 Z\text{-}0.01491\ln^3 Z$$

The detection of the electron fluence in the present experiment is very similar to that used by Hunger and Küchler's. The correction factor (due to the escaped secondary electrons) is given by

$$f = 1/(1-\eta_d) \qquad (3.21)$$

where η_d is the backscattering coefficient for the detector. The backscattering from the detector surface can be reduced by applying a negative bias voltage onto a grid made of micro mesh placed on top of the detector's surface. The calculated correction factor is plotted in Fig.3.15. The fluence measured then is corrected with the above result.

A Faraday cup is combined with the calorimetric method for measuring the electron fluence. The schematic arrangement is given in Fig.3.10. The total electron charge collected in the cup is displayed on a potentiometer, and the electron fluence rate is found from the formula

$$\phi = j / (1.6 \times 10^{-19} C) \ (1/cm^2\text{-sec}) \qquad (3.22)$$

where j (=i/s) is the current density in A/cm^2 measured ($s=\pi r^2$ representing the surface area of the cup normal to the direction of the incident particles assuming parallel beam). The dose-rate $\dot{D}$ in Gy/sec is given by

$$\dot{D} = 1.6 \times 10^{-10} \phi \, S/\rho \qquad (3.23)$$

or in Eq.(3.22), by integrating ϕ, the fluence $\Phi = \int \phi(t)dt$, from the stopping power S or L, of the electrons, to get the total dose, D in gray, $D = 1.6 \times 10^{-9} \Phi L/\rho$.

Normally, the electron fluence is monitored by the fixed detector which can be corrected by the backscattering factor. As said earlier, the irradiation field is expected to be a uniform one of diameter greater than, say, 10 mm, which will be the sampling surface area. A second detector which is movable, mounted on the sampling holder, has been used to measure the uniformity. The result is given in Fig.3.16. It is seen that the irradiation field, within a radius of 10 mm, deviates by a maximum about 10% from that at the centre. Uniformity is therefore reasonably good. The result in Fig.3.16 has been normalized for clarity.

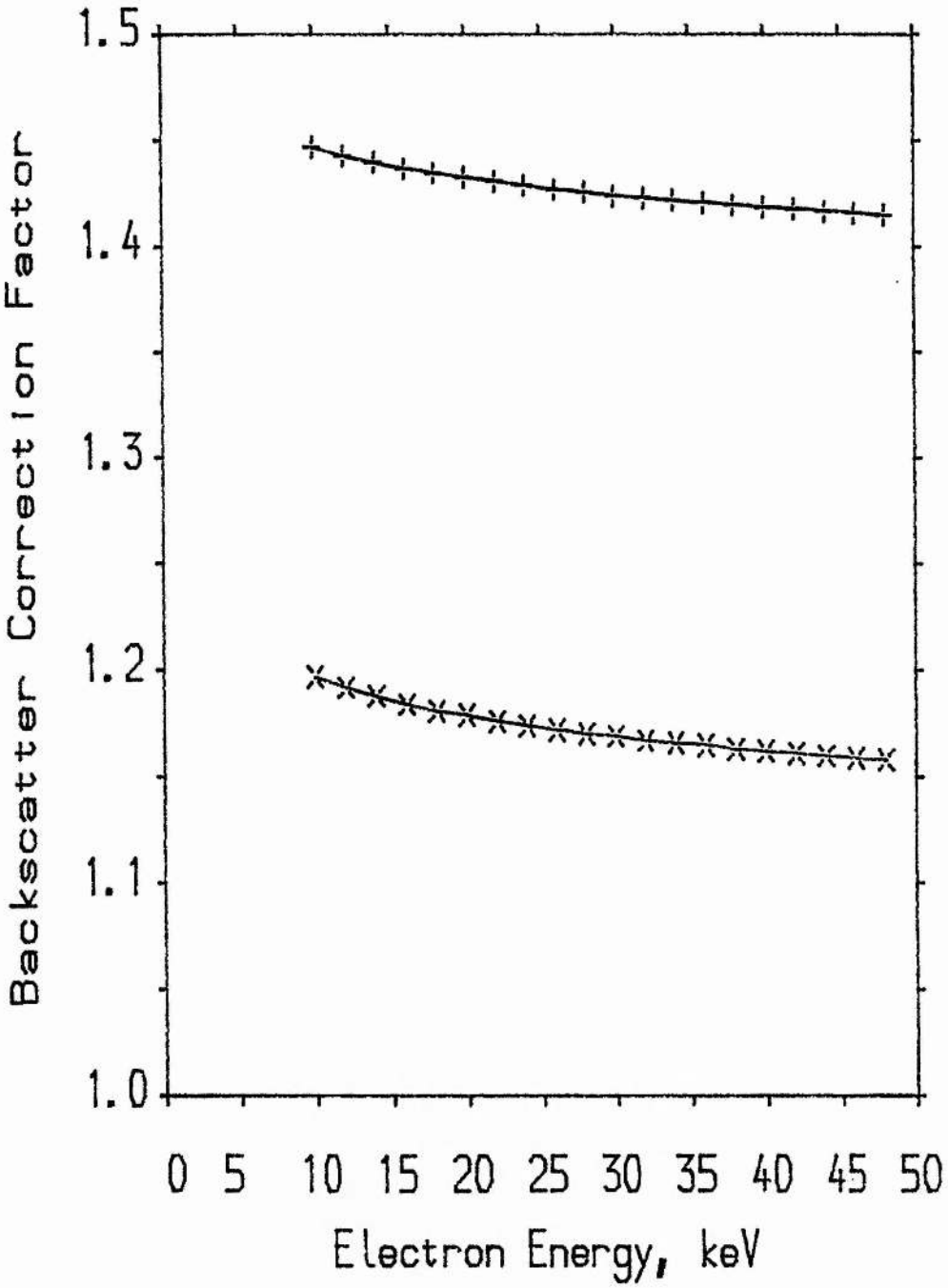

Fig. 3.15 Backscattering correction factors. Above: backscattering on copper; below: backscattering on aluminum.

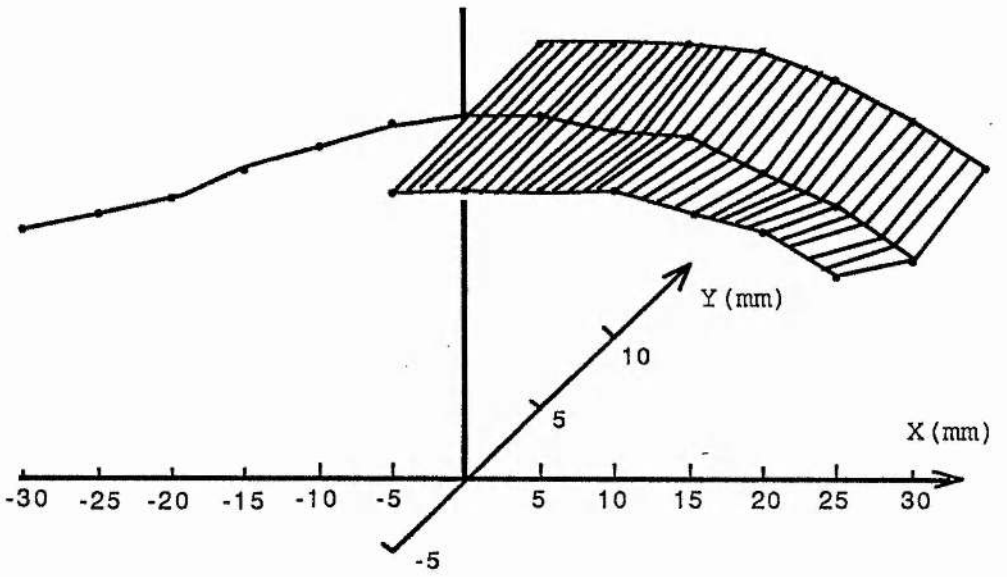

Fig.3.16 Graphical representation of the electron irradiation field normalized to the centre point of interest. X: the forward direction of the sampling rod; Y: the left direction of the sampling rod.

3.3.3 Alpha irradiation dosimetry

Ionization methods of dosimetry have been discussed extensively both in experimental application by Boag (1966) and in the Bragg-Gray theory by Burlin (1968). For example, conventional cavity ionization chambers are one of the most commonly used devices, particularly for the dosimetry of photon beams.

The extrapolation chamber is a special type of the ionization chamber first devised by Failla in 1937 for the purpose of measuring the superficial dose in an irradiated material. This type of chamber has been reported for the measurement of the dosimetry of β-ray sources, the dose-rate in electron beams (cf. Boag, 1966) and for α-ray dosimetry (Datta *et al.*, 1976). Such a chamber was therefore designed and built by the present author to measure the doses to the cells from the alpha particles.

When an ionization chamber is exposed to radiation, as the voltage difference between the electrodes of the chamber increases, at first almost linearly with voltage, and later more slowly, until the ionization current finally approaches the saturation value, i_s. This relation when i (current) from the collector is plotted against V (voltage) is called the saturation curve. It is known that at low collecting voltages, some of the ions, produced in the gas filled in the cavity of the chamber, meet and neutralize with the others of opposite sign before they can reach the collector. This phenomenon is called recombination and can be reduced, for example, by increasing the field strength or by

reducing the separation between the electrodes. So that until the collected current is independent of the applied voltage in a certain range. And then the appropriate quantity, *e.g.*, the fluence rate of the incident particles, may be calculated.

The saturation current may be estimated in an extrapolation ionization chamber using Mie's theory as discussed by Greening (1964), who reviewed the theoretical principles and used data of photons' works for the analysis. For a parallel-plate ionization chamber with separation d (cm), at an ionization rate $\dot{q}$ (esu/cm^{-3}-s^{-1}), the ionization current i is given by

$$i = f \dot{q} d \tag{3.24}$$

where f is the collection efficiency. Assuming the ionization current is carried by positive and negative ions having mobilities k_1 and k_2 (cm^2/s-V) respectively, and recombination coefficient r (cm^3/s), Greening showed that

$$i_s = i \left[1 + \frac{1}{6} \frac{r/e}{(k_1+k_2)/2(k_1k_2)^{1/2}} \frac{d^4\dot{q}}{V^2} \right]$$

$$= i \left(1 + K d^4 \dot{q} / V^2\right) \tag{3.25}$$

where K was found to be 225 (±12%) for series measurements, V is the high voltage applied to the plates. From this, it is deduced that (Boag, 1966)

$$i = \dot{q} d \left(1 - \frac{m^2 d^3}{6} \frac{i}{V^2}\right) \qquad (3.26)$$

where m is a mixed constant equal to 36.7 ± 2.2 (s $cm^{-1} esu^{-1} V^2)^{1/2}$ or, in SI unit, $(2.01 \pm 0.12) \times 10^7$ (s $m^{-1} C^{-1} V^2)^{1/2}$. Therefore, a plot of i versus i/V^2 should give a straight line, the intercept of which on the $i/V^2=0$ axis should give i_s, the slope of the line is $-m^2 d^4 \dot{q}/6$. Eq.(3.26) is valid for $i/i_s > 0.70$ in air experiments.

From the saturation current, i_s, the fluence rate ϕ can be calculated from

$$\phi = (i_s W)/(e A E) \quad (cm^{-2} s^{-1}) \qquad (3.27)$$

where W (33.9 eV), defined in Eq.(1.5), is the mean energy needed to produce an ion pair. A (cm^2) is the window area through which alpha particles enter the ionization chamber, e is the electron charge, and E is the total energy loss of an alpha particle after travelling through the distance d.

It is found that Greening plotted i/i_s, the normalized ionizing current versus $(i/i_s)^2/V^2$ and $(i/i_s)/V^2$ respectively, using published data for ^{60}Co radiation. He showed that better linearity exists in the latter relationship described by Mie (1904) than in the former by Boag (cf. Boag, 1966). Datta *et al.* (1976) applied this theory to alpha particle dosimetry using an extrapolation air ionization chamber with parallel plates. The present work followed a similar procedure.

However, according to Boag (1966; 1987), if initial (and/or geminate) recombination (which is applied to the recombination of positive and negative ions formed within the track of a single ionizing particle) is dominant, one should find a linear relationship between 1/i and 1/X (where X is the field strength) in the near-saturation region (*e.g.*, $i/i_s>0.7$)

$$1/i = 1/i_s + \text{constant}/X \qquad (3.28)$$

whereas if only general recombination (it proceeds once the processes of thermal diffusion and ionic drift have destroyed the initial track structure, *i.e.* positive and negative ion formed by different ionizing particles meet and recombine as they drift towards the opposite electrodes) is present the relationship should be

$$1/i = 1/i_s + \text{constant}/X^2 \qquad (3.29)$$

Furthermore, for α particles, the theoretical treatment of columnar recombination, by Jaffe may be considered. The theoretical saturation current I may be determined by

$$1/i = 1/I + g\, f(x)/I \qquad (3.30)$$

Extensive experimental data may be needed to determine the parameter g and the function f(x). Nevertheless, Boag pointed out that, it is easy in theory, but may often be very difficult

experimentally to distinguish these recombinations. Some initial recombination must always occur, it is only of importance when the ion density in the track is high-as, for instance, in α particle tracks even at atmospheric pressure.

The dosimetric measurements were performed in an example arrangement similar to Datta *et al.*'s (1976). The air chamber used here is similar to that of the real irradiation situation shown in Fig.3.9. A pair of 5 cm diameter petri dishes performed the parallel plates. These were placed above the disc alpha source. The inner surfaces of both plates are fully covered with a copper foil. The top one was connected to a Keithley Electrometer as the charge collector, and the high voltage was applied to the other plate, the collector plate was surrounded with a circular piece of copper foil as the guard ring which was earthed. A small hole was driven in the centre of the window so that the sensitive volume of the chamber could be varied by changing either the window size or the collector to window distance. The saturation current determined at the required distance (window to source) and from which the fluence rates are calculated are given in Table 3.2. A curve of 1/i plotted vs. 1/V (or d/V, d=1 cm) is given in Fig.3.17.

It was found that for the curium source, the fluence rate determined from the saturation current i_s at 1 cm reduced to about 40% when the window diameter was reduced from 5 mm to 2 mm. Also, it changed (to 37%) from the centre to the near edge of the source. Similar change was found when the distance

between the window and the source was increased. For the americium source, if the window diameter was reduced, the measurement of the ionizing current became difficult. But the uniformity of the fluence rate of the second source (ca.$\pm$4% of the median value) was much better than the former one.

Therefore, the cell survival data by ^{244}Cm irradiation might involve some larger error due to the inherent non-uniformity at the short distance. It may be suggested that, for a more strict requirment of the irradiation by this ^{244}Cm source, a collimator is needed. On the other hand, the cell survival data by ^{241}Am were satisfactory, this was also because due to the prolonged irradiation which might have reduced the statistical error of the incident particles distribution.

A rigorous analysis of the error involved in the dose-rate could be done by weighing the LET spectrum of the incident alpha particles from a non- collimated disc source, at the point of interest. However, the error can be estimated approximately as follows.

Consider the diameters of the ^{241}Am source and the cell sample are 6 mm and 10 mm respectively. They are separated at a normal distance of 10 mm. The longest possible distance between the source and a cell at the edge of the sample will be about 13 mm. An alpha particle can lose a total minimum energy of about 1.64 MeV (*i.e.* in 10 mm air, 3.5 μm in the petri dish film, 3.5 μm in the cell), or a maximum 2.03 MeV (13 mm in air, 7.0 μm in the media), the respective LET values are 110 and 118 keV/μm at the

corresponding residual energies. Then from the fluence rate given in Table 3.2, the dose-rate is found to be 0.017 or 0.016 Gy/min at the above two groups of values. It is seen that although for a cell at the edge is exposed to a bit higher LET particles, due to the slightly reduced fluence rate at the same place, the balanced effective dose-rate does not seem to be changed very much in this example, compared to a cell in the centre of the sample which may be exposed to the particles of minimum LET but slightly higher fluence rate.

Table 3.2 Fluence rate of α particles determined from the saturation current by the extrapolation air ionization chamber (window to colletor distance d=1.0 cm; window diameter, 2 mm for plain data and 5 mm for bold data).

alpha source	window-source distance (cm)	saturation current (pA)	fluence rate ($cm^{-2}min^{-1}$)
	1.0	**977**	**5.94×10^7**
	1.0	64.1	2.43×10^7
^{244}Cm	1.0*	23.6	8.95×10^6
	2.0	**341**	**1.67×10^7**
	2.0	16.2	4.95×10^6
	2.0*	8.35	2.55×10^6
	1.0	**1.83**	**9.67×10^4**
^{241}Am	**1.0****	**1.57**	**8.93×10^4**

Notes: *, **- 3 mm or 5 mm eccentrically from the aligned centre;

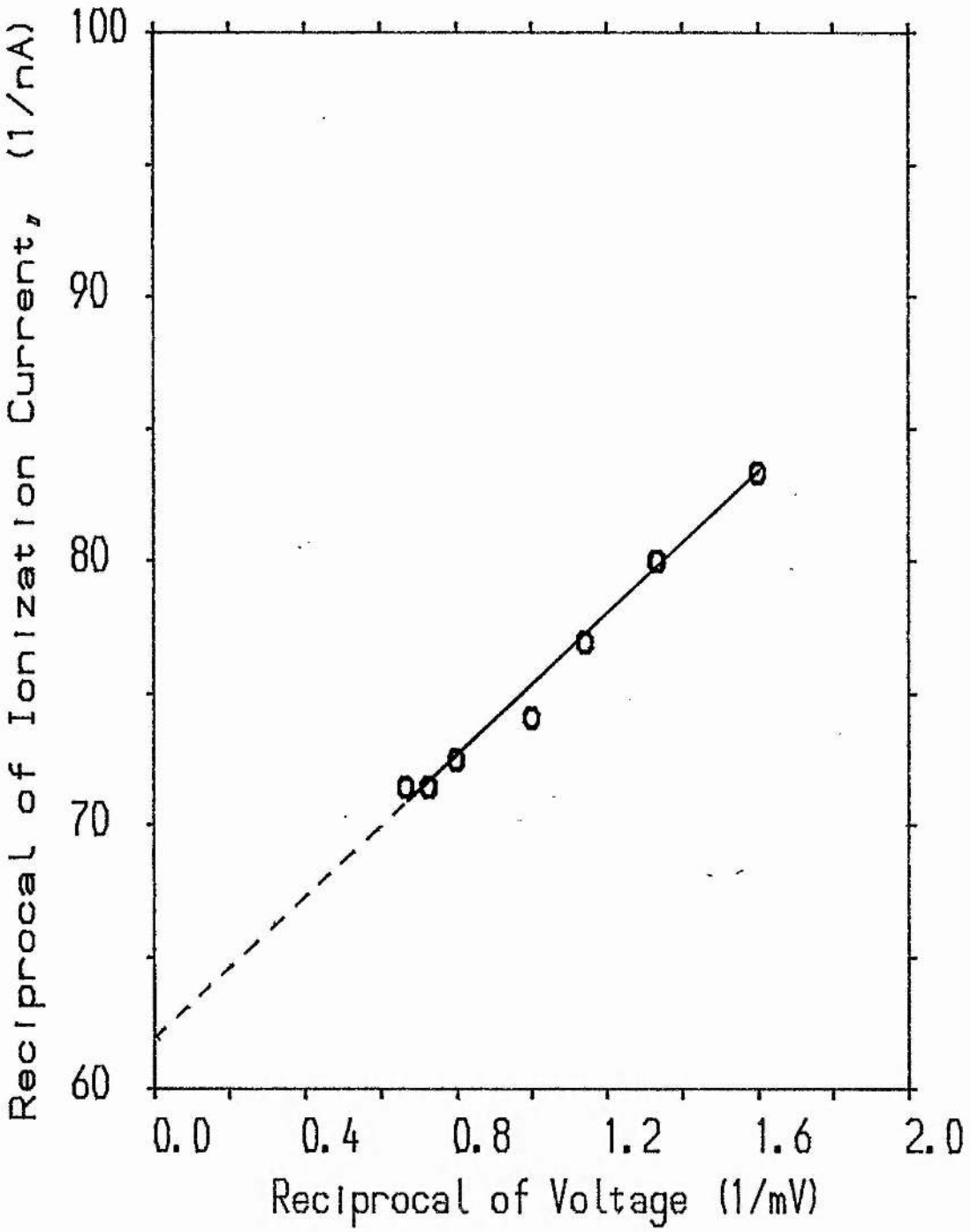

Fig. 3.17 A curve to determine the saturation ionization current for Cm-244 alpha source at 2 cm (window diameter is 2 mm). The saturation current is extrapolated to be 16.2 pA.

CHAPTER IV

EXPERIMENTAL: BIOLOGICAL ASPECTS

4.1 Materials and Methods

Chinese hamster V-79 lung cells were chosen for the investigation so that survival results obtained may be more readily compared with data from the literature. The biological experiments were performed in the cell culture laboratory in the Department of Anatomy and Experimental Pathology.

About $5x10^6$ cells (in 10% DMSO medium) stored in liquid nitrogen were thawed at 37 ^{0}C for the culture, and syringed into a 75 cm^3 culture flask. 15 ml of Eagle's MEM (minimum essential medium) with 10% FCS (foetal calf serum), 1 ml G (glutamine), and 1 ml P/S (penicillin, streptomycin) was carefully added into the flask under gentle agitation. The median pH value was maintained by gassing the flask with 5% CO_2 + 95% air. The procedures were performed in the air flow lamina under sterilised conditions. The culture medium is not a strict factor in the present study. For V79 cells, F10 medium, F12 medium and Eagle's medium are all reported to be satisfactory (Szechter & Schwarz, 1977; Mitchell *et al.*, 1979; Held, 1986).

Incubation for 3-5 days at 37 ^{0}C will give rise to an

exponential growing culture for irradiation colony assay purposes. A subculture could be made for continuing the experiment. To avoid multiplicities the cells were pipetted about ten times up and down in preparing the subculture particularly in diluting the cell mediums for the cell colony assay. Under the microscope, very few clumps of two or three cells could be seen in the sample.

Trypsinization of the colony cells is achieved by treatment with 5% (BACTO) trypsin (DIFCO Labs, Detroit, prepared in 10 ml distilled or deionized water), *i.e.*, 1 ml trypsin solution is added into 19 ml DPBS (dulbeccos phosphate buffered saline, Mg^{2+} and Ca^{2+} free) for less than 10 minutes to release the cells from being attached to the bottom of the flask after the incubation. Longer times for the cell in trypsin may be harmful, since the pancreatic proteolytic enzyme, trypsin, catalyzes the hydrolysis of the peptide bonds of the cellular proteins. But the remaining trypsin does not have to be washed as the immediately added serum can inactivate it (cf. Kruse & Patterson, 1973).

Cell numbers were determined for the x-ray reference experiment by the Coulter Counter (Model Z_BI). 1 ml cell medium in 20 ml Isoton (Azide-free balanced electrolyte solution), counts 0.5 ml, the Coulter Counter was scaled. 3 ml of 1-5x10^4 cells/ml were irradiated in a conical tube. Dilution was made before the cells were plated into the 5 ml culture dishes (Cel-Cult, STERILIN Ltd., FELTHAM). After incubation for 7 days, the cell colonies were stained in methylene blue (3g/l) in 30% alcohol for 15 minutes. By counting the colonies, the plating efficiency was found to be 40-80% calculated from the controlled petri dishes.

The irradiation was carried out using a 250-kV (STABILIPAN) x-ray machine at a dose-rate of 0.709 Gy/min at 14 mA with 0.5 mm Cu filtration. The survival fraction is the ratio of the colonies counted to the cells seeded and corrected for the plating efficiency. By plotting the survival fraction against the doses, the survival curve is obtained. The result of x-ray irradiation is given in Chapter V together with the results for electron and alpha particle irradiation.

4.2 Monolayer Cell Culture Technique

Of specific interest in the present study is analysis of the data obtained for the radiation effect in mammalian cells in terms of physical and biological quantities. For electron and alpha particle irradiation, therefore, monolayer cultured cells were necessary.

Barendsen and Beusker (1960) and Cox *et al.* (1979) have used Melinex (polyester) film sealed by Araldite, polymerized at 160 ^{0}C onto a petri dish, or a glass cylinder using an alkali-etched method. Simmons *et al.* (1983) used specially constructed dish with a Mylar film stretched across it to form the base of the dish. The thickness of the films used were all reported 6 μm.

In the present cell colony assay studies, a polyester film (Melinex, Goodfellow) of 3.5 μm thickness was used for the monolayer cell experiments. The petri dishes of 3 cm diameter used were culture grade. The procedure of preparing a monolayer sample is as follows.

2 ml of about $5x10^5$ exponential growing cells were pipetted into the dish, and gassed for 30 seconds. A cut piece of 4x4 cm^2 film, which had just been wiped with ethyl alcohol twice was dried by facing the cleaned surface towards the lamina flow filter direction. With very careful handling the prepared film could be substituted for the petri dish cover. The film was trimmed to a round piece (ca. 3.5 cm diameter) so that it covered the open top of the dish and that it could be properly taped along the outer surface of the petri dish. A dish well-sealed in the described manner had a flat surface which could withstand low vacuum pumping (*e.g.*, <0.1 torr). The original cover was still useful to protect the fine film cover from being pricked on a hard contact or during transport. Both scissors and tweezers used were soaked in alcohol for a minute and flamed now and then before being used for each sample.

The double covered petri dish should be turned upside down before being placed in the incubator overnight to enable the cells to attach. The controlled number of the plated cells ensured that the cells would attach on the polyester surface with minimum overlapping. This was checked under the microscope. Without overnight incubation, it took a few minutes for the cells to become a sediment deposited immediately on the polyester surface. This observation is meaningful in future for studying irradiation when the cells are in spherical form.

Before irradiation, the polyester surface was cleaned again with ethanol such that no dust or debris would affect the thickness of the film. After the exposure, the surface was cleaned twice, then

cut as near as possible around the centre of about 1 cm (maximum less than 1.5 cm) diameter piece, and dropped into a fresh petri dish, into which 1 ml trypsin was added for washing. The trypsin was then discarded. 1 ml of fresh trypsin was added for 20 seconds and again discarded before incubating for 10 minutes. 2.5 ml fresh medium could be added into the trypsinized dish now, then at least four counts were taken for each sample with a NEUBAUER chamber counter. The rest of the processing technique was the same as that for the conventional culture method.

CHAPTER V

EXPERIMENTAL RESULTS AND DISCUSSION

5.1 X-ray Irradiations

5.1.1 Results of x-ray irradiation

Conventional study on dose or dose-rate effect experiments is almost always carried out with x-rays as the reference radiation. This is because x-ray irradiation has, historically, always been generally available and is still frequently used in radiation research. Thus, the cell colony assay study was started from x-ray irradiation in the present research.

The observed survival curve for V79 cells by x-ray irradiation is shown in Fig.5.1. The survival fraction is defined as the ratio of the number of the colonies survived, N, to the number of the cells plated, N_0, and then scaled by the plating efficiency, P.E., *i.e.*,

$$S = N/(N_0 \times P.E.) \qquad (5.1)$$

It assumes that one colony was grown from one plated cell. In Fig.5.1(a), a survival curve (fitted with Eq.2.4) of x-ray irradiationis is shown. In Fig.5.1(b) and (c), the data are fitted with the two-component model defined by Eq.(2.6) and with the dual-action

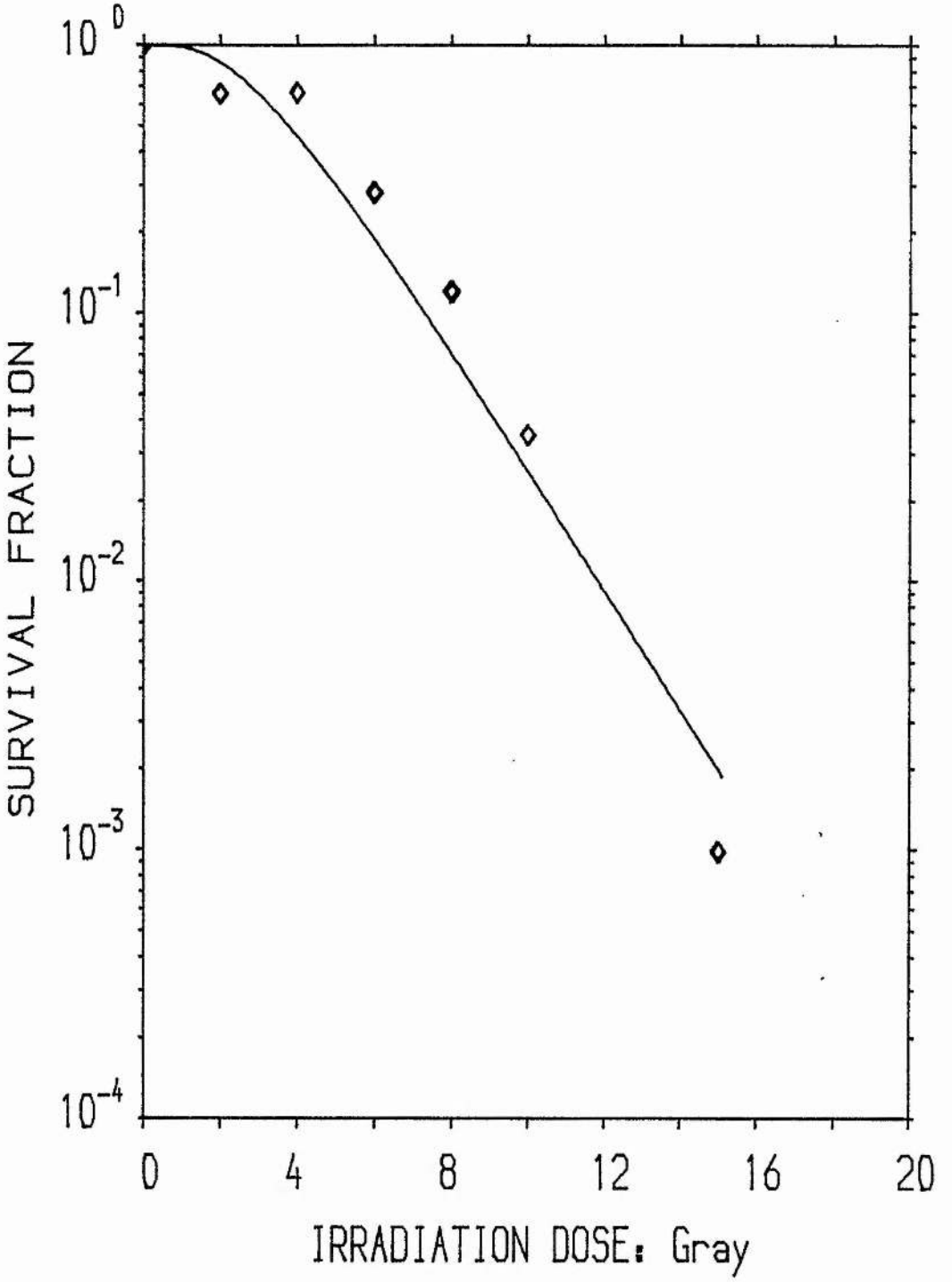

Fig. 5.1 (a) Dose effect result of V-79 cells by 250 kV x-ray irradiation, at dose-rate of 0.709 Gy/min (0.5 Cu filtration).

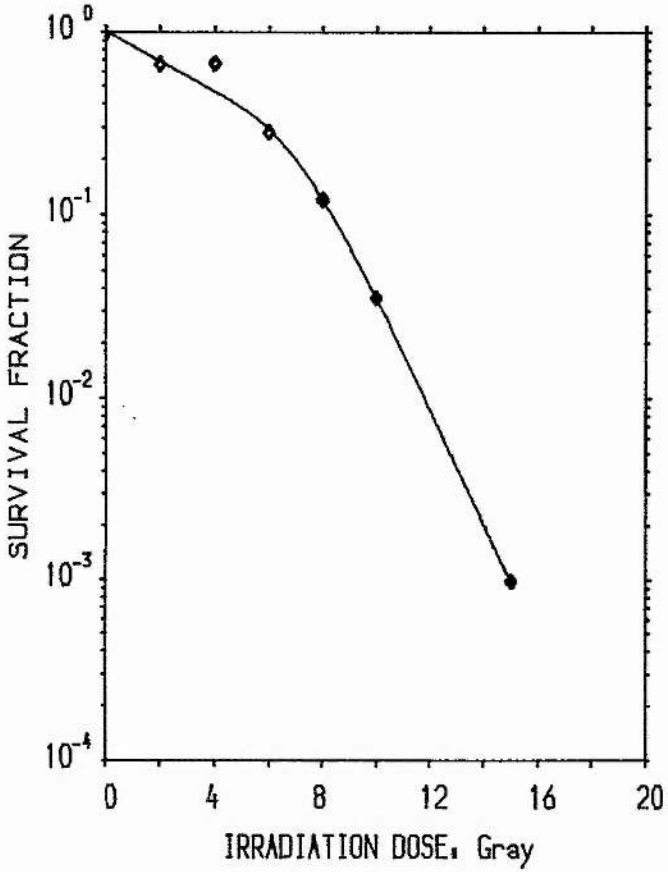

Fig. 5.1 (b) Dose effect result of V-79 cells by 250 kV x-ray irradiation, at dose-rate of 0.709 Gy/min (0.5 Cu filtration).

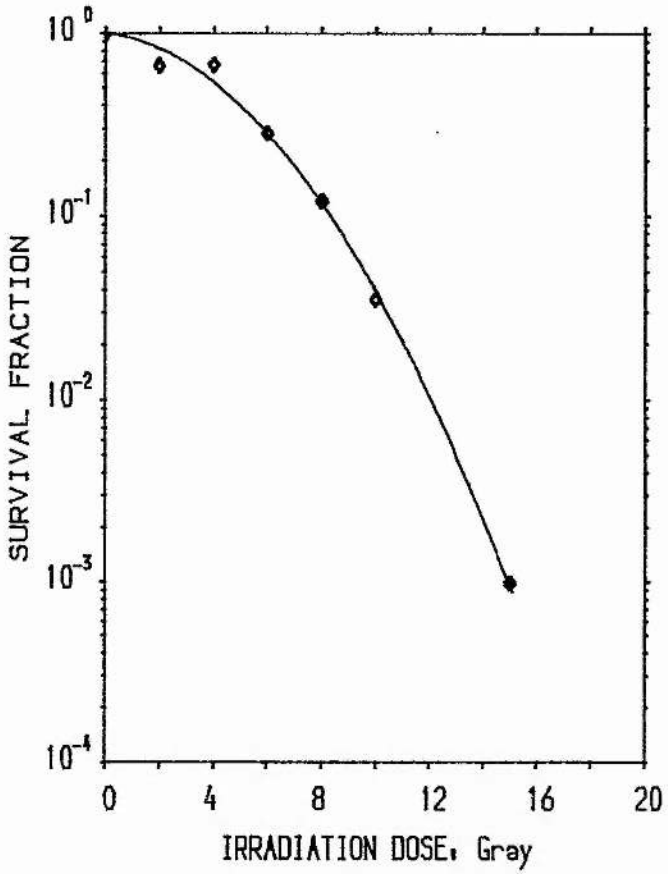

Fig. 5.1 (c) Dose effect result of V-79 cells by 250 kV x-ray irradiation, at dose-rate of 0.709 Gy/min (0.5 Cu filtration).

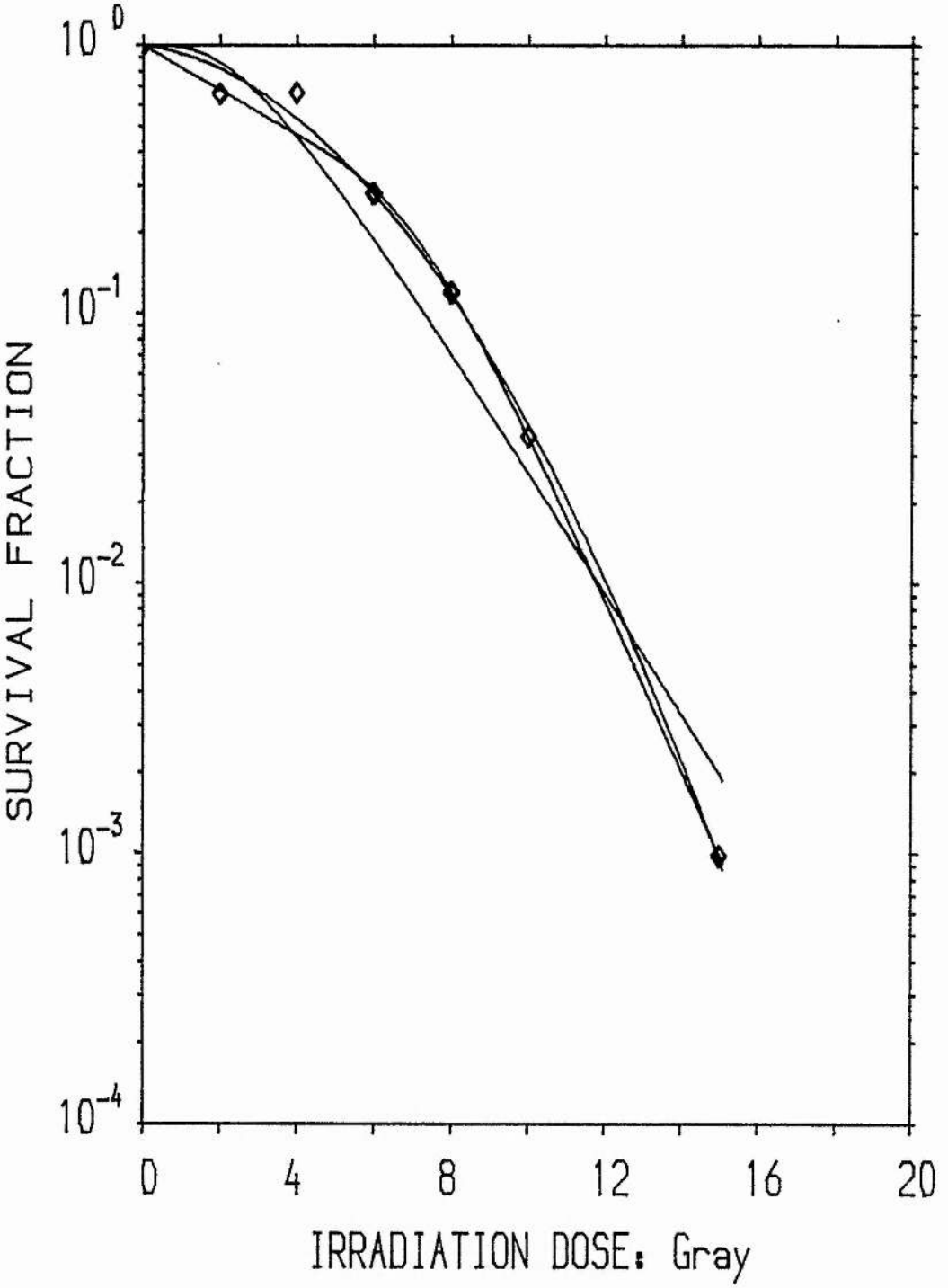

Fig. 5.1(d) Dose effect result of V-79 cells by 250 kV x-ray irradiation, at dose-rate of 0.709 Gy/min (0.5 Cu filtration).

model given in Eq.(2.7). A general comparison is given in Fig.5.1(d) where the three curves are fitted by the three models. The purpose of plotting these figures is merely for a comparison with the results in the reference. The fitted D_0 is 1.79 Gy and n is 4.5 for V79 cells irradiated by x-rays. The result is found to be consistent with published results obtained under similar conditions. Details for x-ray irradiation as well as for the irradiation using electrons and alpha particles is given in Chapter IV. All the experimental data are listed in Appendix B. The errors of the data are analysed according to the reference (Xiao, 1980). The data are processed by a non-linear fitting procedure (Bevinton, 1969; Gilbert, 1969), see Appendix C.

5.1.2 Discussion

Both x-ray and electron irradiations are considered as low LET particles since the calculated values are less than 10 kev/μm for x-rays and around 1 keV/μm for electrons in aqueous medium. Biological evidence has shown that the LET term is an ambiguous quantity, *e.g.*, two different types of radiation may have the same LET but can have different biological efficiencies (ICRU, 1983; ICRU, 1986). Furthermore, although it is easy to calculate the LET value of a specified particle, it is difficult to measure it precisely in experiment because of the range of values present.

On the other hand microdosimetry has an advantage as the microdosimeter can measure the energy deposition events down to one micrometer scale regardless of the difficulty in calculation.

For example, it has been found that in evaluation of the biological effectiveness at low doses, the dose mean (which represents the mean value of the distribution of L or y) for 250 kV_p x-ray are $\bar{L}_D$=2.2 keV/μm, $\bar{y}_D$=3.5 keV/μm, and for ^{60}Co γ radiation, $\bar{L}_D$=0.3 keV/μm and $\bar{y}_D$=1.6 keV/μm, when y is determined in 1 μm diameter sites. The observed RBE values near 2 or 3 are similar to the ratio of the values of $\bar{y}_D$, in the above example, but much less than the ratio of the $\bar{L}_D$ values (ICRU, 1986).

Precise quantitative analysis of x-ray irradiations is more difficult compared with heavy ion particle irradiations, particularly when the continuous photon spectrum of a specified x-ray machine is unknown. Therefore, the radiation effect of x-rays in mammalian cells is conventionally expressed as a function of dose.

An interesting research on x-ray irradiation is to use characteristic x-rays, of which the effective photon energy is well defined. The soft characteristic x-rays produced by bombarding aluminium or carbon targets can give low energy monoenergetic photons of 1.5 keV or 0.3 keV. Characteristic carbon-K x-rays have been used to irradiate the entire cell and are found to be the most damaging biologically of all the photons (Goodhead *et al.*, 1979). The original version of ultra-soft x-ray results was based on the estimated ranges of the photo- electrons and Auger electrons produced in the photoelectric interaction of x-rays and oxygen atom (dominant element in the cell). The conclusions made were that lethal damage could be produced efficiently by individual

tracks, thus the critical damage could result entirely from highly localized energy depositions; no need for 'interaction of sublesions' or 'accumulation of sublethal damage'; and these conclusions can be extended to hard x-ray and γ-ray irradiations (Goodhead, 1983).

From an extensive survey on published survival data of x-ray and γ-ray irradiations to mammalian cells (Chen, 1984; Chen & Watt, 1986) in which the damage effect was expressed as a function of the specific ionization of the secondary electron slowing down spectra, a log- linear relationship (Eq.2.15) was revealed leading to a clearer conclusion, different in concept from any previously published. When the photon results were compared with the heavy ion results (Cannell & Watt, 1985), it was found that the critical damage is determined by the quantity of ionization events rather than the quantity of energy deposition. The most effective damage effect is observed at the optimum specific ionization (cf. Sec.2.3.1).

5.2 Electron Irradiations

5.2.1 Results of electron irradiation

For the electron irradiation experiment, the cells were placed in a different vacuum as described in the last chapter. Precautions had to be taken to ensure that the cells cultured in a petri dish were not affected by their environment. Consequently a test lasting up to 10 minutes was undertaken in which the cells were positioned on the sampling rod and left inside the vacuum

chamber for different times but without irradiation. No apparent difference was observed in the plating efficiency. The result is given in Appendix B1.2.

A survival curve, shown in Fig.5.2, is plotted against the irradiation time for the electron irradiation. The electrons were accelerated at 40 kV, and penetrated first through the window of 5 μm thickness Melinex film and then the 3.5 μm film cover of the petri dish containing the cell culture sample. The effective energy of electrons in the cellular medium is obtained from the calculated electron spectra given in the table in Appendix A3.

From the table, and the plotted graph, the incident energy of the electrons at the cell centre is deduced to be 25 keV. From the measured fluence rate, the total dose delivered is deduced from Eq.(3.23). However, understanding of the action of low energy electrons is more clearly revealed in terms of the irradiation time or the fluence than in terms of absorbed dose. Therefore, the quantities used for the analysis are the irradiation time and the fluence rate. In order to compare the survival for electron irradiation with those of photons or ions data from the literature, the data were again processed by fitting to the target model. The fitted electron fluence at 37% survival on the linear portion Φ_{37} is 2.508×10^9 cm^{-2} by the non-linear fitting method.

5.2.2 Discussion

Only a few studies have been reported for low energy electron irradiations of mammalian cells due to the difficulties in

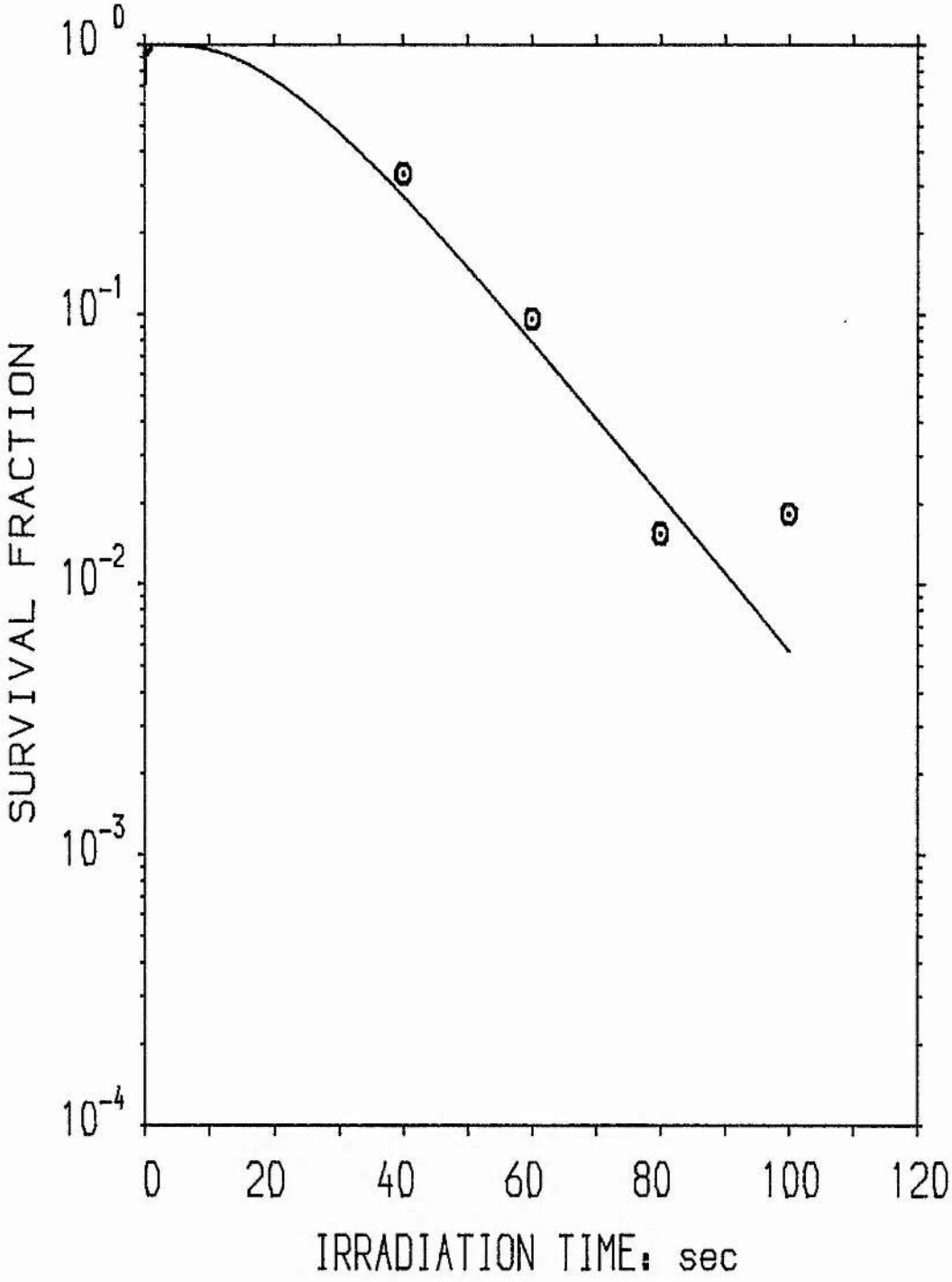

Fig. 5.2 Survival fraction expressed as a function of irradiation time, for V-79 cells by 25 keV electrons at 1.67×10^{8} cm^{-2} $-sec^{-1}$ (0.296 Gy/sec).

Table 5.1 Comparison of survival fraction by 25 keV electrons irradiation to asynchronous Chinese hamster cells

Variations	Present experiment (V-79 cells)	Zermeno & Cole (Don-C cells)
Condition of irradiation to the cells	Cells growing in culture, normal pressure. Broad electron beam	Cells in hydrated state, anoxic. Pencil electron beam
Fluence rate ($cm^{-2}s^{-1}$)	0.167×10^9	19 mm movement in 25 s (sample diameter 13 mm); scan 0.9 cm^2/s
q_{37}, nC/cm^2	0.401	0.20
ϕ_{37}, $\times 10^9$ cm^{-2}	2.508	1.25

experiment. Cole had developed techniques for low-voltage electron irradiation of fully hydrated specimens and applied the technique to the irradiation of viral, bacterial, and later mammalian systems (Cole *et al.*, 1963; Zermeno & Cole, 1969). The characteristics of the reported technique were that, the cells were maintained in hydrated condition, and the samples were cooled to 2 ^{0}C during irradiation, as the sample needed to be exposed at low pressure, therefore, the irradiation was carried out *in vacuo* under an anoxic condition.

In the present research, after the completion of the electron accelerator, a preliminary test irradiation has been tried for the V79 cells. The result is shown in Fig.5.2. The present result is compared with Zermeno & Cole's electron data in Table 5.1. The units used are based on the electron fluence rate rather than on the absorbed dose because of the ambiguity involved. One of the differences is that, the fluence of electron irradiation in the present experiment was about an order of magnitude lower than that of Zermeno and Cole's. The fluence for 37% survival of the present result for the cells exposed to the broad beam of electrons was about twice of the reference electron data of Zermeno and Cole. The fluence rate was kept constant during the whole experiment (Appendix B1.2): any possible factors which may affect the cellular biology was reduced to a minimum in the experimental arrangement. For example, the cells were attached to the film surface in the nutrient medium throughout the irradiation.

We may conclude that the condition of the present electron

irradiation is compatible with these experiments performed with x-rays or heavy ions. If a quantitative analysis is pursued in future, direct comparison can be made between the result of the present electron irradiation and other irradiations. Also, longer time of electron exposure can be practised on the present experimental facility. Although more experiments and more data are expected in future studies, the method of differential vacuum system for the monolayer cell culture irradiation by low energy electrons has been demonstrated successful.

5.3 Alpha Particle Irradiations

5.3.1 Results of alpha particle irradiation

For high LET irradiations by alpha particles, results reported in the literature are at higher dose-rate. The present fluence rate or equivalent dose-rate is at least an order lower than that in the references, cf. Table 5.2. To test the experimental procedure, two high fluence rates, referred to as acute irradiation, were obtained from a ^{244}Cm alpha source under normal pressure. The variance of the fluence rates were obtained when the petri dish sample was at 1.0 cm and 2.0 cm respectively. The dosimetry measurement of alpha particles has been shown earlier in Table 3.2. The survival data by alpha irradiation are plotted as a function of irradiation time in Fig.5.3. Both are pure exponential relations.

Further experiments were performed for chronic exposures at room temperature using an ^{241}Am α source. The averaged

Table 5.2 A comparison of some results of alpha irradiation to Chinese hamster cells

Authors	Alpha source, disc diameter	Source to cell surface distance	E_{eff} (MeV)	LET (kev/μm)	dD/dt (Gy/min)	ϕ ($cm^{-2} min^{-1}$)	D_0 (Gy)	(Depth from cell surface)
Datta et al, 1976 (CHO cells)	Am-241 (4.70 MeV) 0.5 cm	2.7 cm air	0.82	215		3.36×10^5	0.29	(4.0 μm)
		2.3 cm air	1.70	170	0.30	6.00×10^5	0.70	
		1.8 cm air	2.55	140	0.60	1.14×10^6	1.50	
Thacker et al, 1982 (V79-4 cells)	Pu-238 (5.59 MeV) 2.0 cm	65mm He,3mm air + 2x2.5 μm Hostphan	2.60	141	18.84		0.83	(3.5 μm)
Simmons et al,1983 (V79 cells)	Cm-242, 10 cm (6.11 MeV)	1.0 cm air + 6 μm Mylar	5.0	91		3.75×10^5	0.75	(3.5 μm)
Min et al, 1985 (V79 cells)	Pu-238, 10 cm (5.59 MeV)		4.4	100	0.376		0.75	
Present, 1987 (V79 cells)	Cm-244, 0.6 cm (5.80 MeV)	2.0 cm air + 3.5 μm Melinex	2.98	129	2.06	1.00×10^7	1.29	(3.5 μm)
	Am-241, 0.6 cm (5.48 MeV)	1.0 cm air + 3.5 μm Melinex	3.90	108	0.016	9.20×10^4	1.01	

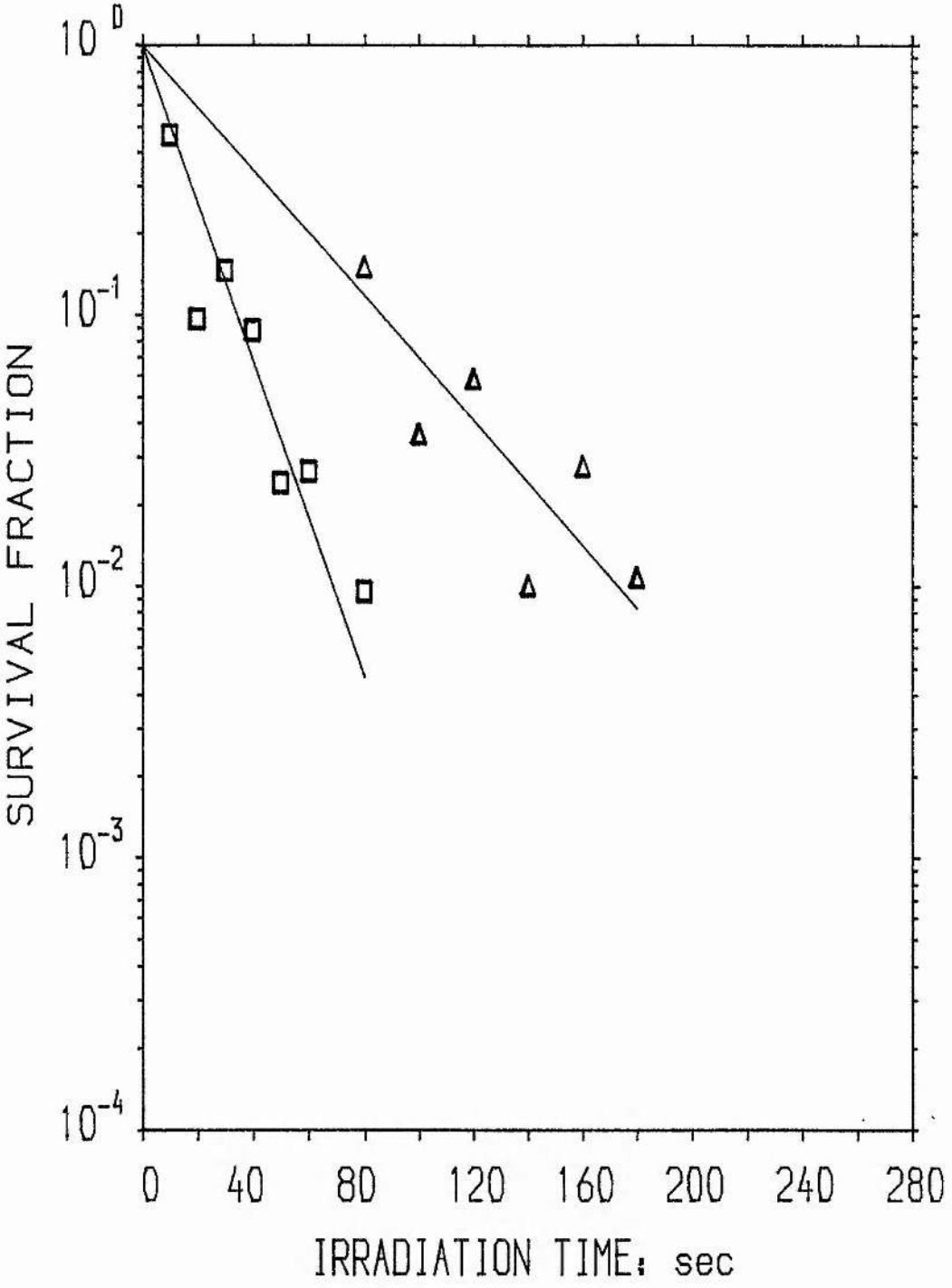

Fig. 5.3 Survival of V-79 cells exposed to Cm-244 alpha particles. Sample-source distance, triangles :20 mm; and squares: 10 mm.

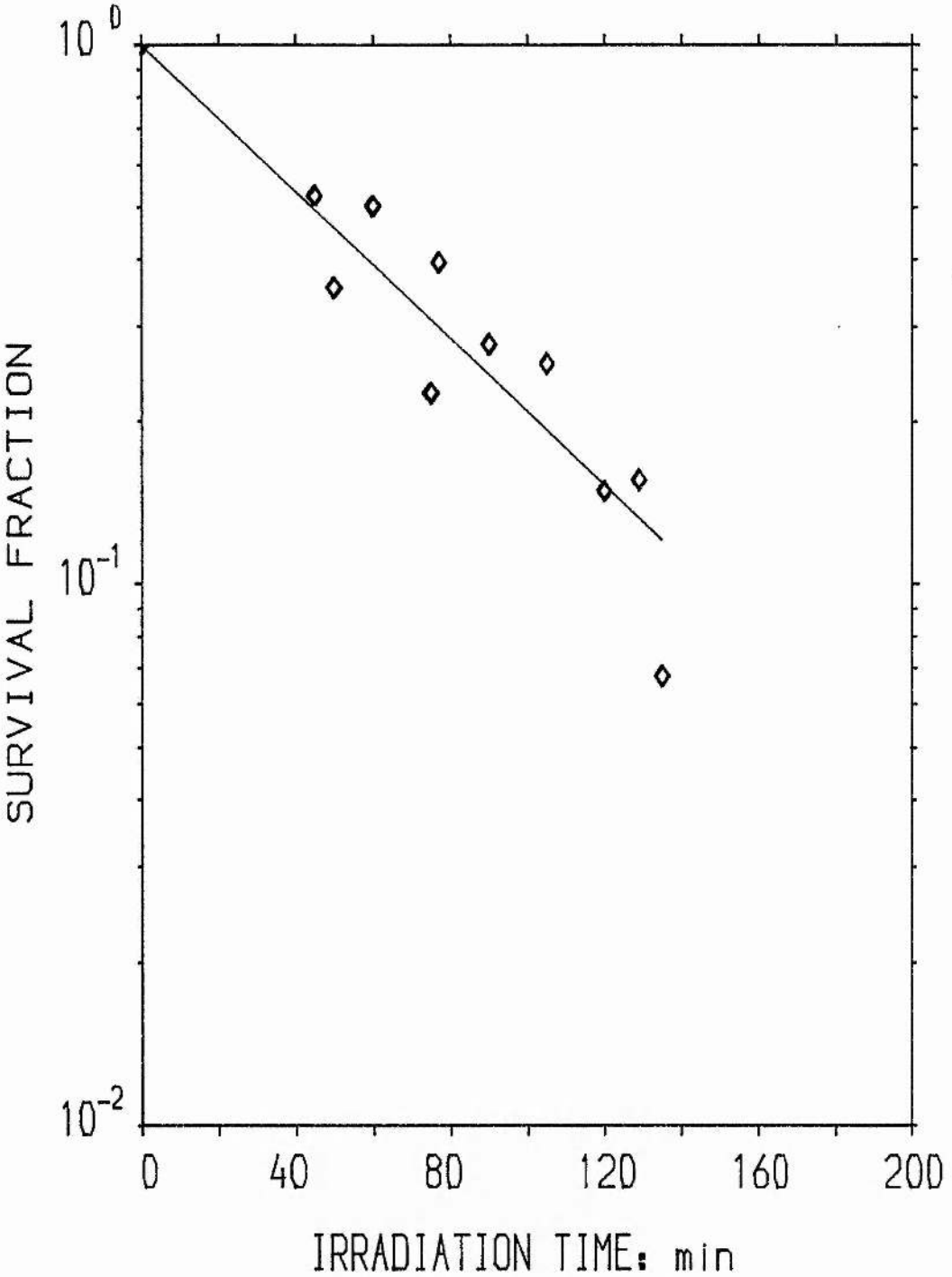

Fig. 5.4 Survival fraction expressed as a function of irradiation time, for V-79 Cells by Am-241 at fluence rate of 1532 cm^{-2}-sec^{-1} (0.0168 Gy/min). D_{37} = 63.8 min.

survival data from several runs are plotted in Fig.5.4. As more than two hours were allowed to irradiate the cell samples, the chronic irradiation data are suitable for fitting the proposed DNA-rupture model introduced in Sec.2.4.

5.3.2 Test of the DNA-rupture model

For the americium-241 alpha particle irradiation at 10 mm in air, the fluence rate of the alpha particles was measured to be 9.2×10^4 cm^{-2} min^{-1} using an extrapolation ionization chamber. The non-uniformity of the dosimetry distribution was less than 5%. Other physical quantities were calculated as in Appendix A2. The calculation was based on the consideration that the alpha particles traversed through 10 mm air and 3.5 μm polyester film cover before reaching the cellular surface. For monolayer culture, the cells are flatttened. The nuclear volume of V79 cells is reported (*e.g.* , Geard, 1985). Separate studies on monolayer culture of V79 cells confirmed that the cell thickness on Mylar film is about 3.5 μm (Min *et al.*, 1985), which is used in the present calculation.

From these known quantities, the alpha particle energy was taken to be 3.62 MeV, or

$E/A = 0.905$ MeV/amu,

$z^{*2}/\beta^2 = 1937$,

$T_{max} = 1.98$ keV,

$I_S = 540$ ionizations/μm or

$\lambda = 1.84$ nm

according to Eqs.(1.13), (1.15) and (1.16). These quantities were put into the mathematical expression of the DNA-rupture model, through non-linear fitting method, the fitted parameters were as follows

$$\ln S = -0.0414 \int_0^{t_1} \{1 - \exp[-10\, e^{-(720-t)/225}]\}\, dt \qquad (5.2)$$

or the individual value of the parameters is

$\sigma_g = 45.0\ \mu m^2$,

$t_f = 720$ min,

$t_r = 225$ min, and

$p_1 n_0 = 10.0$.

The theoretical fitted data were plotted with the experimental data in Fig.5.5. As discussed in Sec.2.4, the above parameters, σ_g stands for the projected cross section of DNA molecules under risk, t_f the damage fixation time, t_r the time required for a cell killing event to be repaired, and p_1 is the efficiency to produce one double strand break event (for heavy ions at λ=1.84 nm, let p_1=1, see Eq.2.16), n_0 is the mean number of DNA molecules at risk, and consequently the product $p_1 n_0$ is the total number of the double strand breaks in an irradiated cell.

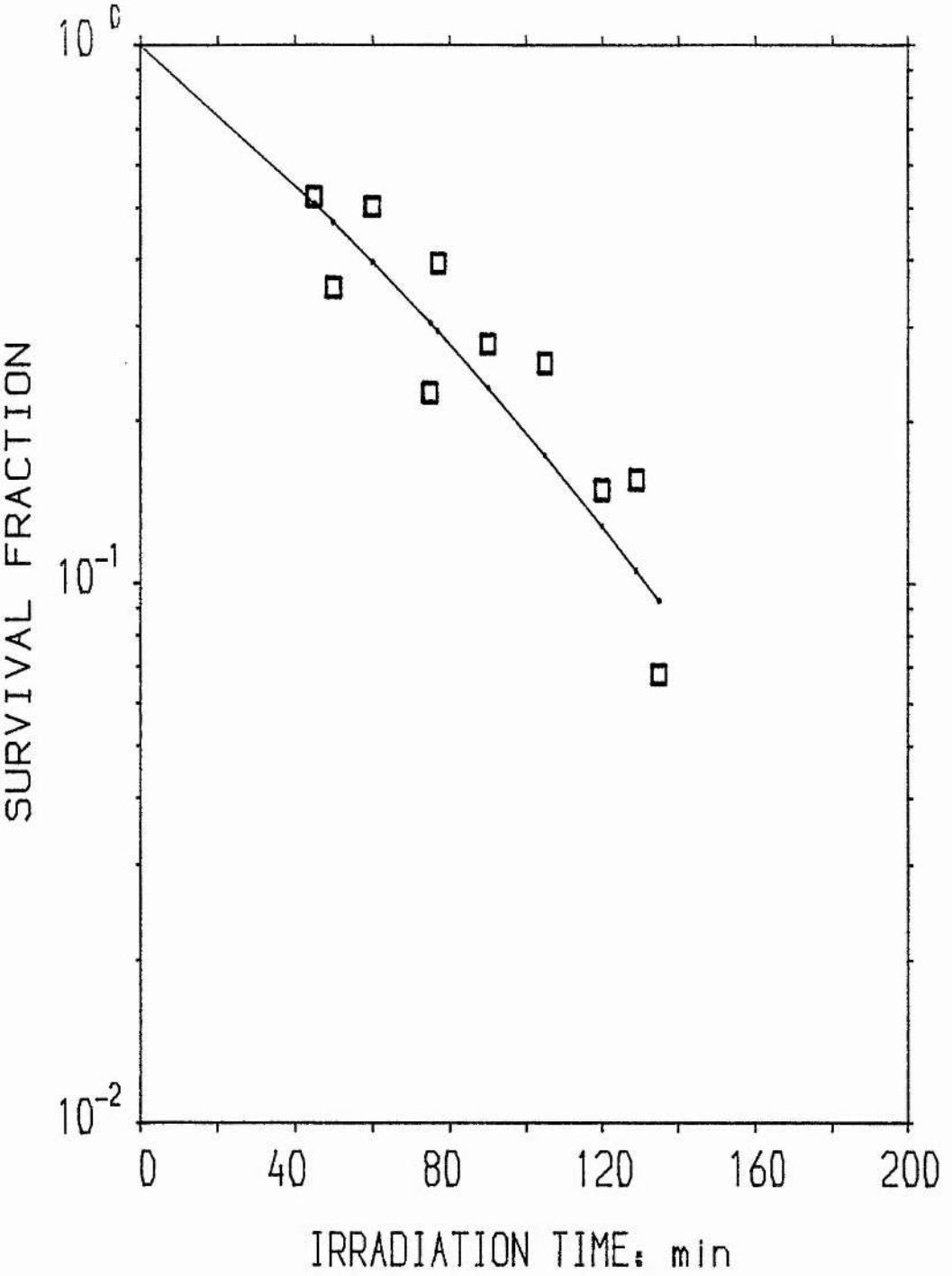

Fig. 5.5 Survival fraction expressed as a function of irradiation time, for V-79 Cells by Am-241 at fluence rate of 9.2×10^{4} cm^{-2} min^{-1}. Solid curve: fitted by the DNA-rupture model.

5.3.3 Discussion

The relative biological effects of alpha particles or heavy ions to x-rays are still justified by the recent RBE values quoted by ICRU (ICRU,1986). In a plot of RBEs versus LETs for different cell lines the maximum RBEs vary from one LET value to another (ICRU, 1970). While the tentative quantities were plotted versus the values of specific ionization, the maximum RBEs all shifted to the optimum specific ionization value (Watt *et al.*, 1985).

On the basis of the above finding, either RBE or LET can be a misleading parameter when adopted for modelling. Therefore, the proposal of the DNA-rupture model assumes that the radiation damage effect is related to the specific ionization value, and the efficiency parameter p_1, a function of the specific ionization, is introduced. Consequently, one can assume that the interaction between the radiation particles and the DNA strands is a single track action, and that dual action is not probable. Therefore the final effect is independent of the dose rate.

It is seen that for the experimental data tested, the damage repair time is about 4 hours, which is a similar answer compared with a separate theoretical research reported by Metting *et al.* (see Table 2.1) whose theory is dose rate squared dependent. Secondly, the damage fixation time was expected and obtained longer than the repair time. Thirdly, and finally the fitted value of DNA cross section at risk, together with the number of damaged DNA molecules gave a theoretical quantity in good accordance with an

estimated quantity based on the experimental study on DNA strand breaks.

The survival data of 250 kV_p x-ray irradiation by Metting *et al.* (1985) are fitted by the model, the result is given in Fig.5.6. From the given dose-rate, the fluence rate of the δ-rays is evaluated using the same method as reported before (Chen & Watt, 1986). That is, the average energy of the photons is evaluated to be 62 keV, and the mean energy of the secondary electrons, $E_{s,e}$, is evaluated as 0.85 keV, and the linear energy transfer, for the secondary electrons produced by the photons, is 11.6 keV/μm. The calculated fluence rate is 1.347×10^6 cm^{-2}-min^{-1} at the dose rate of 0.025 Gy/min. Then, the extracted parameters are as follows

$\sigma_g = 6.0\ \mu m^2$

$t_f = 852$ min,

$t_r = 456$ min, and

$p_1 n_0 = 0.5$.

The above fitted quantities for the x-rays irradiation are comparable with that for alpha particles irradiation. Further discussion is referred to the reference (Chen *et al.*, 1987).

However, we may point out that, as a new modelling approach, the model is under development. Nevertheless, the model explains well the experimental data obtained by alpha chronic irradiation as well as the data from the reference. An

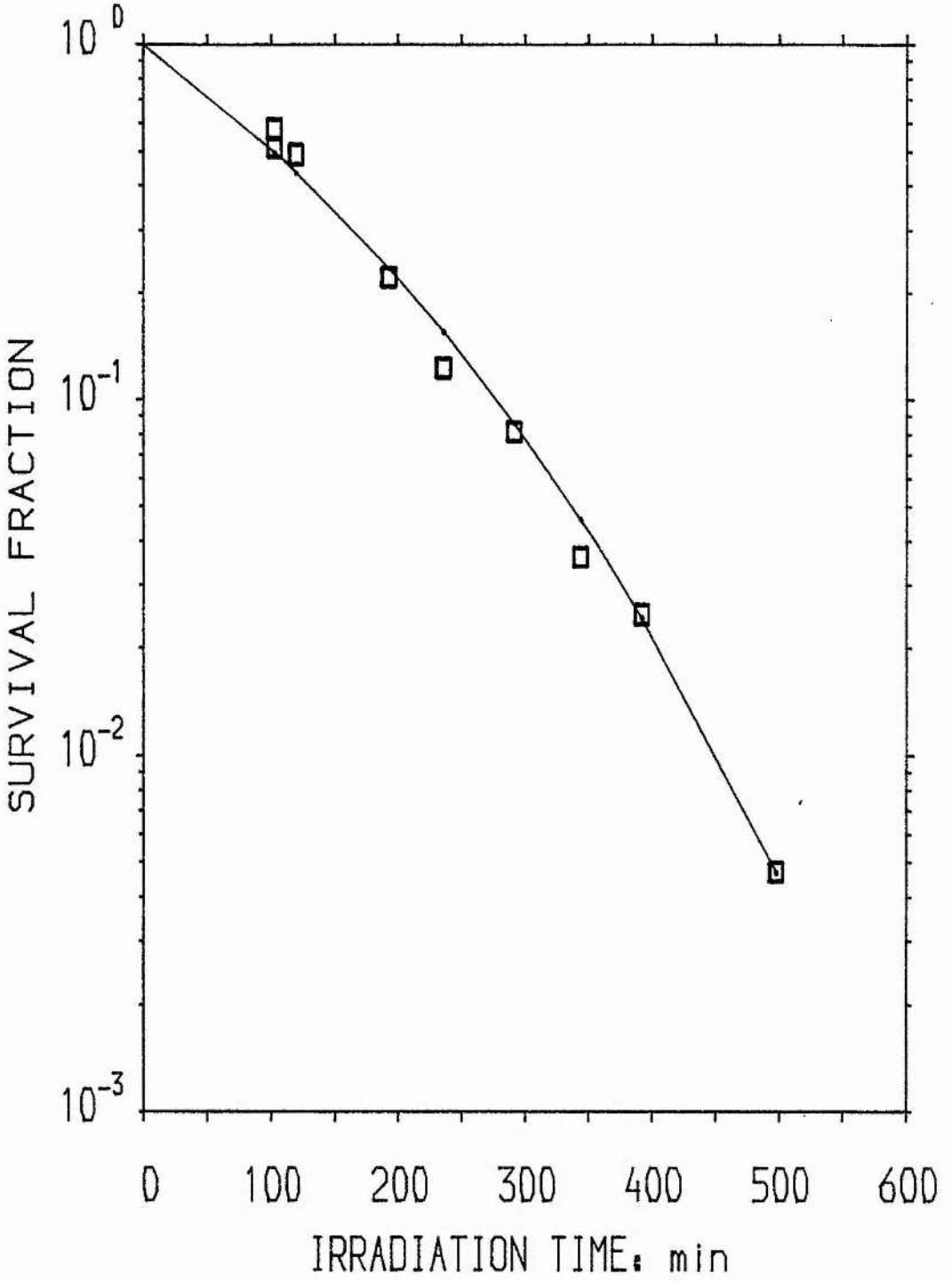

Fig. 5.6 Dose effect result of CHO-K1 cells by 250 kV x-ray irradiation, at fluence rate of 1.347×10^{6} cm^{-2} min^{-1} (0.025 Gy/min, Metting et al., 1985).

interesting feature of the model is that the concept of repair is revised such that the time available for repair or recovery is dose rate independent. The parameters, extracted from the model, have given a reasonable explanation of the present experimental results (Watt, 1987; Chen *et al.*, 1987; Watt *et al.*, 1987).

5.4 Conclusions

5.4.1 Remark on experiments

Experimental works have been performed using different types of ionizing radiations. These included x-rays from a conventional x-ray machine, low energy electrons produced by an accelerator set up for the long term study in this laboratory, and alpha particles from an acute source and a chronic source.

In the literature, there are few data for electrons published compared to the larger amount for x-rays, ions or even neutron irradiation. For future studies, an electron accelerator has been constructed and initial tests have been carried out by irradiation of V79 cells. The survival data showed that the conditions were fulfilled to the original design.

Survival data by alpha particles were performed to relate to LET quantities at higher dose rates in the published research. We have, however, successfully used very low fluence rates to irradiate cells plated by the recently established monolayer technique and obtained suitable results for the theoretical analyses.

Comparison between the present results and the results in

the literature have been made between x-rays and electrons. When more results by electron irradiation become available through future research, a better understanding of radiation damage effect by both x-rays and electrons may be achieved as a linkage between all the different types of ionizing particles.

5.4.2 Remark on theory

The research project began with a survey of published survival data of the effect of ionizing radiation on mammalian cells *in vitro*. The results have been analysed using the specific or primary ionization parameter which is a physical quantity describing the interaction between ionizing particles and matter and a new explanation for the damage mechanism was made. This quantity is a unit excluding energy. It is proposed that the mechanism of radiation damage is dependent on the number of ionization events and the optimum effect occurs when the mean free path of the incident particle is equivalent to the DNA strand spacing. The theoretical model was therefore established on that basis (Watt, 1987).

By testing the model with the experimental data obtained recently, conclusions may be made that at low doses and low dose rates, the radiation action mechanism is a single track action dominantly in the mammalian cells *in vitro* , and that the radiation action is irradiation time dependent not 'dose' rate dependent.

5.4.3 Remark on future study

Both the theoretical and experimental results suggest promising future research on the relationship between cell survival and ionizing radiation time particularly at low doses and low dose rates.

On biological aspects, the monolayer cell culture method has been proved to be a reliable and simple technique for track segment experiments as long as careful procedure is obeyed. On physical aspects, a new irradiation method by low energy electrons has been made available and demonstrated by the experimental results. With use of different alpha particle fluence rates, more survival data could be obtained to test the single track action theory such that at some later stage other biological factors as well as chemical factors may be taken into the mathematical expression of the DNA-rupture model.

In the field of radiological protection against ionizing radiation damage effect, a main interest is how to predict the probability of ultimate health effects resulting from a radiation field. The theoretical modelling of radiation damage effect for extrapolating of health effects to low doses and low dose rates can in turn cause improvement of treatment in radiotherapy.

For example, Watt *et al.* (1985) calculated the optimum characteristic quantities of some heavy ions for possible efficient radiotherapy purpose (Table 5.3). It can be seen that in the table, the optimum quantities of the particles are not the LET values recognized, or the delta ray energy of a specified particle, since

Table 5.3 Energy transfer data for ions with mean free path for primary ionisation λ=2 nm (after Watt *et al.*, 1985)

Ion type	E/A (Mev/amu)	LET (keV/μm)	T_{max} (keV)
$_2H^1$	0.223	64	0.2
$_4He^2$	0.94	108	2.0
$_6Li^3$	2.22	132	5.3
$_{12}C^6$	8.5	185	20.0
$_{20}Ne^{10}$	25.0	215	59.4
$_{40}Ar^{18}$	88.0	260	210.0

the energy deposition is not the determinant factor according to our studies. From deuteron's data ($_2H^1$), the optimum energy of neutron in theory to be used is about 0.7 MeV, This is found in accordance with some experimental results (*e.g.*, Lloyd *et al.* , 1976).

Above all, the study on the mechanisms of radiation damage effect to biological systems will give a better understanding of the dominant factors responsible for damage in the complex chain of events between initial exposure to the radiation and the subsequent biological damage.

Appendix A Stopping Power Formulae

A1. General formulae for electrons and ions (ICRU, 1984)

From Bethe's theory (1933), the collision stopping power is due to energy transfers from the incident particle to bound atomic electrons,

$$\frac{1}{\rho}S_{col} = \frac{1}{\rho}S_{col}(W<W_c) + \frac{1}{\rho}S_{col}(W>W_c) \qquad (A1.1)$$

where the energy transfers W to atomic electrons in inelastic collisions are divided into two classes as $W<W_c$ and $W>W_c$. The leading factor N_AZ/A represents the number of atomic electrons per gram of the medium, and $d\sigma/dW$ the cross section (per atomic electrons). The main result of the Bethe theory is

$$\frac{1}{\rho}S_{col}(W<W_c) = \frac{2\pi N_A r_e^2 mc^2}{2}\frac{Z}{A}z^2\left[\ln\frac{2mc^2\beta^2W_c}{(1-\beta^2)I} - \beta^2\right] \qquad (A1.2)$$

The above equation is valid when the velocity of the projectile is large compared with the velocities of the atomic electrons. For the K-shell, it is valid for $(Z/137\beta)<<1$. The stopping power for $W>W_c$ is

$$\frac{1}{\rho}S_{col}(W>W_c) = \frac{N_A Z}{A}\int_{W_c}^{W_{max}} W\frac{d\sigma}{dW}dW \qquad (A1.3)$$

the final expression for ions is developed as

$$\frac{1}{\rho}S_{col} = 2k_L\frac{Z}{A}\frac{z^2}{\beta^2}\left[\ln\frac{2mc^2\beta^2}{(1-\beta^2)I} - \beta^2\right] \qquad (A1.4)$$

In the latest study, the term in the square bracket has been improved to be $L(\beta)$ and

$$L(\beta) = L_0(\beta) + z\,L_1(\beta) + z^2\,L_2(\beta) \qquad (A1.5)$$

is called the stopping number per atomic electron,

$$L_0(\beta) = \ln\frac{2mc^2\beta^2}{(1-\beta^2)I} - \beta^2 - \frac{C}{Z} - \frac{\delta}{2} \qquad (A1.6)$$

The last two terms in the above are shell correction named after Livingston and Bethe (1937), and a density-effect correction first predicted by Swann (1938) and calculated by Fermi (1940). The other two terms in Eq.(A1.5), zL_1 and z^2L_2 are called Barkas correction and Bloch correction (or z^3, z^4 effects). They are important at high energies. To be simple, all corrections made to Bethe's formula can be summed into a total correction term χ

$$\chi = \frac{C}{Z} + \frac{\delta}{2} - zL_1(\beta) - z^2L_2(\beta) \qquad (A1.7)$$

In the constant term $N=N_A Z/A$ represents the number of atomic electrons per gram of the medium, as N_A is Avogadro's number, Z and A are atomic number and atomic weight, $r_e=2.818\times10^{-13}$ cm^2 is the classical electron radius, hence

$$k_L = 2\pi N_A r_e^2 mc^2$$

$$= 2\pi(6.022045\times10^{23}\text{mol}^{-1})\times(7.940775\times10^{-26}\text{cm}^2) \times (0.5110034\text{MeV})$$

$$= 0.153536 \text{ MeV cm}^2/\text{g-mol} \qquad \text{(A1.8)}$$

For electrons (-) or positrons (+) in Eq.(1.7), $L_e(\beta)$ is

$$L_e(\beta) = \ln(T/I)^2 + \ln(1+\tau/2) + F^{\pm}(\tau) - \delta \qquad \text{(A1.9)}$$

where $\tau=T/mc^2$ is the incident electron demensionless unit and I the mean excitation energy, and

$$F^-(\tau)=(1-\beta^2)\,[1+\tau^2/8 - (2\tau+1)\ln 2] \qquad \text{(A1.10)}$$

To get the restricted stopping power S^{Δ}/ρ for electrons or positrons, simply replace $G^{\pm}(\tau,\eta)$ for $F^{\pm}(\tau)$ in Eq.(A1.9), and

$$G^-(\tau,\eta) = -1 - \beta^2 + \ln[4(1-\eta)\eta] + (1-\eta)^{-1} + (1-\beta^2)\,[\tau^2\eta^2/2 + (2\tau+1)\ln(1-\eta)] \qquad \text{(A1.11)}$$

where $\eta=\Delta/T$ is the fractional energy cut-off.

A complete computer programme (Fortran 77) for calculating the stopping powers for electrons has been compiled

and is given in Appendix C. For high energies, in the programme, the density correction has referred to the consideration by Uehara (1986).

The calculated results for electrons were tabulated in Tables A3.1 and A3.2, and plotted in Figs. A3.1 and A3.2. For alpha particles, the results were given in Tables A3.3, A3.4 and Fig. A3.2. Only the first three numbers of the data may be effective, the rest are printed for text formatting reason.

A2. Empirical formula for ions

Although the sophisticated formulae for the calculation of the stopping power of ions were available, the results from various authors were often slightly different. The present results for alpha particles were obtained by using the empirical formulae (Powers, 1978), the results of which were found to be consistent.

Table A3.1 Electron attenuation data in polyester (R in μm)
Initial electron energy (10-100 keV)

R	10.00	20.00	30.00	40.00	50.00	60.00	70.00	80.00	90.00	100.00
1	6.11	17.74	28.34	38.67	48.87	59.01	69.11	79.19	89.25	99.30
2	0.42	15.25	26.61	37.30	47.72	58.00	68.21	78.37	88.49	98.59
3		12.46	24.80	35.89	46.55	56.99	67.30	77.54	87.73	97.88
4		9.18	22.88	34.45	45.36	55.96	66.39	76.71	86.96	97.17
5		5.02	20.84	32.96	44.14	54.91	65.46	75.87	86.19	96.45
6			18.65	31.42	42.90	53.86	64.53	75.03	85.42	95.73
7			16.26	29.82	41.64	52.79	63.59	74.18	84.64	95.01
8			13.60	28.15	40.34	51.70	62.63	73.32	83.86	94.28
9			10.54	26.41	39.02	50.59	61.67	72.46	83.07	93.55
10			6.81	24.59	37.66	49.47	60.70	71.59	82.28	92.82
11			1.57	22.66	36.26	48.33	59.72	70.71	81.48	92.08
12				20.60	34.83	47.17	58.72	69.83	80.67	91.34
13				18.39	33.35	45.99	57.71	68.94	79.86	90.60
14				15.97	31.82	44.79	56.69	68.04	79.05	89.84
15				13.28	30.24	43.56	55.66	67.13	78.23	89.09
16				10.16	28.59	42.31	54.61	66.21	77.40	88.33
17				6.32	26.87	41.03	53.55	65.28	76.57	87.57
18				0.77	25.07	39.72	52.47	64.35	75.73	86.80
19					23.17	38.38	51.38	63.40	74.89	86.03
20					21.15	37.01	50.27	62.45	74.04	85.26

Table A3.2 Electron attenuation data in water (R in μm)
Initial electron energy (10-100 keV)

R	10.00	20.00	30.00	40.00	50.00	60.00	70.00	80.00	90.00	100.00
1	6.07	17.71	28.32	38.65	48.86	59.00	69.10	79.18	89.24	99.29
2	0.28	15.19	26.57	37.27	47.69	57.98	68.19	78.35	88.47	98.57
3		12.36	24.73	35.84	46.51	56.95	67.27	77.51	87.70	97.86
4		9.02	22.79	34.38	45.30	55.91	66.34	76.67	86.93	97.13
5		4.76	20.72	32.87	44.07	54.85	65.41	75.82	86.15	96.41
6			18.49	31.31	42.82	53.78	64.46	74.97	85.37	95.68
7			16.06	29.68	41.53	52.70	63.51	74.11	84.58	94.95
8			13.34	27.99	40.22	51.60	62.54	73.24	83.78	94.21
9			10.20	26.23	38.88	50.48	61.57	72.37	82.99	93.48
10			6.33	24.37	37.50	49.34	60.58	71.49	82.18	92.73
11			0.72	22.40	36.08	48.18	59.59	70.60	81.37	91.99
12				20.31	34.63	47.01	58.58	69.70	80.56	91.23
13				18.04	33.12	45.81	57.56	68.80	79.74	90.48
14				15.56	31.57	44.59	56.52	67.89	78.92	89.72
15				12.78	29.96	43.35	55.47	66.97	78.09	88.96
16				9.53	28.28	42.08	54.41	66.04	77.25	88.19
17				5.45	26.53	40.78	53.34	65.10	76.41	87.42
18					24.69	39.45	52.24	64.15	75.56	86.64
19					22.74	38.08	51.13	63.19	74.70	85.86
20					20.67	36.68	50.01	62.22	73.84	85.08

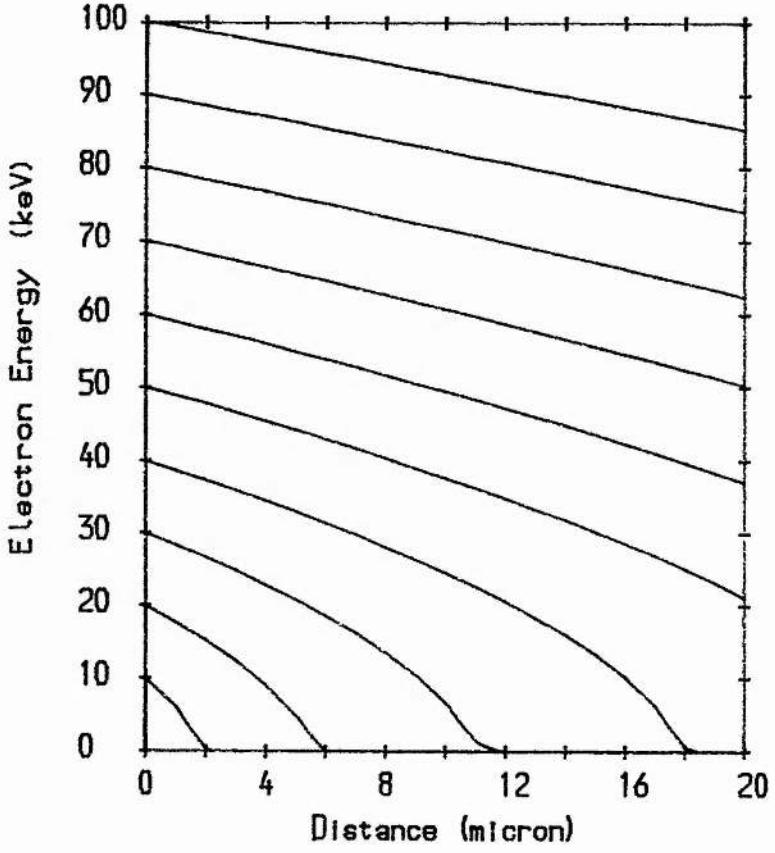

Fig. A3.1 Attenuated electron spectra in polyester

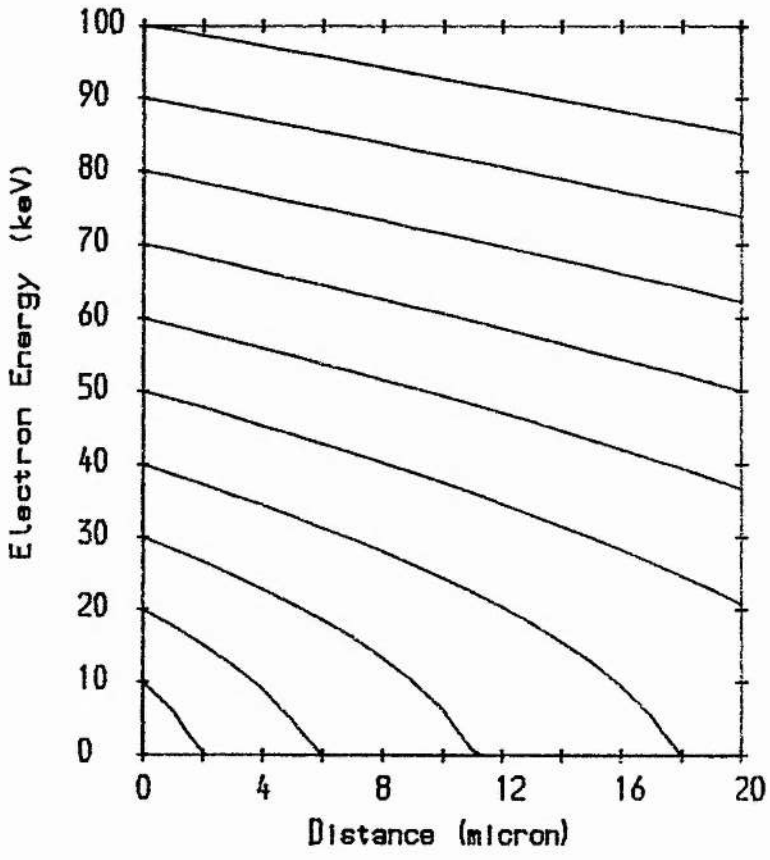

Fig. A3.2 Attenuated electron spectra in water

Table A3.3 Calculated data of energy attenuation (MeV) and stopping power (MeV-cm^2/g) of Cm-244 (5.80 MeV). In air: mm; in water: μm.

R(mm;μm)	E-dE(air)	SP(air)	E-dE(water)	SP(water)
1	5.712	730.135	5.718	818.649
2	5.624	738.316	5.635	827.912
3	5.535	746.802	5.552	837.501
4	5.444	755.613	5.467	847.434
5	5.352	764.767	5.381	857.732
6	5.260	774.290	5.294	868.418
7	5.166	784.210	5.206	879.515
8	5.071	794.552	5.117	891.051
9	4.974	805.347	5.027	903.053
10	4.877	816.634	4.935	915.554
11	4.777	828.449	4.842	928.588
12	4.677	840.833	4.748	942.192
13	4.575	853.839	4.653	956.407
14	4.471	867.517	4.555	971.279
15	4.366	881.929	4.457	986.858
16	4.259	897.143	4.356	1003.199
17	4.149	913.239	4.254	1020.363
18	4.038	930.305	4.151	1038.418
19	3.925	948.442	4.045	1057.440
20	3.810	967.772	3.937	1077.512
21	3.692	988.429	3.827	1098.730
22	3.571	1010.576	3.715	1121.198
23	3.448	1034.401	3.601	1145.035
24	3.322	1060.128	3.484	1170.374
25	3.193	1088.027	3.364	1197.367
26	3.060	1118.423	3.241	1226.186
27	2.923	1151.714	3.116	1257.025
28	2.782	1188.393	2.986	1290.109
29	2.636	1229.080	2.854	1325.695
30	2.486	1274.571	2.718	1364.085
31	2.329	1325.906	2.577	1405.637
32	2.166	1384.490	2.432	1450.789
33	1.995	1452.296	2.282	1500.101
34	1.815	1532.257	2.126	1554.331
35	1.625	1629.065	1.965	1614.561
36	1.422	1750.028	1.797	1682.316
37	1.202	1898.844	1.621	1759.408
38	0.965	2032.796	1.436	1846.753
39	0.718	2033.252	1.242	1941.619
40	0.479	1927.400	1.038	2036.582

Table A3.4 Calculated data of energy attenuation (MeV) and stopping power (MeV-cm^2/g) of Am-241 (5.48 MeV). In air: mm; in water: μm.

R(mm;μm)	E-dE(air)	SP(air)	E-dE(water)	SP(water)
1	5.389	761.096	5.394	856.117
2	5.297	770.471	5.308	866.742
3	5.203	780.231	5.220	877.774
4	5.109	790.401	5.131	889.240
5	5.013	801.013	5.041	901.169
6	4.915	812.102	4.950	913.591
7	4.817	823.702	4.857	926.540
8	4.717	835.856	4.763	940.053
9	4.615	848.607	4.667	954.171
10	4.512	862.013	4.571	968.938
11	4.408	876.125	4.472	984.404
12	4.301	891.014	4.372	1000.624
13	4.193	906.750	4.270	1017.657
14	4.083	923.419	4.167	1035.570
15	3.970	941.119	4.061	1054.437
16	3.856	959.961	3.954	1074.341
17	3.739	980.075	3.844	1095.375
18	3.620	1001.611	3.733	1117.643
19	3.497	1024.746	3.618	1141.260
20	3.372	1049.689	3.502	1166.358
21	3.244	1076.693	3.382	1193.085
22	3.113	1106.057	3.260	1221.610
23	2.978	1138.147	3.135	1252.124
24	2.838	1173.417	3.007	1284.845
25	2.695	1212.432	2.875	1320.026
26	2.546	1255.911	2.739	1357.962
27	2.392	1304.786	2.599	1398.999
28	2.231	1360.299	2.455	1443.563
29	2.064	1424.165	2.305	1492.189
30	1.888	1498.871	2.151	1545.599
31	1.702	1588.282	1.990	1604.815
32	1.504	1698.671	1.823	1671.291
33	1.291	1837.306	1.649	1746.834
34	1.061	1988.579	1.465	1832.645
35	0.816	2053.651	1.273	1926.754
36	0.572	1973.870	1.070	2022.184
37	0.343	1800.897	0.859	2115.120
38	0.152	1301.690	0.637	2217.147
39	0.035	634.426	0.408	2286.656
40			0.198	2105.307

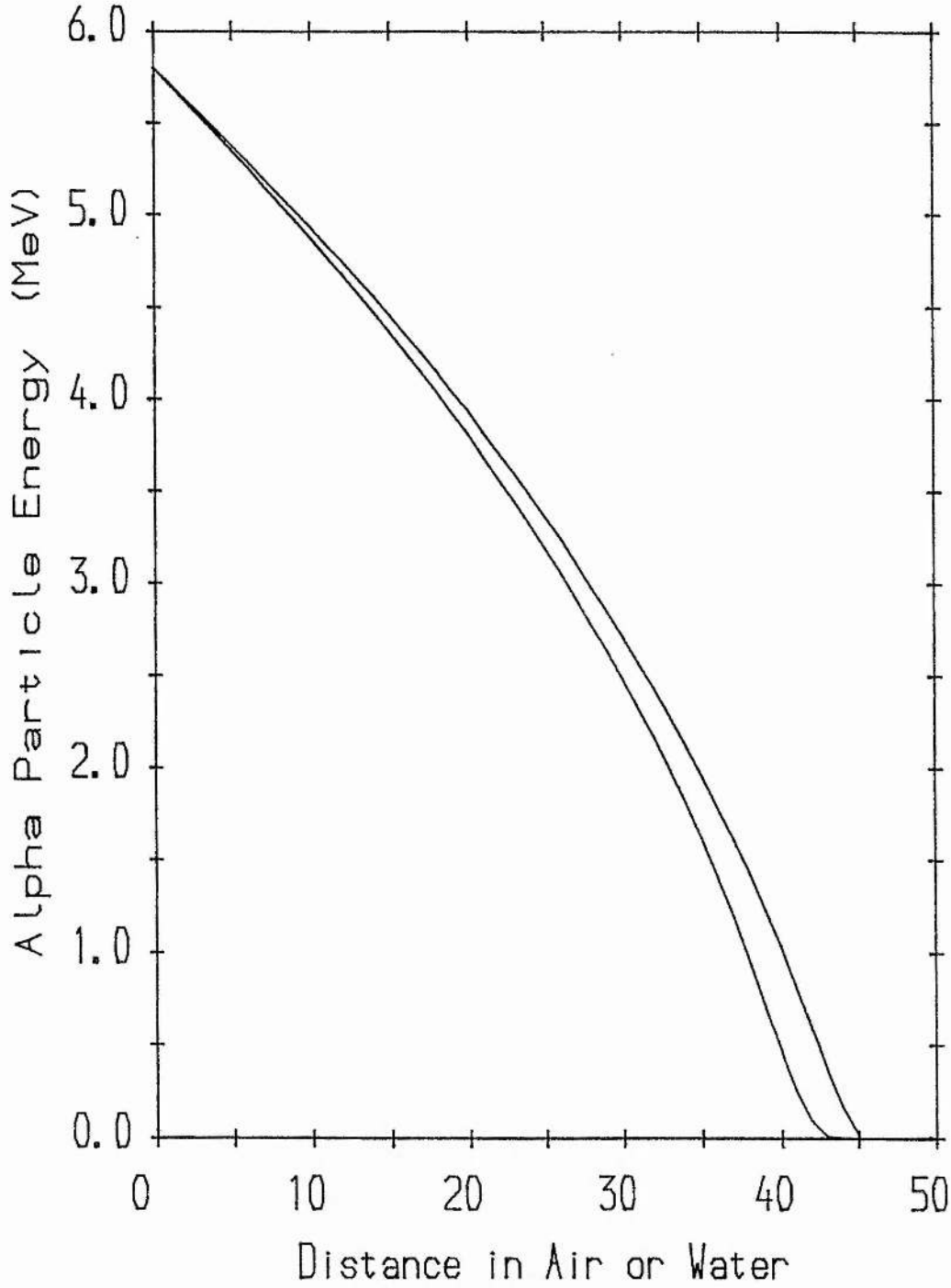

Fig. A3.3 Attenuated alpha spectra
Below: air (mm); Above: water (μm)

Appendix B Experimental Data

(Survival data for colony assay)

B1.1 250 kV X-rays Irradiation (STABLIPAN, SIEMENS, 14 mA, 0.5 Cu filtration)

Dose-rate: 0.709 Gy/min (Exp. No. 3010041185)

Min	Cells Plated	Colonies Counted	S.F.	σ_{n-1}
0	152	59, 63	(0.401	0.0186)
2	305	97, 102	0.814	0.0289
4	305	107, 108	0.879	0.0058
6	1525	173, 248	0.344	0.0867
8	1525	101, 138	0.195	0.0428
10	15250	310, 362	0.0549	0.00601
			(Exp. No. 1411201185)	
0	58	34, 40	(0.638	0.0731)
2	150	44, 52	0.502	0.0591
4	137	39, 40	0.452	0.0081
6	543	69, 81	0.216	0.0245
8	3346	86, 104	0.0445	0.00596
10	4550	44, 45	0.0153	0.00024
15	80000	50	0.000980	
	Dose-rate: 4.72 Gy/min (at 8.5 cm)		(Exp. No. 2005260586)	
0	223	116	(0.520)	
4	446	21, 33	0.116	0.0366
8	4460	39, 40	0.0170	0.00305
10	4460	10, 12	0.00474	0.000610
15	22300	9, 10	0.000819	0.0000610

Averaged Results (data used in Fig. 5.1, 0.709 Gy/min)

2	0.658	0.2206
4	0.666	0.3019
6	0.280	0.0905
8	0.120	0.1064
10	0.0351	0.02800
15	0.000980	

B1.2 Electrons irradiation (25 keV)

In vacuum chamber test (no radiation) (Exp. No. 3012070187)

Min	Cells Plated	Colonies Counted		S.F.	σ_{n-1}
0	101	48,	67	(0.569	0.1330)
2	165	82,	95	0.536	0.0557
4	169	94,	98	0.568	0.0167
6	178	72,	94	0.466	0.0874
8	217	lost			
10	216	100,	144	0.565	0.1440

Current density, j (pA/cm^2) (Exp. No. 1802250287)

Sec	j	Cells Plated	Colonies Counted		S.F.	σ_{n-1}
0	(26.8)	186	116,	125	(0.648	0.0342)
20	26.1	139	lost			
40	26.1	356	71,	81	0.329	0.0031
60	28.0	833	52		0.0963	
80	26.8	703	6,	8	0.0154	0.00310
100	26.8	9080	89,	125	0.0182	0.00433

B1.3 Acute alpha irradiations (^{244}Cm)

Sec	Cells Plated	Colonies Counted		S.F.	σ_{n-1}
	At 10 mm, ϕ: *ca.* 5×10^5 cm^{-2}s^{-1}				(Exp. No. 0301100187)
0	93	30,	43	(0.392	0.0990)
10	231	16,	19	0.193	0.0234
20	762	18,	26	0.0736	0.01894
30	710	27,	55	0.147	0.0711
40	1330	28,	34	0.0594	0.00814
50	1008	3		0.00759	
					(Exp. No. 1001170187)
0	88	69,	69	(0.784)	
10	160	92,	93	0.737	0.0056
20	872	42,	57	0.0724	0.01551
30	613	68,	70	0.144	0.0029
40	1001	52,	61	0.0720	0.00811
50	1162	32,	42	0.0406	0.00776
		(*from 1202180287)			(Exp. No. 0402110287)
0	27	12,	12	(0.444)	
20	132	6,	11	0.145	0.0603
40	220	13		0.133	
60	339	3,	5	0.0266	0.00940
80	9450	33		0.00786	
80*	9360	54,	70	0.0113	0.00206

Averaged results (data used in Fig.5.3)

10				0.465	0.3847
20				0.0970	0.04157
30				0.146	0.00212
40				0.0881	0.03936
50				0.0241	0.02334
60				0.0266	0.00940
80				0.00958	0.002432
At 20 mm, $\phi = 1.670 \times 10^5$ cm^{-2}s^{-1}		(*from 20032703)			(Exp. No. 1202180287)
0	120	69,	72	(0.588	0.0177)
80	412	31,	42	0.151	0.0321
120	1410	47,	50	0.0585	0.00256
160	6880	161,	177	0.0418	0.00280
160*	1190	15		0.0137	
200	3970	80,	81	0.0345	0.00030
240	17120	180,	240	0.0209	0.00421

(Exp. No. 2304300487)

0	88	31,	37	(0.386	0.0482)
100	283	3,	5	0.0366	0.01295
140	1408	3,	8	0.0101	0.00650
180	1440	4,	8	0.0108	0.00509
260	8060	61,	81	0.0228	0.00454

B1.4 Chronic alpha irradiation (^{241}Am)

Min	Cells Plated	Colonies Counted		S.F.	σ_{n-1}
	At 10 mm, $\phi = 1.532 \times 10^3$ cm^{-2}s^{-1}			(Exp. No. 2502040387)	
0	83	51		(0.614)	
60	113	34,	39	0.526	0.0510
90	50	8,	11	0.310	0.0691
120	161	13		0.132	
				(Exp. No. 0503120387)	
0	108	71,	74	(0.671	0.0196)
60	185	49,	70	0.479	0.1196
90	225	37,	37	0.245	
120	717	77,	83	0.166	0.0088
				(Exp. No. 2003270387)	
0	99	88,	94	0.919	0.0429
45	139	66,	68	0.524	0.0111
75	89	18,	19	0.226	0.0086
105	244	57,	58	0.256	0.0032
135	933	58,	58	0.0676	
				(Exp. No. 2304300487)	
0	88	31,	37	0.386	0.0482
50	278	30,	46	0.354	0.1054
77	444	66,	69	0.394	0.0124
129	786	46,	49	0.156	0.0070

Averaged results (data used in Fig.5.4)

45	0.524	0.0111
50	0.354	0.1054
60	0.502	0.0332
75	0.226	0.0086
77	0.394	0.0124
90	0.278	0.0460
105	0.256	0.0030
120	0.149	0.0240
129	0.156	0.0070
135	0.0676	

Appendix C Computing Programmes

C1.1 Programme for electrons calculation

```
      IMPLICIT DOUBLE PRECISION (A-H, O-Z)
      DIMENSION ZJ(8),ZA(8),AJ(8),RJ(8),EI(8),WJP(3),JCJ(3)
      Dimension TT(10,64),T(10),WJW(3)
      DIMENSION D(8,64),SPC(8,64),SPL(8,64),SPCP(8,64),SPLP(8,64)
      Character*20 Textw, Textp, Text
      DATA WJP/0.041959,0.625017,0.333025/, JCJ/1,6,8/
      Data WJW/0.111894, 0.0, 0.888106/
      Data T/10.0,20.0,30.0,40.0,50.0,60.0,70.0,80.0,90.0,100.0/
      Data Textw,Textp/'water (R in micron)','polyester(R in um)'/
      Do 2 k=1,10
2     TT(k,1)=T(k)*0.001

      Ncon=2
      Do 106 Nstep=1,Ncon
      Do 105 k=1,10
      Do 100 i=1,20
      SP=0.0
      Do 50 j=1,3,Nstep
      IF (Nstep .EQ. 2) goto 18
16    Text=Textp
      WJ=WJP(J)
      RD=1.40
      Goto 24
18    Text=Textw
22    WJ=WJW(J)
      RD=1.0
      If (Ncon .eq. 3) Goto 55
24    JC1=JCJ(J)
      IE1=i
      TX=TT(k,i)

      CALL STOPOWER (SP,JC1,IE1,TX)
      SP=SP+SP*WJ
50    CONTINUE
      DR=1.0
      DE=SP*RD*DR*0.1
      Goto 62
c     For E>10 keV, Call Stopfit is valid
55    Text=Textw
      Call Stopfit (SP,k,i,TT)
      DE=SP*1.0
62    TT(k,i+1)=TT(k,i)-DE*1e-3
      If (TT(k,i+1)) 102,105,100
100   Continue
102   TT(k,i+1)=-0.0
105   Continue
      Write (m,902)
      Write (m,903) Text
c     Output of e E in keV now:
```

```
      Write (m,904) (T(k),k=1,10)
      Do 115 i=1,20
      Do 115 k=1,10
115   TT(k,i+1)=TT(k,i+1)*1e3
      DO 120 i=1,20
120   Write (m,905) i,(TT(k,i+1),k=1,10)
      Goto 106
110   Write (m,910)
106   Continue
902   Format (//' Initial Electron Energy (10-100 keV)')
903   Format (' Electron attenuation in ',A20)
904   Format (6x,10f8.3)
905   Format (1x,i3,2x,10f8.3)
920   Stop
      End

      Subroutine Stopfit (SP,k,i,TT)
      Implicit Double Precision (A-H, O-Z)
      Dimension TT(10,64)
      TX=TT(k,i)
      If (TX .GT. 0.3) Goto 200
      AX=(DLOG(TX**2.d0)-8.00637)/3.40120
      AS=1.8205-1.1598*AX+0.16429*AX*AX
      GOTO 300
200   AX=(DLOG(TX**2)-13.30469)/1.89712
      AS=0.63749-0.12199*AX+0.091112*AX*AX
c     Convert the above in MeV-cm2/g into kev/micon (for water)
300   SP=AS*0.1
      RETURN
      END

      SUBROUTINE STOPOWER (SP,JC1,IE1,TX)
      IMPLICIT DOUBLE PRECISION (A-H, O-Z)
      DIMENSION ZJ(8),ZA(8),AJ(8),RJ(8),EI(8),T(64)
      DIMENSION D(8,64),SPC(8,64),SPL(8,64),SPCP(8,64),SPLP(8,64)
      DATA C/2.998D8/, PI/3.1415926/, QE/1.6D-19/, PC/6.62517D-34/
      DATA RME/9.11D-31/, RES/7.940775D-26/, AVN/6.022045D23/
      EME=1.0D-6*RME*C*C/QE
      CFS=1.D0/137.03604D0
      M=6
      JC2=JC1
      IE2=IE1
      EC=0.01e-3

      DO 900 JC=JC1,JC2
C     Input data of Z,A(g/mol),I(eV),R(g/cm3)
      OPEN (11,STATUS='OLD',FILE='ZAIR.DAT')
      READ (11,60) TEXT
      DO 40 OI=1,100
60    FORMAT (A70)
61    FORMAT (I4,7X,F10.7,F7.3,E12.8)
      READ (11,61) IZ,AJ(JC),EI(JC),RJ(JC)
      ZJ(JC)=IZ*1.0
      ZA(JC)=ZJ(JC)/AJ(JC)
      IF (IZ .EQ. JC) GOTO 41
40    CONTINUE
41    CLOSE (11)
C     Plasma energy: PE(MeV), Mean excitation energy: EI(MeV)
      PE =28.816*SQRT(RJ(JC)*ZJ(JC)/AJ(JC))*1.D-6
```

```
      PES=PE*PE
      EI(JC)=EI(JC)*1.D-6

      DO 800 IE=IE1,IE2
      T(IE)=TX
      E=T(IE)+EME
      VCS=1.D0-(EME/E)*(EME/E)
C     if (137*sqrt(vcs) .lt.10) then stop(for strict calcn)
      ETA=EC/T(IE)
      TAO=T(IE)/EME

C     Correction term (non-shell correction): F- (contin.)
      F =(1-VCS)*(1.D0+TAO*TAO/8.D0-(2.D0*TAO+1.D0)*DLOG2)
C     Correction term (non-shell correction): G- (restrictd.)
      G1=-1.D0-VCS+DLOG(4.D0*(1.D0-ETA)*ETA)
      G3=(2.D0*TAO+1.D0)*DLOG(1.D0-ETA)
      G2=(TAO*ETA)*(TAO*ETA)/2.D0+G3
      G =G1+1.D0/(1.D0-ETA)+(1.D0-VCS)*G2
C     Correction term(non-shell correction): F+(for e+: contin.)
      F1=23.D0+14.D0/(TAO+2.D0)+10.D0/(TAO+2.D0)**2
      F2=(VCS/12.D0)*(F1+4.D0/(TAO+2.D0)**3)
      FC=2.D0*DLOG2-F2
C     Correction term(non-shell correction): G+(for e+: restrictd.)
      U =1.D0/(TAO+2.D0)
      G1=1.D0+(2.D0-U*U)*ETA
      G2=(3.D0+U*U)*(U*TAO/2.D0)*ETA*ETA
      G3=(1.D0+U*TAO)*(U*U*TAO*TAO/3.D0)*ETA*ETA*ETA
      G4=(U*U*U*ETA*ETA*ETA/4.D0)*ETA**4
      GC=DLOG(4.D0*ETA)-VCS*(G1-G2+G3-G4)
C     Delta(density) correction: D
      DX=DLOG(VCS/(1.0-VCS))/4.606
      DC=-2.0*DLOG(EI(JC)*1.0D6/28.816*SQRT(RJ(JC)*ZA(JC)))-1.0
      DN=-DC
C     For solid, liquid with I<100 eV (Z=3,4,5)
      IF (ZJ(JC).GE.3 .AND. ZJ(JC).LE.5 .or. zj(jc).eq.10.0) THEN
      X1=2.0
        IF (DN .LT. 3.681) THEN
      X0=0.2
        ELSE
      X0=0.326*DN-1.0
        END IF
C     For solid, liquid with I>=100 eV (Z>=11)
      ELSE IF (ZJ(JC) .GE. 11) THEN
      X1=3.0
        IF (DN .LT. 5.215) THEN
      X0=0.2
        ELSE
      X0=0.326*DN-1.5
        END IF
C     For gases at normal T, P (Z=1,2,6,...10)
      ELSE
        IF (DN .LE. 12.25) THEN
      X1=4.0
        ELSE
      X1=5.0
        END IF
        IF (DN .LE. 10.0) THEN
      X0=1.6
        ELSE IF (DN .GT. 10.0 .AND. DN .LE. 10.5) THEN
```

```
      X0=1.7
        ELSE IF (DN .GT. 10.5 .AND. DN .LE. 11.0) THEN
      X0=1.8
        ELSE IF (DN .GT. 11.0 .AND. DN .LE. 11.5) THEN
      X0=1.9
        ELSE IF (DN .GT. 11.5 .AND. DN .LT. 13.804) THEN
      X0=2.0
        ELSE IF (DN .GE. 13.804) THEN
      X0=0.326*DN-2.5
        END IF
      END IF
      IF (ZJ(JC) .GE. 3) THEN
      DM=3.0
      ELSE
      XA=DN/4.606
      DM=(X1-X0)/(XA-X0)
      END IF
      DA=(DN-4.606*X0)/(X1-X0)**DM
C     Density correction results:
      IF (DX .LE. X0) THEN
      D(JC,IE)=0.0
      ELSE IF (DX .GT. X0 .AND. DX .LE. X1) THEN
      D(JC,IE)=4.606*DX+DC+DA*(X1-DX)**DM
      ELSE IF (DX .GT. X1) THEN
      D(JC,IE)=4.606*DX+C
      END IF
C     Continuous or restricted S.P.(differs in corr.term)
      S1=2.D0*PI*RES*EME*ZJ(JC)*AVN/(VCS*AJ(JC))
      S2=2.D0*DLOG(T(IE)/EI(JC))
C     Stopping power in units of MeV cm2/g
      SPC(JC,IE)=S1*(S2+DLOG(1.D0+TAO/2.D0)+F-D(JC,IE))
      SPL(JC,IE)=S1*(S2+DLOG(1.D0+TAO/2.D0)+G-D(JC,IE))
      SPCP(JC,IE)=S1*(S2+DLOG(1.D0+TAO/2.D0)+FC-D(JC,IE))
      SPLP(JC,IE)=S1*(S2+DLOG(1.D0+TAO/2.D0)+GC-D(JC,IE))
      SP=SPC(JC,IE)
800   CONTINUE
900   CONTINUE
      RETURN
      END
```

C1.2 Programme for alpha particles calculation

```
      Program Alpha
      Dimension FF(7), FA(7),FW(7),XE(2,45001),YE(2,45001)
      Character*90 Text1, Text2, Text3
      Data Text1/' Attenuated Energy Spectra of Cm-244 (5.80 MeV)'/
      Data Text2/' Attenuated Energy Spectra of Am-241 (5.48 MeV)'/
      Data Text3/'      R(mm;um)        E-dE(air)    SP(air)
     +  E-dE(water)        SP(water)'/
      Data E0/5.80/,R0/45000./,AVN/6.022045e23/,Iw/7/
      Data RDa/1.205e-3/,RDw/1.0/,MWa/28.60/,MWw/18.015/
      Data FA/58.9353,2.7406,85.0793,57.2387,0.6799,0.5,2.0/
      Data FW/26.7537,1.3717,90.8007,77.1587,2.3264,0.5,2.0/
      Open (unit=7, status='new', file='a.dat')
```

```
      IR=int(R0)
      XE(1,1)=E0
      XE(2,1)=E0
      Write (Iw,99950)
      If (E0 .eq. 5.80) Goto 2
      If (E0 .eq. 5.48) Goto 4
2     Write (Iw,99910) Text1
      Goto 6
4     Write (Iw,99910) Text2
6     Write (Iw,99910) Text3

      Do 500 JC=1,2
      If (JC-1) 15,15,25
15    RD=RDa
      MW=MWa
      Do 18 k=1,7
18    FF(k)=FA(k)
      Goto 55
25    RD=RDw
      MW=MWw
      Do 28 k=1,7
28    FF(k)=FW(k)
55    Do 100 i=1,IR-1
      TE=XE(jc,i)

      Call SPFIT(FF,TE,SP)
c     Convert SP in 1e-15eVcm2/molecule into MeVcm2/g
      SP=SP*AVN*1.e-6/MW
c     Increment of energy lost(keV) in one micron:
      DE=SP*RD*0.1
      YE(jc,i+1)=SP
      XE(JC,i+1)=XE(JC,i)-DE*1.e-3
c     As fitting is valid for E> 0.01 MeV
      If (XE(JC,i+1)-0.010) 500,500,100
100   Continue
500   Continue

      k=1
120   Do i=1,45
      j=i*1000+1
      Write (Iw,99930) i,XE(1,j),YE(1,j),XE(2,i+1),YE(2,i+1)
125   If (mod(i,5).eq.0) Write (Iw,*)
150   End do
99910 Format (5x,A70)
99930 Format (6x,i3,3x,4f14.3)
      Close (Iw)
200   Stop
      End

      Subroutine SPFIT (FF,TE,SP)
      Dimension FF(7)
      S1=1.-exp(-FF(2)*TE**(2.+FF(6)))
      S2=FF(1)*log(TE)/TE+FF(3)/TE
      S3=S2*exp(-FF(5)/TE**FF(7))
      SP=1.e-15*S1*(S3+FF(4)/TE**2)
      Return
      End
```

C1.3 Programme for non-linear fitting

```
      PROGRAM Fixation
      IMPLICIT DOUBLE PRECISION (A-H,O-Z)
      External fxias, fchis
      Character*50 Text1,Text2,Text3,Text4
      DIMENSION X(100),Y(100),W(100),YFIT(100),Wt(100),
     &  A(10),dA(10),SA(10), B(10),be(10),der(10),Ik(10),Jk(10),
     &  al(10,10),ary(10,10)

      OPEN (1, STATUS='OLD', FILE='ai.DAT')
      Open (7, Status='new', File='ao.dat')
      Read (1,9900) Text1
      Read (1,9900) Text2
      Read (1,*) ii, Iw, Mode, nm, phi, Acc1, Acc2
      Read (1,*) (A(i),i=1,nm)
      Read (1,*) (dA(i),i=1,nm)
      Read (1,9900) Text3
      READ (1,9901) NP
      DO 10 I=1,NP
10    READ (1,*) X(I),Y(I),W(I)
      CLOSE (1)
      Fl=0.001
      Comp=1.0
c     ii =1,2,3: Scurv fit, Sgrid fit, Yfit(np)
      If (ii-1) 102,101,102
101   Call Scurv (ii,x,y,w,np,nm,mode,a,da,sa,fl,yfit,chis)
      Goto 12
102   CALL SGRID (II,X,Y,W,NP,NM,MODE,A,DA,SA,YFIT,CHIS)
12    if (ii-3) 20,40,20
20    If (ii-1) 202,201,202
201   If ((Comp-Chis)/Chis-Acc1) 40,40,30
202   If ((Comp-Chis)/Chis-Acc2) 40,40,30
30    Comp=Chis
      If (ii-2) 101,102,102
40    Write (Iw,9900) Text1
      WRITE (Iw,9903)
      DO 50 I=1,NP
50    WRITE (Iw,9904) X(I),Y(I),W(I),YFIT(I)
      WRITE (Iw,9905)
      WRITE (Iw,9906) A(1),SA(1),A(2),SA(2),CHIS
      Write (Iw,9908)
      Write (Iw,9906) a(3),sa(3),a(4),sa(4), phi
9900  Format (A)
9901  FORMAT (I3)
9902  FORMAT (1X,F7.2,2F12.6)
9903  FORMAT (/' OUTPUT:',3X,'DOSE',6X,'SFmea',7X,'S.D.(SF)',
     +  4X,'SFfit',/)
9904  FORMAT (10X,F7.2,3F12.6)
9905  FORMAT (/5X,'Sg:/cm2 ',5X,'S.D.(Sg)',4X,' tf:min ',5X,
     +  'S.D.(tf) ',4X,'chi-sqd')
9906  FORMAT (3X,e10.3,4X,e10.3,2X,e10.3,3X,e10.3,3X,e10.3)
9908  Format (/5x,'tr:min  ',5x,'S.D.(tr)',4x,' pn ',9x,'S.D.(pn) ',
     +  4x,'phi:1/cm2-min')

200   CONTINUE
```

```
      Close (Iw)
      STOP
      END

      FUNCTION FCHIS(Y,W,NP,NFREE,MODE,YFIT)
      IMPLICIT DOUBLE PRECISION (A-H,O-Z)
      DIMENSION Y(100),W(100),YFIT(100)
      FCHIS=0.0
      DO 80 I=1, NP
      IF (MODE) 62, 64, 66
62    CHI=(Y(I)-YFIT(I))/Y(I)
      GOTO 70
64    CHI=Y(I)-YFIT(I)
      GOTO 70
66    CHI=(Y(I)-YFIT(I))/W(I)**2
70    FCHIS=FCHIS+CHI**2
      FCHIS=FCHIS/(1.0*NFREE)
80    CONTINUE
      RETURN
      END

      SUBROUTINE SGRID(II,X,Y,W,NP,NM,MODE,A,DA,SA,YFIT,CHIS)
      IMPLICIT DOUBLE PRECISION (A-H,O-Z)
      DIMENSION X(100),Y(100),W(100),A(10),DA(10),SA(10),YFIT(100)
      NFREE=NP-NM
      FREE=NFREE*1.
      CHIS=0.D0
      IF (NFREE) 300, 300, 110
110   If (ii-3) 120,191,120
120   DO 200 J=1, NM
121   DO 122 I=1, NP
      Call FxiaS (ii,x,i,a,Surv)
122   Yfit(i)=Surv
123   CHIS1=FCHIS(Y,W,NP,NFREE,MODE,YFIT)
      FN=0.D0
      D=DA(J)
141   A(J)=A(J)+D
      DO 143 I=1, NP
      Call FxiaS (ii,x,i,a,Surv)
143   YFIT(I)=Surv
144   CHIS2=FCHIS(Y,W,NP,NFREE,MODE,YFIT)
145   IF (CHIS1-CHIS2) 151,141,161

151   D=-D
      A(J)=A(J)+D
      DO 154 I=1, NP
      Call FxiaS (ii,x,i,a,Surv)
154   YFIT(I)=Surv
      SAVE=CHIS1
      CHIS1=CHIS2
157   CHIS2=SAVE

161   FN=FN+1.D0
      A(J)=A(J)+D
      DO 164 I=1,NP
      Call FxiaS (ii,x,i,a,Surv)
164   YFIT(I)=Surv
      CHIS3=FCHIS(Y,W,NP,NFREE,MODE,YFIT)
166   IF (CHIS3-CHIS2) 171, 161, 181
```

```
171   CHIS1=CHIS2
      CHIS2=CHIS3
      GOTO 161

181   D=D*(1.D0/(1.D0+(CHIS1-CHIS2)/(CHIS3-CHIS2))+0.5D0)
182   A(J)=A(J)-D
183   SA(J)=DA(J)*SQRT(2.D0/(FREE*(CHIS3-2.D0*CHIS2+CHIS1)))
184   DA(J)=DA(J)*FN/3.
200   CONTINUE

191   DO 192 I=1,NP
      Call FxiaS (ii,x,i,a,Surv)
192   YFIT(I)=Surv
193   CHIS=FCHIS(Y,W,NP,NFREE,MODE,YFIT)
300   RETURN
      END

      Subroutine FxiaS (ii,x,i,a,Surv)
      Implicit Double Precision (a-h, o-z)
      Dimension x(100),a(10)
102   AA=0.0
      BB=X(I)
      HH=(BB-AA)/2.D0
112   t=AA
      ASSIGN 122 TO LE
      GOTO 120
114   t=BB
      ASSIGN 124 TO LE
      GOTO 120
116   t=AA+HH
      ASSIGN 126 TO LE
      GOTO 120
118   ASSIGN 154 TO LE
120   Fun=1.-Dexp(-a(4)*Dexp(-(a(2)-t)/a(3)))

      GOTO LE, (122,124,126,154)
122   S1A=Fun
      ASSIGN 114 TO IL
      GOTO 150
124   S1B=Fun
      S1=S1A+S1B
      ASSIGN 116 TO IL
      GOTO 150
126   S4=Fun
      SS=HH*(S1+4.D0*S4)/3.D0
      S2=0.D0
      ASSIGN 152 TO IL

150   GOTO IL, (114,116,152)
152   S2=S4+S2
      S4=0.D0
      HH=HH/2.D0
      t =AA+HH
      GOTO 118
154   S4=S4+Fun
      t =t+2.D0*HH

      IF (t-BB) 118,160,160
160   SP=HH*(S1+4.D0*S4+2.D0*S2)/3.D0
```

```
      IF (DABS(SP-SS)-0.001*DABS(SP)) 164,164,162
162   SS=SP
      GOTO 152
c     fr=phi
164   fr=9.2e4
      Surv=Dexp(fr*(-a(1))*SS)
      Return
      End

      Subroutine Scurv (ii,x,y,w,np,nm,mode,a,da,sa,fl,yfit,chis)
      Implicit Double Precision (A-H, O-Z)
      Dimension x(1),y(1),w(1),a(4),da(1),sa(1),yfit(1)
      Dimension wt(100),al(10,10),be(10),der(10),ary(10,10),b(10)
11    Nfree=np-nm
      If (Nfree) 13,13,20
13    Chis= 0.
      Go to 110

20    Do 30 i=1,np
21    If (mode) 22,27,29
22    If (y(i)) 25,27,23
23    Wt(i)= 1./y(i)
      Go to 30
25    Wt(i)= 1./(-y(i))
      Go to 30
27    Wt(i)= 1.
      Go to 30
29    Wt(i)= 1./W(i)**2
30    Continue

31    Do 34 j=1,nm
      Be(j)= 0.
      Do 34 k=1,j
34    Al(j,k)= 0.
41    Do 50 i=1,np
      Call Fderiv (ii,x,i,a,da,nm,der)
      Do 46 j=1,nm
      Call FxiaS (ii,x,i,a,Surv)
      Be(j)= be(j)+wt(i)*(y(i)-Surv)*der(j)
      Do 46 k=1,j
46    Al(j,k)= al(j,k)+wt(i)*der(j)*der(k)
50    Continue
51    Do 53 j=1,nm
      Do 53 k=1,j
53    Al(k,j)= al(j,k)

61    Do 62 i=1,np
      Call FxiaS (ii,x,i,a,Surv)
62    Yfit(i)=Surv
63    Chis1=fchis(y,w,np,nfree,mode,yfit)

71    Do 74 j=1,nm
      Do 73 k=1,nm
73    Ary(j,k)=al(j,k)/sqrt(al(j,j)*al(k,k))
74    Ary(j,j)= 1.+fl
80    Call Matinv (ary,nm,det)
81    Do 84 j=1,nm
      B(j)=A(j)
      Do 84 k=1,nm
```

```
84    B(j)=B(j)+be(k)*ary(j,k)/sqrt(al(j,j)*al(k,k))

91    Do 92 i=1,np
      Call FxiaS (ii,x,i,b,Surv)
92    Yfit(i)=Surv
93    Chis=fchis(y,w,np,nfree,mode,yfit)
      If (chis1-chis) 95,101,101
95    Fl= 10.*fl
      Go to 71

101   Do 103 j=1,nm
      A(j)=B(j)
103   SA(j)=sqrt(ary(j,j)/al(j,j))
      Fl= fl/10.
110   Return
      End

      Subroutine Fderiv (ii,x,i,a,da,nm,der)
      IMPLICIT DOUBLE PRECISION (A-H,O-Z)
      Dimension x(50),a(4),da(4),der(10)
11    Do 18 j=1,nm
      Aj=A(j)
      Delta= DA(j)
      A(j)=  Aj+Delta
      Call FxiaS (ii,x,i,a,Surv)
      Yfi=Surv
c        Yfi=FXIAS(ii,x,i,a)
      A(j)= Aj-Delta
      Call FxiaS (ii,x,i,a,Surv)
      Der(j)= (yfi-Surv)/(2.*Delta)
18    A(j)=Aj
      Return
      End

      Subroutine Matinv (ary,norder,det)
      IMPLICIT DOUBLE PRECISION (A-H,O-Z)
      Dimension Ary(10,10),Ik(10),Jk(10)
10    Det=1.
11    Do 100 k=1,norder
      Amax= 0.
21    Do 30 i=k,norder
      Do 30 j=k,norder
23    If (Dabs(Amax)-Dabs(Ary(i,j))) 24,24,30
24    Amax= Ary(i,j)
      Ik(k)= i
      Jk(k)= j
30    Continue

31    If (Amax) 41,32,41
32    Det= 0.
      Go to 140
41    i= Ik(k)
      If (i-k) 21,51,43
43    Do 50 j=1,norder
      Save=Ary(k,j)
      Ary(k,j)= Ary(i,j)
50    Ary(i,j)= -Save
51    j= Jk(k)
      If (j-k) 21,61,53
```

```
53      Do 60 i=1,norder
        Save= Ary(i,k)
        Ary(i,k)= Ary(i,j)
60      Ary(i,j)= -Save

61      Do 70 i=1,norder
        If (i-k) 63,70,63
63      Ary(i,k)= -Ary(i,k)/Amax
70      Continue
71      Do 80 i=1,norder
        DO 80 j=1,norder
        If (i-k) 74,80,74
74      If (j-k) 75,80,75
75      Ary(i,j)= Ary(i,j)+Ary(i,k)*Ary(k,j)
80      Continue
81      Do 90 j=1,norder
        If (j-k) 83,90,83
83      Ary(k,j)= Ary(k,j)/Amax
90      Continue
        Ary(k,k)= 1./Amax
100     Det= Det*Amax

101     Do 130 L=1,norder
        k= norder-L+1
        j= Ik(k)
        If (j-k) 111,111,105
105     Do 110 i=1,norder
        Save= Ary(i,k)
        Ary(i,k)= -Ary(i,j)
110     Ary(i,j)= Save
111     i= Jk(k)
        If (i-k) 130,130,113
113     Do 120 j=1,norder
        Save= Ary(k,j)
        Ary(k,j)= -Ary(i,j)
120     Ary(i,j)= Save
130     Continue
140     Return
        End
c       Reference: Bevington, 1969.
```

References

Al-Ahmad, K.O.(1984). Stopping Power and Range Measurements of Low Energy Electrons (<10 keV) in Solids. Ph.D. Thesis. Dundee University.

Attix, F.H., Roesch, W.C. and Tochilin, E. Radiation Dosimetry (2nd ed). Vol I (1968): Fundamentals. Vol II (1966): Instrumentation. Vol III (1969): Sources, Fields, Measurements, and Applications. Academic Press. New York. London.

Barendsen, G.W. and Beusker, T.L.J.(1960). Effects of different radiations on human cells in tissue culture: I. Irradiation techniques and dosimetry. Radiat. Res. **13**, 832-840.

Barkas, H.(1963). Nuclear Research Emulsion, Vol.1, New York, Academic Press.

Bevington, P.R.(1969). Data Reduction and Error Analysis for the Physical Sciences. New York, McGraw-Hill.

Bichsel, H.(1968). Charged-particle interactions. p.157-228. In "Radiation Dosimetry", Vol I. See Attix *et al* .

Boag, J.W.(1966). Ionization chambers. p.1-72. In "Radiation Dosimetry", Vol II. See Attix *et al* . (1987), Ionization chambers. p.169-244. In "The Dosimetry of Ionizing Radiation", Vol.II. Eds. K.R. Kase, B.E. Bjarngard & F.H. Attix. Aca. Pr., Inc.

Boice, J.D. and Fraumeni, J.F.(1984). Radiation Carcinogenesis: Epidemiology and Biological Significance. Raven Press. New York.

Boutillon, M. and Perroche-Roux, A.M.(1987). Re-evaluation of the W Value for electrons in air. Phys. Med. Biol. **32**(2), 213-219.

Braby, L.A. and Roesch, W.C.(1978). Testing of dose-rate models with *Chlamydomonas reinhardi* . Radiat. Res. **76**, 259-270.

Brown, J.M.(1977). The shape of the dose-response curve for radiation carcinogenesis: Extrapolation to low doses. Radiat. Res. **71**, 34-50.

Burlin, T.E.(1968). Cavity-chamber theory. p.331-392. In "Radiation Dosimetry", Vol I. See Attix *et al* .

Butts, J.J. and Katz, R.(1967). Theory of RBE for heavy ion bombardment of dry enzymes and viruses. Radiat. Res. **30**, 855-871.

Cannell, R.J. and Watt, D.E.(1985). Biophysical mechanisms of damage by fast ions to mammalian cells *in vitro* . Phys. Med. Biol. **30**(3), 255-258.

Chadwick, K.H. and Leenhouts, H.P.(1981). The Molecular Theory of Radiation Biology. Springer-Verlag. Berlin, Herdelgerg, New York.

Chatterjee, A and Magee, J.L.(1985). Theoretical investigation of the production of strand breaks in DNA by water radicals. Radiat. Prot. Dos. **13**(1-4), 137-140.

Chen, C.-Z.(1984). An Appraisal of Models for the Specification of Biological Damage by Ionizing Radiations of X-rays and Gamma-rays. M.Sc. Dissertation. St. Andrews University.

Chen, C.-Z., McGuire, A. and Watt, D.E.(1987). Test of a DNA-rupture model of radiation action. Session **B32-1V**, 8th ICRR. 19-24 July, 1987. Edinburgh.

Chen, C.-Z. and Watt, D.E.(1986). Biophysical mechanism of radiation damage to mammalian cells by x and γ-rays. Int. J. Radiat. Biol. **49**(1), 131-142.

Coggle, J.E.(1983). Biological Effects of Radiation (2nd ed). Taylor & Francis Inc. New York. (1985). Radiation Carcinogenesis. in "The Molecular Basis of Cancer". Eds. Peter B. Farmer and John M. Walker. Croom Helm. London. Sydney.

Cohen, B.L.(1980). The cancer risk from low-level radiation. Health Phys. **39**(4), 659-678.

Cole, A., Cooper, W.G., Shonka, F., Corry, P.M., Humphrey, R.M. and Ansevin, A.T.(1974). DNA scission in hamster cells and isolated nuclei studied by low-voltage electron beam irradiation. Radiat. Res. **60**, 1-33.

Cole, A., Humphrey, R.M. and Dewey, W.C.(1963). Low-voltage electron beam irradiation of normal and 5-bromouridine deoxyriboside-treated L-P59 mouse fibroblast cells in vitro. Nature, **199**, 780-782.

Cox, R., Thacker, J. and Goodhead, D.T.(1977). Inactivation and mutation of cultured mammalian cells by aluminium characteristic ultrasoft x-rays (II). Int. J. Radiat. Biol., **31**, 561-576.

Datta, R. Cole, A. and Robinson, S.(1976). Use of track-end alpha particles from ^{241}Am to study radiosensitive sites in CHO cells. Radiat. Res. **65**, 139-151.

Dertinger, H. and Jung, H.(1970). Molecular Radiation Biology.

Springer, Berlin Heidelberg New York.

Dugle, D.L., Gillespie, G.J. and Chapman, J.D.(1976). DNA strand breaks, repair, and survival in x-irradiated mammalian cells. Proc. Natl. Acad. Sci., USA. **73**, 809-812.

Elkind, M.M.(1984). Repair processes in radiation biology (Failla Memorial Lecture). Radiat. Res. **100**, 425-449.

Elkind, M.M., Han, A. and Hill, C.K.(1984). Error-free and error-prone repair in radiation-induced neoplastic cell transformation. p.303-318. In Boice & Fraumeni(1984).

Freeman, S.E., Blackett, A.D., Monteleone, D.C., Setlow, R.B., Sutherland, B.M. and Sutherland J.C.(1986). Quantitation of radiation-, chemical-, or enzyme-induced single strand breaks in nonradioactive DNA by alkaline gel electrophoresis: Application to pyrimidine dimers. Anal. Biochem. **158**, 119-129.

Geard, C.R.(1985). Chromosomal aberration production by "track segment" charged particles as a function of linear energy transfer. Radiat. Prot. Dos. **13**(1-4), 199-204.

Gilbert, C.W.(1969). Computer programmes for fitting puck and probit survival curves. Int. J. Radiat. Biol., **16**(4), 323-332.

Goodhead, D.T.(1983). Cellular effects of ultrasoft x-radiation. Implications for mechanism of radiation cell killing. In "The Biological Basis of Radiotherapy". p.81-92. Eds. Steel, Adams & Peckham. Elsevier Science Publishers B.V. (1984), Deductions from cellular studies of inactivation, mutatagenesis and transformation. p.369-385, see Boice & Fraumeni.

Goodhead, D.T.(1987a). Biophysical models of radiation action; introductory review. Session **S26-1**, 8th ICRR, 19-24 July, 1987. Edinburgh. (1987b), Relationship of microdosimetric techniques to applications in biological systems. p.1-90. In "The Dosimetry of Ionizing Radiation", Vol.II. Eds. K.R. Kase, B.E. Bjarngard & F.H. Attix. Aca. Pr., Inc.

Goodhead, D.T., Thacker, J. and Cox, R.(1979). Effectiveness of 0.3 keV carbon ultrasoft x-rays for the inactivation and mutation of cultured mammalian cells. Int. J. Radiat. Biol., **36**, 101-114.

Greening, J.R.(1964). Saturation characteristics of parallel- plate ionization chambers. Phys. Med. Biol. **9**, 143-154. (1986). Instability of radiation protection quantities. *ibid.* **31**, 191.

Hall, E.J.(1972). Radiation dose-rate: a factor of importance in radiobiology and radiotherapy (review article). Br. J. Radiol. **45**, 81-97. (1978). Radiobiology for Radiologist (2nd Edn). Harper & Row, Publishers. New Yorw. London.

Hamm, R.N., Wright, H.A., Katz, R., Turner, J. and Ritchie, R.H.(1978). Calculated yields and slowing-down spectra for electrons in liquid water: Implications for electron and photon RBE. Phys. Med. Biol. **23**(6), 1149-61.

Hamm, R.N., Wright, H.A., Ritchie, R.H., Turner, J.E. and Turner, T.P.(1975). Monte Carlo calculation of transport of electrons through liquid water. Proc. 5th Symp. Microdos. p.1037-1053. Eds. J. Booz, H.G. Ebert & B.G.R. Smith. EUR 5452 d-e-f.

Held, K.D., Bren, G.D. and Melder, D.C.(1986). Interactions of radioprotectors and oxygen in cultured mammalian cells. II. Effects of dithiothreitol on radiation-induced DNA damage and comparison with cell survival. Radiat. Res. **108**, 296-306.

Hunger, H-J. and Kuchler, L.(1979). Measurement of the electron backscattering coefficient for quantitative EPMA in the energy range of 4 to 40 keV. Phys. Stat. Sol. **A56**, K45-K48.

ICRP(1977). Pub. 26, Annals of the ICRP1, No.3, Pergamon Press, Oxford.

ICRU(1964). ICRU Rep. **10 b**, Physical Aspects of Irradiation. NBS Handbook 85 (U.S. Government Printing Office, Washington D.C.).

ICRU(1969). Radiation Dosimetry: X-Rays and Gamma Rays with Maximum Photon Energies between 0.6 and 50 MeV. Rep. **14**, ICRU, Washington D.C.

ICRU(1970). Linear Energy Transfer. Rep. **18**, ICRU, Washington D.C.

ICRU(1979a). Quantitative Concepts and Dosimetry in Radiobiology. Rep.**30**, ICRU, Washington D.C. (1979b), Average Energy Required to Produce an Ion Pair. Rep.**31**, ICRU, Washington D.C.

ICRU(1980). Radiation Quantities and Units. Rep. **33**, ICRU, Washington D.C.

ICRU(1983). Microdosimetry. Rep. **36**, ICRU, Bethesda, Md.

ICRU(1984). Stopping Powers for Electrons and Positrons. Rep. **37**, ICRU, Bethesda, Md.

ICRU(1986). The Quality Factor in Radiation Protection. Rep. **40**, ICRU, Bethesda, Md.

Iskef, H.(1981). Stopping Power and Range of Low Energy Electrons (20 eV to 10 keV). Ph.D. Thesis. Dundee University.

Kassis, A.I., Adelstein, S.J., Haydock, C. and Sastry, K.S.R.(1980). Radiotoxicity of ^{75}Se and ^{35}S: Theory and application to cellular

model. Radiat. Res. **84**, 407-425.

Katz, R., AAckerson, B., Homayoonfar, M. and Sharma, S.C.(1971). Inactivation of cells by heavy ion bombardment. Radiat. Res., **47**, 402-425.

Katz, R., Sharma, S.C. and Homayoonfar, M.(1972). The structure of particle tracks, in "Topics in Radiation Dosimetry", Supp 1, p.317-384. Eds. H. Frank & F.H. Attix. Academic Press. New York. London.

Kavenoff, R. and Zimm, B.H.(1973). Chromosome-sized DNA molecules. Chromosoma **41**, 1-27.

Kellerer, A.M. and Rossi, H.H.(1971). RBE and the primary mechanism of radiation action. Radiat. Res. **47**, 15-34. (1972). The theory of dual radiation action. Curr. Top. Radiat. Res., **Q.8**, 402-425. (1972). ibid, **Q.8**, 85-158. (1978). A generalized formulation of dual radiation action. Radiat. Res. **75**, 471-488.

Kiefer, J.(1985). Cellular and subcellular effects of very heavy ions. Int. J. Radiat. Biol. **48**(6), 873-892.

Kiefer, J., Rase, S., Schneider, E., Stratten, H., Kraft, G. and Leisem, H.(1982). Heavy ion effects on yeast cells: Induction of canavine resistant mutants. Int. J. Radiat. Biol. **42**, 591-600.

Koch, C.J. and Painter, R.B.(1975). The effect of extreme hypoxia on the repair of DNA single-strand breaks in mammalian cells **64**, 256-269.

Kruse, P.F. and Patterson, M.K.(1973). Tissue Culture Methods and Applications. Academic Press. New York. San Francisco. London.

Laughlin, J.S. and Genna, S.(1968). Calorimetry. p.389-441. In "Radiation Dosimetry", Vol II. See Attix *et al* .

Little, J.B., Hahn, G.M., Frindal, E. and Tubiana, M.(1973). Radiol., **106**, 689-694.

Lloyd, D.C., Purrott, R.J., Dolphin, G.W. and Edwards, A.A.(1976). Chromosome aberrations induced in human lymphocytes. Int. J. Raidiat. Biol. **29**, 169-182.

Metting, N.F., Braby, L.A., Roesch, W.C. and Nelson, J.M.(1985). Dose-rate evidence for two kinds of radiation damage in stationary- phase mammalian cells. Radiat. Res. **103**, 204-218.

Millar, B.C., Fielden, E.M. and Millar, J.L.(1978). Interpretation of survival-curve data for Chinese hamster cells, line V-79 using the multi-target, multi-target with initial slope, and α, β equations. Intl. J. Radiat. Biol. **33**, 599-603.

Min, T., Cohn, P. and Simmons, J.A.(1985). The sensitivity of three diploid human cell lines to alpha-irradiation. Proc. 2nd Workshop on Lung Dosimetry. Cambridge, 1985.

Mitchell, J.B., Bedford, J.S. and Bailey, S.M.(1979). Dose-rate effects on the cell cycle and survival of S3 HeLa and V79 cells. Radiat. Res., **79**, 520-536.

Mozumder, A. and Magee, J.L.(1966). Model of tracks of ionizing radiation for radical reaction mechanisms. Radiat. Res. **28**, 203-214.

Munson, R.J., Bance, D.A., Stretch, A. and Goodhead, D.T.(1979). Mutation and inactivation of cultured mammalian cells exposed to beams of accelerated heavy ions. I. Irradiation facilities and methods. Int. J. Radiat. Biol. **36**, 127-136.

Okada, S.(1970). DNA as target molecule responsible for cell killing. in "Radiation Biochemistry", Vol.1. p.103-147. Eds. K.I. Altman, G.B. Gerber and S. Okada. Academic Press. New York. London.

Pochin, E.(1983). Harm to the cell and harm to the individual. p3-15. In "Biological Effects of Low-Level Radiation", Vienna, IAEA.

Powers, D.(1978). Unpublished.

Ritchie, R.H., Hamm, R.N., Turner, J. and Wright, H.A.(1978). The interaction of swift electrons with liquid water, 6th Microdosimetry, p.345-354. Eds. J. Booz & H.G. Ebert. EUR6064 DE-EN-FR.

Roesch, W.C.(1972). Hit theory for low-LET radiation (abstract). Radiat. Res. **51**, 480.

Roos, H. and Kellerer, A.M.(1986). An alpha irradiation device for cell studies. IMSK, 86/108 (private communication).

Rossi, H.H.(1972). The role of microdosimetry in radiobiology and radiation protection. Proc. 3rd Symp. Microdos. Eds. H.G. Ebert, CEC, Luxemburg.

Rossi, H.H. and Rosenzweig, W.(1955). A device for the measurement of dose as a function of specific ionization. Radiology, **64**, 404.

Shen, X. and Fu, Y.(1983). Radiation-induced binding of thymine with amino acids- a model system to study radiation-induced cross-links between DNA and protein. Session **A3-39**, Proc. 7th ICRR. Amsterdam, Martinus Nijhoff Publishers.

Simmons, J.A., Cohn, P. and Min, T.(1983). Sensitivity of lung cells

to alpha particle irradiation. Session **B7-27**, Proc. 7th ICRR. Amsterdam, Martinus Nijhoff Publishers.

Simpson, J.A. and Kuyatt, C.E.(1963). Design of low voltage electron gun. Rev. Sci. Instr. **34**(3), 265-268.

Sutherland, J.C., Lin, B.-H., Monteleone, D.C., Mugavero, J., Sutherland, B.M. aand Trunk, J.(1987b). Electronic imaging system for direct and rapid quantitation of fluorescence from electrophoretic gels: Application to ethidium bromide-stained DNA. Anal. Biochem., **163**, 446-457.

Sutherland, J.C., Monteleone, D.C., Mugavero, J.H. and Trunk, J.(1987). Unidirectional pulsed field electrophoresis of single and double stranded DNA in agarose. Anal. Biochem., **162**, 511-520.

Szechter, A. and Schwarz, D.(1977). Dose-rate effects, fractionation, and cell survival at lowered temperatures. Radiat. Res., **71**, 593-619.

Thomas, G.E. and Watt, D.E.(1985). A track structure description of the inactivation of enzymes and viruses by fast ions. Radiat. Effects, **84**, 107-116.

Tobleman, W.T. and Cole, A.(1974). Repair of sublethal damage and oxygen enhancement ratio for low-voltage electron beam irradiation. Radiat. Res. **60**, 355-360.

Todd, P.W., Lyman, J.T., Armer, R.A., Skarsgard, L.D. and Deering, R.A.(1968). Dosimetry and apparatus for heavy ion irradiation of mammalian cells in vitro. Radiat. Res. **34**, 1-23.

Tung, C.J. and Chen, P.J.(1982). Energy-loss and range stragglings for electrons in water. Proc. 8th Symp. Microdos. p.243-254. Eds. J. Booz and H.G. Ebert. Luxemburg. CEC.

Uehara, S.(1986). The development of a Monte Carlo code simulating electron- photon showers and its evaluation by various transport benchmarks. Nucl. Instr. Meth. **B14**, 559-570.

Upton, A.C.(1977). Radiobiological effects of low doses: Implication for radiological protection. Radiat. Res. **71**, 51-74.

Virsik, R.P., Blohm, R., Hermann, K.-P., Modler, H. and Harder, D.(1982). Chromosome aberrations and the mechanism of "primary lesion interaction". Proc. 8th Symp. Microdos. p.409-422. Eds. J. Booz and H.G. Ebert. Julich.

Waibel, E. and Grosswendt, B.(1978). Determination of W values and backscatter coefficients for slow electrons in air. Radiat. Res. **76**, 241-249.

Watt, D.E.(1975). Hit Cross-sections in single target theory. Phys. Med. Biol. **20**, 944-954.

Watt, D.E.(1987). An approach to unified dosimetry for assessment of radiation effect. Session **B21-2V**, 8th ICRR. 19-24 July, 1987. Edinburgh.

Watt, D.E., Al-Affan, I.A.M., Chen, C.-Z. and Thomas, G.E.(1985). Identification of biophysical mechanisms of damage by ionising radiation, Radiat. Prot. Dosi.(Microdosimetry, Proc. Ninth Symp. Microdos., May 20-24, Toulouse, France) **13**(1-4), 285-294.

Watt, D.E., Cannell, R.J. and Thomas, G.E.(1984). Ion beams in quality determination for radiation protection. Intl. Symp. on 3-day in Depth Review on the Nuclear Accelerator Impact in the Inter-disciplinary Field. 30 May-1 June, Padova. Eds. P. Mazzoli and G. Moschini.

Watt, D.E. and Chen, C.-Z.(1985). Unpublished Data.

Watt, D.E., Chen, C.-Z., Kadiri, L. and Younis, A.(1987). Towards a unified system for expression of biological damage by ionizing radiation. Bri. Nucl. Energy Soc., 11-12 May, 1987. London.

Xiao, M.-Y. (1980). Evaluation of Experimental Errors and Data Processing. Kouxue Chubanshe, Beijing.

Zermeno, A. and Cole, A.(1969). Radiosensitive structure of metaphase and interphase hamster cells as studied by low-voltage electron beam irradiation. Radiat. Res. **39**, 669-684.

INT. J. RADIAT. BIOL., 1986, VOL. 49, NO. 1, 131–142

Biophysical mechanism of radiation damage to mammalian cells by X- and γ-rays

C. Z. CHEN and D. E. WATT

Department of Physics, University of St Andrews, St Andrews KY16 9SS, U.K.

(*Received 13 November 1984; final version received 20 June 1985; accepted 25 June 1985*)

Published information on the reproductive death in mammalian cells irradiated by a wide range of X- and γ-ray energies has been re-analysed to extract intrinsic efficiencies of damage for the secondary electrons in transient equilibrium. On a log-log plot, a linear dependence on the track average l.e.t. and the average specific primary ionization is found, indicating that either serves as a good quality parameter. The soft X-ray data are consistent with this conclusion. Upon comparison with data for fast heavy ion irradiations, the average specific primary ionization is shown to be applicable independently of radiation type whereas track average l.e.t. is not. Furthermore it is revealed that electrons are most damaging near the end of their range but their efficiency is only about 10–20 per cent of that of fast ions at the same quality, possibly due to the influence of multiple scatter on the electron penetration depth.

It is deduced that, for the dose rates involved, the damage by electrons is predominantly by intra-track action and not inter-track action. The results are consistent with the suggestion that optimum damage occurs when the mean free path between ionizations is equivalent to the strand separation in the double-stranded DNA.

Indexing terms: radiation quality, mammalian cell survival.

1. Introduction

Identification of the physical quantities which are appropriate for the specification of radiation quality in biological systems is of fundamental importance in the prediction of radiation effects at low doses and in the dosimetry and application of radiation.

During the last decade progress in experimental and theoretical studies of charged particle track interactions has enabled accurate calculations down to energies at the end of the particle range. Recently, when this type of information was applied to published data for the induction of reproductive death in mammalian cells by fast heavy ions, good correlation was obtained in terms of the specific primary ionization (Cannell and Watt 1985, Watt *et al.* 1984). The results suggest that the degree of radiation effect is determined by the mean free path between ionizations and that the energy transfer per primary ionization is relatively unimportant.

For example, when comparison is made for data points with the same specific primary ionization, the data of Blakely *et al.* (1979), obtained with fast ions, having maximum delta-ray energies up to 1·6 MeV, do not differ significantly from the data of Skarsgard *et al.* (1967) and Thacker *et al.* (1979) which have maximum delta-rays up to only 25 keV. Similarly, for yeast cells (Kiefer *et al.* 1982), the ions used have delta-ray yields ranging from ten to one hundred times greater than that occurring for the onset of primary track saturation, yet the intrinsic efficiency for damage is only about 2·0.

The intrinsic efficiency for damage per charged particle track is found to reach an optimum value when the mean free path for primary ionizations is equal to the strand spacing in double-stranded DNA, namely when the specific primary ionization (in water) is about $5{\cdot}5 \times 10^6$ ionizations $cm^2\,g^{-1}$ independently of fast heavy particle type. From this it may be predicted that electrons with the optimum specific primary ionization should act with the same maximum intrinsic efficiency as the heavy ions. In an attempt to gain information on electrons we have analysed published survival data for induction of reproductive death in mammalian cells irradiated by gamma and X-ray fields covering a wide energy range—from 1·25 MeV to 300 eV.

2. Correlation of data

Several sets of survival data for X- and γ-irradiations of mammalian cells have been collated (tables 1–3). Three types of mammalian cells were involved: human carcinoma cells (HeLa); Chinese hamster ovary cells (CHO) and Chinese hamster lung cells (V79). The cells were irradiated *in vitro*. The results of the published papers on mammalian cells were analysed using the values of D_0 which were obtained either from the original authors (in most cases) or by determining the average slope over the approximately linear portion of the published survival curves.

The D_0 values and the results of other relevant calculations are listed in tables 1–3. For γ-rays from ^{60}Co and ^{137}Cs, the effective energy of the photons, $E_{h\nu}$, is taken to be 1252 keV and 662 keV, respectively. For the bremsstrahlung from X-ray machines, the $E_{h\nu}$ value is determined from the HVL (half value layer) or from the filtration thickness, quoted by the original authors and by reference to a catalogue of standard spectra (Seelentag *et al.* 1979).

For this general analysis, some of the factors which might have a second-order influence on the dose–effect curves have been disregarded. However, one of these, the radiation dose-rate has been limited to within two orders of magnitude in the collected data, i.e. 0·14–1·6 Gy min^{-1} for HeLa cells, 0·14–9 Gy min^{-1} for CHO cells, and 1·5–50 Gy min^{-1} for V79 cells. The cells were irradiated *in vitro* in air or in oxygen. No added chemical protectors or sensitizers were present.

The track average l.e.t. (in water), L_T, for the equilibrium slowing down spectra of secondary electrons generated from the primary differential compton and photo-electron distributions released by the incident photons were calculated following McGinnies' work (1959) modified to extend the validity down to 30 eV electron energy using theoretical and empirical relationships (Ashley *et al.* 1978, Iskef *et al.* 1983, Al-Ahmad and Watt 1984). From the track average l.e.t. for the equilibrium electron spectrum, the effective electron energy, E_{se}, was determined by comparison with the energy of primary electrons which would give the same l.e.t. Having selected E_{se}, the corresponding value of I_s was determined as follows. For electron energies above 10 keV, a binary encounter formula divided by a factor of 2 is used for the calculation, i.e. the specific primary ionization is given by

$$I_s = \frac{0{\cdot}3387}{2\beta^2} \ln (2{\cdot}325 \times 10^4 \beta^2) \text{ ionizations } \mu m^{-1}$$

The above equation is modified by the factor of 2 in the denominator as this is found to give better normalization to ensure a smooth join to the calculated results for electron energies below 10 keV in liquid water (Tung and Chen 1982).

Table 1. Cross-section ratio and damage efficiency per primary ionization in human carcinoma (HeLa) cells.

	D_o (Gy)	$E_{h\nu}$ (keV)	E_{pe} (keV)	E_{se} (keV)	$\bar{L}_T$ (keV/μm)	$\bar{I}_s$ (μm^{-1})	σ_e ($10^{-8}cm^2$)	σ_e/σ_g ($\times 10^{-2}$)	σ_R/I_s (nm)
Malone *et al.* (1974) Zeitz *et al.* (1977)	1·22 ± 0·08	1252	160	35	0·88	11·5	0·115	0·23	0·201
Djordjevic (1979)	1·35	662	80	19	1·40	18·5	0·166	0·33	0·179
Malone *et al.* (1974)	1·14	200	16	4·5	4·30	59·0	0·604	1·21	0·205
Nias *et al.* (1968, 1969, 1973)	1·46	150	11	3·3	5·42	74	0·594	1·19	0·161
Busse *et al.* (1977) Waldren *et al.* (1978)	1·23 ± 0·11	80	4·7	1·30	9·3	150	1·21	2·42	0·161
Djordjevic *et al.* (1968)	1·15	60	3·5	1·0	11·0	200	1·53	3·06	0·153
Zeitz *et al.* (1977)	0·91	20·4	3·0	0·8	11·8	220	2·08	4·14	0·189
Malone *et al.* (1971)	1·33	25	2·7	0·76	12·2	240	1·47	2·94	0·122

$\sigma_g \simeq 5 \times 10^{-7}$ cm^2

†E_{pe} is the effective mean electron energy (l.e.t. weighted) for the primary photo-electrons and Compton electron distribution.

‡E_{se} is the effective mean electron energy (l.e.t. weighted) for the slowing down spectrum in transient equilibrium.

Table 2. Cross-section ratio and damage efficiency per primary ionization in Chinese hamster ovary (CHO) cells.

Reference	D_o (Gy)	E_{hv} (keV)	E_{pe} (keV)	E_{se} (keV)	$\bar{L}_T$ (keV/μm)	$\bar{I}_s$ (μm^{-1})	σ_e (10^{-8} cm^2)	σ_e/σ_g ($\times 10^{-2}$)	σ_R/I_s (nm)
Gragg *et al.* (1976)									
Railton *et al.* (1973, 1974)									
Michaels *et al.* (1978)	1·72±0·20	1252	160	35	0·88	11·5	0·082	0·164	0·142
Seymour and Mothershill (1981)									
Malone *et al.* (1974)									
Rao and Hopwood (1982)	1·29	662	80	19	1·40	18·5	0·174	0·347	0·188
Malone *et al.* (1974)	1·89	200	16	4·5	4·3	59	0·364	0·728	0·123
Harris *et al.* (1975)	1·25	100	6·5	1·85	7·6	116	0·973	1·946	0·168
Dikomey (1982)	~0·96	~90	5·6	1·6	8·3	130	1·383	2·767	0·213
Elkind and Sutton (1959)	~1·20	~12	5·2	1·45	8·7	140	1·160	2·320	0·166
Waldren and Rasko (1978)	1·60	80	4·7	1·30	9·3	150	0·930	1·860	0·124
Raaphorst and Dewey (1979)	1·30	49	2·85	0·80	12·0	225	1·477	2·954	0·131
Lehnert (1979)	1·25	25	2·6	0·73	12·5	245	1·60	3·200	0·131

Table 3. Cross-section ratio and damage efficiency per primary ionization in Chinese hamster lung (V79) cells.

Reference	D_o (Gy)	E_{hv} (keV)	E_{pe} (keV)	E_{se} (keV)	$\bar{L}_T$ (keV/μm)	$\bar{I}_s$ (μm^{-1})	σ_e (10^{-8} cm^2)	σ_e/σ_g ($\times 10^{-2}$)	σ_R/I_s (nm)
Millar *et al.* (1978)									
Murthy *et al.* (1979)									
Adams *et al.* (1981)	1·97 ± 0·14	1252	160	35	0·88	11·5	0·071	0·143	0·124
Schlag *et al.* (1978, 1981)									
Raaphorst and Kruuv (1978)	1·75 ± 0·64	662	80	19	1·40	18·5	0·128	0·256	0·138
Koch and Kruuv (1971)									
Ben-Hur *et al.* (1974)									
Ngo *et al.* (1977)	1·67 ± 0·14	~120	9·0	2·6	6·2	88	0·594	1·188	0·135
Chapman *et al.* (1971)									
Waldren and Rasko (1978)									
Harris *et al.* (1975)	1·45	100	6·5	1·85	7·6	13	0·834	1·677	0·148
McNally (1976)	1·33	95	6·0	1·7	8·0	125	0·962	1·925	0·154
Piro *et al.* (1975)	1·46	.11	6·0	1·7	8·0	125	0·877	1·753	0·140
Utsumi and Elkind (1979)									
Han and Elkind (1977)	1·34 ± 0·19	~12	5·3	1·5	8·6	130	1·027	2·054	0·158
Elkind and Sutton (1959)									
Ngo *et al.* (1981)	2·21	80	4·7	1·3	9·3	150	0·673	1·347	0·090
Burki and Carrano (1973)	1·54	~40	2·5	0·7	12·7	250	1·319	2·639	0·106
Goodhead and Thacker (1977)	~1·04	1·5	0·34	0·12	22·8	680	3·508	7·015	0·103
Goodhead *et al.* (1979)	~0·79	0·3	0·12	0·056	25·6	700	5·18	10·37	0·148

3. Results

For X- and γ-irradiations the effect cross-sections, σ_e in cm^2, were calculated from

$$\sigma_e = 1{\cdot}6 \times 10^{-9} \bar{L}_T / D_0$$

where $\bar{L}_T$ is the track average l.e.t. in keV μm^{-1} for the electron spectrum at transient equilibrium and D_0 is in gray. The σ_e values are normalized to a numerical value taken for the geometrical cross-section, σ_g, of the cell nuclei. A nominal value of 5×10^{-7} cm^2 is taken as a compromise between the uncertainty in nuclear size in different experimental arrangements (e.g. Zermeno and Cole 1969, Todd 1975) and the realization that it may be more appropriate to normalize to the cross-sectional area of the DNA content. The ratio $\sigma_R = \sigma_e / \sigma_g$ represents the intrinsic efficiency for the damage specified.

When the intrinsic efficiency for damage is plotted versus $\bar{L}_T$ or $\bar{I}_s$ on a logarithmic scale a linear relationship is obtained for all photon energies (figure 1 (*a*), (*b*)). Mathematical representations of the data, determined by the least squares method, are

$$\sigma_R = (1{\cdot}91^{+0{\cdot}53}_{-0{\cdot}41}) \times 10^{-3} \bar{L}_T^{1{\cdot}12 \pm 0{\cdot}08}$$

and

$$\sigma_R = (1{\cdot}82^{+0{\cdot}55}_{-0{\cdot}42}) \times 10^{-4} \bar{I}_s^{0{\cdot}95 \pm 0{\cdot}03}$$

where the errors are standard deviations about the mean.

Another quantity of interest is the efficiency per primary ionization (or per delta-ray yield) for the equilibrium electron spectra i.e. $\alpha \sigma_R / \bar{I}_s$. As is expected from the equations above this is also constant but with a tendency to decrease at the lowest photon energies i.e. at the highest $\bar{I}_s$ values. The results can be represented by

$$\sigma_R / \bar{I}_s = (0{\cdot}182^{+0{\cdot}055}_{-0{\cdot}042}) \bar{I}_s^{-0{\cdot}047 \pm 0{\cdot}033}$$

Comparison of the latter three equations with the data points is made in figures 1 (*a*) and (*b*) and 2 (solid lines).

4. Discussion and conclusions

Reference to figure 1 shows that the intrinsic efficiency for damage by X- and γ-rays is linearly related to $\bar{L}_T$, and to $\bar{I}_s$ for the equilibrium electron spectrum, when plotted on a logarithmic scale. The points for 1·5 keV Al K X-rays and 0·3 keV carbon characteristic K X-rays (Goodhead *et al.* 1979) are seen to be consistent with the general trend. Carbon K X-rays are predicted to be the most damaging of all photons because their secondary electrons have specific primary ionization around the region of maximum effectiveness.

The intrinsic efficiency for damage per primary ionization (or per delta-ray) generated by electrons entering the cell nucleus is approximately constant independently of both $\bar{L}_T$ and $\bar{I}_s$ (figure 2). The latter implies that the excess energy transfer per primary ionization along an equilibrium spectrum track is of minor, and possibly negligible importance as may be predicted from the work of Zermeno and Cole (1969) who have demonstrated that electrons must have an energy of about 10 keV to penetrate the cell cytoplasm and damage the nucleus. Thus delta-rays must have energies near to or greater than this value to enhance the observed damage cross-section beyond that for the primary target nucleus. Additionally, as the probability

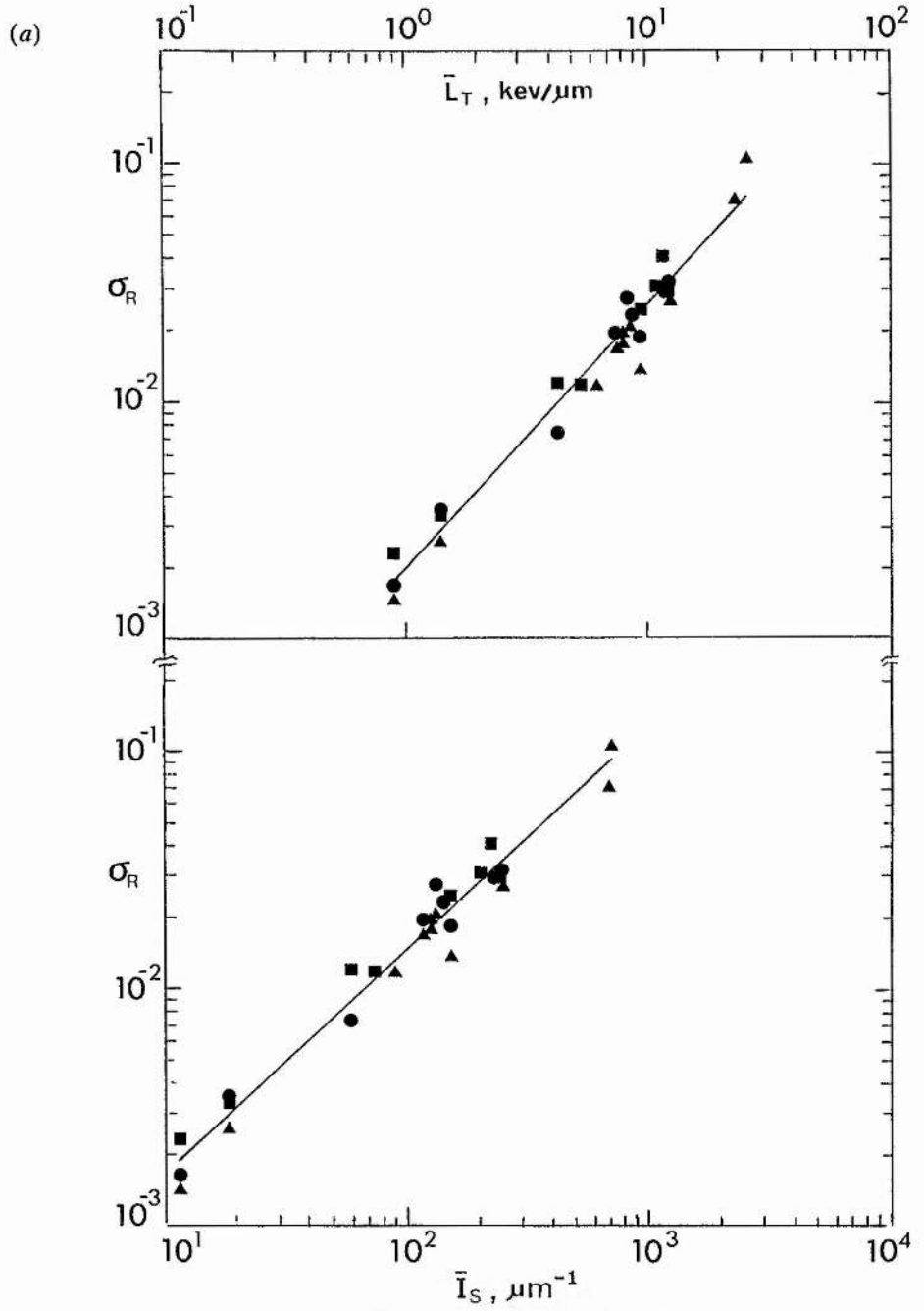

Figure 1. Intrinsic efficiency, for damage by secondary electrons produced in X-and γ-irradiation of CHO (●), HeLa (■) and V-79 cells (▲), plotted as a function (*a*) of the track average l.e.t., $\bar{L}_T$, and (*b*) the mean specific primary ionization, $\bar{I}_s$. References are given in tables 1–3.

of damage by electrons increases rapidly towards the end of the electron track (figure 1 and 3) so, to a good approximation, it can be said that electrons only produce significant damage if they come to rest in the cell nucleus and that their initial kinetic energies are relatively unimportant.

Examination of the data in figure 1 shows that either $\bar{L}_T$ or $\bar{I}_s$ are satisfactory

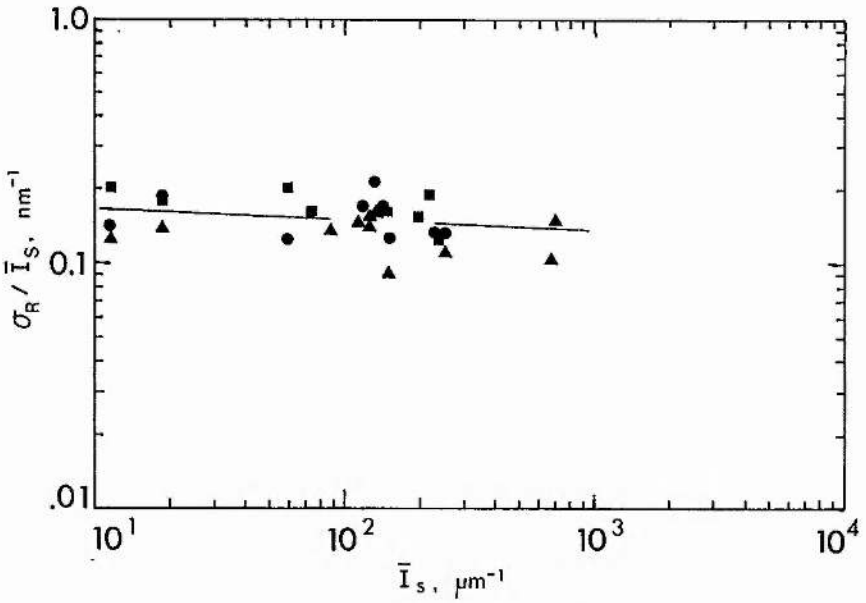

Figure 2. The intrinsic efficiency per primary ionization ($\sigma_R/\bar{I}_s$), plotted as a function of $\bar{I}_s$, approximately constant for photon energies ranging from ^{60}Co to $C_{k\alpha}$ X-rays indicating that the energy transfer per collision, for electrons in the equilibrium slowing down spectrum, is of relatively minor importance.

quality parameters. However, when the heavy ion data are taken into account, I_s is found to be distinctly superior to L_T (Cannell and Watt 1985).

Virsik *et al.* (1983) have reported a good correlation of electron, photon and neutron data with dose-restricted l.e.t. However, restricted l.e.t., which bears a good proportional relationship to the specific primary ionization, is in the wrong dimensional units to permit direct identification of the critical 1·8 nm spacing identified here.

A comparison between the photon data and a typical set of heavy ion data is shown in figure 3. Several interesting features can be deduced from the comparison. First, maximum effective primary ionization for X- and γ-rays can only just exceed the optimum value of 5×10^6 ions cm^2 g^{-1}. This is because electrons can achieve this value only when their energies lie between 250 eV and 50 eV and consequently they reach maximum damage efficiency at the end of their ranges. Secondly, the magnitude of the intrinsic efficiency for X- and γ-rays is always very much less than that for heavy ions with the same specific primary ionization, even for ^{60}Co γ-rays (Watt *et al.* 1985). A probable explanation is that because the equilibrium slowing down electron spectrum contains an abundance of low energy electrons for all photon energies (Hamm *et al.* 1978) and, although these are the most damaging, nevertheless, because of multiple scatter, only a small percentage ($\sim$10 per cent) will have sufficient projected range to penetrate both strands of the DNA thereby reducing the probability of damage. The results are consistent with the deduction that the dominant damage mechanism is a process which reaches an optimum value when the mean free path between primary ionizations along the charged particle tracks corresponds to the spacing between strands in double-stranded DNA.

Thirdly, the effect cross-sections for X- and γ-rays have been deduced from the D_0 values, which lie beyond the shoulder in the dose–response curves. As the intrinsic efficiencies are more closely proportional to the specific primary ionization,

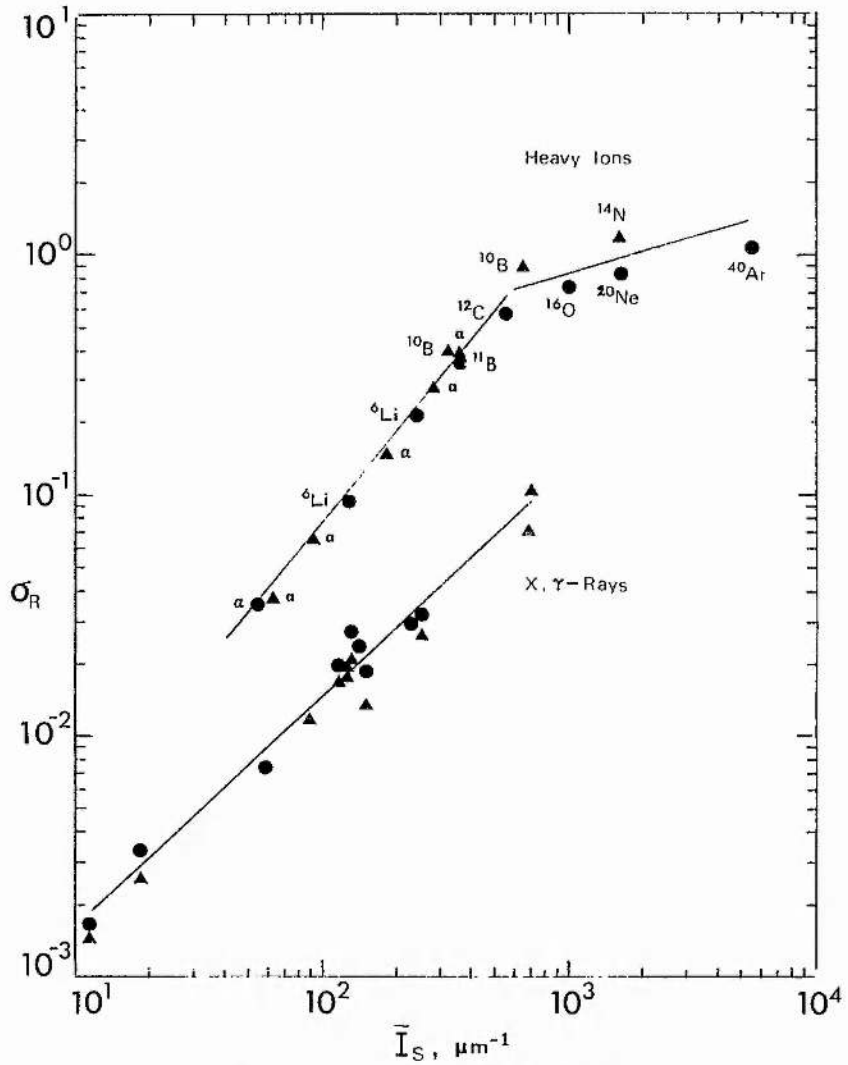

Figure 3. Results for X- and γ-rays from figure 1 (*b*) (tables 2 and 3) are compared with the intrinsic efficiencies for fast accelerated ions (CH cells (●), Skarsgard *et al.* (1967); V-79 cells (▲), Thacker *et al.* (1979)). At the same value of $\bar{I}_s$ the photon data are about an order of magnitude smaller than the ion data (see text). Also as σ_R is more nearly proportional to $\bar{I}_s$ than to $(\bar{I}_s)^{\frac{1}{2}}$ for the photons, electron intratrack action appears to dominate the damage mechanism.

I_s, than to $(I_s)^{\frac{1}{2}}$ it can be implied that most of the observed damage is due to intra-track effects rather than to inter-track effects.

Acknowledgment

Grateful acknowledgment is made to the following bodies for financial support: Sino-British Fellowship Trust; Universities' China Committee, The Henry Lester Trust, St Andrews University and the Chinese Academy of Sciences. This work is part of a program supported by the EEC contract no B10-A-463-81-UK.

References

Adams, G. E., Fielden, E. M., Hardy, C., Millar, B. C., Stratford, I. J., and Williamson, C., 1981, Radiosensitization of hypoxic mammalian cells in vitro by some 5-substituted-4-introimidazoles. *International Journal of Radiation Biology*, **40**, 153–161.

AL-AHMAD, K. O., and WATT, D. E., 1984, Stopping powers for low energy electrons (10 keV) in solid polyethylene. *Journal of Physics D: Applied Physics*, **17**, 1899–1904.

ASHLEY, J. C., TUNG, C. J., and RITCHIE, R. H., 1978, Inelastic interactions of electrons with polystyrene: Calculations of mean free paths, stopping powers, and csda ranges. *IEEE Transactions in Nuclear Science*, **NS-25**, 1566–1570.

BEN-HUR, E., ELKIND, M. M., and BRONK, B. V., 1974, Thermally enhanced radioresponse of cultured Chinese hamster cells: Inhibition of repair of sublethal damage and enhancement of lethal damage. *Radiation Research*, **58**, 38–51.

BLAKELY, E. A., TOBIAS, C. A., YANG, C. H., SMITH, K. C., and LYMAN, J. T., 1979, Inactivation of human kidney cells by high-energy monoenergetic heavy-ion beams. *Radiation Research*, **80**, 122–160.

BURKI, H. J., and CARRANO, A. V., 1973, Relative radiosensitivities of tetraploid and diploid Chinese hamster cells in culture exposed to ionizing radiation. *Mutation Research*, **17**, 277–282.

BUSSE, P. M., BOSE, S. K., JONES, R. W., and TOLMACH, L. J., 1977, The action of caffeine on x-irradiated HeLa cells. II. Synergistic lethality. *Radiation Research*, **71**, 666–677.

CANNELL, R. J., and WATT, D. E., 1985, Biophysical mechanisms of damage by fast ions to mammalian cells in vitro. *Physics in Medicine and Biology*, **30**, (3), 255–258.

CHAPMAN, J. D., WEBB, R. G., and BORSA, J., 1971, Radiosensitization of mammalian cells by p-nitroacetophenone. I. Characterization in asynchronous and synchronous populations. *International Journal of Radiation Biology*, **19**, 561–573.

DIKOMEY, E., 1982, Effect of hyperthermia at 42 and 45°C on repair of radiation-induced DNA strand breaks in CHO cells. *International Journal of Radiation Biology*, **41**, 603–614.

DJORDJEVIC, B., 1979, Modification of radiation response in HeLa cells by misonidazole. *International Journal of Radiation Biology*, **36**, 601–612.

DJORDJEVIC, B., KIM, J. H., and KIM, S. H., 1968, Modification of radiation response in synchronised HeLa cells by metabolic inhibitors. I. Effect of an inhibitor of RNA synthesis, puromycin aminonucleoside. *International Journal of Radiation Biology*, **14**, 1–7.

ELKIND, M. M., and SUTTON, H., 1959, X-ray damage and recovery in mammalian cells in mammalian cells in culture. *Nature*, **184**, 1293–1295.

GOODHEAD, D. T., and THACKER, J., 1977, Inactivation and mutation of cultured mammalian cells by aluminium characteristic ultrasoft X-rays: I. Properties of aluminium X-rays and preliminary experiments with Chinese hamster cells. *International Journal of Radiation Biology*, **31**, 541–559.

GOODHEAD, D. T., THACKER, J., and COX, R., 1979, Effectiveness of 0·3 keV carbon ultrasoft x-rays for the inactivation and mutation of cultured mammalian cells. *International Journal of Radiation Biology*, **36**, 101–114.

GRAGG, R. L., HUMPHREY, R. M., and MEYN, R. E., 1976, The response of Chinese hamster ovary cells to fast neutron radiotherapy beams. I. Relative biological effectiveness and oxygen enhancement ratio. *Radiation Research*, **65**, 71–82.

HAMM, R. N., WRIGHT, H. A., KATZ, R., TURNER, J., and RITCHIE, R. H., 1978, Calculated yields and slowing-down spectra for electrons in liquid water: Implications for electron and photon RBE. *Physics in Medicine and Biology*, **23**, (6), 1149–1161.

HAN, A., and ELKIND, M. M., 1977, Additive action of ionizing and non-ionizing radiations throughout the Chinese hamster cell-cycle. *International Journal of Radiation Biology*, **31**, 275–282.

HARRIS, J. W., POWER, J. A., and KOCK, C. J., 1975, Radiosensitization of hypoxic mammalian cells by diamide. I. Effects of experimental conditions on survival. *Radiation Research*, **64**, 270–280.

ISKEF, H., CUNNINGHAM, J. W., and WATT, D. E., 1983, Project Projected ranges and effective stopping powers of electrons with energy between 20 eV and 10 keV. *Physics in Medicine and Biology*, **28**, (5), 535–545.

KIEFER, J., RASE, S., SCHNEIDER, E., STRATTEN, H., KRAFT, G., and LIESEM, H., 1982, Heavy ion effects on yeast cells: Industion of canavanine-resistant mutants. *International Journal of Radiation Biology*, **42**, 591–600.

KOCH, C. J., and KRUUV, J., 1971, The effect of extreme hypoxia on recovery after irradiation by synchronized mammalian cells. *Radiation Research*, **48**, 74–85.

LEHNERT, S., 1979, Modification of radiation response of CHO cells by 1-methyl-3-isobutylxanthine. I. Reduction of D_0. *Radiation Research*, **78,** 1–12.

MALONE, J. F., FOSTER, C. J., ORR, J. S., and SOLOMONIDES, E., 1971, The effects on the survival of HeLa S-3 cells of independent variations in the sizes of the first and the second X-ray dose in split dose experiments. *International Journal of Radiation Biology*, **20,** 225–231.

MALONE, J. F., PORTER, D., and HENDRY, J. H., 1974, The r.b.e. of ^{60}Co gamma rays with respect to 300 kVp X-rays for the survival of HeLa S-3 and CHO cells, irradiated in different states of proliferation. *International Journal of Radiation Biology*, **26,** 355–362.

MCGINNIES, R. T., 1959, *Energy Spectrum Resulting from Electron Slowing Down,* National Bureau of Standards Circular 597, Washington.

MCNALLY, N. J., 1976, The effect of a change in radiation quality on the ability of electron affinic sensitizers to sensitize hypoxic cells. *International Journal of Radiation Biology*, **29,** 191–196.

MICHAELS, H. B., EPP, E. R., LING, C. C., and PETERSON, E. C., 1978, Oxygen sensitization of CHO cells at ultrahigh dose rates: prelude to oxygen diffusion studies. *Radiation Research*, **76,** 510–521.

MILLAR, B. C., FIELDEN, E. M., and MILLAR, J. L., 1978, Interpretation of survival-curve data for Chinese hamster cells, line V-79 using the multi-target, multi-target with initial slope, and α, β equations. *International Journal of Radiation Biology*, **33,** 599–603.

MURTHY, M. S. S., DEORUKHAKAR, V. V., and RAO, B. S., 1979, Hyperthermia inactivation of diploid yeast and the interaction of damage caused by hyperthermia and ionizing radiation. *International Journal of Radiation Biology*, **35,** 333–341.

NGO, F. Q. H., BLAKELY, E. A., and TOBIAS, C. A., 1981, Sequential exposures of mammalian cells the low linear energy transfer and high linear energy transfer radiations: I. lethal effects following X-ray and neon ion irradiation. *Radiation Research*, **87,** 59–78.

NGO, F. Q. H., HAN, and ELKIN, M. M., 1977, On the repair of sub-lethal damage in V79 Chinese hamster cells resulting from irradiation with fast neutrons or fast neutrons combined with X-rays. *International Journal of Radiation Biology*, **32,** 507–511.

NIAS, A. H. W., and EBERT, M., 1969, Effects of single and continuous irradiation of HeLa cells at −196°C. *International Journal of Radiation Biology*, **16,** 31–41.

NIAS, A. H. W., GREENE, D., FOX, M., and THOMAS, R. L., 1968, Effect of 14 MeV monoenergetic neutrons on HeLa and P388F cells *in vitro*. *International Journal of Radiation Biology*, **13,** 449–456.

NIAS, A. H. W., SWALLOW, A. J., KEENE, J. P., and HODGSON, B. W., 1973, Absence of a fractionation effect in irradiated HeLa cells. *International Journal of Radiation Biology*, **23,** 559–569.

PIRO, A. J., TAYLOR, C. C., and BELLI, J. A., 1975, Interaction between radiation and drug damage in mammalian cells. I. Delayed expression of actinomycin D/X-ray effects in exponential and plateau phase cells. *Radiation Research*, **63,** 346–362.

RAAPHORST, G. P., and DEWEY, W. C., 1979, Fixation of potentially lethal radiation damage by post-irradiation exposure of Chinese hamster cells to 0·5 M or 1·5 M sodium chloride solutions. *International Journal of Radiation Biology*, **36,** 303–315.

RAAPHORST, G. P., and KRUUV, J., 1978, The radiation response of cultured mammalian V79-S171 cells exposed to a wide concentration range of sulphate salt solution. *International Journal of Radiation Biology*, **33,** 173–183.

RAILTON, R., LAWSON, R. C., PORTER, D., and HANNAN, W. J., 1973, Neutron spectrum dependence of r.b.e. and o.e.r. values. *International Journal of Radiation Biology*, **23,** 509–518.

RAILTON, R., PORTER, D., LAWSON, R. C., and HANNAN, W. J., 1974, The oxygen enhancement ratio and relative biological effectiveness for combined irradiations of Chinese hamster cells by neutrons and γ-rays. *International Journal of Radiation Biology*, **25,** 121–127.

RAO, B. S., and HOPWOOD, L. E., 1982, Modification of mutation frequency in plateau phase Chinese hamster ovary cells exposed to γ radiation during recovery from potentially lethal damage. *International Journal of Radiation Biology*, **42,** 501–508.

SCHLAG, H., and LUCKE-HUHLE, C., 1981, The influence of ionization density on the DNA synthetic phase and survival of irradiated mammalian cells. *International Journal of Radication Biology*, **40,** 75–85.

SCHLAG, H., WEIBEZAHN, K. F., and LUCKE-HUHLE, C., 1978, Negative pion irradiation of mammalian cells. II. A comparative analysis of cell-cycle progression after exposure to π-mesons and cobalt γ-rays. *International Journal of Radiation Biology*, **33**, 1–10.

SEELENTAG, W. W., PANZER, W., DREXLER, G., PLATZ, L., and SANTNER, F., 1979, A catalogue of spectra used for the calibration of dosimeters. *GSR Report*, S-560.

SEYMOUR, C. B., and MOTHERSILL, C., 1981, The effect of lactate on the radiation response of CHO-K1 cells in culture. *International Journal of Radiation Biology*, **40**, 283–291.

SKARSGARD, L. D., KIHLMAN, B. A., PARKER, L., PUJARA, C. M., and RICHARDSON, S., 1967, Survival, chromosome abnormalities, and recovery in heavy-ion and X-irradiated mammalian cells. *Radiation Research*, Suppl. 7, 208–221.

THACKER, J., STRETCH, A., and STEPHENS, M. A., 1979, Mutation and inactivation of cultured mammalian cells exposed to beams of accelerated heavy ions. II. Chinese hamster V79 cells. *International Journal of Radiation Biology*, **36**, (2), 137–148.

TODD, P. W., 1975, Heavy ion irradiation of human and Chinese hamster cells in vitro. *Radiation Research*, **61**, 288–297.

TUNG, C. J., and CHIEN, P. J., 1982, Energy-loss and range stragglings for electrons in water. *Proceedings of the Eighth Symposium on Microdosimetry*, edited by J. Booz and H. G. Ebert (Luxemburg: Commission of the European Communities), pp. 243–254.

UTSUMI, H., and ELKIND, M. M., 1979, Potentially lethal damage qualitative differences between ionizing and non-ionizing radiation and implications for 'single-hit' killing. *International Journal of Radiation Biology*, **35**, 373–380.

VIRSIK, R. P., BLOHM, R., HERMANN, K.-P., MODLER, H., and HARDER, D., 1983, Chromosome aberrations and the mechanism of 'primary lesion interaction'. *Proceedings of the Eighth Symposium on Microdosimetry*, edited by J. Booz and H. G. Ebert (Luxemburg: Commission of the European Communities), 8395, 409–422.

WALDREN, C. A., and RASKO, I., 1978, Caffeine enhancement of x-ray killing in cultured human and rodent cells. *Radiation Research*, **73**, 95–110.

WATT, D. E., CANNELL, R. J., and THOMAS, G. E., 1984, *International Symposium on 3-day in depth review on the nuclear acelerator impact in the inter-disciplinary field, 30 May–1 June*, Laboratori Nazionali di Legnaro (Padova), Italy, edited by P. Mazzoli and G. Moschini.

WATT, D. E., AL-AFFAN, I. A. M., CHEN, C. Z., and THOMAS, G. E., 1985, Identification of biophysical mechanisms of damage by ionising radiation. *Radiation Protection Dosimetry* ~~(in the press)~~, 13(1-4), 284-295.

ZEITZ, L., KIM, J. H., and DETKO, J. F., 1977, Determination of relative biological effectiveness (RBE) of soft x-rays. *Radiation Research*, **70**, 552–563.

ZERMENO, A., and COLE, A., 1969, Radiosensitive structure of metaphase and interphase hamster cells as studied by low-voltage electron beam irradiation. *Radiation Research*, **39**, 669–684.

Radiation Protection Dosimetry
Vol. 13 No. 1-4 pp. 285–294 (1985)
Nuclear Technology Publishing

IDENTIFICATION OF BIOPHYSICAL MECHANISMS OF DAMAGE BY IONISING RADIATION

D. E. Watt*, I. A. M. Al-Affan*, C. Z. Chen* and G. E. Thomas†
*Department of Physics, University of St Andrews
St Andrews KY16 9SS, Scotland
†Department of Mathematical Sciences, University of Dundee
Dundee DD1 4HN, Scotland

Abstract — New analyses of published data for the inactivation of enzymes, viruses, and higher cells by accelerated ions and X and gamma rays indicate that the dominant mechanism for reproductive death in mammalian cells is determined by the "matching" of the mean free path between ionisations to the strand separation in double stranded DNA. Electrons have greatly reduced intrinsic efficiencies of action when compared with heavier particles because they can reach the requisite specific primary ionisation only at very low energies when they undergo large range straggling. In all of the systems tested the action of electrons seems to be intra-track rather than inter-track. Additional evidence in support of the proposed mechanism is found in the occurrence of the RBE maxima at the same critical specific primary ionisation of 0.55 per nanometre and independently of radiation type. In view of the foregoing findings microdosemeters measure the wrong quantity, but information of practical value can be obtained by applying saturation corrections which are dependent on radiation type. In radiotherapy best results should be achieved by selection of the appropriate specific primary ionisation rather than the maximum LET for the radiation concerned.

INTRODUCTION

Identification of the main physical mechanisms responsible for radiation damage is necessary to improve our understanding of radiation effects in biology, protection and therapy. For the development of realistic mathematical models of radiation action it is essential to know the main physical processes which are manifestations of the radiation quality, and from which physical parameters descriptive of the quality may be extracted.

Historically, radiation effects have been interpreted in terms of parameters directly related to energy deposition. However, there is an increasing amount of evidence that energy based parameters may not be the most appropriate for interpretation of radiation effects in biological systems. Examples of such evidence are:

(i) Inactivation of enzymes in the dry state and in vacuum where particles of different energy but of the same type and with the same LET have effect cross sections differing by an order of magnitude[1].

(ii) The apparently anomalously high damage per unit dose caused by K shell vacancies associated with incorporated electron capture nuclides[2] and by photoelectric interactions by soft X ray irradiation[3].

(iii) Predictions from classical microdosimetry theory that neutrons of intermediate energy (~ 7 keV) will have approximately the same effect as tritium β rays, which seems unlikely because of the fundamental differences in the physical interaction of these radiations[4].

With the object of identifying the main mechanisms responsible for radiation damage a similarity treatment has been developed whereby the general trends of radiation effects may be expressed for any specified biological endpoint in a "universal" manner which, ideally, would be independent of both target and radiation type. Towards this objective published data for inactivation of enzymes, viruses, yeast and mammalian cells, by accelerated ions, X and γ rays have been re-analysed[1,5-7].

The philosophy of approach was guided by earlier work on hit and target theory and by experimental studies on enzymes in the dry state under vacuum when it became clear that the degree of damage was determined predominantly by the type of physical interaction and not necessarily by the amount of energy transfer[8,1]. Therefore, to avoid direct dependence on parameters based on energy it was decided to quantify the degree of radiation damage by the cross section for radiation effect σ_e for the incident charged particles. Also, rather than speculate on the sizes of radiosensitive volumes and become involved with the associated complex parameter k (the radiosensitivity), the radiation effect is expressed in terms of the (more fundamentally explicit) quantity intrinsic efficiency of action, ε, for the charged particle track which actually enters a well defined geometric cross

sectional area σ_g of the irradiated specimen. Thus $\varepsilon = \sigma_e/\sigma_g$, where σ_g is taken for the whole molecule in the case of enzymes, the cross sectional area within the protein coat for viruses, and the cross sectional area of the nucleus for cells.

Results have been obtained from published data for the following targets with mean chord length, $\bar{d}$, indicated.

(i) Enzymes: lysozyme, trypsin, Rnase, Dnase, and β galactosidase irradiated in the dry state by fast ions ranging from protons to argon ($\bar{d}$ = 3 nm to 10 nm)[9-12].

(ii) Viruses: tobacco mosaic virus, Newcastle disease, influenza A, *Staph.* K, S-13, vaccinia, φX-174 and T1-phage ($\bar{d}$ = 16 to 76 nm)[13-17].

(iii) Yeast cells irradiated by fast alpha particles to uranium ions ($\bar{d}$ = 1360 nm)[18].

(iv) Mammalian cells: T1-human kidney; Chinese hamster CH2B2 and V79 cells irradiated by fast helium to uranium ions[19-23] ($\bar{d} \sim 4000$ nm).

(v) Mammalian cells: HeLa human carcinoma, Chinese hamster ovary and Chinese hamster lung V79 cells irradiated by soft X rays to ^{60}Co γ rays[35,36,38-75] ($\bar{d}$ = 4000 nm).

CALCULATION OF BASIC DATA

Effect cross sections

The microscopic cross section for induction of the effect by individual charged particle radiations can be extracted from the dose survival curves, assuming unit density, from the formula

$$\sigma_e = \frac{1.6 \times 10^{-9}\,\bar{L}_T}{D} \qquad (1)$$

where $\bar{L}_T$ is the track average LET in keV.μm^{-1} for the relevant charged particle energy spectrum, σ_e is in cm^2 and D in Gy. For accelerated ions in track segment experiments, $\bar{L}_T$ is calculated for the primary ion tracks and D is taken as that corresponding to 37% survival fraction. For X and gamma irradiations, the effect is due to the slowing down recoil electron spectrum in transient equilibrium. Consequently $\bar{L}_T$ refers to the track average LET for that spectrum and D in Equation 1 was taken either as the value of D_0 (the slope of the dose-response curve at high doses) quoted by the original authors or by averaging the slope over the approximately linear portion of the survival curve.

Relative biological effectiveness, RBE

For comparative purposes it is useful to compare the RBE with the simple ratio of effect cross sections, although the latter is the more fundamental measure of relative effects. The RBE of radiation type 1 with respect to the reference radiation type 2 is given by

$$\mathrm{RBE}_{1,2} = \frac{\sigma_1}{\sigma_2}\frac{\bar{L}_{T,2}}{\bar{L}_{T,1}} \qquad (2)$$

where the LET ratio reintroduces the dependence on energy deposition.

Inherent in Equations 1 and 2 is the assumption of a pure exponential response but this is thought to be acceptable for the present purposes.

Basic physical data for accelerated ions and electrons

All results were computed for liquid water of unit density. Calculations of LET, delta ray energy spectra and yields, maximum delta ray energies and range-energy relationships relied mainly on standard Bethe type formulae[24] and on empirical relationships developed in this laboratory for application to low energies[25-29]. In the stopping power formulae, inner shell corrections were included but the Barkas and Bloch (Z_1^3,Z_1^4) effects were ignored. Ziegler's format for the effective charge on the projectiles[30], with some improvements, were used to scale data for protons to heavier projectiles. Delta ray yields were assumed to be constant below 100 eV down to a 30 eV threshold.

For accelerated ions, the specific primary ionisation (I_i) could be deduced either from the relation

$$I_i = \frac{L_\infty}{(\bar{T}_\delta + W)} \qquad (3)$$

or

$$I_i = k\frac{z^2}{\beta^2}\left(\frac{1}{I_1} - \frac{1}{T_{\delta,\max}}\right) \qquad (4)$$

In these equations the mean energy required to produce an ion pair, W, and I_1, the mean ionisation potential for water were each taken to be 30 eV. $\bar{T}_\delta$ is the frequency weighted average energy for the delta ray spectrum. Both methods of calculation agreed to within a few per cent.

For electrons, the specific primary ionisation, I_i as ionisations per μm, was calculated[7] from

$$I_i = \frac{0.3387}{2\beta^2}\ln(2.325 \times 10^4\,\beta^2) \qquad (5)$$

at energies >10 keV. Data from Tung and Chen[28] were used at energies below 10 keV.

Electron spectra at transient equilibrium for photons

As the effect of photon dose is due to the cumulative action of the electrons in the equilibrium slowing down spectrum, the relevant cross section is for an electron at an energy representative of this spectrum. Therefore, in addition to details of the slowing down spectrum and the track average LET,

an "effective" electron energy must be determined and involves decisions on the correct weighting parameter for averaging. This will be discussed below.

The original bremsstrahlung spectra for the X ray irradiations were taken either from the original publications or deduced from the known filtration using Seelentag's data[31]. The primary photoelectron and differential compton electron distributions, allowing for coherent scatter, were then computed for each photon energy band. For each electron energy band, the McGinnies method[32] was used for calculation of the slowing down spectra. The lower threshold cut-off was extended from 400 eV to 20 eV by incorporating Sugiyama's theory of stopping power[33]. In this, modifications are made to the Z_1, Z_2 and mean excitation potential, I, to enable application of the Bethe formula to low energies. A facility was built into the computer program to allow the compounding of results for individual electron energy bands into the complex weighted primary electron spectra and initial photon spectrum by using a constant channel width throughout. Channel widths were selected on a logarithmic scale to simplify the variation of channel width whilst preserving the important E/2 location corresponding to maximum energy transfer for electrons and following McGinnies' suggestion. The program provides results for the differential track length, differential electron fluence spectrum, track average LET, dose average LET, the concentration of equilibrium electrons and the total fluence of equilibrium electrons per primary electron.

Effective electron energy for the slowing down spectrum

Correct weighting of the electron spectrum to determine an effective electron energy requires foreknowledge of the radiation damage mechanisms. As an initial step the effective electron energy was determined by first calculating the track average LET for the slowing down spectrum and then finding the primary electron energy which would give this value. From what we deduce from the present results concerning the damage mechanism it would have been more accurate to have determined the effective energy for the track average of the specific primary ionisation but it is not expected that this would make an important difference for photons[7].

INTERPRETATION OF RESULTS

Enzymes (dry state)[1]

(i)The intrinsic efficiency for radiation action as a function of LET is a moderately good "universal" parameter, as it is independent of enzyme type within the experimental errors which, however, may be as much as a factor of two (see Figure 1 in Reference 1).
(ii) Radiation action is predominantly due to delta rays as evidenced by (a) the relatively small degree of saturation ($\lesssim$2 times) at high LET, (b) the intercept of the extrapolated ε against L curve with the ^{60}Co point at low LET[1], and (c) the magnitude of the intrinsic efficiency which can greatly exceed unity (see Figure 1 in Reference 1).
(iii) The data can be adequately predicted using a single hit, single target, model where a hit is a single ionisation and the target is the whole molecule[8].

Viruses

For those viruses not containing double stranded DNA the conclusions are similar to those for enzymes. However, to obtain the moderately good agreement between the theoretical and experimental intrinsic efficiencies (see Figure 2 in Reference 5) a sophisticated hit-target model is required in which the following detail must be taken into account[5]: random traversals and near misses of the target; distributions in energy, range and angle of emission of the delta rays; the presence of an insensitive coat surrounding the virus.

Results for T1-phage, which contains double stranded DNA, exhibit two interesting characteristics: (i) the observed intrinsic efficiency is two to four times smaller than predicted by simple hit-target theory and by comparison with the results for φX-174 which contains only single stranded DNA. (ii) There is a pronounced change in slope when the intrinsic efficiency is plotted against either LET or specific primary ionisation. The inflection in the curve occurs at the point where the mean free path for ionisation is about 1.8 nm – a dimension which is immediately suggestive of the spacing between the strands in double stranded DNA[6] (Figure 1).

Yeast cells

The yeast cell data of Kiefer *et al.*[18] are for irradiation conditions under which there is a large amount of saturation. The measured efficiencies for damage are much smaller than predicted by single or double hit, single target theory which includes full correction for saturation[34]. Also, despite the enormous delta ray yield, the observed efficiencies rarely exceed 2.5 and are frequently near unity (Figure 1).

Mammalian cells

All the data show a similar general trend when the intrinsic efficiencies are plotted as a function of specific primary ionisation, that is, a steep initial

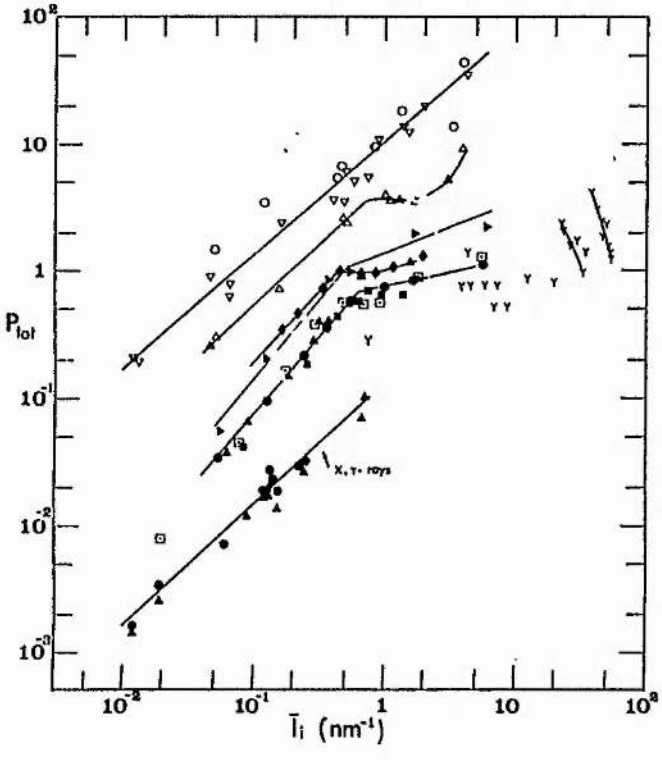

Proton and higher Z ions

▽ trypsin	(9, 10, 12)	◆ TI cells	(22)
○ φX-174	(16, 17)	■ TI cells	(23)
△ TI-phage	(16, 77)	⊡ TI cells	(79)
Y yeast cells	(18)	▲ V-79 cells	(20)
● CH2B2 cells	(19)	▶ V-79 cells	(78)

X and gamma rays

● CHO cells ▲ V-79 cells (3, 7, 38-75, 82)

Figure 1. P_{tot}, the total probability, or the intrinsic efficiency for damage for radiations ranging from photons to protons and higher Z ions in enzymes, bacteriophages, yeast cells and mammalian cells is shown as a function of the mean specific primary ionisation ($\bar{I}_i$). Numbers in brackets are references for data sets.

slope with a point of inflection, when the mean free path between ionisations is about 1.8 nm, followed by a much more gradual slope (Figure 1). The point of inflection is LET dependent but when referred to specific primary ionisation it is independent of radiation type, suggesting that specific primary ionisation is the more fundamental and significant parameter.

Because of the 1.8 nm spacing between ionisations for optimum damage, the much reduced intrinsic efficiency of action and the apparently low sensitivity to maximum δ ray energy and yield, it is suggested that this is good evidence, based purely on physi track structure considerations and the survival cur that double strand breakage in DNA is the ma cause of cell death. Confirmation of this conclusion supported by comparison of results for T1-pha (with double strand DNA) which has an optimu response with those for φX-174 phage (with sing strand DNA) which does not[6] (Figure 1).

Mammalian cells: X and gamma ray data

Analysis of the data for accelerated ions revea that there is an important relationship between th mean free path for primary ionisation and the spaci between the strands in double stranded DNA whi acts as a major damage mechanism. One ma surmise, therefore, that electrons with the optimu mean free path for ionisation should have the san intrinsic efficiency for damage as the other charge particles. Consequently, in an attempt to extra information on damage by electron tracks, analysis X and gamma irradiations of mammalian cells w pursued[7].

Mean intrinsic efficiencies for the slowing dow equilibrium spectra of electrons were determined f the X and gamma irradiation induction of ce reproductive death. A linear dependence (log-lo plot) is found on the track average LET and th average specific primary ionisation, indicating th either serves as a good quality parameter. The so characteristic X ray data[3,7] are consistent with th conclusion. However, the knowledge that the specif primary ionisation is of the greater importance, indicated in the analyses of the accelerated ion coupled with the fact that the specific prima ionisation is a more fundamental parameter tha LET (or restricted LET), leads one naturally to i selection as an important candidate for th specification of radiation damage.

Perhaps surprisingly, reference to Figure 1 show that the intrinsic efficiency for damage by electron (X and gamma data) is nearly an order of magnitud less than that for accelerated ions at the same specif primary ionisation. A possible explanation is tha electrons are only capable of reaching the requisit specific primary ionisation of about 0.5 pe nanometre at the very end of their tracks when the energies fall below 250 eV and their extrapolate range is a few nanometres. The pronounce skewness of their transmission curves due to multipl scattering means that relatively few electrons whic interact with the first strand in the DNA ar physically capable of reaching the second strand t consolidate the damage. Other evidence for th anomalously low efficiency for electron tracks given in the following discussion.

CONCLUSIONS, WITH DISCUSSION

Accelerated ions

From detailed track structure analyses of dose-survival curves we have identified the dominant damage mechanism for inactivation as being due to a single hit (ionisation) anywhere within the target molecule for enzymes and within the region surrounded by the protein coat for viruses not containing double stranded DNA. Because single hit action is sufficient and the insensitive structures are small or negligible, good correlation is obtained with LET in small targets irradiated by accelerated ions as the spatial distribution of the delta rays can contribute importantly to the intrinsic efficiency for damage. In other words, provided saturation effects are properly taken into account, all the ionisations are effective and LET, *in those special circumstances*, is a significant parameter. However, the sophisticated single hit, single target, model described elsewhere[5] confirms the importance of the individual interactions rather than the actual energy deposition in the form of LET.

Examination of the data for targets (including the mammalian cells) which contain double stranded (ds) DNA provides a much more exciting picture. For these, three main features are observed: (i) the point of inflection for primary ionisation rates near 0.55 per nanometre; (ii) the common nature of the point of inflection for all target types (with ds DNA) and for all types of accelerated ion; (iii) the much smaller intrinsic efficiencies observed for targets containing ds DNA compared with those observed for similar sized targets not containing ds DNA. All of these features strongly indicate that the dominant damage mechanism is caused by intra-track action in which an interaction is necessary in each of the two neighbouring strands spaced at about 1.8 nm in the DNA. It is concluded that the mean free path between ionisations is the dominant fundamental physical parameter of the radiation which determines the radiation action and the effect will be a maximum (ignoring delta rays for the moment) when this "matches" the strand spacing. The "duplex matching" will be subject to the normal stochastic fluctuations.

Thomas[34] has calculated that the probability of damage by this type of "resonance" behaviour is much more consistent with the observed probabilities than is a simple two-hit action. The possibility of a resonance action has been contemplated before, albeit on the basis of absorbed energy[35], and there is abundant radiobiological evidence that the double stranded DNA has special importance (e.g., Chadwick and Leenhouts[36]). More evidence will be presented below which further supports the foregoing argument.

Electrons

Information on the action of electrons is obtained from three sources: (i) direct irradiation with external electron beams[37]; (ii) X and gamma irradiations; and (iii) the extraction of delta ray effects from experiments with accelerated ions.

Experiments[37] with external electron irradiation of mammalian cells prove that electrons require about 10 keV to traverse the insensitive cytoplasm and that there is a sensitive structure within the nucleus of estimated dimension 2.5 nm[80]. The intrinsic efficiency of damage for a primary 10 keV electron (including the effects of the slowing down cascade developed at the end of the range) is about 2×10^{-3} [76].

To extract damage probabilities from the photon and accelerated ion data we note that the total probability of damage

$$\varepsilon = P(i) + I_i \bar{d}\, \overline{P(j)} \qquad (6)$$

where P(i) is the intrinsic efficiency of damage for the radiation on the primary target alone, in which $I_i.\bar{d}$ ionisations occur on average, and $\overline{P(j)}$ is the mean intrinsic efficiency of damage for the delta ray spectrum. This assumes that the electrons forming the delta ray penumbra act separately in individual secondary targets. Without foreknowledge of the actual inactivation mechanism we cannot calculate P(i) but we know that in the saturation condition $I_i > 0.55\ nm^{-1}$, P(i) = 1, in which case $P(j) = (\varepsilon - 1)/I_i.\bar{d}$ represents the mean intrinsic efficiency $(\bar{\varepsilon}_j)$ for a single delta ray with average energy representative of the delta ray spectrum.

Results for enzymes, viruses and higher cells are shown in Figure 2. Note that for mammalian cells the value of $\bar{\varepsilon}_j = (4\text{–}5 \times 10^{-5})$ for delta rays compares closely with the value extracted directly from the equilibrium electron spectra for the photon data (see Figure 3 in Reference 7, divide by $\bar{d}$ and get $\bar{\varepsilon}_j = 4 \times 10^{-5}$). In calculating the latter value it is assumed that the action in the primary target is small compared with the last term in Equation 6 above.

Direct confirmation of the low intrinsic efficiency for electrons is obtained by the observation that the intrinsic efficiency for damage by accelerated ions is relatively insensitive to the delta ray energy spectrum, as can be seen by comparison of the results shown in Figure 1, in which the maximum delta ray energies range up to 15 keV (Barendsen *et al.*[23]), to > 1 MeV (Blakely *et al.*[22]), and to > 3 MeV (Kraft *et al.*[21]), yet the intrinsic efficiencies above the saturation values do not change by more than a factor of 3 despite the very large delta ray yields and energies. A dependence of the intrinsic efficiency on delta ray energy, at maximum energies > 10 keV[37], is revealed in the analysis of the yeast cell and V-79 cell data in Figures 1 and 2.

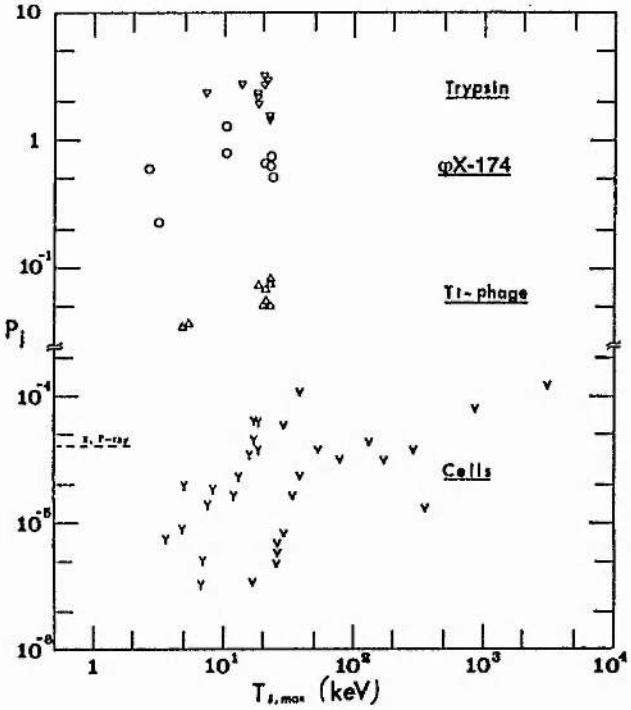

Figure 2. P_j, the probability of damage for a single electron representative of the delta ray spectrum of heavy ion tracks plotted against the maximum delta ray energy T_{max} (keV). Symbols are as in Figure 1, plus V to denote V-79 cells[21]. The dashed line indicates the value of P_j in mammalian cells for a typical slowed down secondary electron in the cascade spectrum.

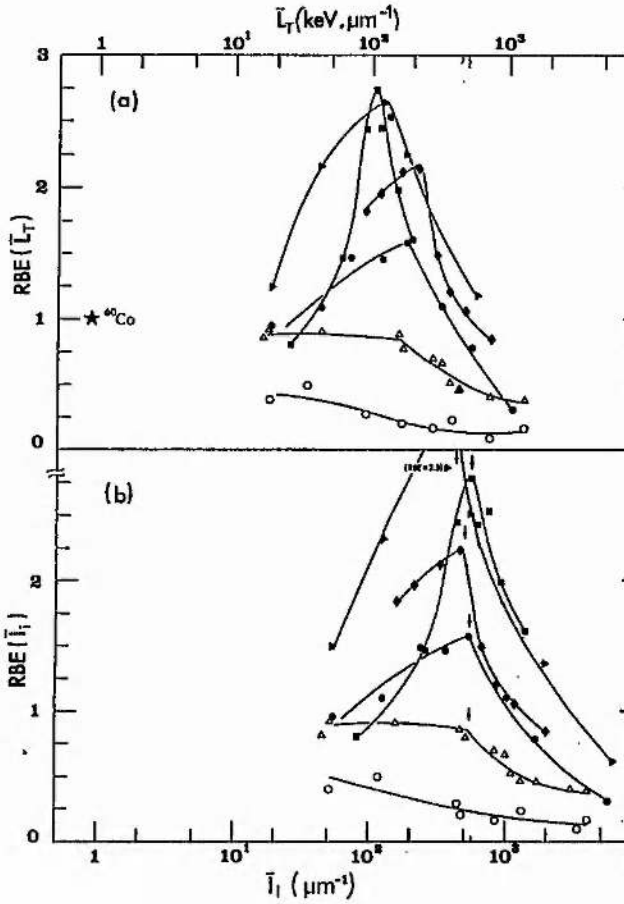

Figure 3. RBEs, determined using Equation 2, are shown a function of L_T and of I_i. In the latter case the bet grouping of the maxima, their common value of $I_i \sim 50$-μm^{-1}, and the apparent independence of radiation type consistent with the interpretation of the damage mechanis described in the text. The symbol notation is as used Figure 1.

The probability of lethal damage by electrons clearly depends on the ratio of insensitive to sensitive regions along the electron track; the mean chord length through the sensitive region; and the fact that the mean free path for specific primary ionisation along the electron track reaches the optimum value for damage only at the very end of its range where it has a significantly reduced probability of interacting with the double strands because of the degree of multiple scattering and the resulting skewness of the number relative to penetration range curve. There could also be a solid angle effect. The results shown in Figure 2 seem consistent with these arguments.

Furthermore, it can be argued that the action of electrons is predominantly intra-track rather than inter-track, otherwise the X and gamma ray data in Figure 1 would show a dependence on $(I_i^{1/2})$ rather than being directly proportional to I_i[7]. This observation, combined with the low damaging efficiency of electrons, challenges the widely accepted view concerning the degree of importance of the D^2 component in the application of dual action models to mammalian cells for the dose range studied (up to 50 Gy delivered at rates from 0.14 to 17 Gy.min^{-1}).

Additional evidence in support of the damage mechanism described here can be found from consideration of RBEs, microdosimetry ar radiobiology as discussed in the following sections.

Relative biological effectiveness

Usually the maximum in the RBE-LET curve associated with the onset of saturation, wi progressively increasing energy wastage. Th maximum RBE occurs at different LET according ion type. If the same data are shown as a function I_i a more self consistent representation is achieved all the maxima lie at the same position ($\lambda_i \sim< 1$ nm) independently of both target type and radiatio type (Figure 3).

Microdosimetry

If the lethal damage mechanism is indee dependent on the degree of matching between th

mean free path for ionisation and the spacing of the strands in DNA then classical microdosimetry measures the wrong quantity in a dosemeter of the wrong size! However, the situation can be improved by introducing saturation corrections dependent on radiation type and determined by relating y_0, the lineal energy corresponding to the onset of saturation, to the optimum specific primary ionisation of 0.55 per nanometre as discussed elsewhere[4].

Blohm and Harder[81] have considered other aspects of the role of primary ionisation in microdosimetry.

Table 1. Energy transfer data for ions with mean free path for primary ionisation $\lambda_i = 2$ nm.

Ion type	E (MeV.amu^{-1})	LET (keV.μm^{-1})	$T_{\delta,max}$ (keV)
H	0.223	64	0.2
He	0.94	108	2.0
Li	2.22	132	5.3
C	8.5	185	20.0
Ne	25.0	215	59.4
Ar	88.0	260	210.0

Radiobiology and radiotherapy

Radiotherapy normally aims at depositing the maximum amount of energy in the localised area of the tumour. From the results obtained here the optimum damage occurs at I_i values of about 0.5 per nanometre and not at the maximum LET for the specified radiation. Table 1 shows typical physical data for fast ions along with their maximum delta ray energies, as these latter are presumably more subject to the influence of modifying factors.

As protons with energy near 200 keV will produce optimum damage (Table 1) one can predict that neutrons with energy around 400 keV will be the most efficient at inducing cell reproductive death. There is good radiobiological evidence that this is so.

From the data given in Figure 1 and Equation 2 it can be predicted that, for reproductive death, the maximum possible RBE with respect to ^{60}Co γ rays will be about 9 for mammalian cells irradiated with neutrons or accelerated ions. The implication is that the higher RBEs observed at low doses and dose rates is a consequence of repair of electron induced damage.

REFERENCES

1. Watt, D. E., Al-Kazwini, A. T., Al-Shaibani, H. M. A. and Twaij, D. A. A. *Studies in Enzyme Inactivation as a Prelude to Damage Modelling.* IN Proc. 7th Symp. on Microdosimetry, EUR 7147 (London: Harwood Academic) pp. 201-209 (1981).
2. Booz, J., Humm, J., Charlton, D. E. Poplun, E. and Feinendegen, L. E. *Microdosimetry of the Auger Effect: the Biological Significance of Auger-electron Cascades of Phosphorus after Low Energy Photon Interaction with DNA.* IN Proc. 8th Symp. on Microdosimetry, eds. J. Booz and H. G. Ebert, EUR 8395 (London: Harwood Academic) pp. 625-638 (1983).
3. Goodhead, D. T., Thacker, J. and Cox, R. *Effectiveness of 0.3 keV Carbon Ultrasoft X-rays for the Inactivation and Mutation of Cultured Mammalian Cells.* Int. J. Radiat. Biol. **31**, 541-559 (1979).
4. Al-Affan, I. A. M. and Watt, D. E. *Saturation Values of Lineal Energy in Microdosimetry: Quality Factor.* Radiat. Prot. Dosim. **11**, 1, 66-67 (1985).
5. Thomas, G. E. and Watt, D. E. *A Track Structure Description of the Inactivation of Enzymes and Viruses by Fast Ions.* Radiat. Effects **84**, 107-116 (1985).
6. Cannell, R. J. and Watt, D. E. *Biophysical Mechanisms of Damage by Fast Ions to Mammalian Cells in vitro.* Phys. Med. Biol. **30**, 255-258 (1985).
7. Chen, C. Z. and Watt, D. E. *Biophysical Mechanism of Radiation Damage to Mammalian Cells by X and γ-rays.* Int. J. Radiat. Biol. in press (1985).
8. Watt, D. E. *Hit Cross-sections in Single Target Theory.* Phys. Med. Biol. **20**, 944-954 (1975).
9. Brustad, T. Radiat. Res. Suppl. **2**, 65 (1960).
10. Brustad, T. *Inactivation at Various Temperatures of the Esterase Activity of Dried Trypsin by Radiations of Different LET.* Radiat. Res. Suppl. **7**, 74-86 (1967).
11. Gunther, W. and Jung, H. Z. Naturf. **22b**, 313 (1967).
12. Dolphin, G. W. and Hutchinson, F. *The Action of Fast Carbon and Heavier Ions on Biological Materials I: The Inactivation of Dried Enzymes.* Radiat. Res. **13**, 403-414 (1960).
13. Lea, D. E. *Actions of Radiation on Living Cells* (Cambridge University Press) 2nd edn (1956).
14. Pollard, E. C. and Dimond, A. E. Phytopathology **46**, 214-218 (1956).
15. Jagger, J. and Pollard, E. C. Radiat. Res. **4**, 1-8 (1956).

16. Shambra, P. E. and Hutchinson, F. *The Action of Fast Heavy Ions on Biological Material II. Effects on T1 and φX-1 Bacteriophage and Double-strand and Single-strand DNA.* Radiat. Res. **23**, 514-526 (1964).
17. Yatagai, F., Kitayama, S. and Matsuyama, A. *Inactivation of Phage φX-174 by Accelerated Ions.* Radiat. Res. **77**, 2 258 (1979).
18. Kiefer, J., Rase, S., Schneider, E., Stratten, H., Kraft, G. and Liesem, H. *Heavy Ion Effects on Yeast Cells: Induct of Canavine Resistant Mutants.* Int. J. Radiat. Biol. **42**, 591-600 (1982).
19. Skarsgard, L. D., Kihlman, B. A., Parker, L., Pujara, C. M. and Richardson, S. *Survival, Chromosome Abnormaliti and Recovery in Heavy-ion and X-irradiated Mammalian Cells.* Radiat. Res. Suppl. **7**, 208-221 (1967).
20. Thacker, J., Stretch, A. and Stephens, M. A. *Mutation and Inactivation of Cultured Mammalian Cells Exposed Beams of Accelerated Heavy Ions. II. Chinese Hamster V-79 Cells.* Int. J. Radiat. Biol. **36**, 137-148 (1979).
21. Kraft, G., Blakely, E. A., Hieber, L., Kraft-Weyrather, W., Miltenburger, H. G., Muller, W., Schuber, M., Tobi C. A. and Wulf, H. *HZE Effects on Mammalian Cells.* Advances Space Res. to be published (1985).
22. Blakely, E. A., Tobias, C. A., Yang, T. C. H., Smith, K. C. and Lyman, J. T. *Inactivation of Human Kidney Cells High-energy Monoenergetic Heavy-ion Beams.* Radiat. Res. **80**, 122-160 (1979).
23. Barendsen, G. W., Koot, C. J., van Kersen, R. R., Bewley, D. K., Field, S. B. and Parnell, C. J. *The Effect of Oxyg on Impairment of the Proliferative Capacity of Human Cells in Culture by Ionising Radiations of Different LET.* Int. Radiat. Biol. **10**, 317-327 (1967).
24. ICRU. *Stopping Powers for Electrons and Positrons.* Report 39 (ICRU Publications, 7910 Woodmount Ave, Bethes MD 20814, USA) (1984).
25. Iskef, H., Cunningham, J. W. and Watt, D. E. *Projected Ranges and Effective Stopping Powers of Electrons w Energy Between 20 eV and 10 eV.* Phys. Med. Bio. **28**, 535-545 (1983).
26. Al-Ahmad, K. O. and Watt, D. E. *Stopping Powers and Extrapolated Ranges for Electrons (1 to 10 keV) in Metals.* Phys. D: Appl. Phys. **16**, 2257-2267 (1983).
27. Al-Ahmad, K. O. and Watt, D. E. *Stopping Power of Low Energy Electrons (10 keV) in Solid Polyethylene.* J. Ph D: Appl. Phys. **17**, 1899-1904 (1984).
28. Tung, C. J. and Chen, P. J. *Energy Loss and Range Stragglings for Electrons in Water.* IN Proc. 8th Symp. Microdosimetry, EUR 8395 (London: Harwood Academic) pp. 243-254 (1983).
29. Ashley, J. C. *Stopping Power of Liquid Water for Low Energy Electrons.* Radiat. Res. **89**, 25-31 (1982).
30. Ziegler, J. F. *The Stopping and Ranges of Ions in Matter. Vol. 5 Handbook of Stopping Cross-sections for Energetic Io in all Elements.* (Oxford: Pergamon Press) (1980).
31. Seelentag, W. W., Panzer, W., Drexler, G., Platz, L. and Santner, F. *A Catalogue of Spectra Used for the Calibrati of Dosimeters.* GSR Report S-560 (1979).
32. McGinnies, R. T. *Energy Spectrum Resulting from Electron Slowing Down.* Circular 597 (National Bureau Standards, Washington, DC) (1959).
33. Sugiyama, H. *Stopping Power Formula for Intermediate Energy Electrons.* Phys. Med. Biol. (in press) (1985).
34. Thomas, G. E. *Modelling Radiation Damage by Fast Ionizing Particles.* PhD Thesis, University of Dundee (1985).
35. Yamaguchi, H. and Waker, A. J. *A Resonance Model for Radiation Action.* IN Proc. 8th Symp. on Microdosimet eds. J. Booz and H. G. Ebert, EUR 8395 (London: Harwood Academic) pp. 497-506 (1983).
36. Chadwick, K. H. and Leenhouts, H. P. *The Molecular Theory of Radiation Biology.* (Heidelberg: Springer-Verla (1981).
37. Zermano, A. and Cole, A. *Radiosensitive Structure of Metaphase and Inter-phase Hamster Cells as Studied by L Voltage Electron Beam Irradiation.* Radiat. Res. **39**, 669-684 (1969).
38. Adams, G. E., Fielden, E. M., Hardy, C., Millar, B. C., Stratford, I. J. and Williamson, C. *Radiosensitization Hypoxic Mammalian Cells in Vitro by some 5-Substituted-4-Introimidazoles.* Int. J. Radiat. Biol. **40**, 153-161 (1981
39. Ben-Hur, E., Elkind, M. M. and Bronk, B. V. *Thermally Enhanced Radioresponse of Cultured Chinese Hamster Ce Inhibition of Repair of Sublethal Damage and Enhancement of Lethal Damage.* Radiat. Res. **58**, 38-51 (1974).
40. Burki, H. J. and Carrano, A. V. *Relative Radiosensitivities of Tetraploid and Diploid Chinese Hamster Cells in Cult Exposed to Ionizing Radiation.* Mutat. Res. **17**, 277-282 (1973).
41. Busse, P. M., Bose, S. K., Jones, R. W. and Tolmach, L. J. *The Action of Caffeine on X-irradiated HeLa Cells. Synergistic Lethality.* Radiat. Res. **71**, 666-677 (1977).
42. Chapman, J. D., Webb, R. G. and Borsa, J. *Radiosensitisation of Mammalian Cells by p-nitroacetophenone. Characterization in Asynchronous and Synchronous Populations.* Int. J. Radiat. Biol. **19**, 561-573 (1971).
43. Dikomey, E. *Effect of Hyperthermia at 42 and 45°C on Repair of Radiation-Induced DNA Strand Breaks in CHO Ce* Int. J. Radiat. Biol. **41**, 603-614 (1982).
44. Djordjevic, B. *Modification of Radiation Response in HeLa Cells by Misonidazole.* Int. J. Radiat. Biol. **36**, 601-6 (1979).

45. Djordjevic, B., Kim, J. H. and Kim. S. H. *Modification of Radiation Response in Synchronised HeLa Cells by Metabolic Inhibitors. I. Effect of an Inhibitor of RNA Synthesis, Puromycin Aminonucleoside.* Int. J. Radiat. Biol. **14**, 1-7 (1968).
46. Elkind, M. M. and Sutton, H. *X-ray Damage and Recovery in Mammalian Cells in Culture.* Nature (Lond.) **184**, 1293-1295 (1959).
47. Gragg, R. L., Humphrey, R. M. and Meyn, R. E. *The Response of Chinese Hamster Ovary Cells to Fast Neutron Radiotherapy Beams. I. Relative Biological Effectiveness and Oxygen Enhancement Ratio.* Radiat. Res. **65**, 71-82 (1976).
48. Han, A. and Elkind, M. M. *Additive Action of Ionizing and Non-ionizing Radiations throughout the Chinese Hamster Cell-cycle.* Int. J. Radiat. Biol. **31**, 275-282 (1977).
49. Harris, J. W., Power, J. A. and Kock, C. J. *Radiosensitization of Hypoxic Mammalian Cells by Diamide. I. Effects of Experimental Conditions on Survival.* Radiat. Res. **64**, 270-280 (1975).
50. Koch, C. J. and Kruuv, J. *The Effect of Extreme Hypoxia on Recovery after Irradiation by Synchronised Mammalian Cells.* Radiat. Res. **48**, 74-85 (1971).
51. Lehnert, S. *Modification of Radiation Response of CHO Cells by 1-methyl-3-isobutylxanthine. I. Reduction of D.* Radiat. Res. **78**, 1-12 (1979).
52. Malone, J. F., Foster, C. J., Orr, J. S. and Solomonides, E. *The Effects on the Survival of HeLa S-3 Cells of Independent Variations in the Sizes of the First and the Second X-ray Dose in Split Dose Experiments.* Int. J. Radiat. Biol. **20**, 225-231 (1971).
53. Malone, J. F., Porter, D. and Hendry, J. H. *The r.b.e. of ^{60}Co Gamma Rays with Respect to 300 kVp X-rays for the Survival of HeLa S-3 and CHO Cells, Irradiated in Different States of Proliferation.* Radiat. Res. **26**, 355-362 (1971).
54. McNally, N. J. *The Effect of a Change in Radiation Quality on the Ability of Electron Affinic Sensitizers to Sensitize Hypoxic Cells.* Int. J. Radiat. Biol. **29**, 191-196 (1976).
55. Michaels, H. B., Epp, E. R., Ling, C. C. and Peterson, E. C. *Oxygen Sensitization of CHO Cells at Ultrahigh Dose Rates: Prelude to Oxygen Diffusion Studies.* Radiat. Res. **76**, 510-521 (1978).
56. Millar, B. C., Fielden, E. M. and Millar, J. L. *Interpretation of Survival-curve Data for Chinese Hamster Cells, Line V-79 using the Multi-target, Multi-target with Initial Slope, and* α, β, equations. Int. J. Radiat. Biol. **33**, 599-603 (1978).
57. Murthy, M. S. S., Deorukhakar, V. V. and Rao, B. S. *Hyperthermia Inactivation of Diploid Yeast and the Interaction of Damage Caused by Hyperthermia and Ionizing Radiation.* Int. J. Radiat. Biol. **35**, 333-341 (1979).
58. Ngo, F. Q. H., Blakely, E. A. and Tobias, C. A. *Sequential Exposures of Mammalian Cells to the Low Linear Energy Transfer and High Linear Energy Transfer Radiations: I. Lethal Effects Following X-ray and Neon Ion Irradiation.* Radiat. Res. **87**, 59-78 (1981).
59. Ngo, F. Q. H., Han, A. and Elkind, M. M. *On the Repair of Sub-lethal Damage in V79 Chinese Hamster Cells Resulting from Irradiation with Fast Neutrons or Fast Neutrons Combined with X-rays.* Int. J. Radiat. Biol. **32**, 507-511 (1977).
60. Nias, A. H. W. and Ebert, M. *Effects of Single and Continuous Irradiation of HeLa Cells at –196±C.* Int J. Radiat. Biol. **16**, 31-41 (1969).
61. Nias, A. H. W., Greene, D., Fox, M. and Thomas, R. L. *Effects of 14 MeV Monoenergetic Neutrons on HeLa and P388F Cells in Vitro.* Int. J. Radiat. Biol. **13**, 449-456 (1968).
62. Nias, A. H. W., Swallow, A. J., Keene, J. P. and Hodgson, B. W. *Absence of a Fractionation Effect in Irradiated HeLa Cells.* Int. J. Radiat. Biol. **23**, 559-569 (1973).
63. Piro, A. J., Taylor, C. C. and Belli, J. A. *Interaction between Radiation and Drug Damage in Mammalian Cells. I. Delayed Expression of Actinomycin D/X-ray Effects in Exponential and Plateau Phase Cells.* Radiat. Res. **63**, 346-362 (1975).
64. Raaphorst, G. P. and Dewey, W. C. *Fixation of Potentially Lethal Radiation Damage by Post-Irradiation Exposure of Chinese Hamster Cells to 0.5 M or 1.5 M Sodium Chloride Solutions.* Int. J. Radiat. Biol. **36**, 303-315 (1979).
65. Raaphorst, G. P. and Kruuv, J. *The Radiation Response of Cultured Mammalian V79-S171 Cells Exposed to a Wide Concentration Range of Sulphate Salt Solution.* Int. J. Radiat. Biol. **33**, 173-183 (1978).
66. Railton, R., Lawson, R. C., Porter, D. and Hannan, W. J. *Neutron Spectrum Dependence of r.b.e. and o.e.r. Values.* Int. J. Radiat. Biol. **23**, 509-518 (1973).
67. Railton, R., Porter, D., Lawson, R. c. and Hannan, W. J. *The Oyxgen Enhancement Ratio and Relative Biological Effectiveness for Combined Irradiations of Chinese Hamster Cells by Neutrons and ?-Rays.* Int. J. Radiat. Biol. **25**, 121-127 (1974).
68. Rao, B. S. and Hopwood, L. E. *Modification of Mutation Frequency in Plateau Phase Chinese Hamster Ovary Cells Exposed to Radiation During Recovery from Potentially Lethal Damage.* Int. J. Radiat. Biol. **42**, 501-508 (1982).
69. Schlag, H. and Lucke-Huhle, C. *The Influence of Ionization density on the DNA Sythetic Phase and Survival of Irradiated Mammalian Cells.* Int. J. Radiat. Biol. **40**, 75-85 (1981).
70. Schlag, H., Weibezahn, K. F. and Lucke-Huhle, C. *Negative Pion Irradiation of Mammalian Cells. II. A Comparative Analysis of Cell-cycle Progression after Exposure to Mesons and Cobalt* γ*-rays.* Int. J. Radiat. Biol. **33**, 1-10 (1978).

71. Seymour, C. B. and Mothersill, C. *The Effect of Lactate on the Radiation Response of CHO-K1 Cells in Culture.* I J. Radiat. Biol. **40**, 283-291 (1981).

72. Utsumi, H. and Elkind, M. M. *Potentially Lethal Damage Qualitative Differences between Ionizing and Non-ioniz Radiation and Implications for 'Single-hit' Killing.* Int. J. Radiat. Biol. **35**, 373-380 (1979).

73. Virsik, R. P., Blohm, R., Hermann, K.-P., Modler, H. and Harder, D. *Chromosome Aberrations and the Mechani of 'Primary Lesion Interaction'.* IN Proc. 8th Symp. on Microdosimetry, eds. J. Booz and H. G. Ebert, EUR 83 (London: Harwood Academic) pp. 409-422 (1983).

74. Waldren, C. A. and Rasko, I. *Caffeine Enhancement of X-ray Killing in Cultured Human and Rodent Cells.* Radi Res. **73**, 95-110 (1978).

75. Zeitz, L., Kim, S. H., Kim, J. H. and Detko, J. F. *Determination of Relative Biological Effectiveness (RBE) of Soft rays.* Radiat. Res. **70**, 552-563 (1977).

76. Watt, D. E., Cannell, R. J. and Thomas, G. E. *Ion Beams in Quality Determination for Radiation Protection.* IN I Symp. on 3-day in depth Review on the Nuclear Accelerator Impact in the Interdisciplinary Field, May 30-June Laboratoire Nazionali di Legnaro, Padova, Italy (1984).

77. Fluke, D. J., Brustad, T. and Birge, A. C. *Inactivation of Dried T1 Bacteriophage by Helium Ions, Carbon Ions a Oxygen Ions: Comparison of Effects for Tracks of Various Ion Density.* Radiat. Res. **13**, 788-808 (1960).

78. Bird, R. P. and Burki, H. J. *Survival of Synchronised Chinese Hamster Cells Exposed to Radiation of Different Lin Energy Transfer.* Int. J. Radiat. Biol. **27** C21, 105-120 (1975).

79. Todd, P. W. *Reversible and Irreversible Effects of Densely Ionizing Radiations upon the Reproductive Capacity Cultured Human Cells.* Med. Coll. Virginia, Q. **1**, 2-14 (1965).

80. Cole, A. *The Study of Radiosensitive Structures with Low Voltage Electron Beams.* IN Cellular Radiation Biolo (Baltimore: Williams and Wilkins) pp. 267-271 (1965).

81. Blohm, R. and Harder, D. *Restricted LET: Still a Good Parameter of Radiation Quality for Electrons and Photo* Radiat. Prot. Dosim. **13**, 1-4, 377-381 (1985).

82. Goodhead, D. T. and Thacker, J. *Inactivation and Mutation of Cultured Mammalian Cells by Aluminium Characteris Ultra-soft X Rays.* Int. J. Radiat. Biol. **31**, 541-559 (1977).

Paper No. 6 BNES Conf. on
Health effects of low dose ionising ra
- recent advances and their impl
11-14, M

Towards a unified system for expression of biological damage by ionizing radiation.

D E WATT, C-Z CHEN, L A KADIRI AND A-R S YOUNIS

Department of Physics
University of St Andrews
North Haugh
ST ANDREWS
Fife KY16 9SS
Scotland, UK

Limitations to our currently adopted system of radiation dosimetry are discussed. Analyses of a wide range of published data on inactivation of enzymes, viruses, bacteria, plant and mammalian cells by electrons, X and γ-rays, and accelerated ions leads to the conclusion that the main radiosensitive sites in higher cells are the double-stranded segments of DNA. The probability of damage is determined by the mean free path for ionization along the charged particle tracks and is optimum when the spacing matches the mean chord length (2 nm) through a DNA segment. Interpretation of these findings leads to the possibility of a more accurate unified system of dosimetry and to the specification of absolute biological effectiveness.

INTRODUCTION

1. The biological effectiveness of ionizing radiation is currently assessed in terms of the absorbed dose (D) and a scaling factor which takes into account the different damaging power of different radiation types. In radiological protection scaling is achieved through the quality factor (Q) and, in radiobiology, by the relative biological effectiveness (RBE). Q is selected so that it always exceeds, by an arbitarily chosen safety factor, the measured RBE for the induction of biological end-points deemed to be of importance eg chromosome aberrations, leukaemia induction, life shortening in animals etc. For dosimetry purposes Q and RBE are expressed as functions of the linear energy transfer (LET) of the radiation, (ref - 1, 2).

2. In radiological protection additivity of the effectiveness of mixed radiation fields, is achieved through the summation of the partial dose equivalents H (= D.Q) for the radiation types involved. Therefore H represents an attempt to correlate the effectiveness of any radiation field in a unified way. There are, however, serious limitations to its application both in theory and practice due to the subjective judgement involved in the degree of inbuilt safety factor; the requirement that the radiation type be known; the necessity for different types of dose equivalent instrumentation for different types of radiation field; the relative nature of Q and RBE; the generally poor unification achieved because different particle types with the same LET, and therefore the same Q's, can have different biological effects.

3. Difficulties with the currently accepted system of dosimetry lie in our lack of knowledge of the basic mechanisms of radiation action and our consequent inability to specify the radiation quality in absolute terms. If this could be done, the construction of a unified system should be relatively easy although its practical implementation may not be as simple and will almost certainly require that a new generation of 'dosimeters' be designed to comply with fundamentally new concepts.

3. Recent studies in this laboratory have led to significant progress towards the absolute specification of radiation quality. A wide range of published data on the action of electrons, X and γ-rays, neutrons and accelerated ions on enzymes, viruses, plant and mammalian cells has been re-interpreted to extract the probabilities of inactivation (ref - 3) or mutation (ref - 4) by single charged particle tracks which actually enter the biological target. The relevant charged particles are those in the equilibrium charged particle spectrum generated in the medium by indirectly ionizing radiation. The probabilites for induction of the specified damage therefore represent the intrinsic efficiencies of action which are absolute measures of the radiation quality. It follows that the absolute biological effectiveness (ABE) can be defined in terms of the product of the relevant charged particle fluence and the intrinsic efficiency (ref - 5). To enable this to be of practical value a method must be found of representing the intrinsic efficiency as a function of physical and biological parameters so that it can be calculated directly and to indicate possibilities for the design of suitable instrumentation.

4. The results of our analyses lead to the conclusion that energy based parameters are unsuitable for the specification of radiation effect in mammalian cells in vitro. Absorbed dose is not a suitable quantity for assessing the magnitude of the radiation field. Radiation quality is not a function of LET, or restricted LET, or microdose parameters although the latter two are closer approximations than the linear stopping power. Therefore quality should not be represented by RBE or Q as presently defined. Consequently the entire basis of our system of dosimetry should be re-examined.

5. Below, evidence is presented to justify these statements. It will be demonstrated from purely physical arguments that the important radiosensitive sites in the cell nucleus are the double stranded segments in the nuclear DNA and that the dominant critical physical parameter of the charged particle radiation is the mean free path between ionizing interactions. Damage is a stochastic process which occurs when the mean spacing between interactions along the charged particle track matches the mean chord distance through a DNA segment (~ 2 nm). Radiation effects depend mainly on the frequency of interactions not the energy transferred in the interactions. Damage is predominantly an intra-track, not inter-track, process for all radiations except at extremely large doses.

Correlation of Survival Data

6. Effect cross-sections normalised to the geometrical cross-section of the radiosensitive sites give effect probabilities, p.

7. Earlier studies on various enzymes showed that although 'p' for fast accelerated ions could be correlated reasonably well as a function of the track average LET slow ions could not and it was concluded that the frequency of interactions had a fundamentally important role in the biophysical mechanism of radiation action. (Ref - 23)

8. Extension of these studies to more complex targets (ref - 5, 6) revealed three significant facts when ds DNA was present: the inactivation probability was reduced by an order of magnitude; a point of inflection, indicating biosensitive structure, appeared in targets containing ds DNA when the spacing between interactions of the relevant charged particle radiation was near 2 nm (figs 1(b), 2(b)); the point of inflection at 2 nm was common to all targets containing ds DNA (eg T1-phage, mammalian and plant cells) and to all ion types (fig 3(d)).

9. From these findings it seems reasonable to accept that ds DNA is the dominant radiosensitive site in mammalian cells. Damage is produced when the radiation track interacts in each strand of the DNA and is optimum when the mean free path (λ) between interactions matches the mean chord length (~ 2 nm) through a segment of the DNA.

10. From the extensive data shown in fig 3 several conclusions can be reached. The initial slope α (gray-1) of the dose-survival curve does not provide a useful means of unifying the data either as a function of reciprocal LET or as a function of the mean free path although use of this latter provides a common point at which α reaches a maximum value dependent on radiation type (figs 3(a) and (b)). In fig 3(a), as α and LET are not suitable quantities for correlating the data in a meaningful way, it follows that absorbed dose cannot be a meaningful quantity for specifying the radiation field.

11. In figs 3 (c) and (d) much better correlation is obtained by use of the inactivation probability (p) which is an absolute measure of the radiation quality. Expressing p as a function of the mean free path between ionizations, rather than of reciprocal LET, is much better for two main reasons: the single point-of-inflection at 2nm independently of radiation type and of plant or mammalian cell type; the realistic representation of the known quality of heavy charged particles with respect to X and γ rays and electrons. Fig 3 (c), which shows X and γ-rays on the same curve as the heavier particles, implies that they have the same quality at the same LET. This is known from radiobiology not to be true. The reason that X and γ rays have lower effectiveness at the same λ is that many of the low energy electrons in the equilibrium spectrum can expend their energies in the cell nucleus without interacting with a sensitive site (ref - 3, 5).

12. If the mean free path between interactions is the physical parameter controlling the radiation action then it follows that the delta rays associated with the heavy ion tracks must have relatively small effect (because λ is the zeroth moment of energy transfer and is independent of the delta ray energy whereas LET is the first mo ment). It is shown elsewhere (ref -5) that this is so. The extrinsic efficiency of electrons in the equilibrium spectrum (ref -14), and of delta rays, ranges from about 4×10^{-5} to 10^{-4} for maximum delta ray energies extending from 10 keV to 1 MeV. (Ref -5). However as up to several thousand delta rays may be released in the cell nucleus by a primary charged particle track the inactivation probability can be enhanced by an amount ranging from a few percent up to a factor of 2 depending on the ion velocity and mean free path.

13. Another important deduction that can be made from the foregoing analyses is that damage is predominantly by intratrack action. Inter-track action, if any, must be very small as may be deduced from the size of the radiosensitive sites (ref - 17) and the observation that the slope of the p v λ graph for $\lambda >$ 2nm is near unity. In other words there is negligible 'dose rate' effect which is contrary to current thinking in many proposed models of repair.

14. The foregoing deductions based on experimental evidence could form the foundations of a unified system of dosimetry.

15. Additionally it will be necessary to correct any instrument reading for recovery or repair of damage to determine the absolute biological effectiveness of the radiation.

16. Some progress towards this has been achieved by the development of a new model of radiation action with recovery of damage (ref - 5). Absolute Biological Effectiveness is expressed in terms of the projected geometrical cross-sectional area of the radiosensitive sites ($\sim 3 \times 10^{-7} cm^2$) for mammalian cells; the total fluence of the charged particle equilibrium field; a recovery time factor which is a function of the mean time to mitosis at which damage can be considered fixed; a mean recovery time; the number of double strand segments and DNA at risk (~ 10 for fast ions, ~ 1 for equilibrium electrons) and the duration of the irradiation. This model is undergoing test (ref -7).

18. Application of effect probabilities to the interpretation of radiation action mechanisms has proved to be a very powerful technique for linking the fundamental physical processes with

the biological endpoint of interest and could make an important contribution to radiotherapy, radiobiology and radiological protection (ref - 4, 19 to 22).

REFERENCES

1. ICRU Report No 16. Linear energy transfer. International Committee on Radiation Units and Measurements, June 15, 1970.
2. ICRU Report No 40. The quality factor in radiation protection. International Committee on Radiation Units and Measurements. April 4, 1986.
3. WATT D E, ALAFFAN I A M, CHEN C Z and THOMAS G E. Identification of biophysical mechanisms of damage by ionizing radiation. Radiat Protect Dos 13, No 1-4, 285-294.
4. KADIRI L A and WATT D E. Determination of total probabilities for cellular mutagenesis in vitro. Submitted to Int J Radiat Biol 1987.
5. WATT D E. On absolute biological effectiveness and unified dosimetry. Submitted to Soc Radiol Protect, June 1987.
6. CANNELL R J and WATT D E. Biophysical mechanism of damage by fast ions to mammalian cells in vitro. Phys Med Biol 30, No 3, 255-258.
7. CHEN C Z, McGUIRE A and WATT D E. Test of a DNA rupture model of radiation action Paper B32 IV, 8th ICRR Congress, Edinburgh, July 1987.
8. YATAGI F, KITAMAMA S and MATSUYAMA A. Inactivation of phage φX-174 by accelerated ions. Radiat Res 77, 250-258, 1979.
9. BRUSTAD T. Inactivation at various temperatures of the esterase activity of dried trypsin by radiations of different LET. Radiat Res Suppl 7, 74-86, 1967.
10. SHAMBRA P E and HUTCHINSON F. The action of fast heavy ions on biological material II. Effects on T1 and φX-174 bacteriophage and ds and ss DNA. Radiat Res 23, 514-526, 1964.
11. BARENSDEN G W, KOOT C J, van KERSEN R R, BEWLEY D K, FIELD S B and PARNELL C J. The effect of oxygen on impairment of the proliferative capacity of human cells. Int J Radiat Biol 10, 317-327, 1967.
12. BLAKELY E A, TOBIAS C A, JANG T C H, SMITH K C and LYMON J T. Inactivation of human kidney cells by high energy monoenergetic heavy ion beams. Radiat Res 80, 122-160, 1979.
13. VIRSIK R P, BLOHM R, HERMANN K P, MODLER H and HARDER D. Chromosome aberrations and the mechanism of 'primary lesion interaction'. In Proc of 8th symp on Microdosimetry. Ed J Booz and H G Ebert. EUR 8395 (London: Harwood Academic), 409-422, 1983.
14. CHEN C Z and WATT D E. Biophysical mechanism of radiation damage to mammalian cells by X and γ rays. Int J of Radiat Biol, 49, (1), 131-142, 1986.
15. SKARSGARD L D, KIHLMAN B A, PARKER L, PUJARA C M and RICHARDSON S. Survival, Chromosome abnormalities and recovery in heavy ion and X-irradiated mammalian cells. Radiat Res Suppl 7, 208-211, 1967.
16. TODD P W. Heavy ion irradiation of human and chinese hamster cells in vitro. Radiat Res 61, 288-297 1975.
17. GOODHEAD D T. Cellular effects of ultra-soft X-radiation. Implications for mechanism of radiation cell killing. In 'The Biological Basis of Radiotherapy' p 81-92, 1983. Editors Steel, Adams and Peckham. Elsevier Science Publishers B V.
18. COX R and MASSON W K. Mutation and inactivation of cultured mammalian cells exposed to beams of accelerated heavy ions III Human diploid fibroblasts. Int J Radiat Biol 36, (2), 149-160, 1979.
19. JAWAD H H and WATT D E. Physical Mechanism for inactivation to metalloenzymes by characteristic X-rays. Int J Radiat Biol 50, (4), 665-674 (to be read in conjunction with refs 20, 21).
20. GOODHEAD D T and NIKJOO H. Physical mechanism for inactivation of metalloenzymes by characteristic X-rays: Analyses of the data of Jawad and Watt. Letter to the Editor Int J Radiat biol 1987.
21. WATT D E and YOUNIS A-R S. Damage to metalloenzymes by characteristic Xrays. Letter to the Editor Int J Radiat Biol 1987.
22. YOUNIS A-R S and WATT D E. Quality of radionuclides incorporated into mammalian cells. Int J Radiat Biol 1988.
23. WATT D E, AL-KAZWINI A T, AL-SHAIBANI H M A and TWAIJ D A A. Studies in enzymes inactivation as a prelude to damage modelling. proc 7th Symp on Microdosimetry, EUR 7147 (London, Harwood Academic) 201-209, 1981.

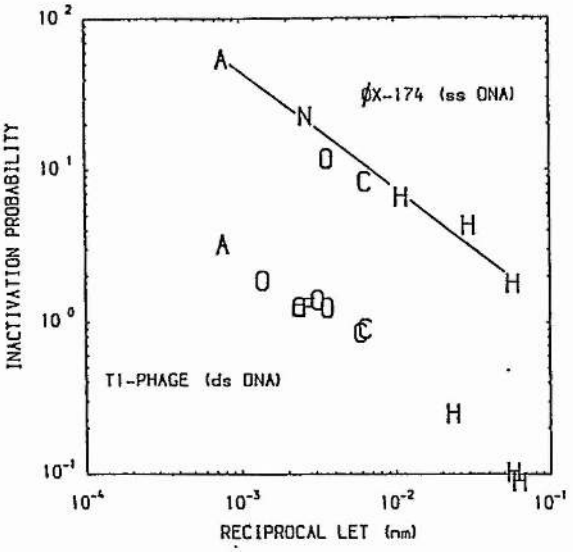

Fig 1(a)

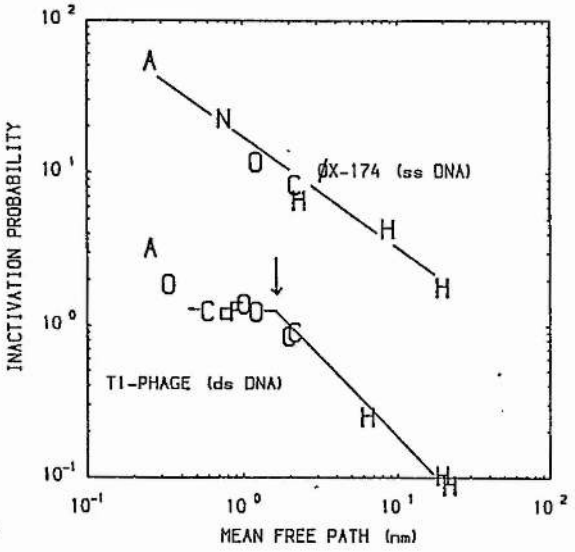

(b)

Fig 1 The probability for inactivation of φX-174 (ss DNA) (ref - 8,9) and T1-phage (ds - DNA) (ref - 8,10) is shown (a) as a function of reciprocal LET and (b) as a function of the mean free path for ionization. Note the point of inflection (arrowed) which occurs only when ds DNA is present.

Symbols: H = helium; C = carbon; N = nitrogen; O = oxygen; F = fluorine; □ = neon; A = argon.

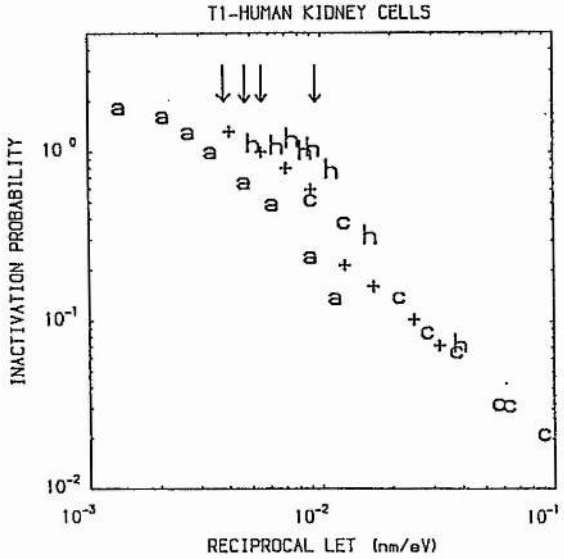

Fig 2(a)

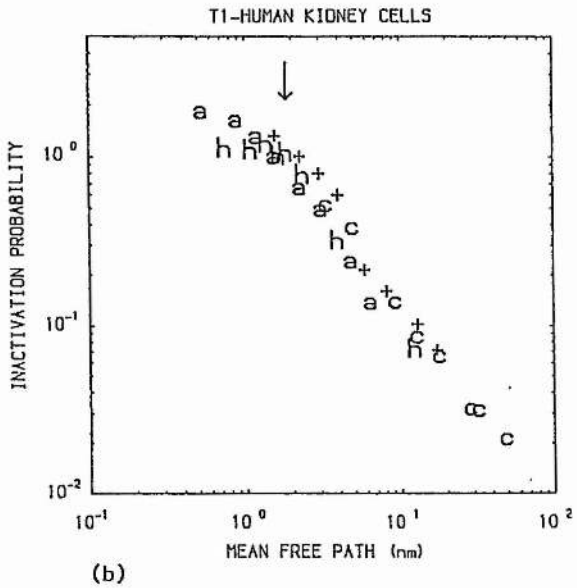

(b)

Fig 2

Optimum damage (p = 1.0) in T1-human kidney cells (ref - 11,12) occurs at different LET (arrowed) depending on ion type viz. at 260, 215, 185 and 108 keV/μm for Ar, Ne, C and He ions respectively (fig 2 (a)). There is a common point of inflection (arrowed) at ~ 2 nm when p is plotted against the mean free path indicating that λ is a better parameter for specifying quality (fig 2 (b)).

Symbols: h = helium; c = carbon; + = neon; a = argon.

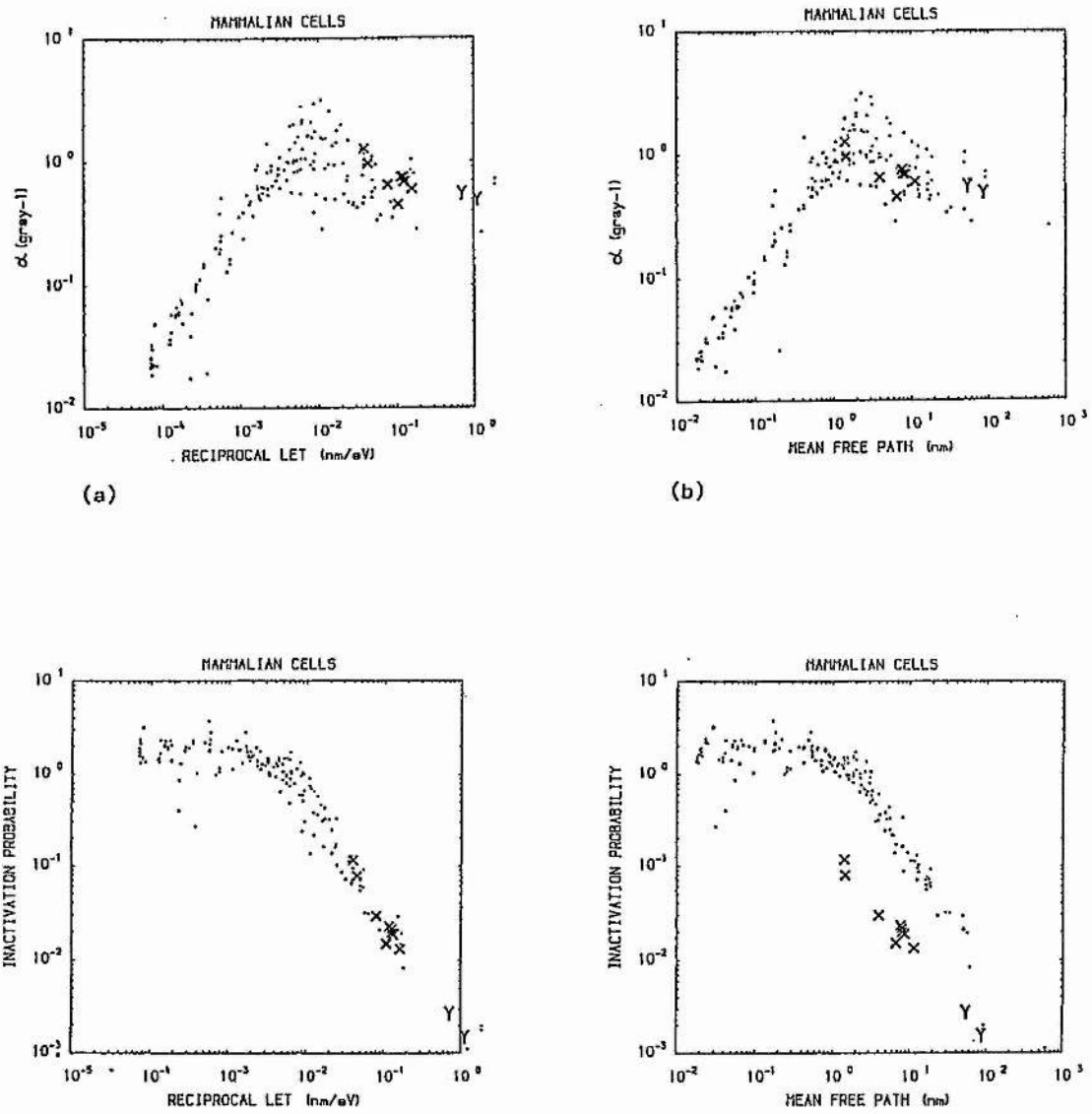

Fig 3

Data for T1-human kidney cells (ref - 11,12); chinese hamster V79 (ref -13, 14); CH2 B2 (ref -15); M31 cells (ref 16) and human diploid fibroblasts HF19 (ref 18) are shown as plots of the initial slope of the survival curves (α gray^{-1}) and of the inactivation probability, p as functions of reciprocal LET and mean free path. Fig 3 (d) shows the good correlation that can be obtained for all target types and radiation types whilst being consistent with the known behaviour of quality for X and γ - rays. See text for discussion.

Session B32-1V: 8th ICRR, Edinburgh, 19-24 July 1987.

DNA-RUPTURE MODEL OF RADIATION ACTION

Chun-Zhang Chen, Alan McGUIRE & David E. WATT*
Department of Physics University of St. Andrews
St. Andrews, KY16 9SS. Scotland, U.K.
**Permanent address: Institute of Biophysics*
Chinese Academy of Sciences. Beijing, China

Abstract

Recent studies of the correlation between biological damage and linear primary ionization of the relevant charged particle tracks has led to the development of a single track model of radiation action in which the production of double-strand breaks in DNA is the dominant damage mechanism in mammalian cells. The model is testable as the shape of the survival curves is predicted to be dependent on irradiation time and not on 'dose' rate.

An appraisal of the validity of this model will be made by reference to published survival data for x-irradiation and in terms of new results obtained with alpha particle irradiation.

Introduction

The correlation between biological damage and linear primary ionization of the relevant charged particle tracks[1,2,3] has led to the development of a single track model of radiation action in DNA by production of DSBs in mammalian cells *in vitro*[4]

$$\ln S = - \sigma_g \phi \int_0^{t_1} [\, 1 - \exp (- p_1 n_0 e^{- (t_f - t)/ t_r})] \, dt$$

where σ_g is the projected cross-section involving the DNA molecules; ϕ is the fluence rate of the incident particles; p_1 stands for the probability relating to the efficiency of one track traversal[3]; n_0 the mean number of segments of DNA molecules at risk. The time factors proposed are: t_f the damage fixation time, t_r the damage repair time and t_1 the total irradiation time.

The model was tested using new data from chronic α irradiation to V79 cells and published data[5] for 250 kV_p x-ray irradiation of CHO-K1 cells. The extracted parameters, particularly the time factors, indicate that the survival curve is indeed dependent on irradiation time and not on 'dose' rate.

Method

A source from ^{241}Am alpha particles was used for the chronic irradiation. The fluence rate was mesured to be $9.2x10^4$ cm^{-2}-min^{-1} at 10 mm from the centre of the 6 mm disc source. The source-sample distance was chosen such that the mean free path of the alpha particles had an optimum damaging value, which is 1.8 nm being equivalent to the DNA double strand spacing [6].

Asynchronous monolayer culture of V79 cells, growing on 3.5 μm Melinix film, were irradiated at room temperature. The obtained data were fitted into the proposed model by a non-linear fitting method.

Results

Conditions	Present Study	From Metting *et al.*, 1985
Irradiation	^{241}Am α particles	250 kV_p x-rays
Fluence rate (cm^{-2} min^{-1})	$9.20X10^4$	$1.35X10^6$
Dose-rate (Gy/min)	0.0168	0.025
	Parameters extracted from the DNA-rupture model	
σ_g, μm^2	45.0	6.0
t_f, min	720	852
t_r, min	225	456
p_1n_0	10.0	0.5

Conclusions

Published data on prolonged irradiations of several hours duration is very limited and, indeed, is available only for x-rays. For the preliminary experiment reported here, using alpha particles, it is clear that the structure of the survival curve can be reproduced on the basis that only intra-track action occurs. However, there are large errors on the magnitude of the four parameters extracted. Better statistics and irradiations with different heavy particle types on the same cell line are required for proper evaluation of the model.

The recovery time for double-strand breaks in DNA seems to be several hours. If the model can be experimentally established there would be important considerations for clinical therapy at low doses.

Acknowledgement: to Drs. A. C. Riches and P. E. Bryant for helpful discussion and biological facilities.

References:

1. Cannell, R. J. and Watt, D. E. (1985). Phys. Med. Biol. **30**, 255-258.
2. Chen, C.-Z. and Watt, D. E. (1986). Int. J. Radiat. Biol. **49**, 131-142.
3. Watt, D. E., Al-Affan, I.A.M., Chen, C.-Z. & Thomas, G.E. (1985). Radiat. Prot. Dosi. **13**, 285-294.
4. Watt, D.E.(1987). Session **B21**- 2V, 8th ICRR.
5. Metting, N.F., Braby, L.A., Roesch, W.C. & Nelson, J.M.(1985).**103**, 204-218.
6. Chen, C.-Z.(1987). Ph.D. Thesis.

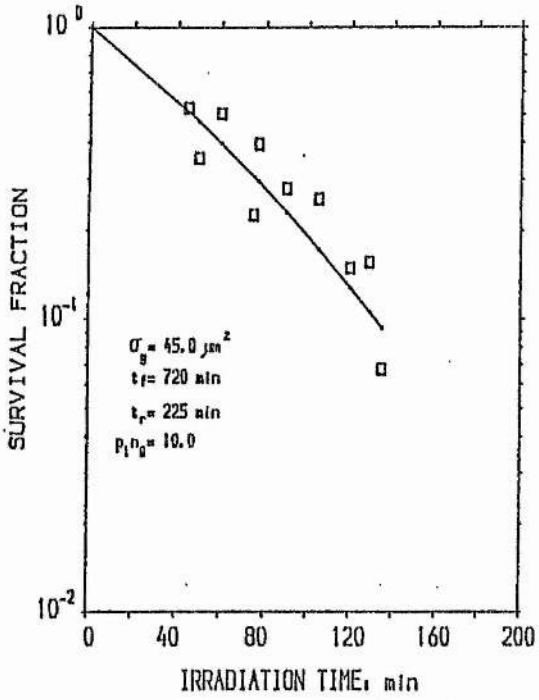

Fig.1 Survival fraction expressed as a function of irradiation time, for V-79 Cells by Am-241 at fluence rate of 9.2×10^4 cm^{-2} min^{-1}. Solid curve: fitted by the DNA-rupture model.

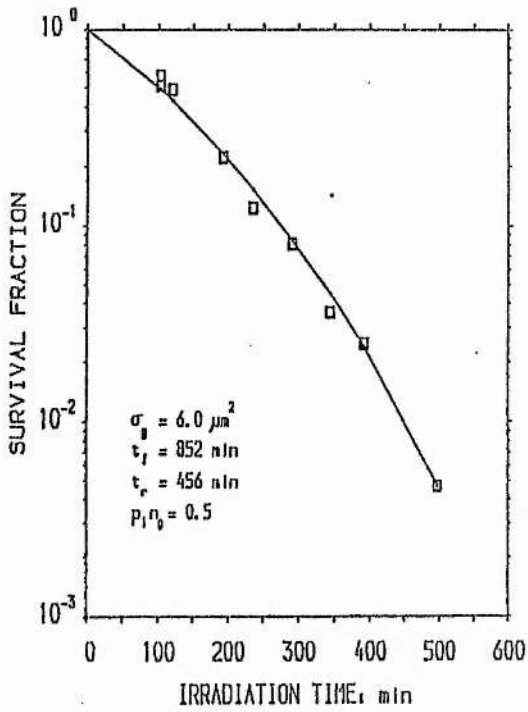

Fig.2 Survival fraction of CHO-K1 cells by 250 kV x-ray irradiation. Fluence rate: 1.347×10^4 cm cm^{-2} min^{-1} (0.025 Gy/min, Metting et al., 1985).